# SELECTIVE INCORPORATION OF THE C-F BOND AS A CONFORMATIONAL TOOL IN QUADRUPLEX DNA LIGAND DESIGN

**Daniel L. Smith**

**A Thesis Submitted for the Degree of PhD**
**at the**
**University of St Andrews**

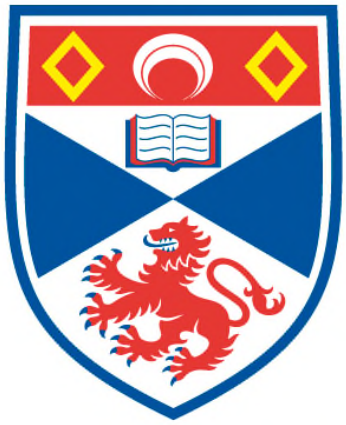

**2012**

**Full metadata for this item is available in**
**St Andrews Research Repository**
**at:**
**http://research-repository.st-andrews.ac.uk/**

**Please use this identifier to cite or link to this item:**
**http://hdl.handle.net/10023/3169**

**This item is protected by original copyright**

# Selective incorporation of the C–F bond as a conformational tool in quadruplex DNA ligand design

University of St Andrews

600 YEARS

School of Chemistry

Daniel L. Smith

June 2012

*Thesis submitted to the University of St Andrews for the degree of Doctor of Philosophy*

Supervisor: Prof. David O'Hagan

**1. Candidate's declarations:**

I, Daniel Smith, hereby certify that this thesis, which is approximately 50,000 words in length, has been written by me, that it is the record of work carried out by me and that it has not been submitted in any previous application for a higher degree.

I was admitted as a research student in September 2008 and as a candidate for the degree of PhD in September 2009; the higher study for which this is a record was carried out in the University of St Andrews between 2008 and 2012

Date: _____ Signature of Candidate:_____

**2. Supervisor's declaration:**

I hereby certify that the candidate has fulfilled the conditions of the Resolution and Regulations appropriate for the degree of Doctor of Philosophy in the University of St Andrews and that the candidate is qualified to submit this thesis in application for that degree.

Date: _____ Signature of Supervisor: _____

**3. Permission for electronic publication:**

In submitting this thesis to the University of St Andrews I understand that I am giving permission for it to be made available for use in accordance with the regulations of the University Library for the time being in force, subject to any copyright vested in the work not being affected thereby. I also understand that the title and the abstract will be published, and that a copy of the work may be made and supplied to any *bona fide* library or research worker, that my thesis will be electronically accessible for personal or research use unless exempt by award of an embargo as requested below, and that the library has the right to migrate my thesis into new electronic forms as required to ensure continued access to the thesis. I have obtained any third-party copyright permissions that may be required in order to allow such access and migration, or have requested the appropriate embargo below.

The following is an agreed request by candidate and supervisor regarding the electronic publication of this thesis:

Embargo on both all of printed copy and electronic copy for the same fixed period of two years on the following ground: publication would preclude future publication.

Date:_____ Signature of Candidate:_____

Signature of Supervisor:_____

*Dedicated to my Papa*

# Acknowledgements

I would like to thank my supervisor Prof. David O'Hagan for the opportunity to conduct research under his supervision. Our many conversations around the project and about science in general have been instrumental throughout my PhD and in my professional development.

I would also like to extend my gratitude towards Dr Nancy Campbell for her tireless work and effort during our collaboration. Her patience and expertise has been of great value.

The work presented in this thesis would have not been possible if it was not for the help, support and skill of all of the technical staff at the School of Chemistry and the BSRC. I am particularly indebted to Melanja Smith for NMR assistance and Caroline Horsburgh for mass spectroscopic analysis. I am also thankful for the assistance of Dr Tomas Lebl with NMR analysis and to Prof. Alexandra Slawin for X-ray crystallography and advice.

Many people have made my time in St Andrews a very memorable and enjoyable experience. All members of the DOH group and the BSRC past and present have contributed in their own special way, however, I would like to particularly acknowledge the following people for their respective contributions: Andrew Nortcliffe for his friendship, invaluable support and advice; Dr Daniel Farran, Dr Jason Schmidberger, Romain Cadou and Thomas Moraux; the forbidden BSRC quartet of Alan, Ray, Stan and Stevie; Nawaf and Fraser for the Dundee commute; Dr Neil Keddie and Dr Michael Corr for their careful proof reading; and finally to my thesis office partner Joanna Wlochal for her sympathetic and supportive attitude.

I am also immensely grateful for the love and support of my family, Marian and Neville Mansell, Steven's Gogo, Robert Kennedy and my friends. Finally and most importantly, I want to acknowledge the love, understanding and motivation from my partner Steven, whom has been instrumental throughout my PhD.

Cancer Research UK generously sponsored this work.

# Table of Contents

## Chapter 2:
## Telomeres, telomerase and quadruplex DNA



## Chapter 3:
## Synthesis and evaluation of fluorinated BSU6039 analogues

## Chapter 4:
## Synthesis of C–F bond incorporated BRACO-19 analogues



## Chapter 5:
## Studies on the selective fluorination of dipeptides

# Abbreviations

| | | |
|---|---|---|
| $\{^1H\}$ | - | proton decoupled |
| 5-FU | - | 5-fluorouracil |
| A | - | adenine |
| Å | - | Angstrom |
| Ala | - | alanine |
| *ap* | - | antiperiplanar |
| aq | - | aqueous |
| Ar | - | aryl |
| ASAP MS | - | atmospheric solids probe analysis mass spectrometry |
| atm | - | atmospheric pressure |
| ax | - | axial |
| Bn | - | benzyl |
| Boc | - | *tert*-butoxycarbonyl |
| br. | - | broad |
| *c* | - | concentration |
| calc. | - | calculated |
| CD | - | circular dichroism |
| CDI | - | 1,1′-carbonyldiimidazole |
| cf. | - | compare |
| concd | - | concentrated |
| COSY | - | correlation spectroscopy |
| CSD | - | Cambridge Structural Database |
| d | - | doublet |
| $d_6$-DMSO | - | deuterated dimethyl sulfoxide |
| DAST | - | diethylaminosulfur trifluoride |
| dba | - | dibenzylideneacetone |
| DBU | - | 1,8-diazabicycloundec-7-ene |
| DCC | - | dicyclohexylcarbodiimide |
| dd | - | doublet of doublets |

| | | |
|---|---|---|
| de | - | diastereomeric excess |
| dec. | - | decomposition |
| δ | - | Nuclear magnetic resonance chemical shift parts per million downfield from a standard |
| $\Delta T_m$ | - | difference in melting temperature |
| Deoxo-Fluor® | - | dimethoxyethylaminosulfur trifluoride |
| DEPT | - | distortionless enhancement by polarization transfer |
| DFI | - | 2,2-difluoro-1,3-dimethylimidazolidine |
| DFT | - | density functional theory |
| DIC | - | *N*,*N*′-diisopropylcarbodiimide |
| DIPEA | - | *N*,*N*-diisopropylethylamine |
| DMAc | - | *N*,*N*-dimethylacetamide |
| DMAP | - | *N*,*N*-dimethylaminopyridine |
| DMF | - | *N*,*N*-dimethylformamide |
| DMSO | - | dimethyl sulfoxide |
| DNA | - | deoxyribonucleic acid |
| dppb | - | 1,4-bis(diphenylphosphino)butane |
| dr | - | diastereomeric ratio |
| $\varepsilon$ | - | molar extinction coefficient |
| $ED_{50}$ | - | dose that is effect in 50% of test subjects |
| EDCI | - | *N*-(3-dimethylaminopropyl)-*N*′-ethylcarbodiimide hydrochloride |
| ee | - | enantiomeric excess |
| EI | - | electron ionisation |
| eq | - | equivalent |
| ES | - | electrospray ionisation |
| EXSY | - | exchange spectroscopy |
| FAM | - | carboxyfluorescein |
| FRET | - | Förster resonance energy transfer |
| FT-IR | - | Fourier transform infrared spectroscopy |
| G | - | guanine |
| g | - | grams |
| $g^-$ | - | *gauche* torsion angle |

| | | |
|---|---|---|
| $g^+$ | - | *gauche* torsion angle |
| $G_0$ | - | resting phase of the cell cycle |
| GABA | - | γ-aminobutyric acid |
| $GABA_{A/B/C}$ | - | γ-aminobutyric acid receptor subclass A/B/C |
| GMP | - | guanosine monophosphate |
| Go | - | any number of guanine nucleotides |
| GP | - | general procedure |
| h | - | hour |
| HATU | - | *O*-(7-azabenzotriazol-1-yl)-*N*,*N*,*N*′,*N*′-tetramethyluronium hexafluorophosphate |
| HBTU | - | *O*-(benzotriazol-1-yl)-*N*,*N*,*N*′,*N*′-tetramethyluronium hexafluorophosphate |
| $H_{eq}$ | - | equatorial hydrogen |
| HMBC | - | heteronuclear multiple-bond correlation spectroscopy |
| HMDS | - | 1,1,1,3,3,3-hexamethyldisilazane |
| HOBt | - | hydroxybenzotriazole |
| HOESY | - | heteronuclear Overhauser effect spectroscopy |
| HPLC | - | high-performance liquid chromatography |
| HRMS | - | high resolution mass spectroscopy |
| HSQC | - | heteronuclear single-quantum correlation spectroscopy |
| hTERT | - | human telomerase reverse transcriptase |
| hTR | - | human telomerase ribonucleic acid |
| Hz | - | Hertz |
| $ID_{50}$ | - | dose that inhibits at 50% of maximum response |
| IR | - | infrared |
| *J* | - | coupling constant |
| L | - | litre |
| $\ell$ | - | path length |
| Lit. | - | literature reference |
| LHS | - | left hand side |
| M | - | molar |
| m | - | multiplet |

| | | |
|---|---|---|
| *m*/*z* | - | mass to charge ratio |
| mg | - | milligrams |
| MHz | - | megahertz |
| min | - | minutes |
| mL | - | milliliters |
| MO | - | molecular orbital |
| MOST | - | morpholinosulfur trifluoride |
| mp | - | melting point |
| n | - | number |
| N/T | - | not tested |
| NFSI | - | *N*-fluorobenzenesulfonamide |
| NHEJ | - | non-homologous end joining |
| NMM | - | *N*-methylmorpholine |
| NMR | - | nuclear magnetic resonance |
| nOe | - | nuclear Overhauser effect |
| NOESY | - | nuclear Overhauser effect spectroscopy |
| *O. nova* | - | *Oxytricha nova* |
| *t*-Bu $P_4$ | - | *tert*-butyl P4 phosphazene |
| P450 | - | specific cytochrome enzyme subtype |
| PDB | - | protein database |
| PET | - | positron emission tomography |
| Ph | - | phenyl |
| Phe | - | phenylalanine |
| Phen | - | phenanthroline |
| $\pi^*$ | - | antibonding π orbital |
| POT1 | - | protection of telomeres 1 protein |
| ppm | - | parts per million |
| PyBrop | - | bromotripyrrolidinophosphonium hexafluorophosphate |
| q | - | quartet |
| $R_f$ | - | retention factor |
| RHS | - | right hand side |
| rRNA | - | ribosomal ribonucleic acid |
| rt | - | room temperature |

| | | |
|---|---|---|
| s | - | singlet |
| Ser | - | serine |
| SET | - | single electron transfer |
| $\sigma^*$ | - | antibonding σ orbital |
| soln. | - | solution |
| ssDNA | - | single stranded deoxyribonucleic acid |
| T | - | thymine |
| t | - | triplet |
| T3P® | - | propylphosphonic anhydride |
| TAMRA | - | carboxytetramethylrhodamine |
| TBAF | - | tetrabutylammonium fluoride |
| TBAI | - | tetrabutylammonium iodide |
| TBDMS | - | *tert*-butyldimethylsilyl |
| TBSOTf | - | *tert*-butyldimethylsilyl trifluoromethanesulfonate |
| $^{tel}EC_{50}$ | - | dose that is 50% effective against the action of telomerase |
| $^{tel}IC_{50}$ | - | dose that results in 50% inhibition of telomerase |
| temp | - | temperature |
| TFAc | - | trifluoroacetate |
| THF | - | tetrahydrofuran |
| TLC | - | thin layer chromatography |
| TRAP | - | telomeric repeat amplification protocol |
| tRNA | - | transfer ribonucleic acid |
| UV-Vis | - | ultraviolet-visible |
| *v*/*v* | - | volume per volume |
| Val | - | valine |
| *w*/*v* | - | weight per volume |
| *w*/*w* | - | weight per weight |
| Xn | - | any number non-guanine nucleotides |
| Xp | - | any number of non-guanine nucleotides involved in loop formation |
| XtalFluorE® | - | morpholinodifluorosulfonium tetrafluoroborate |
| XtalFluorM® | - | (diethylamino)difluorosulfonium tetrafluoroborate |

# Abstract

**Chapter 1** provides a general introduction to organofluorine chemistry and focuses on recent developments in fluorination techniques. It also details how the C–F bond influences conformational and physiochemical properties of organic molecules.

**Chapter 2** highlights the biological role of the telomere, telomerase and quadruplex DNA in cells. It discusses the inhibition of telomerase with small molecules that stabilise quadruplex DNA as a treatment for cancer. An overview of the development of structurally related telomerase inhibitors and recent X-ray crystallographic structural data with BSU6039 and BRACO-19 telomeric DNA is presented.

**Chapter 3** discusses the synthesis of fluorinated BSU6039 analogues for the investigation of the conformational effects of fluorine in 5-membered rings and its influence on binding with quadruplex DNA. These compounds have been successfully co-crystallised with telomeric DNA and their relative stabilisation of telomeric DNA has been assessed. The latter half of this chapter focuses on the co-crystal structures between (*S,S*)- and (*R,R*)-**144** with *Oxytricha nova* telomeric DNA, discussing the key differences between the two stereoisomers.

**Chapter 4** details the synthesis of fluorinated BRACO-19 analogues. The syntheses of such fluorinated analogues were achieved through a base mediated coupling between 3,6-diaminoacridone and an $\alpha$-fluorinated-$\beta$-amino ester. The $\alpha$-fluorinated-$\beta$-amino ester was synthesised through a deoxyfluorination-mediated approach, using the stereochemistry of natural amino acids.

**Chapter 5** describes the stereo- and regio- selectivity of deoxyfluorination reactions with dipeptides bearing the $\beta$-amino alcohol functionality. Understanding this selectivity enabled the development of a method towards $\alpha$-fluorination of tertiary amides. The application of this fluorination method with an orthogonally protected tertiary amide is described.

# Chapter 1

# Synthesis & properties of fluorinated compounds

## 1.1 - A brief history

Alchemists of the 17$^{th}$ century first harnessed the power of fluoric acids by treating fluorspar ($CaF_2$) with strong acid to liberate hydrofluoric acid vapour. This vapour was used to etch glass for decorative purposes. However, the isolation of elemental fluorine remained elusive until the end of the 19$^{th}$ century, with many of great experimentalists, including H. Davy and A.-M. Ampère, dedicating their efforts. The Frenchman Henri Moissan finally isolated elemental fluorine ($F_2$) in 1886, by the electrolysis of $KHF_2$/HF, an accomplishment that contributed to Moissan being awarded the Nobel Prize for Chemistry in 1906.[1] During his attempts to isolate $F_2$, Moissan would often experience the apparatus exploding into flames, as the liberated gas reacted with silicon grease. Moissan took this to conclude that he had in fact produced $F_2$ and proceeded to inform the National Academy with the following statement: *"One can indeed make various hypotheses on the nature of the liberated gas: the simplest would be we are in the presence of fluorine"*.[2]

## 1.2 - Fluorination techniques

Elemental fluorine will react with practically any organic material. In today's chemical research environment, fluorine gas is still actively used by academic groups around the world, despite the requirement for rigorous safety considerations. Chambers and Sandford have developed a method employing microflow reactors to tame $F_2$. With this approach, 1,3-diketones such as **1**, can be mildly fluorinated with 10% $F_2$ in $N_2$, and

then subsequent cyclisation with hydrazine through to mono-fluorinated pyrazoles such as **3**. These represent fluorinated structural motifs for medicinal chemistry applications (Scheme 1.01).[3] This approach results in higher yields over direct fluorination of pyrazoles with electrophilic fluorinating reagents or with elemental fluorine.

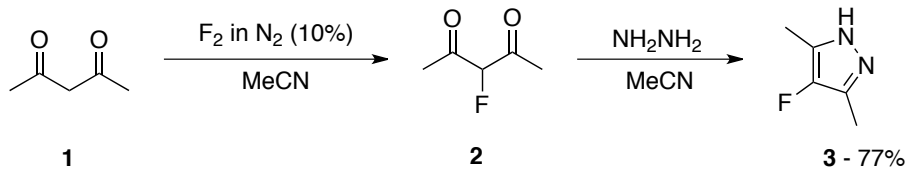


**1** **2** **3** - 77%

**Scheme 1.01.** Synthesis of pyrazoles employing a fluorination flow method.

Despite controlling the reactivity of $F_2$ with flow reactors, elemental fluorine remains difficult to handle and therefore in the last half-century, there have been many novel fluorination methods reported in the literature.[4,5]

## 1.3 - Electrophilic fluorinating reagents

In the 1960's Derek Barton explored the development of the electrophilic reagent $CF_3OF$. Fluoroxy-trifluoromethane can fluorinate activated enolates, but the reagent is toxic and difficult to use.[6] Various second generation electrophilic fluorinating reagents initially inspired by the power of $CF_3OF$ have now become commonplace in organic chemistry (Figure 1.01).

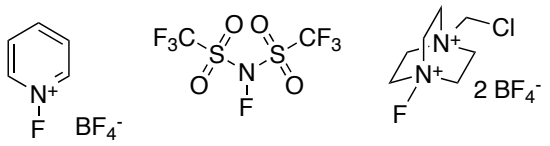


**4** **5** **6**

**Figure 1.01.** Common electrophilic fluorinating reagents.

The first of these reagents were the *N*-fluoropyridinium salts **4** of Umemoto.[7] The reactivity of these salts can be tuned through modification of the pyridinium ring with electron-withdrawing and -donating functional groups. The mode of fluorination is thought to proceed by a single electron transfer (SET) mechanism.

The sulfone amide, *N*-fluorobis[(trifluoromethyl)sulfonyl]imide **5** (NFSI), developed by Desmarteau, is among the most powerful electrophilic fluorinating reagent developed.[8] Differding and co-workers demonstrated the first enantioselective electrophilic fluorination with the chiral *N*-fluoro sultam **7** NFSI.[9] Fluorination of cyclic enolates **8** with sulfone **7**, enabled a modest enantioselectivities of up to 70% ee (Scheme 1.02).

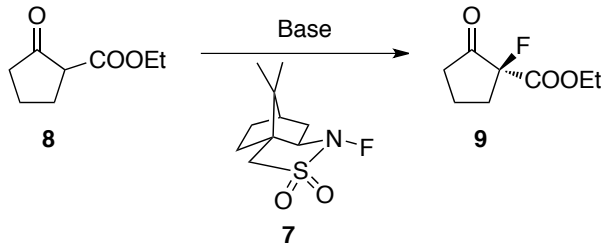


**Scheme 1.02.** The first example of an enantioselective fluorination reaction.

More recently, however, there have been remarkable developments in enantioselective fluorination as demonstrated by MacMillan,[10] Jørgenson[11] and Barbas.[12] In their separate approaches they have demonstrated how organocatalysts in the presence of NFSI can achieve $\alpha$-fluorination of various aldehydes, with enantioselectivities of up to 99% ee in the case of MacMillan's system (Scheme 1.03).

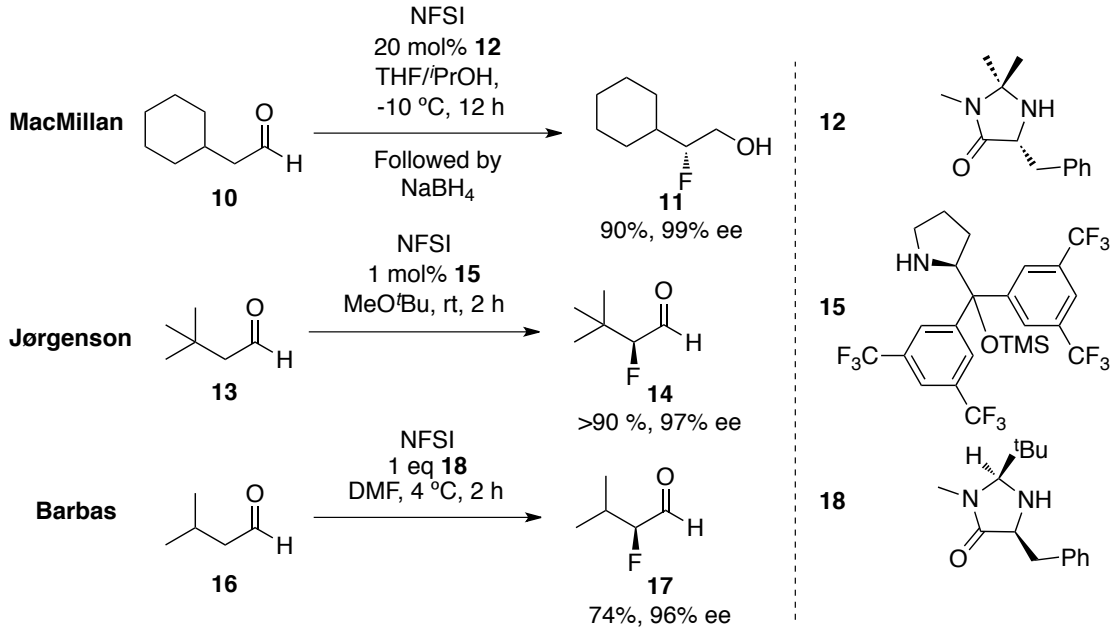


**Scheme 1.03.** Organocatalytic approaches to the $\alpha$-fluorination of aldehydes with NFSI (**5**).

In these examples, the formation of a chiral enamine intermediate results in a diastereoselective interaction with the fluorinating reagent (Scheme 1.04).

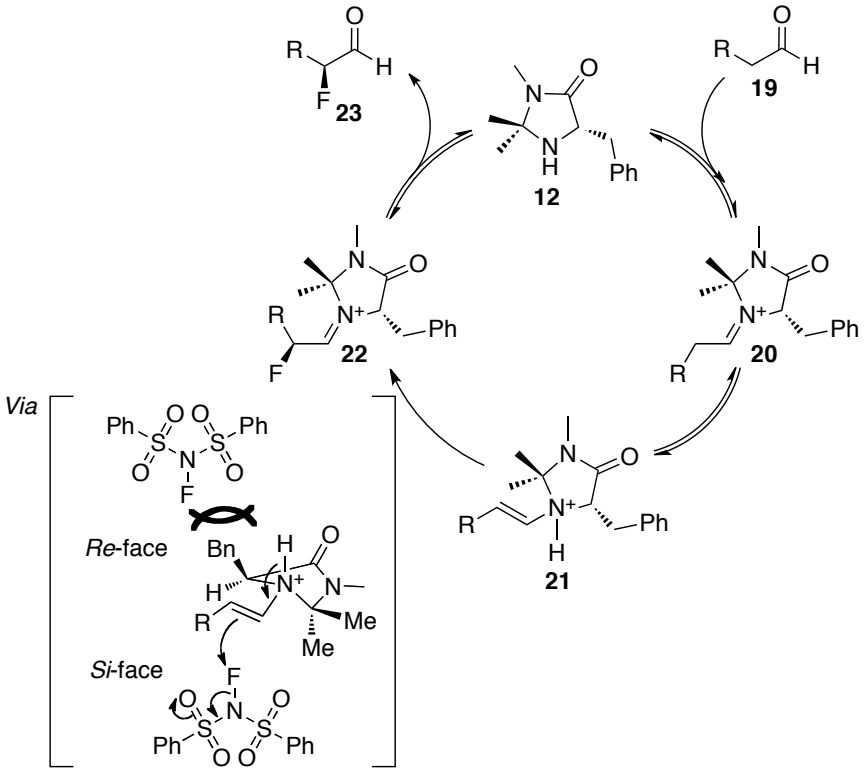


**Scheme 1.04.** Proposed catalytic cycle for fluorination where R = aryl or alkyl. The counterion for intermediates **20**-**22** is dichloroacetic acid.

Transfer of fluorine from the bottom face (the *Re*-face) of the chiral intermediate is blocked by the bulky phenyl moiety (Scheme 1.04, red clash). Thus, NFSI approaches the *Si*-face of the enaminium intermediate **21** to furnish the $\alpha$-fluoro iminium **22**, which generates $\alpha$-fluoro aldehyde **23** following hydrolysis.

Jørgenson used the bulky proline derivative **15** at very low catalyst loading (1 mol%), much lower than that of MacMillan and Barbas. The MacMillan and Barbas catalysts both suffer from higher catalyst loadings, however in the system developed by MacMillan, the yields and level of enantiocontrol were significantly improved (Scheme 1.03).

The most widely used electrophilic fluorinating reagent is the 1,4-diazabicyclo[2.2.2]octane based reagent, selectfluor (**6**) (Figure 1.01).[13] Selectfluor, developed by Banks, is a highly stabile, versatile and reliable fluorinating reagent that has found wide application in synthesis.[13,14] A recent publication in *Science* by Toste and co-workers demonstrated the applicability of selectfluor (**6**) in the enantioselective fluorocyclisation of dihydropyran based substrates such as **24** to fluorinated spiro-oxazoline, such as **26**. (Scheme 1.05).[15]

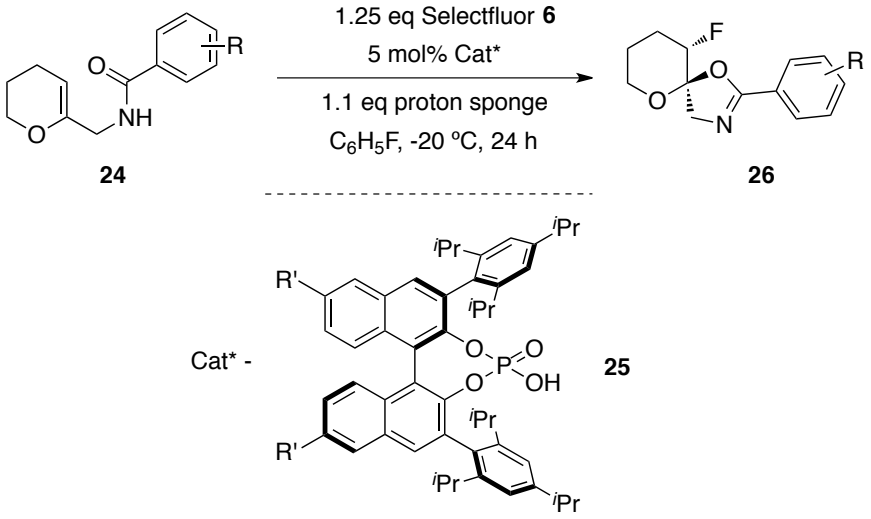


**Scheme 1.05.** Phase transfer catalyst with selectfluor to induce fluorocyclisation. R = H, alkyl, aryl, halide

In this particular transformation, Toste *et al.* formed a chiral cationic fluorinating reagent *in situ*, with phosphoric acid catalyst **25**. Selectfluor is insoluble in non-polar solvents and in this protocol the formation of the chiral selectfluor salt with **25** enables the reaction to proceed in a non-polar solvent and thus increases the substrate scope. Conducting the reaction in a polar medium was found to lead to multiple unidentifiable products.

Ritter and co-workers have pioneered an approach to the fluorination of aromatic heterocycles through the use of the selectfluor $PF_6^-$ salt **28**.[16] They demonstrated that treatment of aryl tributylstannanes (**27**) with silver triflate and selectfluor resulted in the isolation of aryl fluorides such as **29** within 20 min at room temperature (Scheme 1.06).

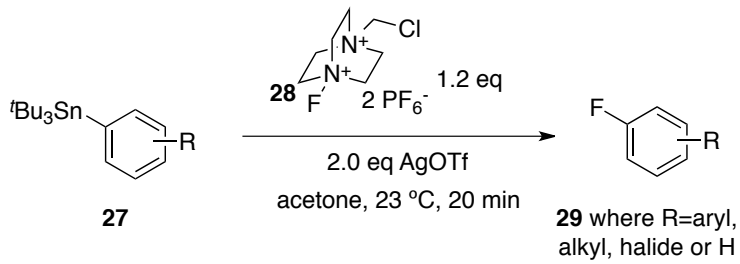


**Scheme 1.06.** Fluorodestannylation through a silver-mediated approach.

This proceeds through a mechanistically complex process that preliminary experimental data demonstrates the involvement of two silver cations in the catalytically active species. Trans-metalation of the aryl stannane followed by oxidative insertion of the fluorine to form a speculative $[(Aryl\text{-}Ag\text{-}F)Ag]^{n+}$ species is though to be key to the process. Reductive elimination to form the Aryl-fluorine bond completes the process.

Gouverneur *et al*. have recently demonstrated this fluorodestannylation in the preparation of fluorine-18 labelled heterocycles with modest radiochemical yields of up to 18% for positron emission tomography (PET).[17]

## 1.4 - Nucleophilic fluorinating reagents

Fluoride ion is a hard nucleophile with high solvation energy. The use of polar coordinating solvents greatly diminishes its nucleophilicity.[18,19] Typical nucleophilic sources of fluoride are: NaF, KF and CsF.[20–22] These alkali metal fluorides can be used to displace activated alcohols, such as **30**, to furnish the corresponding fluorinated derivatives **31** (Scheme 1.07).[4]

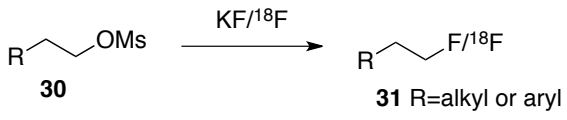


**Scheme 1.07.** General nucleophilic displacement of an activated alcohol with KF. Radiolabelled $K^{18}F$ can be used for the generation of PET radiotracers. R = H, alkyl, aryl.

Many nucleophilic fluorinating reagents are commercially available and offer an array of options for chemists to introduce one more fluorine atoms into organic molecules.

One of the most powerful fluorinating reagents is sulfur tetrafluoride ($SF_4$), which can convert alcohols, ketones and carboxylic acids through to their respective mono-, di- and tri-fluoro analogues.[4]

The development of safer and easier to use sulfur-based fluorination regents was led by Middleton at DuPont in the 1970's.[23] Middleton developed diethylaminosulfur trifluoride **32** (DAST **32**, Figure 1.02), which represented a convenient nucleophilic fluorinating reagent (Scheme 1.08) for the deoxyfluorination of alcohols, with wide applications in synthesis.

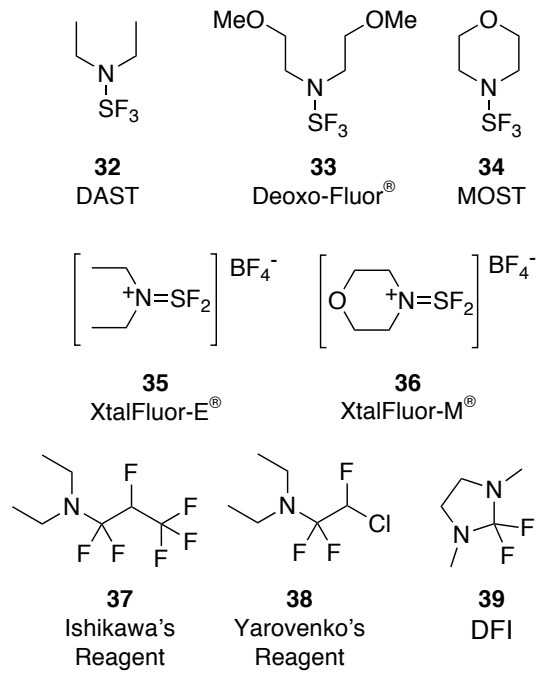


**Figure 1.02**. Nucleophilic fluorinating reagents.

DAST **32** exists in equilibrium between the neutral form **32** and the charged activated species **32'** with a fluoride counter ion. Nucleophilic attack of the lone pair of an alcohol (**40**), to the sulfur of the activated DAST **32'** results in intermediate **41** (Scheme 1.08). This activates the alcohol ready for nucleophilic displacement by the liberated fluoride to yield the fluorinated product **42** (Scheme 1.08). DAST **32** does, however, suffer from thermal sensitivity and can decompose exothermically at temperatures above 90 ºC.

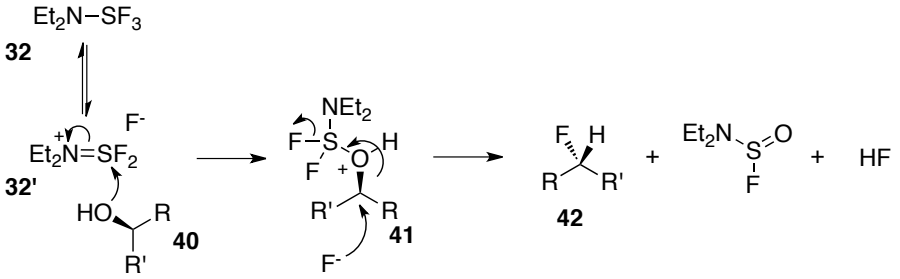


**Scheme 1.08.** General mechanism for fluorination of alcohols (where R = aryl and alkyl) with DAST **32** or Deoxo-Fluor® **33**.

Deoxo-Fluor® **33** and MOST **34** were developed as thermally stable alternatives to DAST **32** (Figure 1.02).[23] Sulfur trifluoride based fluorinating reagents can fluorinate a variety of substrates, however, they are mostly employed for the fluorination of alcohols. DAST **32** can also convert ketones into their respective *gem*-difluoro analogues.[24]

Ishikawa's reagent **37**, Yarovenko's reagent **38** and the 2,2-difluoro-1,3-dimethylimidazolidine (DFI) **39** are nucleophilic fluorinating reagents that are less commonly employed.[4] This lack of application can be explained through their propensity to form side products. For example, DFI **39** can be used to fluorinate alcohols and ketones such as **43** and **46**, however, this often results in elimination to give vinyl and fluoro vinyl side products such as **44** and **48** (Scheme 1.09).[25]

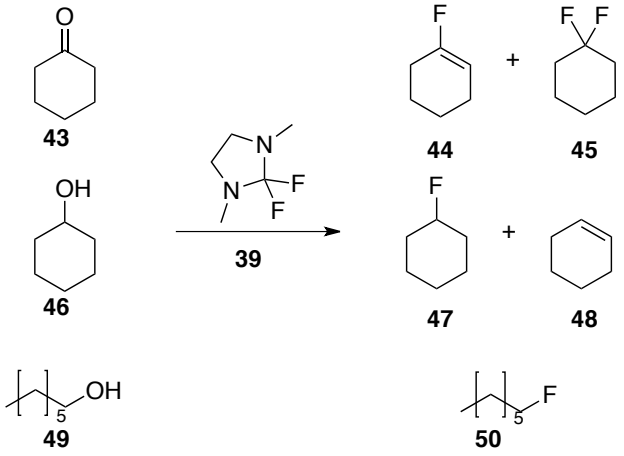


**Scheme 1.09**. Fluorination of alcohols and ketones with DFI **39**.

The tetrafluoroborate salts, XtalFluorE® **35** and M® **36** are recent additions to the list of nucleophilic fluorinating regents (Figure 1.02).[26,27] These air and thermally stable solid salts have been shown to have similar selectivity to DAST **32** or Deoxo-Fluor® **33** with few elimination products observed. However, these reagents require promoter additives such as DBU or $HF.Et_3N$ to enable effective conversion to *gem*-difluoro **51**, mono-fluoro **53** and acyl fluoride **55** derivatives (Scheme 1.10).[27] These reagents, unlike DAST **32** and Deoxo-Fluor® **33**, do not have free fluoride, therefore the promoters are important in generating fluoride for nucleophilic attack at the activated carbon centers.

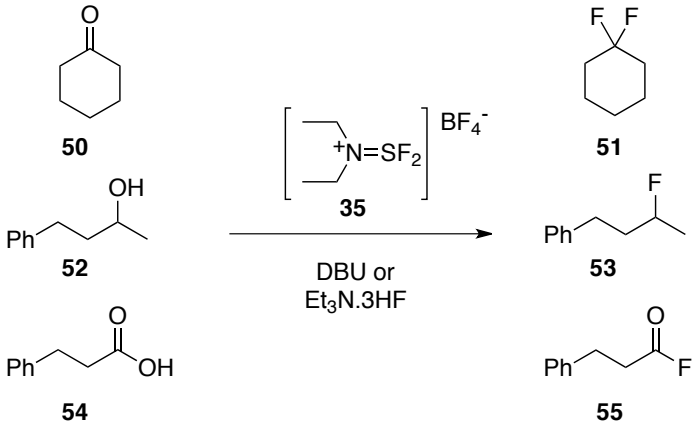


**Scheme 1.10.** Fluorination with XtalFluorE® (**35**).

## 1.5 - Trifluoromethylation of aromatic and heteroaromatic rings

Recent high profile publications have appeared in the literature addressing the development of effective aromatic trifluoromethylation. The most notable of these are from the laboratories of Buchwald,[28] Baran[29] and MacMillan,[30] appearing in *Science*, *PNAS* and *Nature* respectively. Buchwald *et al*., developed a low catalyst loading Pd phosphine based trifluoromethylation procedure that displayed wide substrate tolerance (Scheme 1.11). This method proceeds *via* a classic Pd catalysed mechanism with reductive elimination furnishing the Ar-$CF_3$ product, such as **57**, in yields >70%.

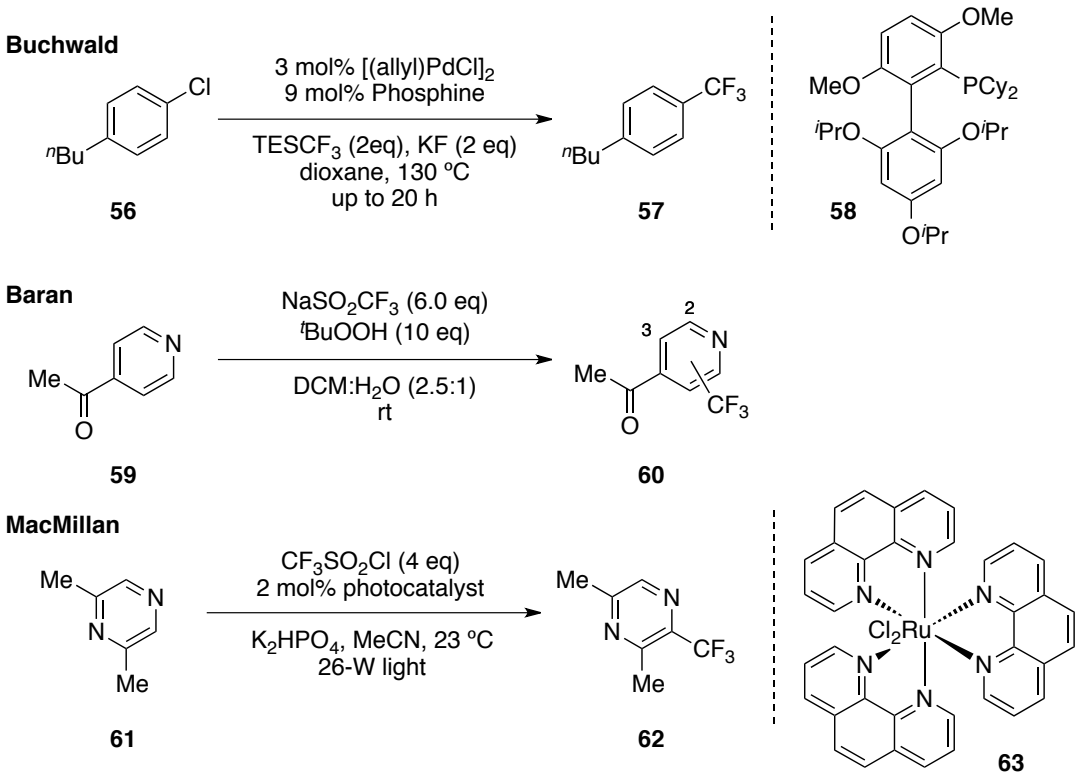


**Scheme 1.11.** Recent advances in the trifluoromethylation of aromatic rings.

The Buchwald palladium catalysed approach provides an efficient procedure for the trifluoromethylation of various building blocks for later assembly into structurally important compounds. The contributions by Baran[29] and MacMillan[30] employ radical trifluoromethylation approaches, which proceed at ambient temperature (Scheme 1.11). Baran *et al*., have shown that the Langlois reagent ($NaSO_2CF_3$),[31] along with *tert*-butyl hydroperoxide can achieve radical trifluoromethylation of unactivated heteroaromatics such as **59** (Scheme 1.11). This occurs in a non-selective fashion under biphasic conditions with trifluoromethylation of **59** occurring at the 2/3- positions (Scheme 1.11). Extending this approach to the trifluoromethylation of medicinally active agents enabled the synthesis of trifluoromethylated analogues **64**-**66** with some selectivity for the more nucleophilic carbon center (Figure 1.03).

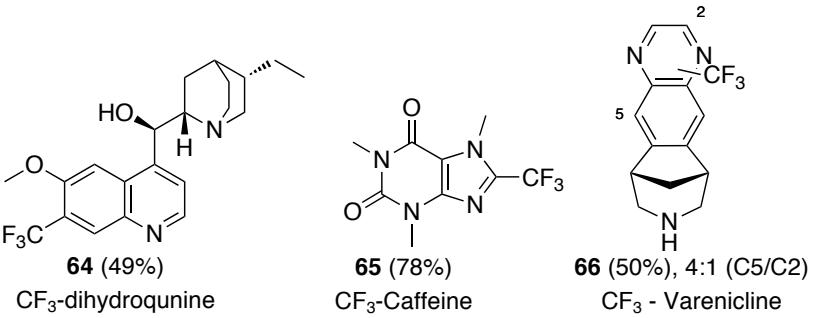


**Figure 1.03.** Selected products using the Baran's trifluoromethylation method.

In a subsequent development, MacMillan *et al*. have demonstrated the applicability of $Ru(phen)_3$ photocatalyst **63** for the initiation of radical trifluoromethylation with various unactivated heteroaromatics such as **61** (Scheme 1.11).[30] This approach also works at ambient temperature and is highly suitable to late stage modifications of pharmacological relevant compounds such as **67-72** (Figure 1.04). The authors report both selective and promiscuous trifluoromethylation with this approach (Figure 1.04). While both outcomes are beneficial, the promiscuous trifluoromethylation is significantly more powerful, enabling the synthesis of various trifluoromethylated regioisomers for the systematic studies of their effects *in vitro*/*vivo*.

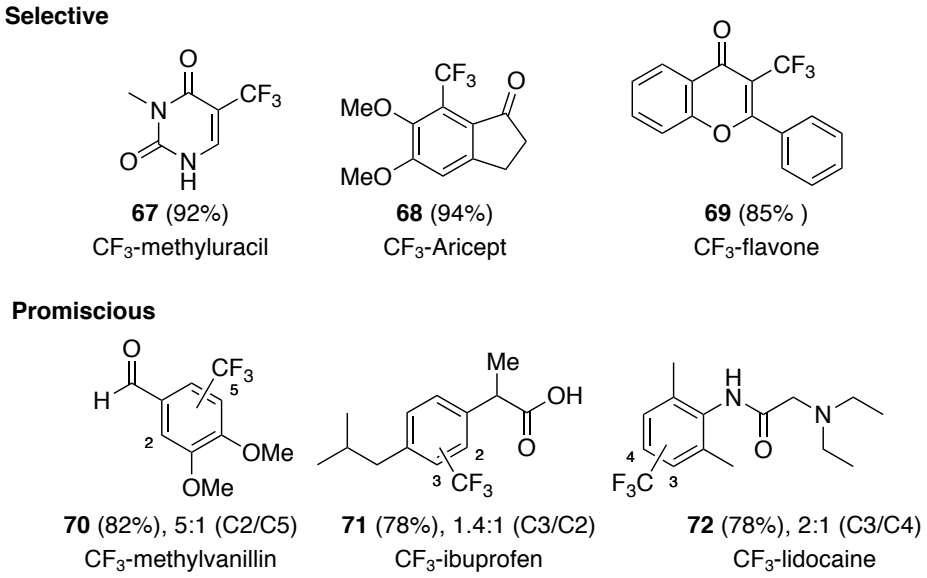


**Figure 1.04.** Typical products of the MacMillan's trifluoromethylation procedure.

Both of the procedures from the MacMillan and Baran laboratories represent significant advances in the trifluoromethylation of aromatic compounds with wide ranging applications. The application of these techniques to rapid profiling of trifluoromethylated drugs in a medicinal chemistry context will be a key aspect of their future application.[32,33]

## 1.6 - Properties of fluorine in organic molecules

Organofluorine compounds have found a multitude of applications from functional materials[34] to pharmaceuticals,[35–37] and agrochemicals.[38] They form a significant proportion of pharmaceutical compounds and agrochemicals, with organofluorine compounds representing approximately 20% of products on the market.[39]

Fluorine has a small van der Waals radius (1.47 Å)[40] and is often regarded as an isostere for hydrogen or oxygen, as its steric influence is intermediate between these atoms.[41] Due to its high electronegativity, fluorine holds onto valence electrons tightly, and as a result, it has a high ionisation energy potential of 1681 kJ $mol^{-1}$ (cf. chlorine 1251 kJ $mol^{-1}$). Fluorine has never been observed as a 'fluoronium' ion ($F^+$), unlike other halogens.[19]

The C–F bond is the strongest single bond in organic chemistry with a dissociation energy of 115.0 kcal $mol^{-1}$, significantly higher than that of other carbon halogen bonds (cf. C–Br - 69 kcal $mol^{-1}$, C–Cl - 79 kcal $mol^{-1}$).[42] This can be attributed to the electronegativity and relative size of the fluorine atom, with the carbon donating electrons to the fluorine such that the carbon becomes $\delta^+$ and the fluorine $\delta^-$. Therefore, it can be assumed that the single bond has some electrostatic character in addition to its covalent nature.[42]

## 1.7 - Acidity and basicity

The strong C–F dipole alters the p$K_a$ or p$K_b$ of neighbouring functional groups (Table 1.1).[43,44] For example, sequential introductions of fluorine on the $\alpha$-carbon of acetic acid results in an increase of acidity of the carboxylic acid, with the p$K_a$ going from 4.76 in acetic acid to 0.52 for trifluoroacetic acid (Table 1.01). This can be explained by a greater electropositive nature of the $\alpha$-carbon supporting the negative charge of the carboxylate through the inductive effect.

| Carboxylic acids | p$K_a$ | Alcohols | p$K_a$ | Bases | p$K_b$ |
|---|---|---|---|---|---|
| $CH_3CO_2H$ | 4.76 | $CH_3CH_2OH$ | 15.9 | $CH_3CH_2NH_2$ | 10.7 |
| $CH_2FCO_2H$ | 2.59 | $CF_3CH_2OH$ | 12.4 | $CH_2FCH_2NH_2$ | 8.97 |
| $CHF_2CO_2H$ | 1.34 | $(CH_3)_3OH$ | 19.2 | $CHF_2CH_2NH_2$ | 7.52 |
| $CF_3CO_2H$ | 0.52 | $(CF_3)_3OH$ | 5.1 | $CF_3CH_2NH_2$ | 5.70 |

**Table 1.01.** p$K_a$ and p$K_b$ of non-fluorinated and fluorinated acids, alcohols and bases.

This effect on acidity or basicity can affect a drugs ability to be transported through biological membranes such as the blood brain barrier. Thus, fluorine incorporation can be used to tailor properties to improve pharmacokinetic profile of a molecule.[36]

## 1.8 - Fluorine in drug metabolism

Within medicinal chemistry, the strong C–F bond has been used to limit the susceptibility of pharmaceuticals to P450 oxidation in the liver.[35] This has been widely applied to the modification of aryl rings for example, in Ezetimibe **74** (Scheme 1.12). Lead optimisation of **73** resulted in an overall increase in potency and stability *in vivo*.[45]

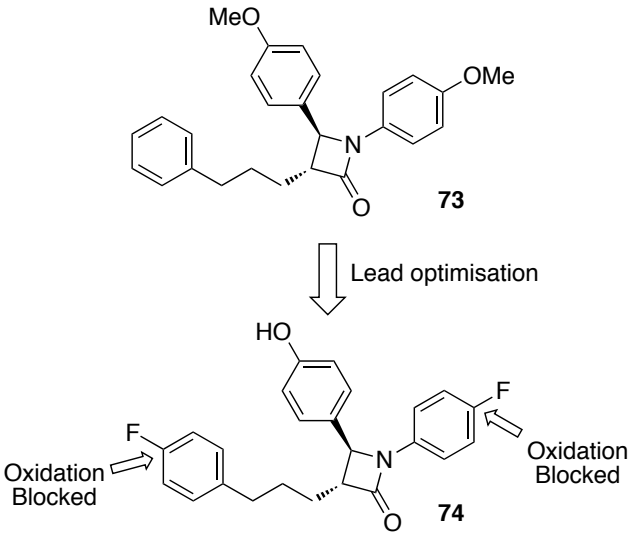


**Scheme 1.12.** Metabolic stability introduced through lead optimisation resulting in greater potency.

## 1.9 - Fluorine based suicide inhibitors

One of the earliest and most successful applications of fluorine within medicinal chemistry was the antineoplastic drug 5-fluorouracil (5-FU) **75** (Scheme 1.13).[46] 5-FU acts by inhibiting the enzyme thymidylate synthase disrupting the biosynthesis of nucleotides for DNA synthesis resulting in cell death (Figure 1.13).

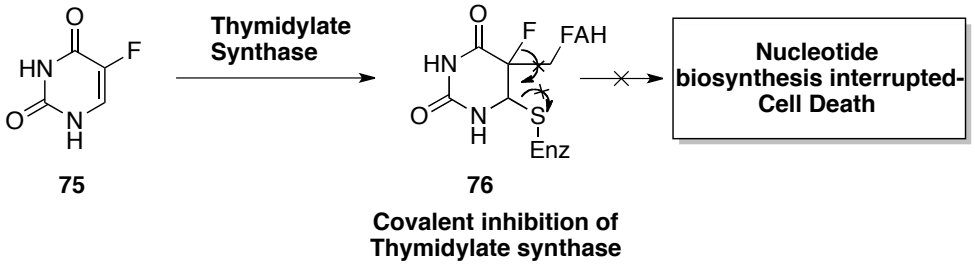


**Scheme 1.13**. 5-FU inhibition of thymidylate synthase through the irreversible covalent blocking of the active site.

Inhibition of the enzyme occurs during the methylation stage. To release the methylated nucleotide, the fluorine must leave as '$F^+$', which cannot happen, and so the 5-FU becomes covalently bound in the active site, thus leaving the enzyme inactive (Scheme 1.13).[47]

## 1.10 - $^{19}$F NMR probes in chemical biology

### *1.10.1 - General applications*

The use of fluorine NMR has been particularly important in chemical biology for example, during the elucidation of the metabolism of fluoro-containing pharmaceuticals,[48,49] or following the biosynthesis of fluorinated natural products *in vitro*.[50,51] The power of $^{19}$F NMR signals in these systems is that the chemical shift of fluorinated compounds varies over a large range (~ 300 ppm) and their spectral complexities are lower compared with $^{1}$H NMR spectra. $^{19}$F NMR has been extended to the study of small molecule-protein or DNA binding studies.[52,53] The synthesis of proteins containing fluorine modified amino acids, offers a route to monitor the binding of small molecules to an active site by observing the chemical shift changes in the $^{19}$F NMR spectrum.[54]

### *1.10.2 - rRNA conformation probes*

The application of $^{19}$F NMR in the study of small molecule probes for determining RNA tertiary structure was reported in 2010 by Micouin and co-workers.[55] Based on previous work, they demonstrated that small diaminocyclopentanes **77** (Figure 1.05) were able to bind to various transfer RNAs without altering the global structure of specific tRNAs.[56,57]

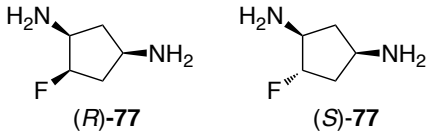


**Figure 1.05.** Small fluorinated NMR probes for RNA structure.

Monitoring the chemical shift differences of the two diastereoisomers of **77** upon binding to tRNA sequences demonstrated the formation of a diastereomeric pair with tRNA (Figure 1.06). The relative chemical shift was found to be tRNA dependent. In each case this shift was dependent on the tertiary structure of the tRNA, as confirmed by variable temperature-NMR (VT-NMR).[55]

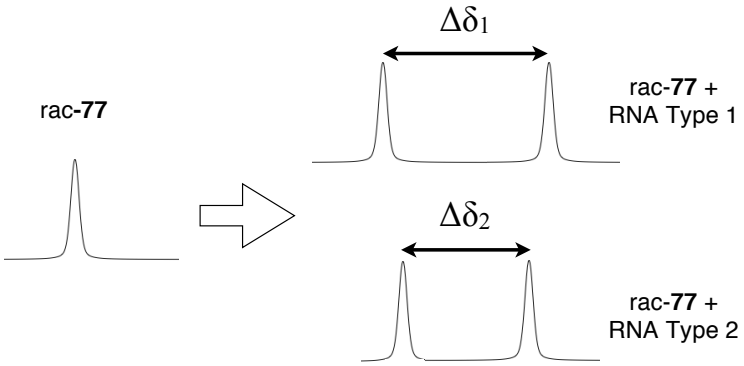


**Figure 1.06.** Changes in the $^{19}$F NMR chemical shift of rac-**77** in response to RNA addition.

This technique allows a potential method to investigate the topological changes in tRNA structure, however the future assessment, in a complex biological environment, may be complicated by non-specific binding of **77**.

### *1.10.3 - Membrane transport kinetics*

$^{19}$F NMR has also been used to explore the transport of the fluorinated glucose analogue *α*/*β*-**78** across erythrocyte (red blood cells) membranes (Figure 1.07).[58]

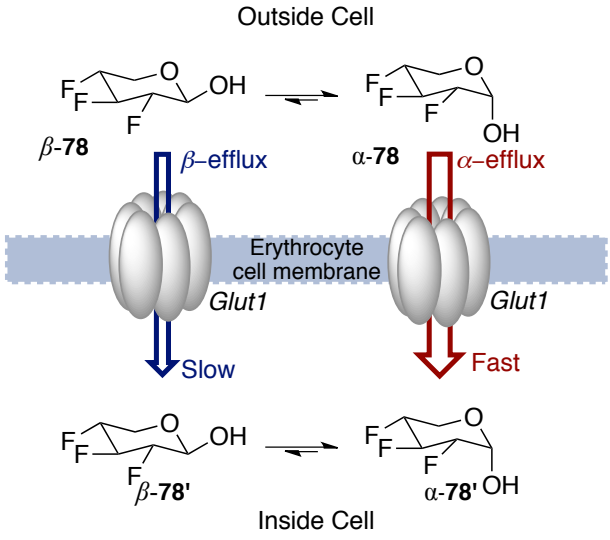


**Figure 1.07**. Trifluoro-glucose analogues *α*/*β*-**78** as a $^{19}$F NMR probes to study efflux enzymes through 2D EXSY experiments.

In the study by O'Hagan *et al*., membrane transport kinetics were assessed by 2D $^{19}F$ Exchange Correlation Spectroscopy NMR (EXSY NMR).[59] The $^{19}F$ NMR signals for both of the intra- and extra-cellular populations of the trifluoroglucose anomers' $\alpha/\beta$-**78** were distinguishable. In the EXSY experiment, the intensity of the cross peaks formed from the retained polarisation from internal to external populations could be correlated to the transmembrane rate constant. It was found that this method generated rate constants that were similar to glucose itself.[60]

## 1.11 - Conformational effects of fluorine

### *1.11.1 - The gauche effect*

The incorporation of a carbon-fluorine bond into organic molecules can have an influence on molecular conformation. A well-documented case is the *gauche* effect in 1,2-difluoroethane **79** (Scheme 1.14). It has been shown that the *gauche* conformers are favoured over the *anti*-conformer by approximately 0.8 kcal mol$^{-1}$.[19]

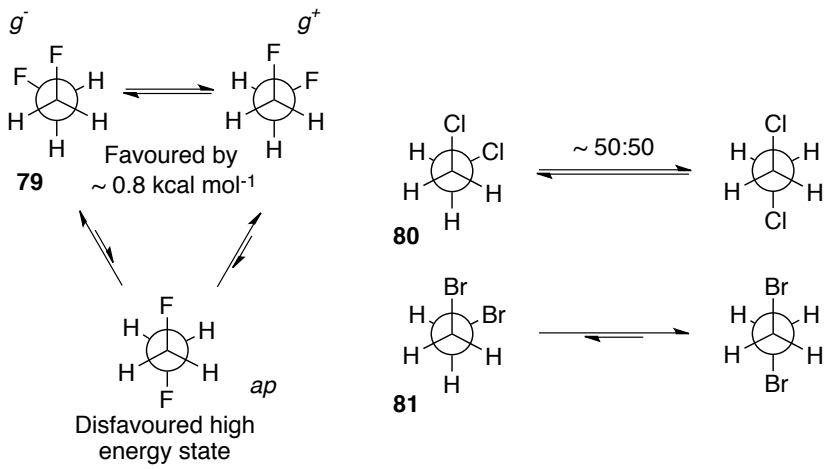


**Scheme 1.14**. The *gauche* effect in 1,2-dihaloethanes.

This is in contrast with 1,2-dichloroethane **80**, which does not show conformational preference and with 1,2-dibromoethane **81**, which has an *anti*-conformer preference. In the case of 1,2-difluoroethane **79**, the *gauche*-conformer is stabilised through hyperconjugative interactions (Figure 1.08).

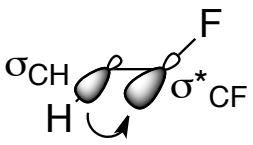


**79**

**Figure 1.08**. Hyperconjugation in 1,2-difluoroethane **79**.

This donation of electron density from the $\sigma_{CH}$ orbital antiperiplanar to the $\sigma^*_{CF}$ orbital stabilises the *gauche* conformer.[61,62] The $\sigma^*_{CF}$ orbital is low in energy and a good acceptor of electron density compared to the other halogens.[63] In the case of 1,2-difluoroethane **79**, there are two hyperconjugative interactions with both C–F bonds orientating antiperiplanar to C–H bonds. The *gauche* effect is also observed in 1,2-fluorohydrins and in other systems whereby the fluorine has a vicinal arrangement with various electron withdrawing groups.[64]

Stereoelectronic effects are important in the molecular preorganization of linear fluoroalkanes containing multiple contiguous vicinal fluorine atoms.[65] The synthesis of the all-*syn* tetra-, penta- and hexa-fluoroalkanes, **82**-**84**[67–69] respectively, results in a defined conformation arising from *gauche* effect contributions and most significantly 1,3-fluorine-fluorine repulsion of ~3.0 kcal mol$^{-1}$ (Figure 1.09).[66]

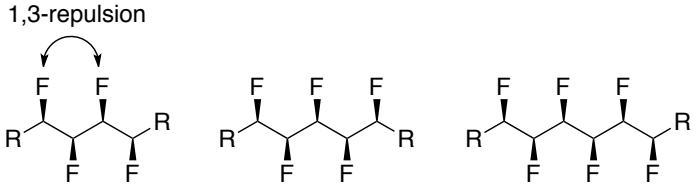


**82** **83** **84**

**Figure 1.09.** The all *syn*-vicinal fluorinated alkane motifs.

This is particularly striking in the hexa-fluoroalkane **84**, where a helical structure is observed in both the solid and solution states (Figure 1.10).[69]

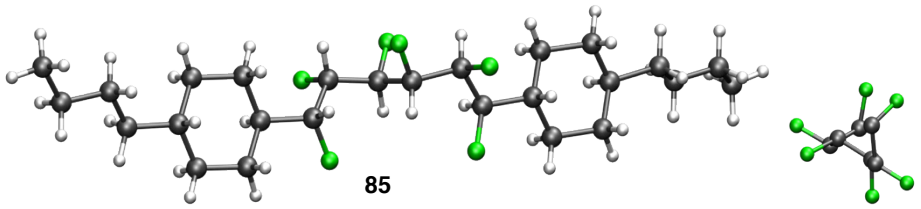


**Figure 1.10**. X-ray crystal structure of the all-*syn* hexa-fluoro alkane demonstrating the helicity induced by 1,3-fluorine-fluorine repulsions.

In a systematic study with various fluorohydrin stereoisomers **87-90** of the HIV-1 protease inhibitor Indinavir **85**, the *gauche* effect has been used to stabilise the preferred extended binding conformation (Figure 1.11).[70]

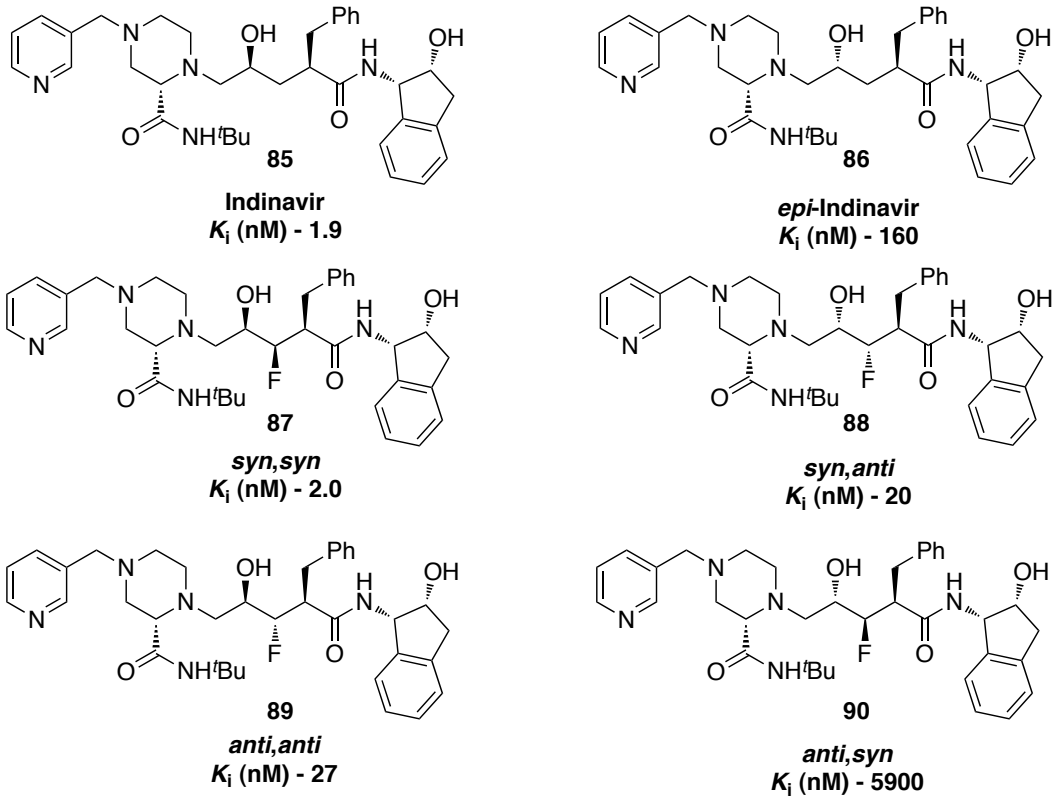


**Figure 1.11.** Fluorinated Indinavir **85** and *epi*-Indinavir **86** demonstrating a conformational preference for target specificity.

The optimal conformation is achieved in the *syn*,*syn* isomer **87**, which has the same efficacy as Indinavir **85**. This conformation is not accommodated in the *anti*,*anti* isomer **89**, which has a lower activity (10 fold decrease). There is a more significant effect in the fluorinated stereoisomers of the less active *epi*-Indinavir **86**. Interestingly the *syn*,*anti* isomer **88** reverses the loss in activity in **86** over **85** by 8 fold, whereas, the *anti*,*syn* **90** shows a dramatic decrease in activity into the millimolar range (Figure 1.11).[70]

### *1.11.2 - The α-fluoroamide effect*

α-Fluoro amides have a clear conformational preference as a result of the C–F bond dipole (1.85 Debye in fluoromethane).[71] In α-fluoro-amides there is a strong preference for the C–F bond to lie *antiperiplanar* to the dipole of the amide carbonyl (Scheme 1.15).[72–74] This is particularly striking for **91** and **92** where there is a stabilisation of 7.5 and 8.0 kcal mol$^{-1}$ respectively for the *anti* conformation.[72]

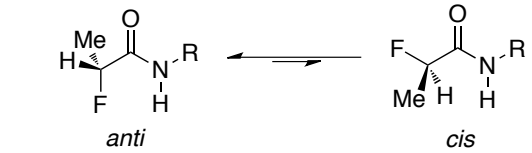


7.5 kcal mol$^{-1}$ - **91**, R = H
8.0 kcal mol$^{-1}$ - **92**, R = Me

**Scheme 1.15.** The α-fluoroamide effect with *anti*-preference relative to the amide carbonyl.

Molecular orbital (MO) calculations by O'Hagan *et al*., demonstrated this preference in *N*-methyl-2-fluoropropionamide.[72] The rotational energy profile for this system is shown in Figure 1.12. There is a clear energy well of ~8.0 kcal mol$^{-1}$ when the C–F bond and amide carbonyl are *anti* to each other.[72]

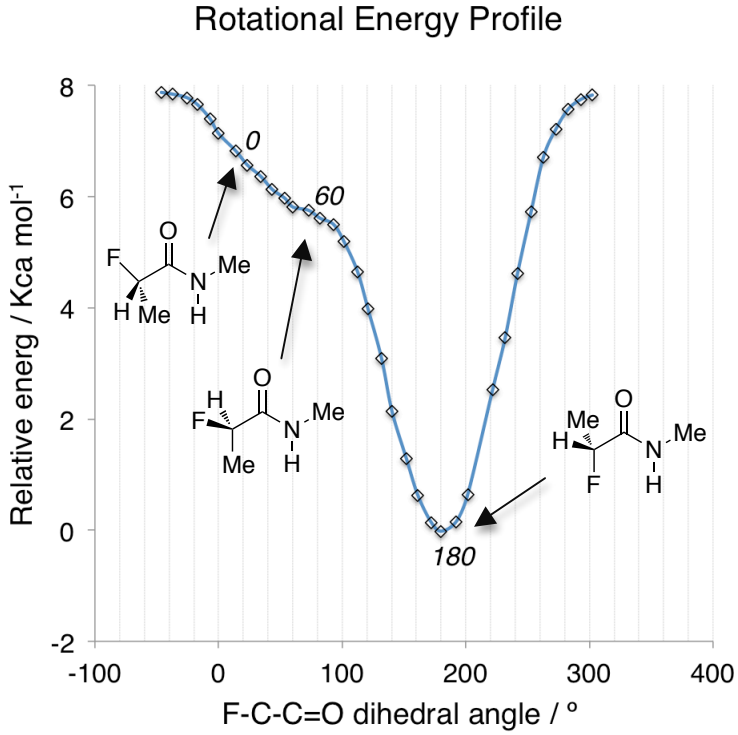


**Figure 1.12.** Rotational energy profile for α-fluoroacetamide **92** showing a conformational well for the *trans*- (*anti*) conformation.

This strong preference arises from at least three stabilizing factors: primarily the relaxation of the dipoles from the C–F and the C=O bonds, such that their combined vectors cancel (Figure 1.13, A); a favourable C–F···H-N electrostatic interaction (Figure 1.13, B); and finally, a stabilising orbital interaction between the amide $\pi^*_{C(O)N}$ orbital and the F $n_p$ orbital (Figure 1.13, C).[75]

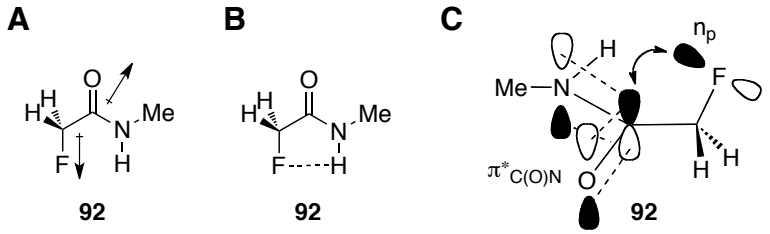


**Figure 1.13.** Stabilising factors for the *anti*-conformation in $\alpha$-fluoroamides.

A study of the *Cambridge Structural Database* (CSD) by Seebach *et al*., reveals that this conformational preference is reflected across a range of open chain compounds in the solid state with typical F–C–C–O dihedral angles of 147º<φ<190º (Figure 1.14).[76]

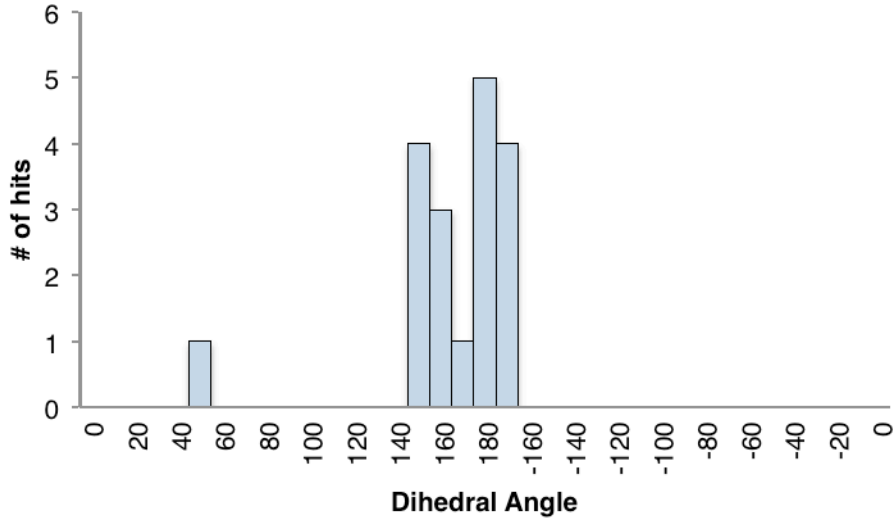


**Figure 1.14**. Dihedral angle prevalence in $\alpha$-fluoro amides.

The notable exception to this is the *synclinal* example with a dihedral angle ~50-60º. Seebach *et al*., also observed this deviation from the anticipated *antiperiplanar* orientation in a study of fluorinated *β*-amino acid conformational effects on peptide conformation.[76] They demonstrated through NMR analysis of the $^4J_{HF}$ coupling constants that the C–F bond orientates perpendicular to the amide plane in the tridecapeptide **93** if it can not adopt an *anti* orientation, thus destroying the helicity of the peptide (Figure 1.15, A).[77] In this example, it was reasoned that the global energy

minimum of the peptide was enough to 'override' the local stabilisation of the C–F bond, which was forced into its next favoured conformation (Figure 1.15, B). This energy preference is apparent in the rotational energy diagram (Figure 1.12) with a plateau around 60º.[72]

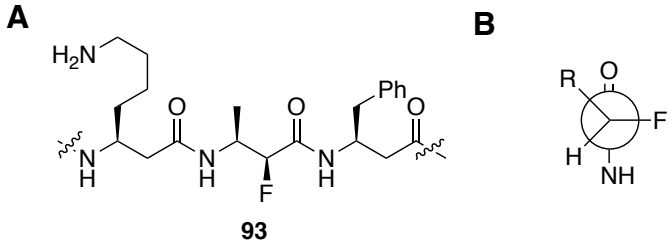


**93**

**Figure 1.15**. The fluorinated tridecapeptide has a favoured solution structure with the C–F bond orientating 90º relative to the carbonyl of the amide.

### *1.11.3 - The Charge-dipole effect*

If the C–F bond is located proximal to a positive charged species, a conformational preference arises resulting from a strong electrostatic interaction.[78] This favours a conformation that might otherwise be unfavourable. For example, in 2-fluoroethylammonium **94**, the C–F and C–$NH_3^+$ orientate preferentially in a *gauche* rather than an *anti* alignment (Scheme 1.16).

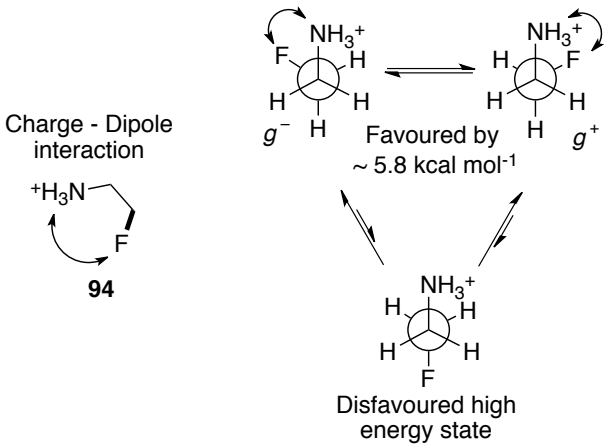


**Scheme 1.16.** Charge-dipole effect in 2-fluoroethylammonium **94**.

DFT calculations on 2-fluoroethylammonium **94** have demonstrated that the *gauche* conformation is preferred by about 5.8 kcal mol$^{-1}$ (Figure 1.16), thus, exerting significant stabilisation for that particular conformation.[78,79] This conformational preference is also observed for protonated alcohol **95** and the *N*-fluoroethylpyridinium ion **96** (Figure 1.16).

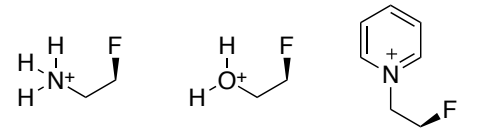


**94** 5.8 kcal mol$^{-1}$ **95** 7.2 kcal mol$^{-1}$ **96** 3.7 kcal mol$^{-1}$

**Figure 1.16**. Conformational preference as a result of the charge-dipole interaction.

In studies by Lankin and Synder[80] the charge-dipole effect was shown to result in a strong axial orientation of the C–F bond in 3-fluoropiperidinium rings **97-99**, where the stabilisation is ~5 kcal mol$^{-1}$. The axial preference was confirmed by NMR and DFT calculations, in addition to X-ray crystallographic analysis of selected compounds. The 3,5-difluoropiperidinium **100** also demonstrated an axial preference, clearly overcoming the repulsive 1,3-diaxial fluorine-fluorine interaction (Figure 1.17).

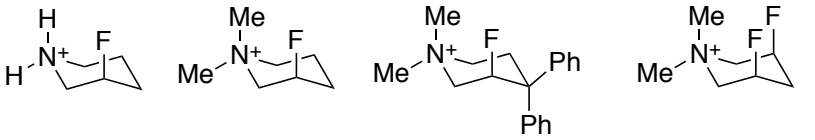


**97** 5.4 kcal mol$^{-1}$ **98** 4.0 kcal mol$^{-1}$ **99** 3.7 kcal mol$^{-1}$ **100** 8.9 kcal mol$^{-1}$

**Figure 1.17.** Charge-dipole effect in fluorinated piperidinium systems with their respective DFT (Becke3 LYP/6–311G(d,p)) calculated energies.

Following from these studies, Gooseman *et al*. demonstrated the charge-dipole effect in 4-and 5-membered rings, **101** and **102** respectively (Figure 1.18), which have no particular conformational preference in their non-fluorinated forms unlike six membered rings.[81,82]

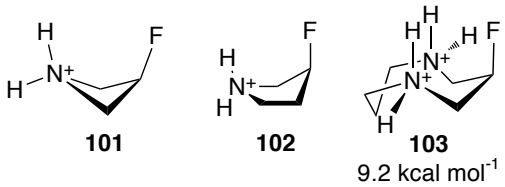


**Figure 1.18**. Charge-dipole effect in small and large fluorinated nitrogen containing heterocycles.

This was confirmed through DFT and X-ray crystallographic analysis, both of which are in strong agreement with that observed in six-membered rings. The effect in larger rings, such as **103** (Figure 1.18), was also found to favour the axial orientation of the C–F bond.[81] It follows that the incorporation of the C–F bond into protonated nitrogen heterocycles offers a way to influence the conformation in a non-covalent manner, which could have an application in drug discovery.

## 1.12 - Applications of the charge-dipole effect

### *1.12.1 - Organocatalysts*

The charge-dipole effect has been explored in both medicinal and organocatalytic arenas.[83] In a study by Gilmour *et al*.[84] an exocyclic C–F bond situated pendant to a pyrrolidine ring (**104**) was shown to induce stereocontrol in the epoxidation of *α,β*-unsaturated aldehydes such as **105a/b** (Scheme 1.17) with excellent enantiomeric control, up to 96% ee in **107b** with good to excellent diastereomeric excess.

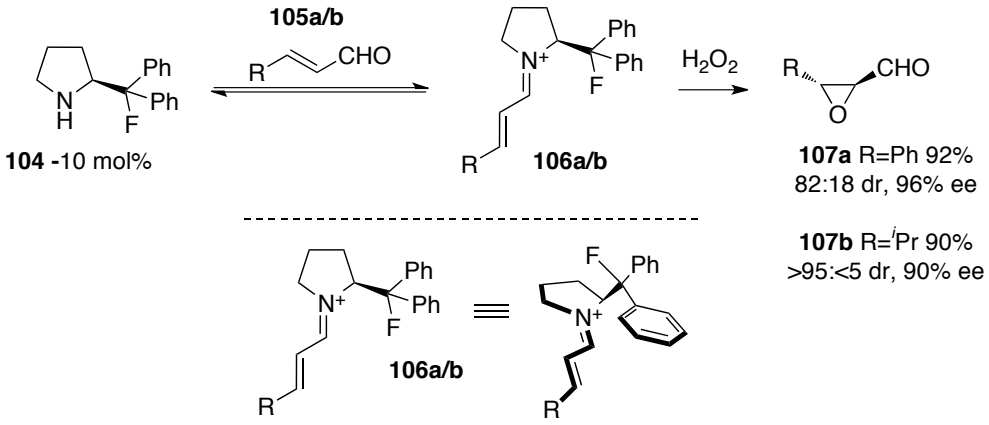


**Scheme 1.17.** Organocatalytic epoxidation of *α,β*-unsaturated aldehydes with the C–F charge-dipole effect driving enantiocontrol.

In this reaction, the intermediate C–F-iminium dihedral angle in **106** was shown to be 58º, thus directing the phenyl moiety to shield one face of the $\pi$-system (3.8/4.3 kcal mol$^{-1}$ *gauche* stabilisation for the *E*-/*Z*- geometry in **106a**/**b**). This therefore delivers the nucleophile to the opposite *Si*-face. The non-fluorinated catalyst **108** proceeds with 23% ee, albeit under different conditions (Scheme 1.18).[85]

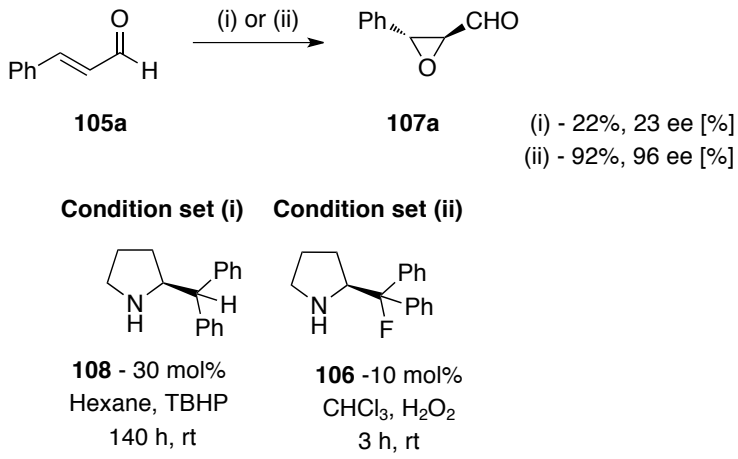


**Scheme 1.18.** Demonstration of the fluorine charge dipole effect and its application in organocatalysis.

### *1.12.2 - Biological exploitation of the C–F bond*

The charge-dipole effect has also been used to probe the molecular binding conformation of GABA **109** to $GABA_{A/C}$ receptors and GABA metabolising enzymes (Figure 1.19).

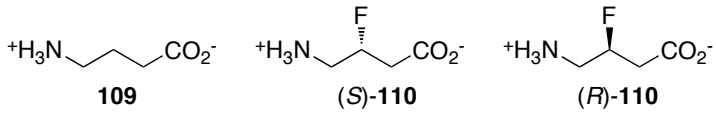


**Figure 1.19.** Fluoro-GABA analogues.

Deniau *et al*. demonstrated that GABA transaminase could discriminate between (*R*)-and (*S*)-3-fluoroGABA **110**.[86] The preferred transaminase binding conformation is readily adopted by (*S*)-**110**, however, this conformation is unfavoured in (*R*)-**110** (Figure 1.20, A).[86] Both (*R*)- and (*S*)-**110** exhibited a similar efficacy for the $GABA_A$ receptor[87] (Figure 1.20, B), however (*R*)-**110** was more active at the $GABA_C$ receptor (Figure 1.20, C).[88]

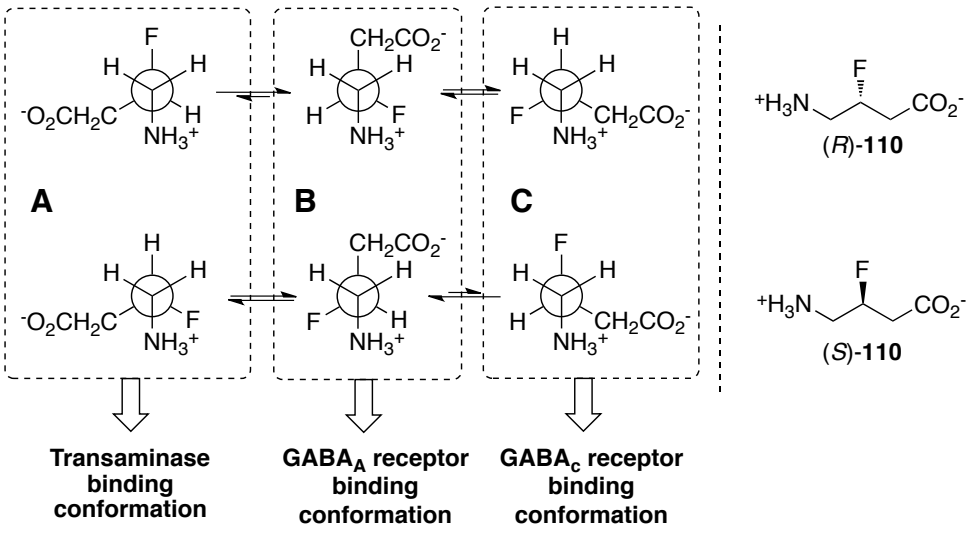


**Figure 1.20.** Preferred binding conformations of the fluorinated GABA analogues **110** to the $GABA_A$ receptor and GABA transaminase.

The charge-dipole effect governs these conformations leading to the observed activities. These studies demonstrate that the fluorine charge-dipole effect is significant in a biological context and can offer information on the favoured binding mode of small molecules to large proteins (Figure 1.21).

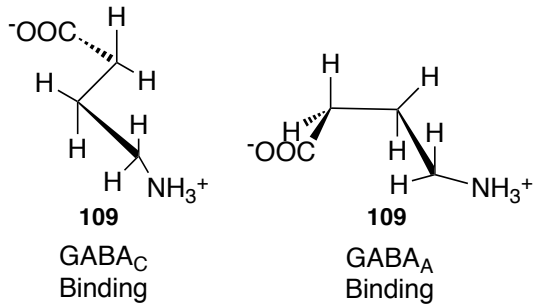


**Figure 1.21.** Binding conformation to $GABA_{A/C}$ receptors of GABA based on fluorinated probes.

It also demonstrated the applicability of this approach in the development of probes to study binding conformations of bioactives in complex molecular environments; thus providing information for the development of new inhibitors to target these receptors.[89]

In a comprehensive study by Hunter *et al*., the $\alpha$-fluoro amide, charge-dipole and fluorine-fluorine *gauche* effects were collectively considered for a conformational study on $\alpha,\beta$-difluoro-γ-amino amides **111** and **112** (Figure 1.22).[90]

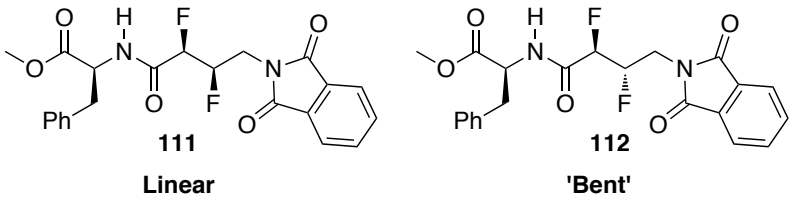


**Figure 1.22.** Conformational differences between *syn*- and *anti*-isomers of the $\alpha,\beta$-difluoro-γ-amino amides **111** and **112**.

In this study, it was possible to demonstrate through NMR solution studies and by X-ray crystallography that both **111** and **112** exhibited an *antiperiplanar* orientation of the C–F bond relative to the amide carbonyl and that the vicinal C–F bonds are *gauche* to each other. The $\beta$-C–F and γ-C–N bonds are also *gauche* in the solid and solution state. The accumulative effect of these interactions results in two distinct and predictable conformations for **111** and **112**.[90] From these compounds, the vicinally 2,3-difluorinated GABA analogues **113-116** were prepared and assessed for their respective activity on $GABA_C$ receptors.[91] It was found that the *syn*-isomers exhibited potent activity over the *anti*-isomers (Figure 1.23).

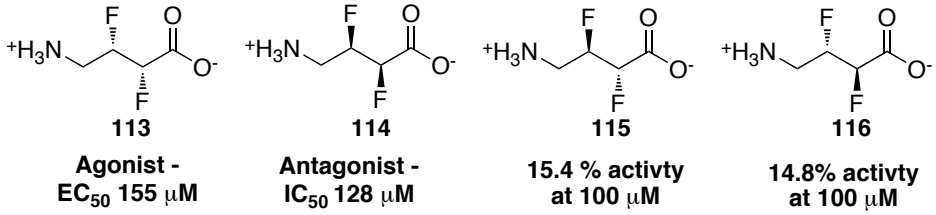


**Figure 1.23.** The four stereoisomers of 2,3-difluorinated GABA analogues and their activity for the $GABA_C$ receptors.

In the *syn*-isomer series, **113** acts as an agonist, whereas **114** was an antagonist. Molecular docking studies of the energy-minimised structures of **113** demonstrate it could adopt the correct binding conformation to accommodate the key contacts important for $GABA_C$ binding, thus supporting its agonist response. Docking of **114** also demonstrated the ability of the carboxylate and amine groups to orientate in the correct manner, however, this also highlighted additional steric interactions with the

receptor that may explain its antagonist activity. The predicted conformation of **113** corresponds with the binding conformation proposed earlier for GABA **109** (Figure 1.21) to the $GABA_C$ receptor. Interestingly **113** and **114** did not exhibit any $GABA_A$ activity whereas **115** and **116** did.[91]

From these studies, it is clear that the charge-dipole and other conformational effects can be used to influence the conformation of otherwise flexible organic molecules. This predictable preorganization has enabled detailed studies on the binding of GABA to its receptors. It is envisaged that this information will enable a better understanding of how to design tailored inhibitors for these receptors.

## 1.13 - Synthesis of fluorinated *β*-amino acids

### *1.13.1 - General methods*

The most common way of incorporating a fluorine substituent into an amino acid involves deoxyfluorination reactions with DAST **32**. Takei *et al*., have employed DAST **32** in the synthesis of *α*-fluoro-*β*[2,3]-homophenylalanine **118** in studies exploring the inhibition of chromotrypsin (Scheme 1.19, A).[92]

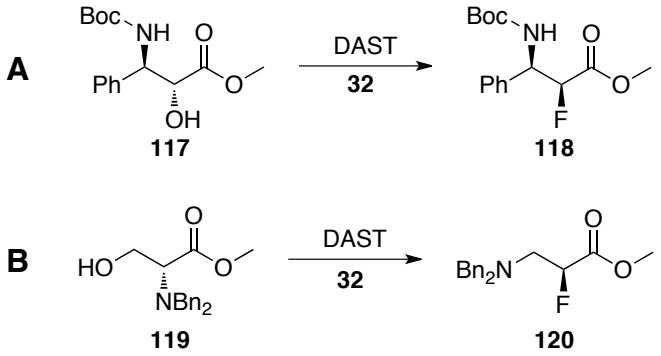


**Scheme 1.19.** The application of DAST **32** to the synthesis of *α*-fluorinated-*β*-amino acids.

DAST **32** was first used in this context in a synthesis of benzyl protected *α*-fluoro-*β*-alanine **120** by Shomek (Scheme 1.19, B).[93] This method has been widely used by Seebach *et al.* for studies on the influence of *α*-fluorinated-*β*-amino acids on *β*-amino peptide structures and exploring their metabolic stability.[94] In example B (Figure 1.19), the fluorination proceeds through an aziridinium intermediate, a mechanism, which will be discussed in more detail in Chapter 4.[95]

These methods rely on stereospecific reactions manipulating the existing stereochemistry of the starting material. Other methods have used stereoselective fluorination reactions to generate new stereogenic centers with fluorine. This approach is discussed in sections 1.13.2 and 1.13.3.

### *1.13.2 - Evans oxazolidine approach*

In 2008, Abell *et al*. demonstrated an Evans oxazolidinone based strategy for the construction of mono-fluorinated $\beta^{2,2}$-amino acids bearing a quaternary stereogenic center (Scheme 1.20).[96] In this approach they were able to fluorinate the oxazolidine derivative of cyclohexyl and phenyl propanoic acids, **120a/b** respectively, by deprotonation and treatment with *N*-fluorobenzenesulfonamide. This gave **121a/b** in high diastereomeric excess and in good yield (>90% de, 79%).

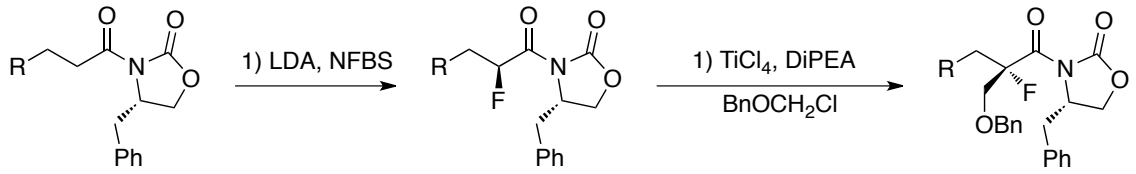


**120a** - R = Ph
**120b** - R = $C_6H_{12}$

**121a** - 79%, 12:1 dr
**121b** - 75%, 12:1 dr

**122a** - 70%
**122b** - 69%

**Scheme 1.20.** Evans auxiliary approach to the synthesis of mono-fluorinated quaternary centers

The alkylation of **121a/b** was achieved with benzyl chloromethyl ether in the presence of base and $TiCl_4$ (Scheme 1.20). Further transformations with **122** enabled the synthesis of **124a/b** in >95% diastereomeric excess (Scheme 1.21). This was the first synthesis of a mono-fluorinated $\beta^{2,2}$ substituted amino acid and offered a versatile approach to the synthesis of diverse fluorinated amino acids (Scheme 1.21).

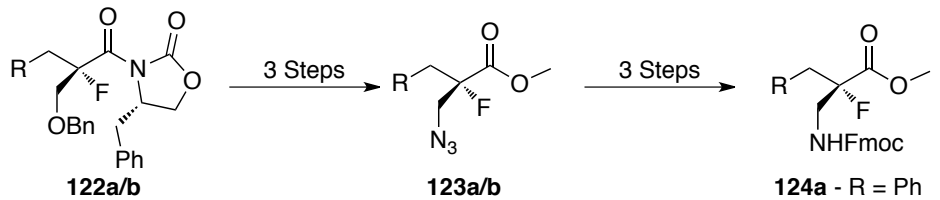


**122a/b**

**123a/b**

**124a** - R = Ph
**124b** - R = $C_6H_{12}$

**Scheme 1.21.** Functionalisation of the fluorinated Evans auxiliaries **122a/b** mono-fluorinated $\beta^{2,2}$ amino acids.

### *1.13.3 - Davies' lithium amide approach*

In a modification of the Davies'[97] diastereoselective addition of lithium amides **126** to $\alpha,\beta$-unsaturated esters **125**, Duggan and co-workers have demonstrated that quenching the intermediate enolates **127** with NFSI **5** results in the isolation of $\alpha$-fluorinated $\beta^{2,3}$-amino acids **128** with high diastereoselectivity (Scheme 1.22).[98]

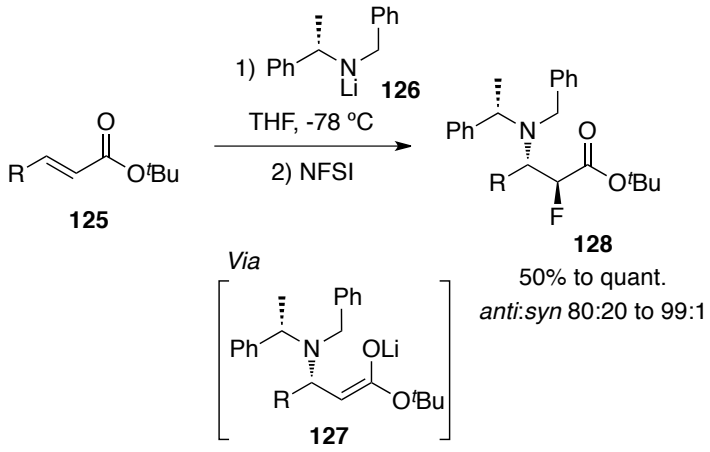


**Scheme 1.22.** Chiral lithium amide addition to $\alpha,\beta$-unsaturated esters in the tandem approach to $\alpha$-fluorinated $\beta^{2,3}$ amino acids. R = alkyl, aryl.

Various $\alpha,\beta$-unsaturated esters **125** could be employed with the chiral lithium amide **126** to provide synthetically useful $\beta$-amino acids **128** through this tandem approach. In a proof of concept study, a stepwise addition-fluorination protocol *via* **129a/b** demonstrated that the isolated $\beta$-amino acids **128a/b** were of low diastereomeric excess (Figure 1.23). Thus, demonstrating the power of their tandem approach (Figure 1.22).

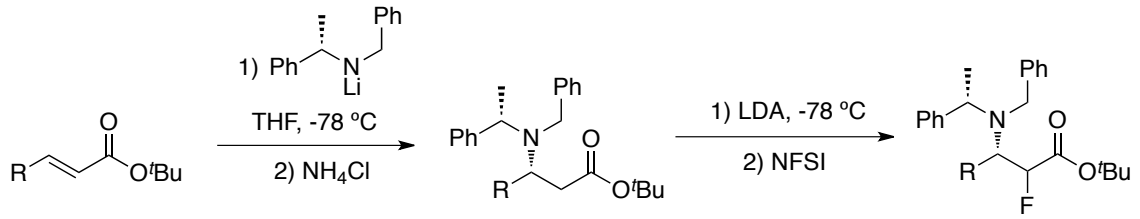


**125a** (R = Ph) **129a** **128a'** - quant, *anti*:*syn* = 61:39
**125b** (R = TBDMSO$(CH_2)_2$) **129b** **128b'** - 93% *anti*:*syn* = 72:28

**Scheme 1.23.** Stepwise approach with poor diastereomeric control of the fluorination step.

Using the tandem approach, the orthogonally protected $\alpha$-fluoro-$\beta^{2,3}$-lysine derivative **130** starting from **128c** was synthesised (Scheme 1.24).

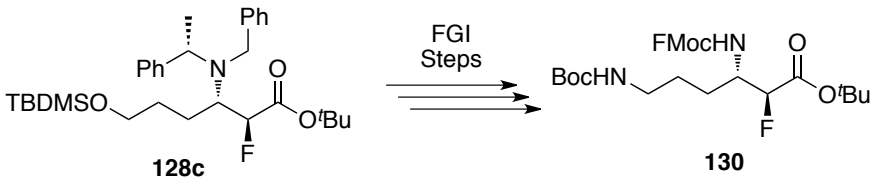


**Scheme 1.24.** Further functionalisation through to an orthogonally protected $\alpha$-fluoro-$\beta^{2,3}$-lysine for synthesis applications.

This method offers a route for generating an array of structurally diverse fluorinated $\beta$-amino acids for the incorporation into medicinally relevant compounds or for the use as chemical probes.

The synthesis of fluorinated amino acids has received a significant level of attention as indicated by the number of reviews and publications in the field.[99] Structural and biological applications of the conformational influence of the C–F bond continue to appear, and the role of the C–F bond in this context may become more widely recognised.

## 1.14 - Conclusion

It is clear, from the discussion in this chapter, that the strategic incorporation of a C–F bond into an organic molecule can result in a conformational bias. This has enabled the elucidation of binding modes of small molecules to enzymes and large receptors.

The following chapter will address the development of quadruplex DNA stabilizing ligands and will offer a biological context for investigating the conformational influence of the C–F bond in a drug-DNA complex.

# Chapter 2

# Telomeres, telomerase and quadruplex DNA

## 2.1 - The 2009 Nobel prize to telomeres

In 2009, the Nobel Prize for Medicine was awarded to Elizabeth H. Blackburn, Carol W. Greider and Jack W. Szostak for their contributions towards our understanding of the telomere and telomerase.[100] Their contributions have budded what is now a very active research area. Blackburn and Szostak were first to demonstrate that the telomeric sequence was conserved across a range of distantly related organisms and that it was fundamental in cell biology.[101] Following this, Blackburn and Greider provided evidence for the enzyme telomerase (Christmas Day 1984), which is responsible for elongation of the telomere.[102] They later demonstrated that telomerase required an RNA component to be catalytically active.[103] These discoveries underpin many of the biochemical and genetic studies focused around the telomeres and its role in cancer, ageing, and inheritable diseases, amongst many others. The following will provide a general review of the telomere and inhibitors of telomerase.

## 2.2 - Telomeres and telomerase

One of the major limitations of replication in eukaryotic cells is for the replication machinery to completely copy to the 3' end of DNA. This is known as the end replication problem.[104] Thus, with each round of replication, a short section of DNA is cleaved from the chromosome. DNA sequences coded at the end of chromosomes are not faithfully copied and this jeopardises genomic stability following each round of cell division. To guard against this, chromosomes have a protective ending known as the telomere (Scheme 2.01).

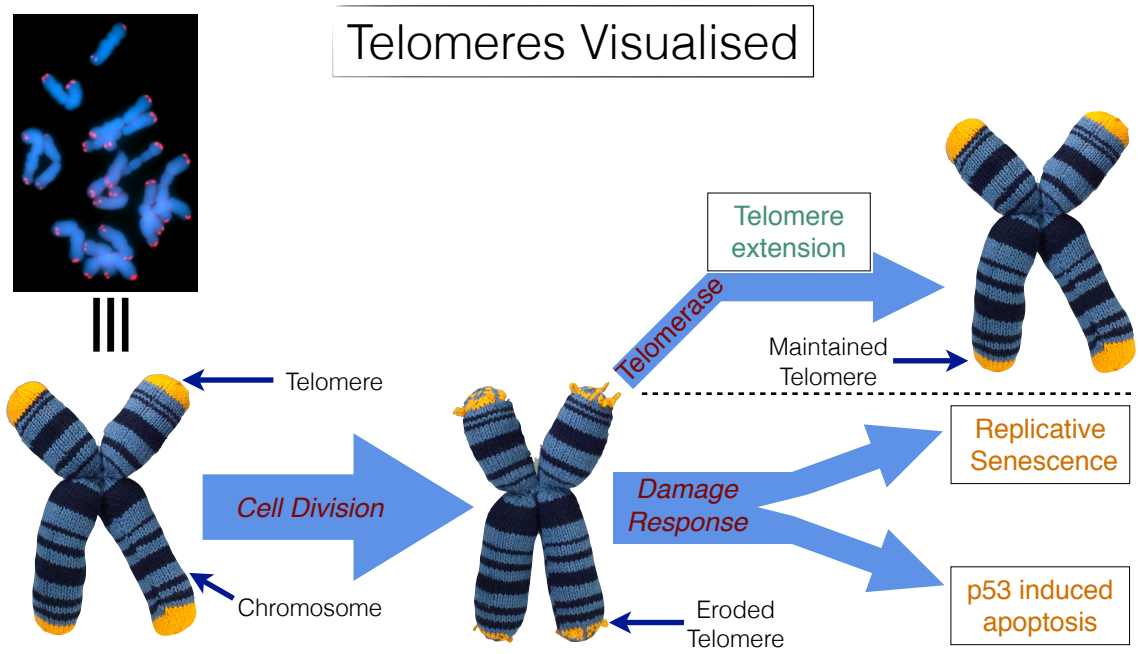


**Scheme 2.01.** Generalised scheme for telomere erosion and elongation at the chromosome end. Knitted chromosomes copyright Science Museum/Science and Society Picture Library 2012.

The telomere is a non-coding sequence of DNA consisting of tandem hexanucleotide repeats dTTAGGG, with an approximate length of 5-8 kilobase pairs.[105] Therefore, each round of cell division results in the loss of approximately 50-200 bases from this non-coding DNA.[106] The cell will replicate until the length of the telomere reaches a critical length, its Hayflick limit,[107] before entering a state of replicative senescence ($G_0$ state), which then initiates p53-mediated cell death.[108] Therefore, the average telomeric length in a colony of cells will decrease over time until it reaches its Hayflick length, unless the cells are replenished by their respective stem cell, which generally have longer, maintained telomeric DNA lengths.

The telomeres in stem and germ-line cells are maintained by an RNA-dependent DNA polymerase.[102,109] This reverse transcriptase adds the TTAGGG nucleotides to the 3' end of the telomere following each round of cell division. The RNA component (hTR) is critical for activity and anneals the 3' end of the telomere,[110,111] templating it into the active site of the catalytic subunit, hTERT. The hTR component is found expressed in somatic cells, however hTERT expression is silenced through various transcriptional regulators,[106] thus somatic cells contain no constitutively active telomerase.[112–114] Both hTR and hTERT components are expressed in stem and germ-line cells, thus active telomerase can maintain the telomeric length in these cells.[113]

## 2.3 - Telomerase and cancer

The nature of the telomere in somatic cells, with its critical length, raises a question around its role in cancer. Cancer cells typically replicate without control and so it would be natural to assume that the average telomeric DNA length in cancer is critically low. However, this is not observed and the telomere lengths in cancers are maintained. This telomeric maintenance can be attributed to the loss of the transcriptional control of hTERT, with 85% of cancers expressing this catalytic domain.[115,116] With both hTR and hTERT found in cancer cells, an active telomerase maintains the telomere length and these cells subsequently avoid activation of cell death pathways. Targeting the action of telomerase offers a unique method of cancer therapy with the bulk of non-cancerous cells not affected by this approach.[108]

Even though the telomere is a section of non-coding DNA, its maintenance and function is controlled by a multitude of protein interactions.[117] The majority of the telomere adheres to normal topological parameters of duplex DNA, with the exception of approximately 200 nucleobases at the 3' end.[118–120] These nucleobases form a single stranded overhang and it is this section of the telomere where the most interesting biological interactions occur and structures form.

## 2.4 - Shelterin complex at the telomere

Single-stranded DNA (ssDNA) in other regions of the genome are quickly recognised as damaged by the cell.[121–123] Detection of ssDNA results in the activation of repair mechanisms or causes the cell to activate apoptotic pathways. To circumvent this for the telomere, there are various proteins that interact with the 3' single stranded overhang and protect it.[117,124] These core protective proteins form the complex known as *shelterin* and specifically bind the TTAGGG repeat of the telomere. *Shelterin* is comprised of eight core protein units, TRF1/2, TIN2, TPP1 and POT1 (Figure 2.01), with five domains available to recognize the telomeric DNA sequence, making it highly specific for telomeric DNA. Knockout studies of the *shelterin* component POT1, resulted in cell-cycle arrest and chromosomal end-to-end fusion as a direct result of *shelterin* complex disruption.[125] For telomerase to elongate the telomere following cell division,

the telomere must be linear and free of any tertiary structure to enable the association of the catalytic and recognition domains of telomerase.[126]

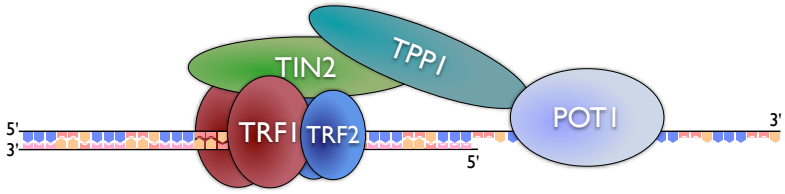


**Figure 2.01**. A simplified representation of *shelterin* proteins associating with telomeric DNA.

## 2.5 - Self-assembly of guanosine

In the 1960's, it was established that solutions of guanosine-5'-monophosphate (5'-GMP) base **131** formed gel-like solutions upon standing (Scheme 2.02).[127] These gel solutions resulted from the formation of square planar quartets of hydrogen-bonded ionophores, which rapidly formed in the presence of monovalent cations.

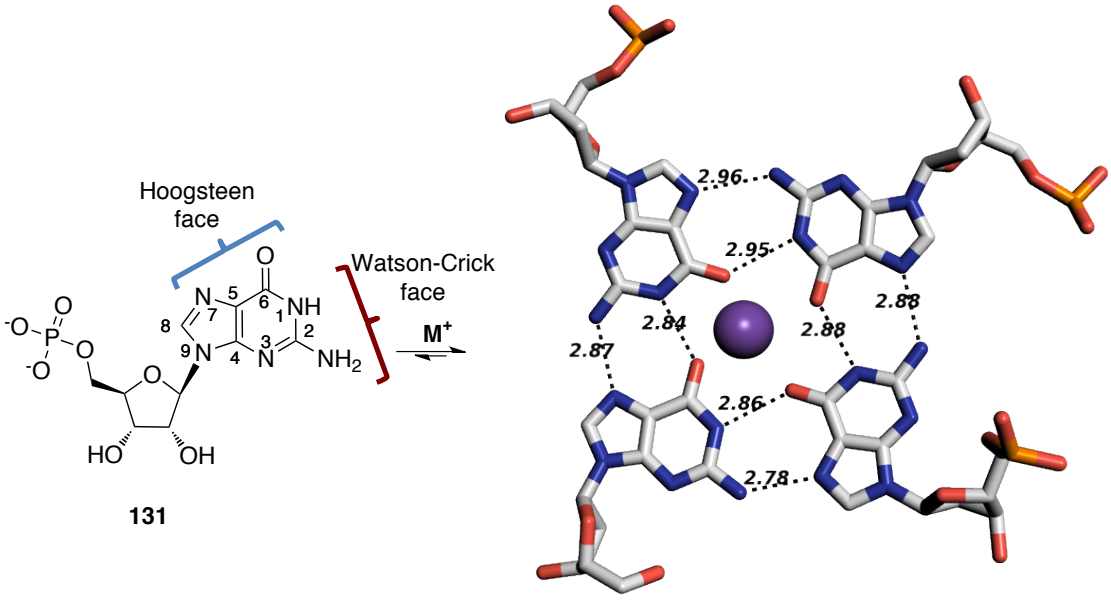


**Scheme 2.02.** The self-assembly of guanosine nucleotides **131** into quartet structures in the presence of mono-valent counter ions. Quartet representation extracted from PDB 1I1H (Ref.-128) with the image created using PyMol.[129] Distances are in Å.

These monovalent cations, primarily $Na^+$ and $K^+$, increase the stability of G-quartets by favourable electrostatic interactions with the $O^6$ atoms of each base. 5'-GMP **131** can form four hydrogen bonds per base by utilizing its Hoogsteen edge along with the

typical Watson-Crick edge as shown in **131** (Scheme 2.02). The hydrogen bond acceptors $N^7$ and $O^6$ on the Hoogsteen edge form hydrogen bonds with the hydrogen bond donors, $N^1$ and $N^2$, on the Watson-Crick edge. Therefore, four individual 5'-GMP **131** nucleotides can form a G-quartet with eight hydrogen bonds in total. [130]

Multiple G-quartets can self-assemble into a G-quadruplex structure through favourable $\pi$-$\pi$ stacking interactions and stabilisation brought about by a bipyramidal antiprismatic bound cation, primarily $K^+$.[131] A further thermodynamic driving force for this assembly is found from the displacement of water that forms unfavourable interactions with each G-quartet. G-quadruplex self-assembly motifs can be between 8 to 30 nm long with each G-quartet rotated round the central axis (Figure 2.02).[132–134]

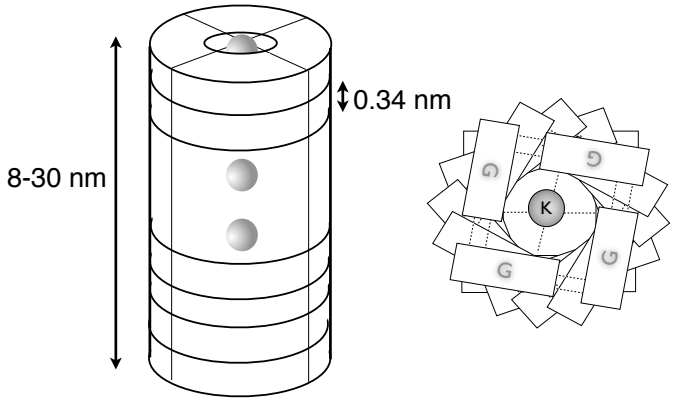


**Figure 2.02.** Representation of guanine tetrads stacking to form a self-assembled G-quadruplex.

## 2.6 - Quadruplex DNA folding and topology

It is likely that guanine-rich telomeric sequences in the human genome will form quadruplexes *in vivo*.[135-137] There are two main types of quadruplex structures that can form with guanine-rich sequences, intramolecular (unimolecular) and intermolecular (bimolecular) forms. Sequences of the type Go·Xp·Go form intermolecular structures and Xn·Go·Xp·Go·Xp·Go·Xp·Go·Xn form intramolecular folds (where Xn is any number non-guanine nucleotide, Go is any number of guanine nucleotides and Xp is any number non-guanine nucleotides involved in loop formation).[135] The topology that one sequence may form over another is firstly governed by the linking nucleotide length and by the presence of different monovalent cations. [138] Go·Xp·Go sequences, such as the *Oxytricha nova* telomeric sequence, $G_4T_4G_4$, will form bimolecular quadruplexes

where two sequences associate to form the quadruplex structure (Figure 2.03). In these structures, Xp will orientate relative to the guanine nucleotides to accommodate their assembly into a quadruplex (Figure 2.03).

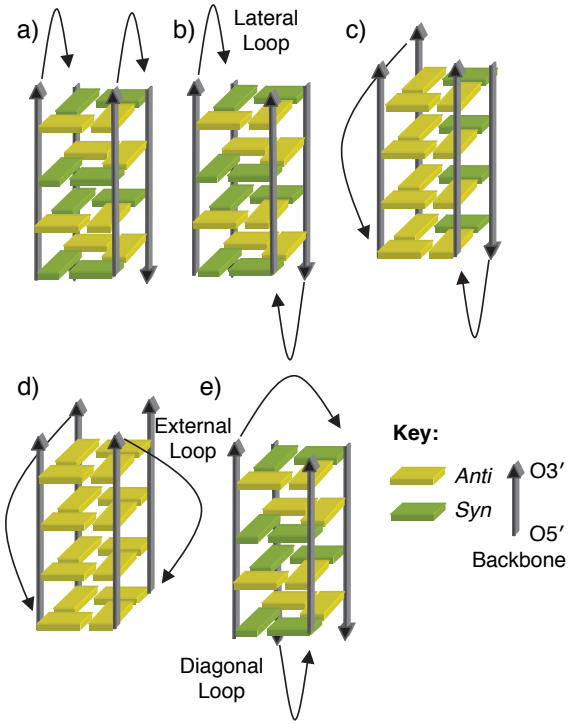


**Figure 2.03.** Arrangement of guanines and linking nucleotides in bimolecular quadruplexes.[139]

The Xp nucleotides can either form external, diagonal or lateral links relative to the quadruplex core, which can result in many complex and diverse quadruplex structures.[130,140] In addition to this, the glycosidic bond in the DNA monomers will also reverse from the favoured *anti* to *syn* bond angle, in an attempt to accommodate the formation of hydrogen bonded quartets.[138] In the *O. nova* sequence, $G_4T_4G_4$, the thymine linking nucleotides associate in a diagonal manner (Figure 2.03, e) relative to the guanine nucleotides (Figure 2.04).[141–143]

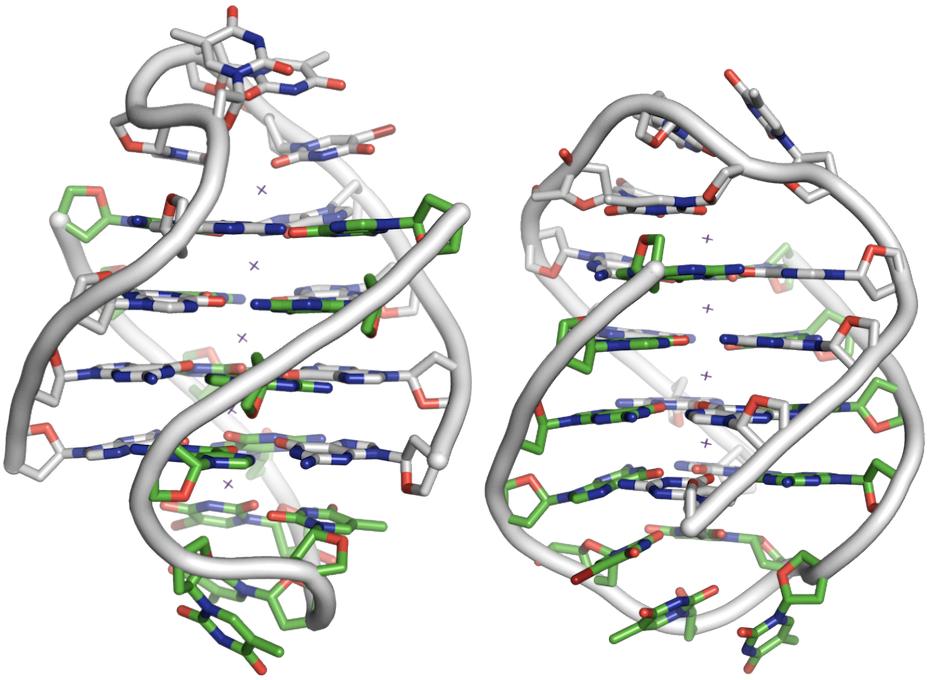

**Figure 2.04.** Crystal structure of the *O. nova* $G_4T_4G_4$ bimolecular quadruplex with two aspect views. Image created with PyMOL[129] using PDB file 1JPQ.[141]

However, the mutant *O. nova* sequence, $G_3T_4G_4$ forms a mismatched quadruplex, which results in a distinct fold compared to $G_4T_4G_4$, with the thymine nucleotides associating in a lateral and diagonal manner.[144] A small sequence change can result in a significant structural modification, highlighting the complexity of quadruplex folds in the solid state, and clearly the dynamics in solution. A further example of this structural complexity is exemplified by reducing the number of nucleotides available for cross-linking. For example, the $G_4T_3G_4$ sequence forms a bimolecular structure with lateral thymine linkages.[145] In this case, two quadruplex structures in the unit cell are observed with both the head-to-head (Figure 2.03, a) and head-to-tail (Figure 2.03, b) quadruplexes formed (Figure 2.05).

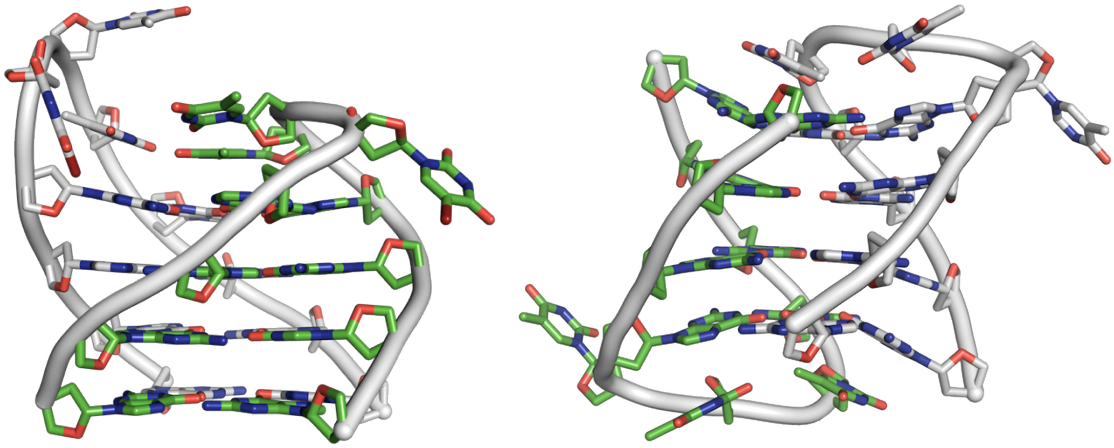

**Figure 2.05.** The two quadruplex DNA structures formed from the $G_4T_3G_4$ sequence. Images created with PDB codes 2AVH & 2AVJ respectively using the PyMOL package.[129]

Unimolecular quadruplexes also form different topological structures (Figure 2.06).[138] Such unimolecular quadruplexes are biologically relevant and are likely to form *in vivo* at the ssDNA ends of the telomere, in addition to regions throughout the genome that have a high guanine content.[146]

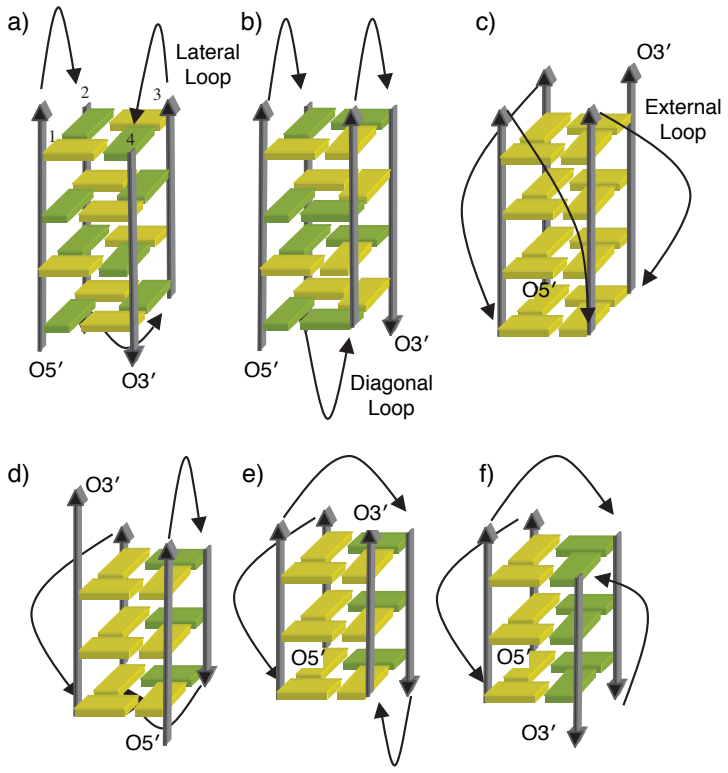


**Figure 2.06.** Arrangement of guanines and linking nucleotides in unimolecular quadruplexes.[139]

In addition to the various ways that the linking polynucleotides can arrange relative to the guanine core, there is also a structural effect from the presence of different monovalent cations.[147] For example, $Na^+$ ion coordinates within the plane of the G-quartet while the larger $K^+$ ion coordinates offset between two G-quartets. As a result, as shown by solution NMR (Figure 2.07, A)[148] and X-ray[149] crystallographic studies (Figure 2.07, B), structures for the human telomeric sequence $d(TG_3(T_2AG_3)_3)$ adopt very distinct folds. In the $Na^+$ NMR structure the $T_2A$ linking nucleotides associate in a lateral and diagonal fashion relative to the guanine tetrads (Figure 2.07, A). In contrast, the linking nucleotides assemble in a diagonal manner (Figure 2.06, C) in the crystal structure with $K^+$, resulting in a distinctive propeller like structure (Figure 2.07, B).

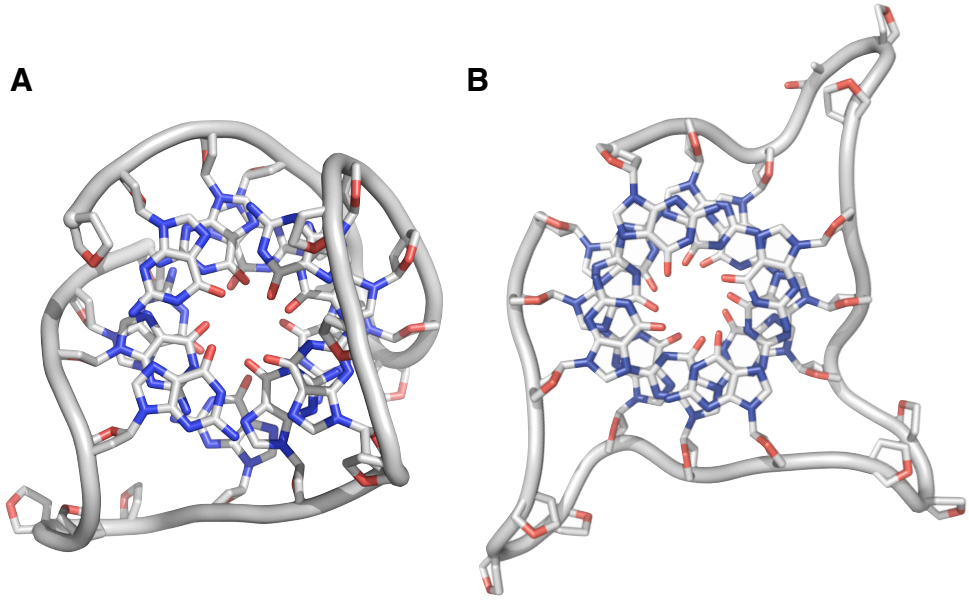


**Figure 2.07**. Unimolecular quadruplex DNA with different counterions **A** – $d[AG_3(T_2AG_3)_3]$ sequence with $Na^+$ counter ion & **B** – with $K^+$ counter ion. Images created from PDB codes 143D (Ref.-148) and 1KF1 (Ref.-149) with PyMol.[129]

Structural studies of the human telomeric DNA sequences are starting to provide a strong foundation in the understanding of how quadruplex DNA topologies arise. This information is important for the rational design of drugs that may interact with these sequences.[140]

## 2.7 - Telomerase inhibition

Zahler and co-workers observed that increasing the $K^+$ concentration induced an inhibitory effect on telomerase action *in vivo*.[150] They concluded that the increased [$K^+$] stabilises quadruplex folds *in vivo* and *in vitro*, and that this may act as a negative feedback mechanism for the maintenance of telomere length. This inhibition of telomerase can be attributed to the disruption of the association between the telomere and telomerase, with the interaction critically dependent on the 3' ssDNA overhang being free and linear. This free topology is required such that the hTERT RNA subunit can anneal with the telomere, thus stable quadruplex DNA structures will inhibit the action of telomerase as they will not uncoil.[151]

## 2.8 - Assessing telomerase inhibition and quadruplex stability

The development of quadruplex DNA stabilising ligands has called for the development of standardised techniques to assess their action *in vitro* and *in vivo*. The following section is a brief overview of the current techniques used.[152]

Circularly polarised light spectroscopy is used to assess the topological arrangement of guanine-rich sequences. Circular dichroism (CD) is a powerful tool to probe and monitor structural changes of quadruplex DNA upon altering the nature and concentration of counter ions.[153,154] CD can also be used to monitor structural changes upon binding of drugs that interact with quadruplex DNA.[152] Other spectroscopic techniques such as NMR[155,156] and X-ray crystallography[157] play significant roles in the structural evaluation of how quadruplex stabilising ligands bind to quadruplex DNA. These techniques taken together provide information on the interactions between drugs and quadruplex DNA and can be used for the systematic development and rational design of new agents.

Fluorescence resonance energy transfer (FRET) assays are used to quantify the level of stabilisation that specific ligands provide to the quadruplex folds.[158] For this technique, modified quadruplex DNA sequences are attached with fluorescent donor and acceptor chromophores at the 3' and 5' ends (Scheme 2.03). Commonly used chromophores are 6-carboxyfluorescein **132** (FAM) and 6-carboxytetramethyl rhodamine **133** (TAMRA) (Scheme 2.03). When the donor and acceptor are in close contact, such as when the quadruplex is folded, the excitation of the donor ligand results in FRET transfer to the acceptor which results in emission of a different wavelength (Scheme 2.03).[159] An increase in temperature will unfold the quadruplex structure to its linear form, thus increasing the distance between the two chromophores, resulting in poor energy transfer with subsequent fluorescence decrease. The addition of a stabilising ligand will cause an increase in the melting temperature of the quadruplex DNA, and the increased stabilisation of the fold results in a higher melting temperature.

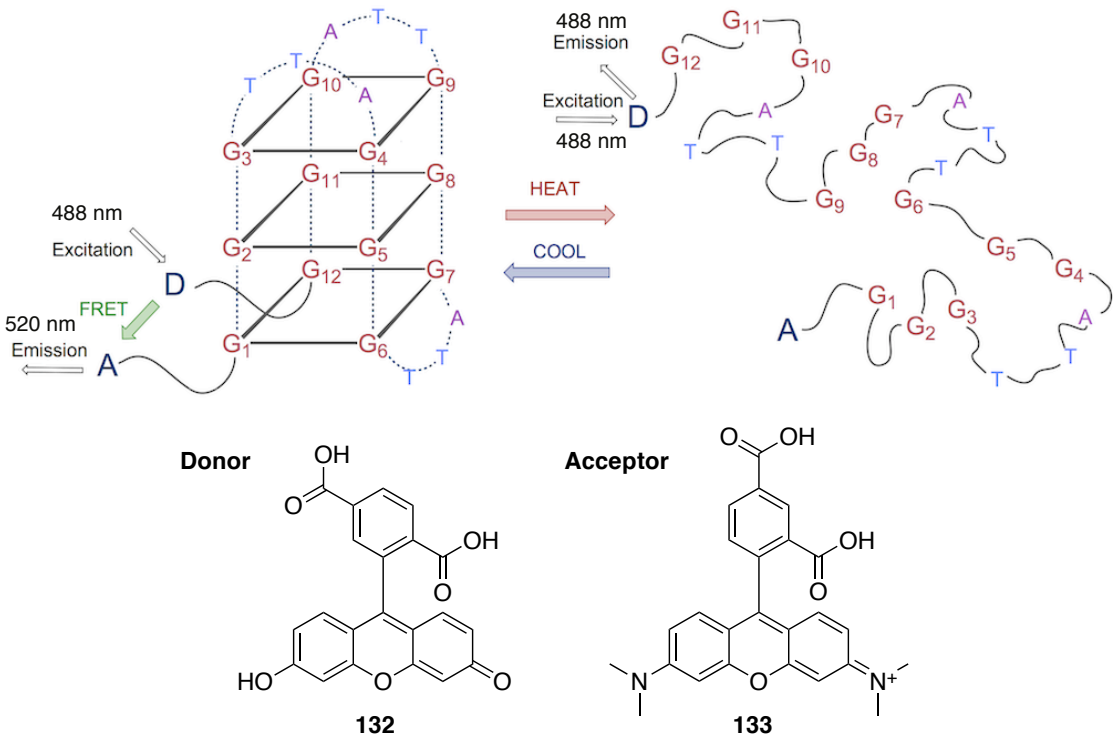


**Scheme 2.03.** General overview of FRET-based analysis of quadruplex stability.

Telomerase inhibition assays provide specific values for the inhibition of telomerase activity *in vitro*. The protocol for this is known as TRAP - Telomeric repeat amplification protocol.[160] The use of a fluorescent primer for the telomerase enzyme enables the evaluation of telomerase inhibition by quadruplex-stabilising drugs. This is

a widely employed protocol in the literature providing $^{tel}IC_{50}$/$^{tel}EC_{50}$ values for a range of ligands.

Good experimental correlation between the FRET and the TRAP assays are observed and generally a higher melting temperature results in better inhibition of the telomerase enzyme. However, a direct correlation and prediction of one value based on the other cannot easily be made.

## 2.9 - Quadruplex DNA stabilising ligands

Various quadruplex DNA stabilising ligands have been identified.[106,161] These include natural products along with various other motifs arising from structure based design strategies.[140,161] A concurrent theme arises with these stabilising ligands, as many are based on a large polyaromatic core with various peripheral cationic side chain substituents. These side chain substituents often interact with the negatively charged phosphate grooves and polynucleotide linkages, while the flat polyaromatic cores capitalise on favourable $\pi$-$\pi$ stacking with a free G-tetrad at the end of the quadruplex DNA fold. It has been observed that larger aromatic cores give rise to greater selectivity of quadruplex DNA over that of duplex DNA, due to the greater $\pi$-bonding surface available from the quadruplex.[135]

A critical evaluation of quadruplex DNA ligands is in their classical cytotoxicity. For an effective quadruplex DNA stabilising ligand, the level of cell cytotoxicity should be at least 10 times higher than the $^{tel}EC_{50}$. Classical anti-cancer/proliferative drugs work on being cytotoxic to the cell, this is not the case for quadruplex DNA ligands. Typically the use of a drug that inhibits telomerase through the stabilisation of quadruplex structures will not demonstrate any signs of activity until multiple rounds of cell division. This would lead to the gradual erosion of the telomere, initiating expression of proteins associated with short or damaged telomeres, resulting in characteristics protein *foci* at the chromosomal ends. The use of other anti-cancer agents would accelerate this process by targeting the cancerous cells from two approaches, with each agent working synergistically with one another.

### *2.9.1 - Natural products and analogues*

The natural product telomestatin **134** is currently the most efficient telomerase inhibitor known, with an $^{tel}IC_{50}$ of 5 nM and is often used as the benchmark for assessment of other telomerase inhibitors (Figure 2.08).[162,163] Telomestatin **134** was isolated from *Streptomyces anulatus* and is comprised of seven oxazole rings with one dehydrothiazole ring.[162] A subsequent total synthesis identified the natural configuration of telomestatin **134** as the (*R*)-enantiomer, in-line with the natural configuration of the amino acid cysteine.[164]

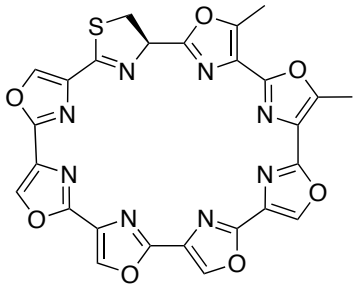


**Figure 2.08.** The natural product telomestatin, a potent inhibitor of telomerase.

Telomestatin has a 70-fold binding selectivity for quadruplex DNA over that of duplex DNA.[163] Quadruplex selectivity is critical for non-specific binding of the ligand to other regions of genomic DNA, with unspecific binding resulting in unwanted cytotoxic effects. Synthetic analogues of telomestatin **134**, such as **135a/b** (Figure 2.09) have been shown to be entirely quadruplex selective over duplex DNA, with the acetate analogue **135b** demonstrating a 2 $\mu$M inhibition of telomerase (Figure 2.09).[165,166]

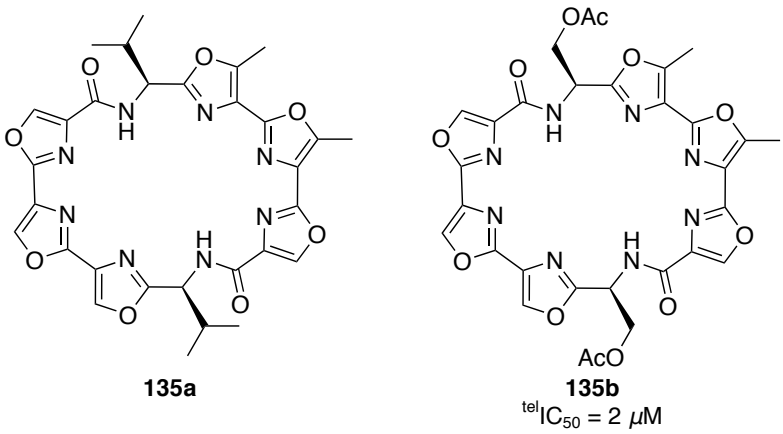


**Figure 2.09.** Analogues of the natural product telomestatin.

### *2.9.2 - Porphyrin based inhibitors*

Porphyrin based inhibitors such as TMPyP4 **136** have poor selectivity for quadruplex DNA, however CD and NMR based studies have shown that porphyrin **136** significantly stabilises quadruplex DNA (Figure 2.10).[167,168] TMPyP4 **136** was shown to inhibit telomerase with an $^{tel}IC_{50}$ of 6.5 $\mu$M as determined by the TRAP assay and a $\Delta T_m$ of 17 ºC from FRET analysis.[169] Subsequent X-ray crystallographic studies of TMPyP4 **136** with bimolecular quadruplex d($TAG_3T_2AG_3$) detailed an unusual major groove complexation between the ligand and the DNA rather than complexing to the G-tetrad face.[170] This may offer an explanation for the poor duplex/quadruplex selectivity.[167,171]

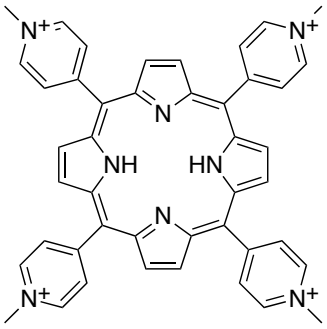


**136**
$\Delta T_m$ = 17.0 ºC
$^{tel}IC_{50}$ = 6.5 $\mu$M

**Figure 2.10.** Structure of the porphyrin based quadruplex DNA stabilizing ligand, TMPyP4 **136**.

### *2.9.3 - Quinacridine ligands*

Dibenzophenanthroline ligands such as **137a-c** have been shown to have good stabilisation potential for quadruplex DNA. Assessing their stabilisation through FRET analysis, found that **137a** and **137b** stabilized the human telomeric sequence by +19.7 ºC and +12.8 ºC respectively (Figure 2.11).[158] In TRAP assays, **137a** and **137b** have also showed an inhibitory effect on telomerase with $^{tel}IC_{50}$ values of 0.028 $\mu$M and 0.5 $\mu$M respectively. These values correlate with the FRET-based observations with the higher stabilising ligand resulting in a greater inhibition of telomerase. The cyclic derivative **137c** was shown to bind by both $\pi$-stacking and groove intercalation with quadruplex DNA with a $\Delta T_m$ of 28 ºC and $^{tel}IC_{50}$ of 0.13 $\mu$M (Figure 2.11).[172]

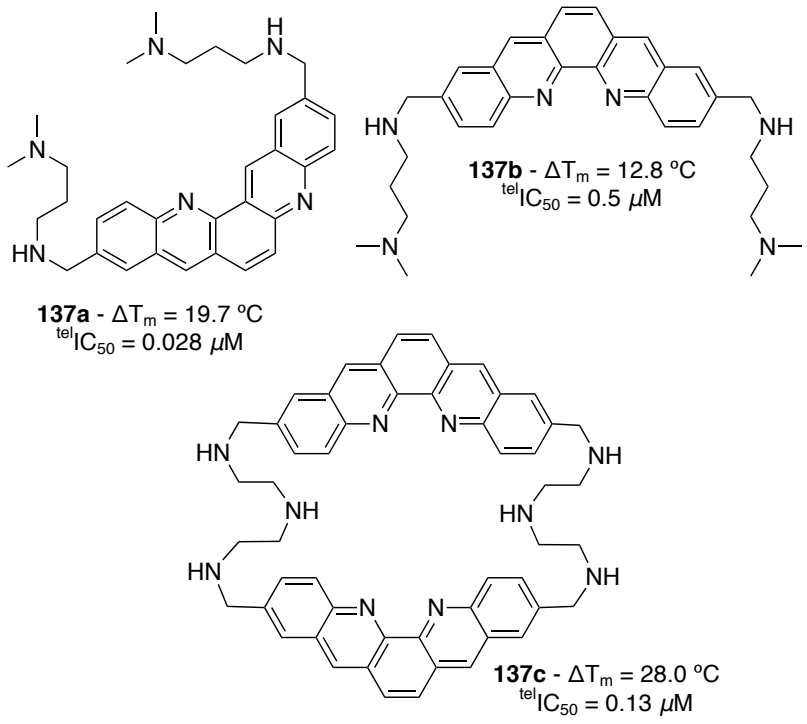


**Figure 2.11.** Structures of the quinacridine based quadruplex DNA stabilizing ligands.

### *2.9.4 - Anthraquinone and fluorenone ligands*

Quadruplex DNA-stabilising ligands developed by Neidle, Hurley and co-workers have led to a plethora of papers detailing the improvements and achievements of designing new ligands based on their early work.[173] Initially, bisamidoanthraquinone ligands **138a-h** had attractive $^{tel}EC_{50}$ values for telomerase inhibition (Figure 2.12).

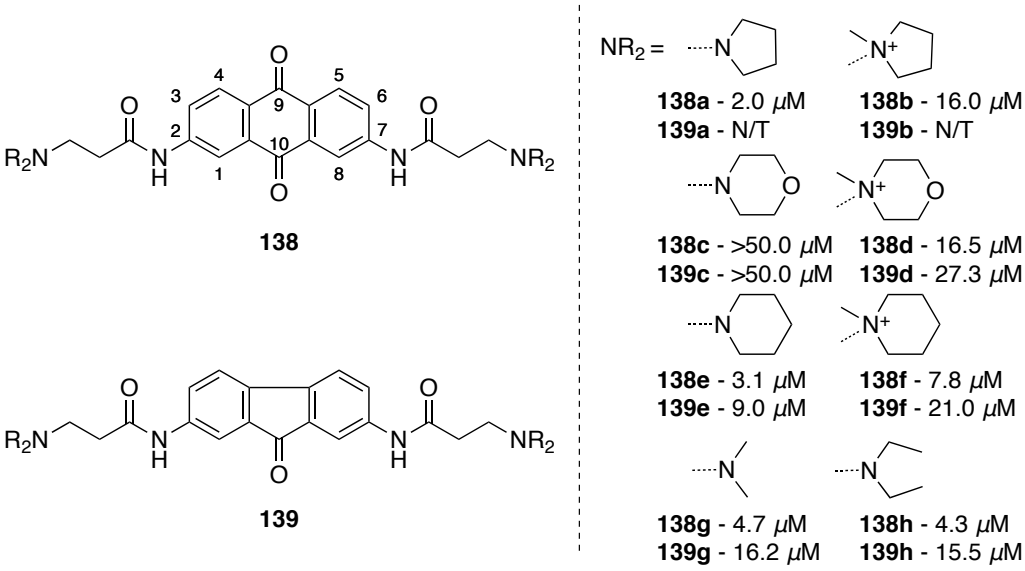


**Figure 2.12.** Structures and $^{tel}EC_{50}$ values of the anthraquinone and fluorenone based ligands.

Systematic studies on the substitution patterns of anthraquinones **138a-h** through the 1,4- 1,8-, 2,6- and 2,7- regioisomers identified the 2,7-regioisomer **138a** as the most potent, with an inhibitory value of 2.0 $\mu$M. The side groups are protonated at physiological pH with the exception of morpholine **138c**. The detrimental effect of neutral ligands can be observed in the $^{tel}EC_{50}$ value for **138c** (>>50 $\mu$M), thus this ligand does not appear to form strong interactions with quadruplex DNA folds. Interestingly, the generation of the $N^+$–Me salts **138b/d/f/h** resulted in an increase in $^{tel}EC_{50}$ values. This may be due to the removal of hydrogen bonds between the ligands and the quadruplex DNA. However, the metabolic cytotoxic effects of **138a-h** were problematic. This lead to the development of fluorenone analogues **139a-h**, which do not suffer the same metabolic fate as **138a-h**. Fluorenones **139a-h** demonstrated $^{tel}IC_{50}$ values between 8-12 $\mu$M and a decrease in metabolic related cytotoxicity compared to the anthraquinones **138a-h** (Figure 2.12).

### *2.9.5 - Acridone and di- and tri-substituted acridine ligands*

Subsequent development of acridone-based ligands **140a-h**,[174] demonstrated that the incorporation of a nitrogen in the aromatic core results in an increased interaction with quadruplex DNA (Figure 2.13). Following these observations, the acridine-based compounds **141a-h**[175,176] were developed in an attempt to arrange the central protonated acridine nitrogen over the negatively polarised central quadruplex core (Figure 2.13). However, the acridine series **141a-h** had low selectivity (1.3:1) for quadruplex DNA over duplex DNA.[177] Of the series, BSU6039 **141a**, which exhibited a $^{tel}EC_{50}$ value of 5.2 $\mu$M, was chosen for subsequent studies.

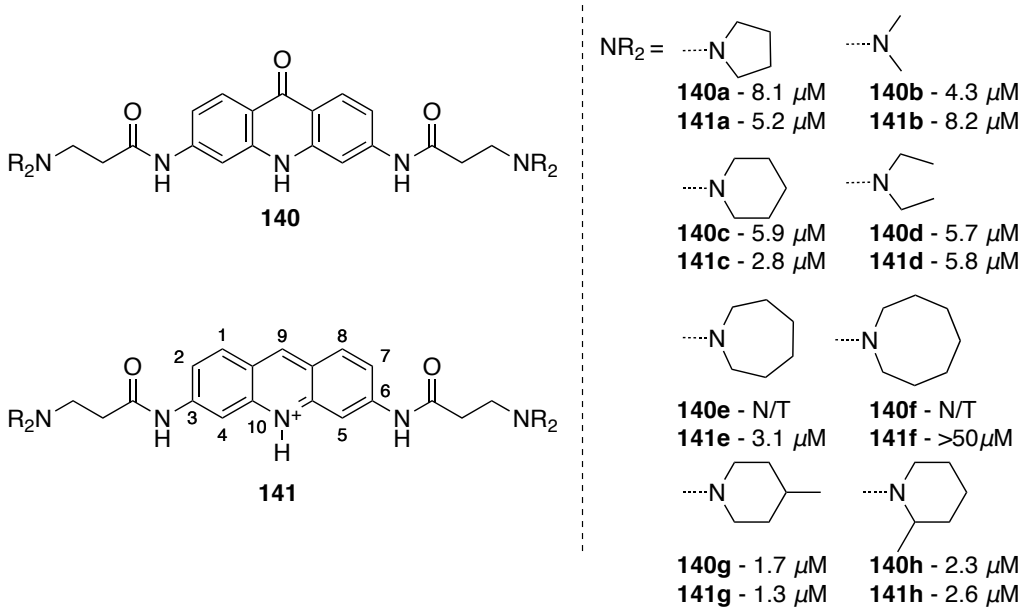


**Figure 2.13.** Structure and $^{tel}EC_{50}$ values for the acridone and acridine 3,6-disubstituted ligands.

Molecular modelling with BSU6039 **141a** suggested that substitution at the 9-position would result in further interactions with a third phosphate groove in the quadruplex fold (Figure 2.14).[177,178] The tri-substituted series **142a-f** was synthesised and it was found that **142a** (BRACO-19) exhibited the most favourable inhibitor characteristics. BRACO-19, with the 4-(dimethylamino)aniline substituent in the 9-position, was 31-fold more selective for quadruplex over duplex DNA and also showed a 44-fold increase in inhibition of telomerase ($^{tel}EC_{50}$ 0.115 $\mu$M) when compared to BSU6039.[174]

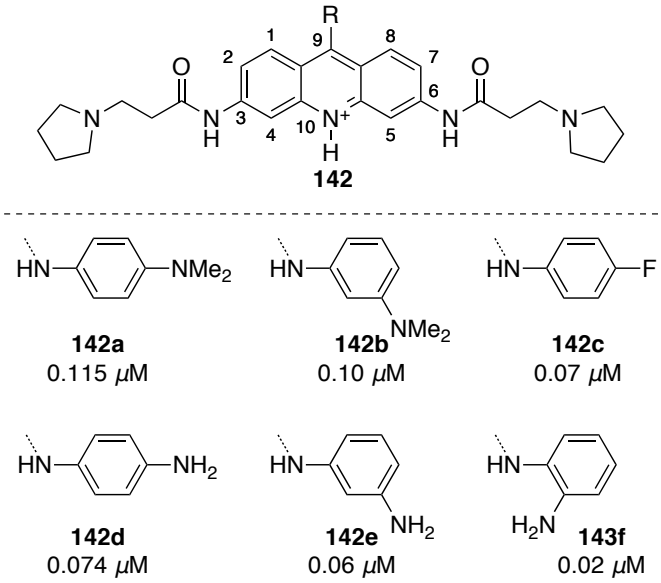


**Figure 2.14.** 3,6,9-Trisubstituted acridine ligands. $^{Tel}EC_{50}$ values are underneath for each 9-position substituent.

## 2.10 - BRACO-19 142a *in vitro* & *in vivo* studies

BRACO-19 **142a** (Figure 2.15) has good *in vitro* efficacy against the prostate cancer cell line DU145.[179] It was shown that after incubation over 7 days with sub-cytotoxic doses of BRACO-19 **142a** that half of the cells entered the $G_0$ phase. After 21 days there was an increase in the expression of the apoptosis associated proteins p21 and p16. It was also noted that non-homologous end-joining (NHEJ) events were occurring during the metaphase of the cell cycle, a feature of dysfunctional telomeres.[121] The data presented here suggests that BRACO-19 **142a** acts as a telomerase inhibitor through quadruplex DNA stabilization and also competes with telomeric binding proteins such as POT1. It has been demonstrated *in vivo* that BRACO-19 **142a** has efficacy towards xenographed uterine cancers in a murine model.[180]

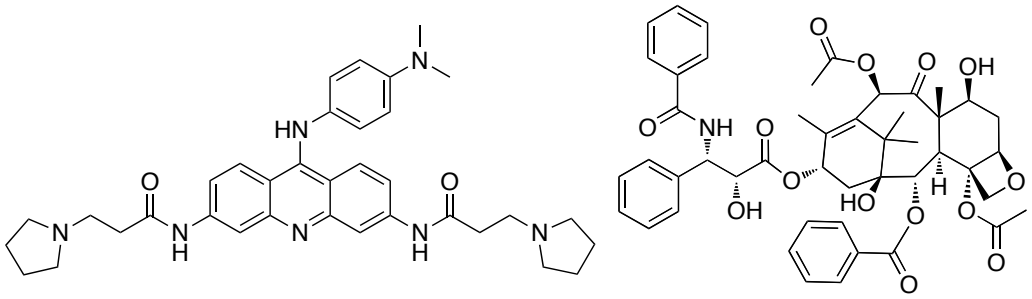

**142a** **143**

**Figure 2.15.** Structure of BRACO-19 **142a** and Paclitaxel **143** (Taxol).

Further studies with BRACO-19 **142a** and the established clinical anti-cancer agent paclitaxel **143** (Figure 2.15) have shown promising synergistic activities.[151] The treatment of A431 human epithelial carcinoma with BRACO-19 **142a** results in an insignificant decrease in tumour size upon intraperitoneal dosage. However, dosing of BRACO-19 **142a** post paclitaxel **143** treatment in these carcinomas resulted in greater tumour shrinkage, with a shortening of the average telomere length, than with paclitaxel alone.[181] This was the first proof of principal study of quadruplex DNA stabilisation as a method for anti-cancer therapy.

## 2.11 - X-ray crystallographic studies with acridine based ligands

### *2.11.1 - BSU6039 **141a** and O. nova DNA*

The crystal structure between BSU6039 **141a** and the bimolecular quadruplex DNA sequence $G_4T_4G_4$ was solved to 1.75 Å and provided an insight into how the acridine based ligands **141a-h** interact with quadruplex DNA (Figure 2.16).[128]

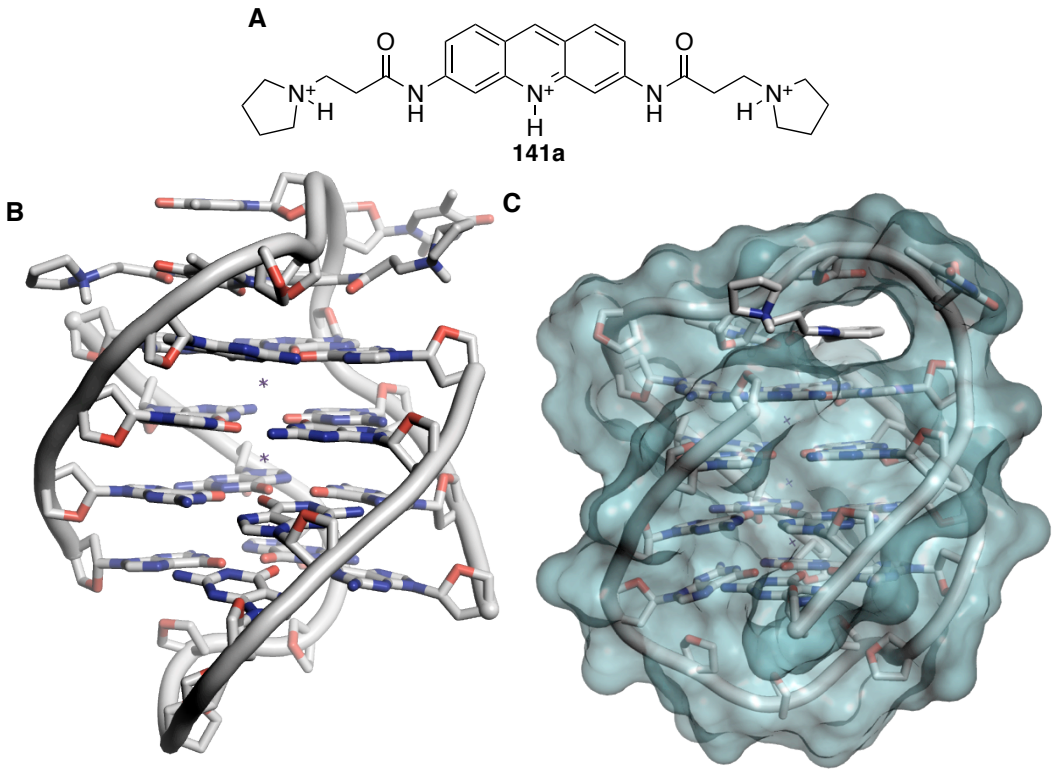


**Figure 2.16.** Crystal structure of BSU6039 **141a** bound to the bimolecular quadruplex fold from the *Oxytricha nova* sequence. **A** – BSU6039 structure, **B** – standard representation with BSU6039 binding in the top section and **C** – Surface representation to show binding cleft. Images created from PDB 1L1H using PyMol.[129]

In this structure, BSU6039 **141a** binds with one quadruplex fold with the thymine linking residues orientating in a diagonal manner across the top face of the quadruplex (Figure 2.16, B). This topology is the same for the native crystal structure (Figure 2.4) with potassium ions and generates two wide phosphate grooves with complementary narrower phosphate grooves along the sides of the quadruplex.[141] The glycosidic angles of the guanine nucleotides in the sequence alternate *syn-anti*, such that the G-tetrad has a *syn-syn-anti-anti* glycosidic arrangement, which enables the hydrogen bonds from the

Hoogsteen and Watson-Crick faces to be accommodated (Figure 2.3). Between the G-tetrads, potassium ions are coordinated to the $O^6$ carbonyls of the G-tetrads, thus further stabilizing the quadruplex structure (Figure 2.16, purple crosses). The diagonal orientation of the thymine loops generates a binding cleft into which BSU6039 **141a** can orientate and $\pi$-$\pi$ stack with the top G-tetrad (Figure 2.16, C). In contrast to the native crystal structure (Figure 2.4), one of the thymine nucleotides twists out of the loop plane and interacts with the central nitrogen and one amide carbonyl of **141a**, forming two hydrogen bonds (Figure 2.17).

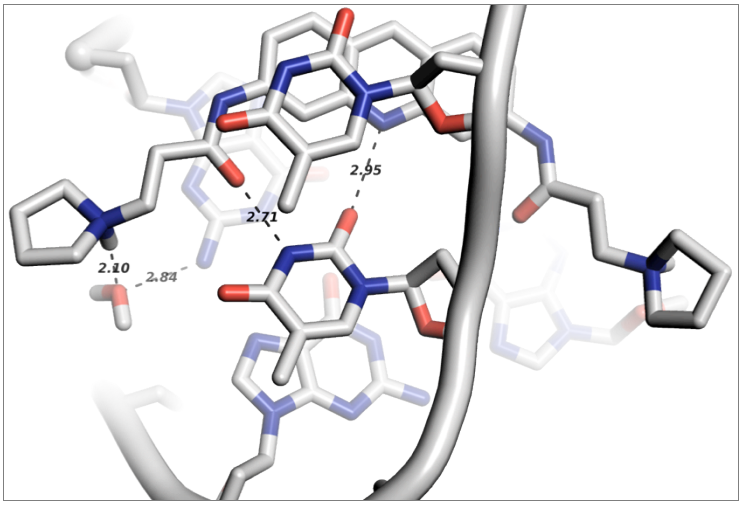


**Figure 2.17.** Top orientated view of the binding between BSU6039 **141a** and the quadruplex fold. Distances are in Å. Image generated from PDB file 1L1H using PyMOL.[129]

Another thymine nucleotide also forms a $\pi$-$\pi$ interaction with the acridine, further stabilising the fold. In the phosphate grooves, there is a highly ordered water lattice. However, the charged pyrrolidino rings of **141a** do not interact through salt bridges with the phosphate backbone and only on one side does the substituent form a hydrogen bond with a water molecule (Figure 2.17). This specific water molecule forms a hydrogen bond with the guanine tetrad. There are no other direct hydrogen bonds in the crystal structure between the quadruplex and the ligand. It has been rationalised that the substituents interact in an electrostatic manner as demonstrated in a range of crystal structures of 3,6-substituted acridines **141a-h** with the *O. nova* sequence.[182]

### *2.11.2 - BRACO-19 **142a** and human DNA*

A subsequent study on the mode of binding of the 3,6,9-substituted acridine ligand **142a** has been published.[183] The crystal structure of BRACO-19 bound to the bimolecular human telomeric G-quadruplex sequence, d($TAG_3T_2AG_3T$), was resolved to 2.5 Å by X-ray crystallography (Figure 2.18).[183]

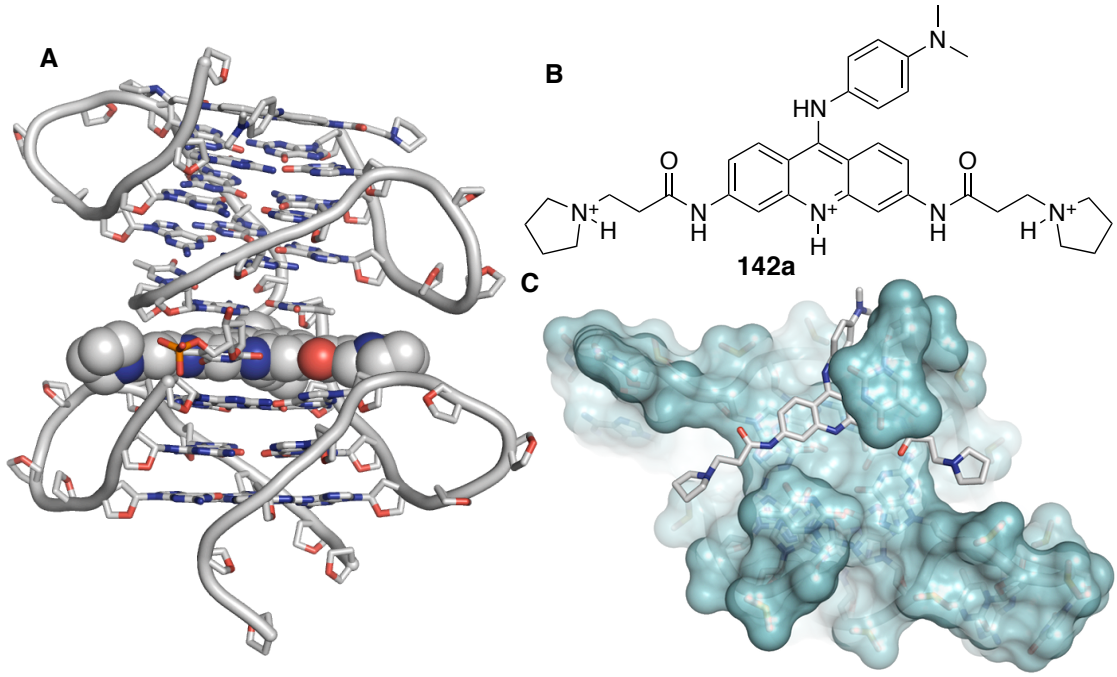


**Figure 2.18.** BRACO-19 bimolecular quadruplex DNA co-complex X-ray crystal structure. **A** – BRACO-19 in a space filling representation sandwiched between two quadruplex folds, **B** – Structure of BRACO-19 for comparison and **C** – Surface representation of the bottom quadruplex clearly demonstrating the phosphate grooves. Images created from the PDB file 3CE5 using PyMol.[129]

This crystal structure and the binding between the quadruplex DNA and the ligand **142a** are very different to that of the *O. nova* structure presented earlier. Each bimolecular quadruplex has propeller linkages, similar to those observed in the native $G_3(T_2AG_3)_3$ sequence (Figure 2.07, B), with an assembly of three planar stacked guanine tetrads. In contrast to the BSU6039 **141a** crystal structure, BRACO-19 **142a** is complexed between two quadruplex folds, forming $\pi$-$\pi$ stacking interactions with the 3' end guanine tetrad of one quadruplex and TA nucleotides of the 5' end from another quadruplex. One linking thymine base is rotated such that it interacts through hydrogen bonding and water-salt bridges with the acridine core of BRACO-19 **142a** (Figure 2.19).

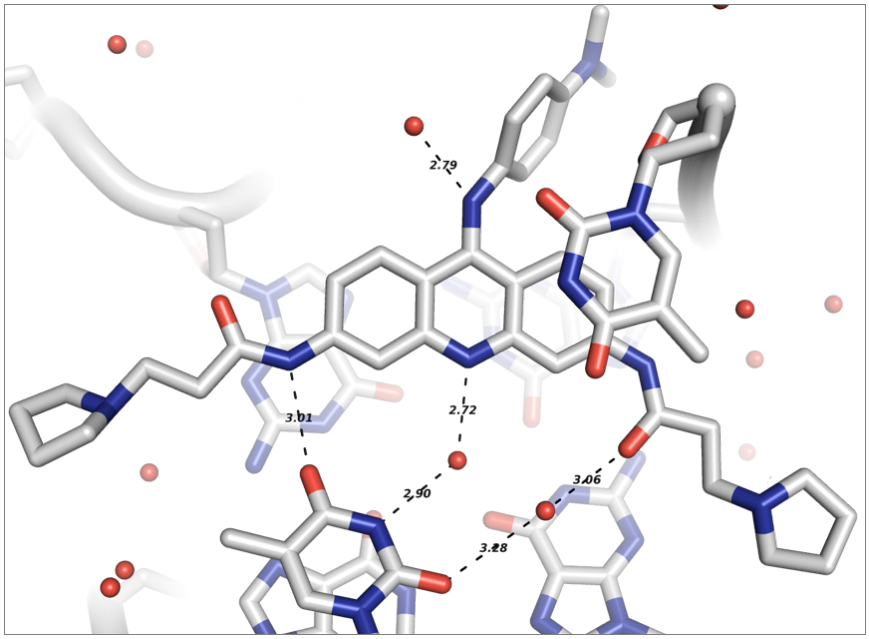


**Figure 2.19**. Top orientated view of the binding between BRACO-19 **142a** and quadruplex DNA. Distances are in Å.

This rotated thymine plays a critical role in the interaction and stabilisation of BRACO-19 **142a** with the quadruplex. The charged 3- and 6- substituents do not form hydrogen bonds with the negatively charged phosphates and interact in an electrostatic manner. The propeller TTA linkages between the guanine tracks generate size specific grooves that accommodate smaller substituents. This is in contrast to the *O. nova* sequence where the diagonal loops generate a cleft able to accommodate a variety of substituents.[182] The overall mode of binding of BRACO-19 **142a** is typically mediated through hydrogen bonding with water to the quadruplex rather than through direct interactions. The synthesis of BRACO-19 **142a** analogues with longer alkyl substituents results in decreased stability.[184] It is likely that the conformational flexibility in these analogues results in a less ordered binding ligand that will not orientate correctly to form hydrogen bonds, even with the water lattice in the phosphate grooves. The interaction between BRACO-19 **142a** and two quadruplex folds is a significant observation and may represent a realistic *in vivo* model. It is reasonable that quadruplex folds occur in a contiguous fashion with one or more quadruplex folds occurring at the ssDNA telomeric end. Therefore, the binding of BRACO-19 **142a** to one quadruplex *in vivo* may induce another quadruplex to 'fold back' and interact similar to that observed in the crystal structure. To date, however, there are no crystal structures of extended telomeric sequences, such as with $d(AG_3(T_2AG_3)_n)$ where $n \geq 7$, that demonstrate two or

more quadruplexes per sequence.[151] The generation of such structural data would be a significant advance in the current understanding of how quadruplex ligands are likely to interact with quadruplex DNA *in vivo*.

## 2.12 - Conclusions

This chapter has provided a brief overview of the biological and structural aspects of telomeres in the cell. It has also discussed the implication of inhibiting enzymes involved in the maintenance of telomere length. The structures of several classes of small molecule inhibitors of telomerase that act through the stabilisation of quadruplex DNA *in vivo* have been described. Detailed assessment of their interaction in the solid state by X-ray crystallography has enabled the development of a generalised view of their mode of action.

# Chapter 3

# Synthesis and evaluation of fluorinated BSU6039 analogues

## 3.1 - Introduction

It is common practice in drug discovery to vary the substituents on the pharmacophore to explore structure activity relationships for a particular inhibitor. In the case of BRACO-19 **142a** and BSU6039 **141a**, it is clear that small ring substituents on the alkyl amino side chains led to a more efficacious inhibitor (Chapter 2.14).[161] These rings are accommodated within the hydrophobic pocket formed by the DNA sequence. The size of the hydrophobic pocket is highly dependent on the individual sequence of the quadruplex DNA used for crystallisation, with the various linker nucleotides assuming different conformations in space (Chapter 2.6).[157] In the case of the *O. nova* sequence, crystallography indicates that the thymine residues allow for a variety of alkyl substituents to be accommodated.[182]

As highlighted in Chapter 1.11, modification of small nitrogen containing heterocycles with $\beta$-fluorine substituents results in a ring conformation whereby the fluorine-carbon bond dipole moment interacts favourably with the $N^+$–H bond dipole on the protonated nitrogen (Figure 3.01).[19]


**101** **97**

**Figure 3.01.** The charge-dipole effect in 5- and 6-membered rings.

This is a dipole-dipole through space interaction. The possibility of incorporating fluorine in this manner into BSU6039 would enable an investigation into the mode of binding and the importance of ring conformation to the stability of quadruplex DNA. In addition, the C–F bond will be expected to lower the p$K_a^H$ of the protonated amine and increase the acidity of the hydrogen for hydrogen bonding. In general, however, a smaller $\Delta pK_a$ between the donor and acceptor results in a stronger hydrogen bond.[185]

Therefore, the aim of this research was to investigate the effect of substituting the pyrrolidino rings of BSU6039 **141a** with a C–F bond at the 3-position and to assess the structural influence by X-ray crystallography of co-crystals with *O. nova* bimolecular quadruplex DNA (Chapter 2.6/2.11).

In order to investigate these effects, it was necessary to synthesise the enantiomers of the fluoro- and hydroxyl- analogues **144** and **145** of BSU6039 (Figure 3.02). These analogues would then be co-crystallised with the $T_4G_4T_4$ *O. nova* quadruplex DNA sequence.

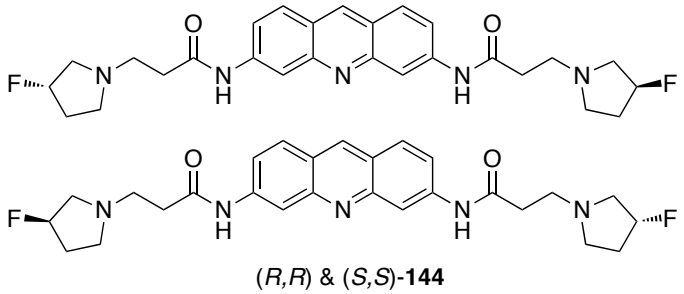

(*R,R*) & (*S,S*)-**144**

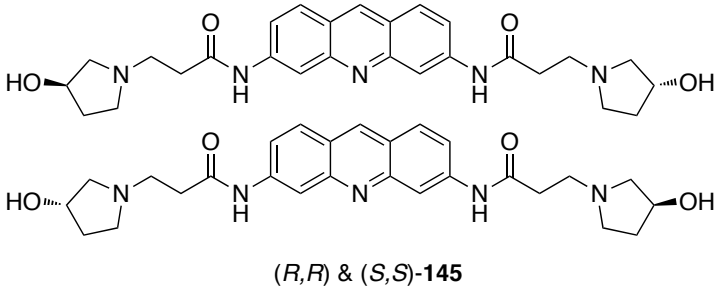

(*R,R*) & (*S,S*)-**145**

**Figure 3.02.** 3-Fluoro- and 3-hydroxyl pyrrolidine analogues of BSU6039 **141a**.

## 3.2 - Synthesis of BSU6039 141a analogues

To access the synthetic targets it was required to prepare the *bis*-chloro intermediate **146** from which **144** and **145** could be synthesised (Scheme 3.01). This intermediate can be accessed by treating proflavin **147** with 3-chloropropionyl chloride **148**.

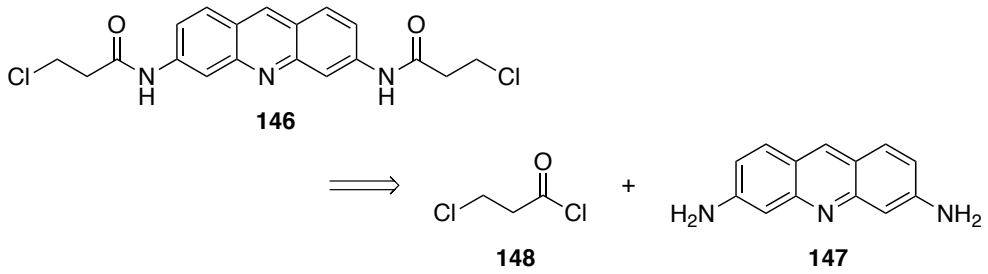


**Scheme 3.01.** Retrosynthetic approach to **146**.

Treatment of diamine **147** with neat 3-chloropropionyl chloride (**148**) under forcing conditions generated the known *bis*-chloro substituted acridine **146** in an excellent yield of 90% (Scheme 3.02).[175]

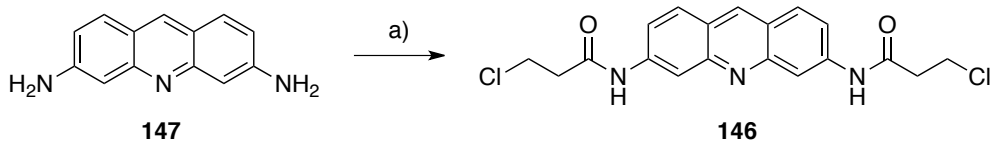


**Scheme 3.02**. *Reagents and conditions*: a) 3-Chloropropionyl chloride (neat), 140 ºC, 4 h, 90%.

The solubility of *bis*-chloro **146** in common solvents was very low, thus it was particularly difficult to purify. In the event, *bis*-chloro **146** was often contaminated with acid chloride **148**. This pungent smelling contaminant remained even after recrystallisation and washing with ethanol and then drying under high vacuum. However, the contamination (NMR analysis) was low and so the product was taken on without further purification. In order to access (*R,R*)-**144**, it was required to treat *bis*-chloro **146** with (3*R*)-fluoropyrrolidine **149** (Scheme 3.03).

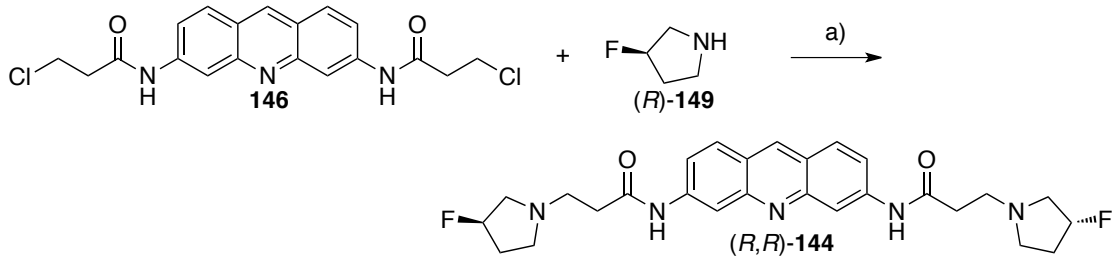


**Scheme 3.03**. *Reagents and conditions*: a) NaI, EtOH, 80 ºC, 3-5 h, 63%.

Treating pyrrolidine (*R*)-**149** with *bis*-chloro **146** in ethanol and with sodium iodide generated (*R,R*)-**144**. Purification of the product mixture by column chromatography required up to 5% triethylamine to obtain a pure sample of (*R,R*)-**144** (63% yield). Repeating the procedure with (*S*)-**149** enabled the isolation of (*S,S*)-**144** also in a satisfactory yield of 65% (Scheme 3.04).

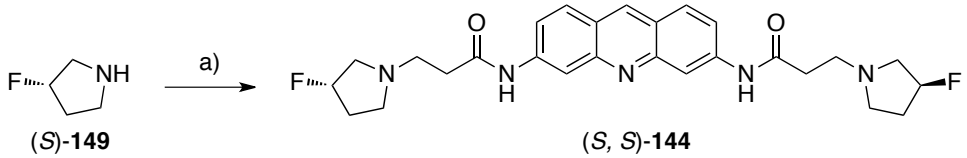


**Scheme 3.04**. *Reagents and conditions*: a) **146**, NaI, EtOH, 80 ºC, 3-5 h, 65%.

In order to obtain (*S,S*)-**145** and (*R,R*)-**145**, the reactions were repeated with (*S*)- or (*R*)-**150**. Products (*S,S*)-**145** and (*R,R*)-**145** could be isolated in satisfactory yields for both ligands (Scheme 3.05).

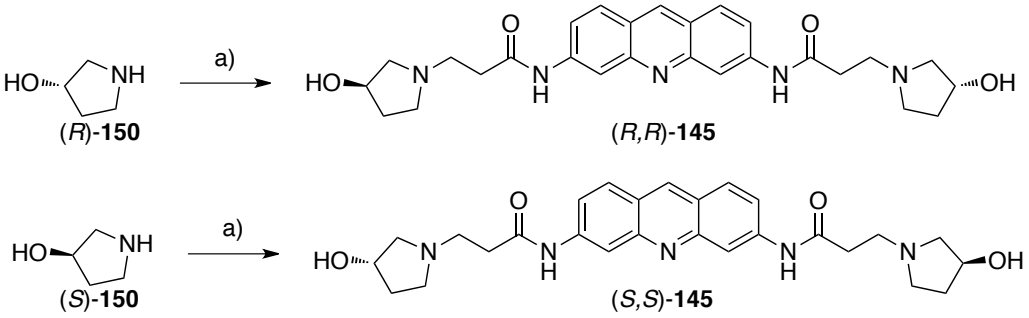


**Scheme 3.05**. *Reagents and conditions*: a) **146**, NaI, EtOH, 80 ºC, 3-5 h, 59%.

## 3.3 - Characterisation of (*S,S*)- and (*R,R*)-144

The proton resonances of the 3-fluoropyrrolidine ring in (*S,S*)- and (*R,R*)-**144** in the $^{1}$H NMR are well defined and can be assigned based on the correlations in the $^{1}$H–$^{1}$H COSY spectrum (Figure 3.03).

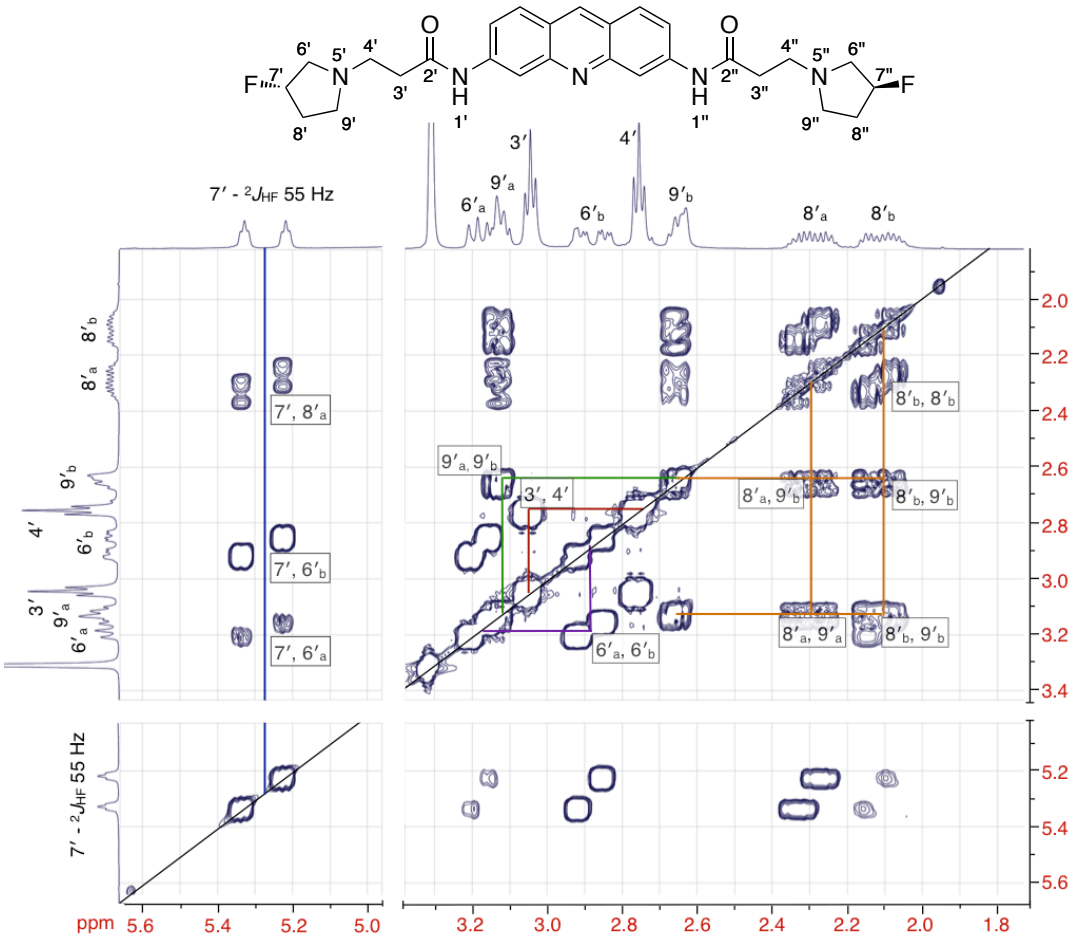


**Figure 3.03.** $^{1}$H-$^{1}$H COSY (500 MHz, $d_6$-DMSO/$CD_3OD$) analysis of (*S,S*)-**144**.

It is likely that the C–F bond does not exhibit a strong preference for a *pseudo*- axial or equatorial C–F bond conformation. Therefore, the unambiguous assignment of *pseudo*-axial and equatorial proton resonances cannot be made and have been designated as $H_a$ and $H_b$ for each resonance. Thus, starting from the distinctive $^{2}J_{HF}$ coupling constants, it was possible to assign the resonance at 5.28 as *H*-7' in **144** (Figure 3.03, blue line). The cross peak pattern from *H*-7' enabled the putative assignment of the resonances belonging to *H*-6'$_{a/b}$ and *H*-8'$_{a/b}$. The relative chemical shift of the resonances at 3.15 and 2.84 ppm and their cross peak isolation (Figure 3.03, purple line) support the assignment of these as the *H*-6'$_{a/b}$ resonances. Therefore, the

resonances at 2.29 and 2.10 ppm can be assigned as *H*-8'$_{a/b}$. The remaining resonances corresponding to *H*-9'$_{a/b}$ are confirmed through the clear cross peaks with *H*-8'$_{a/b}$ (Figure 3.03, orange lines). It is clear from the analysis of **144** that distinct resonances for each proton on the pyrrolidino ring can be observed. The $^{1}$H–$^{1}$H COSY assignments were supported by a $^{1}$H–$^{13}$C HSQC analysis (Figure 3.04).

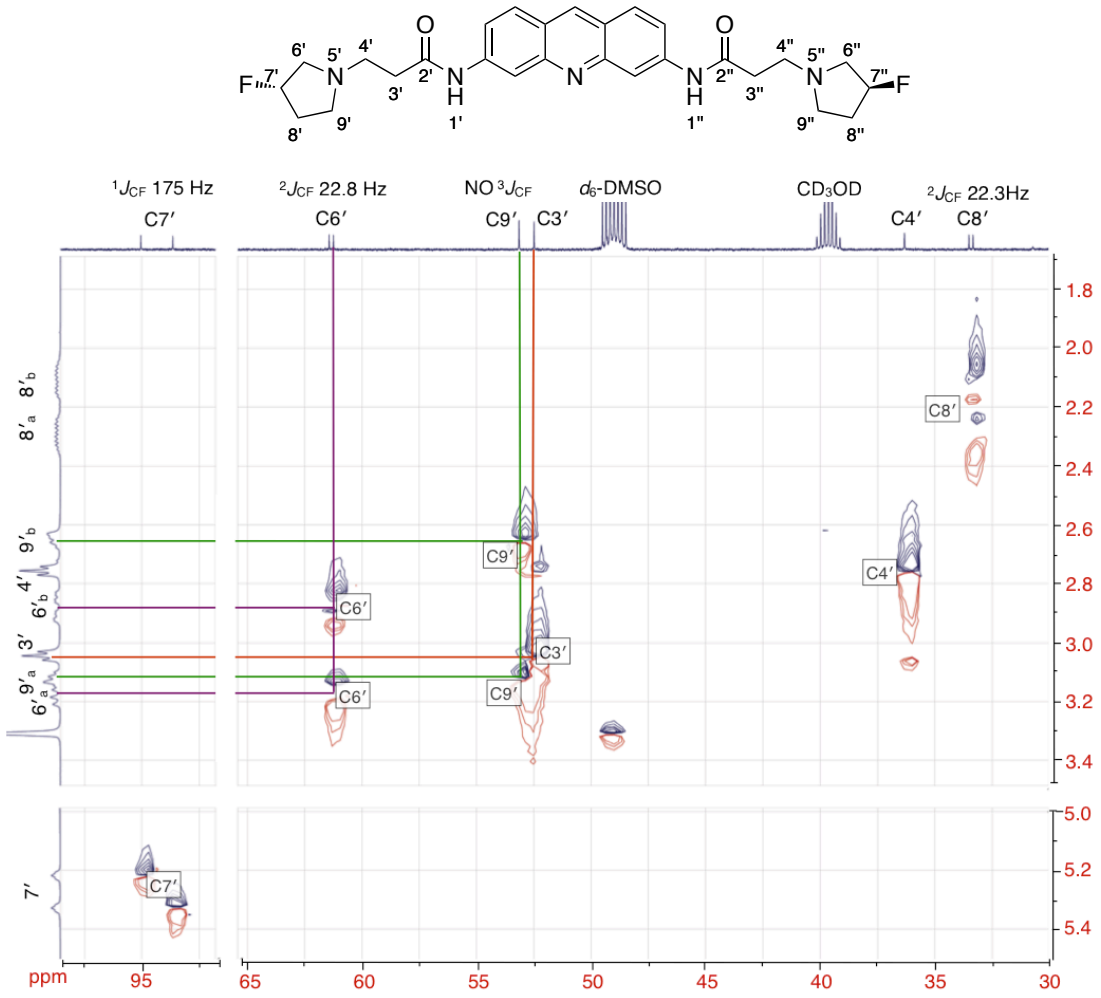


**Figure 3.04.** $^{1}$H–$^{13}$C HSQC (500/125 MHz, $d_6$-DMSO/$CD_3OD$) analysis of (*S,S*)-**144**.

Again, the distinctive $^{1}J_{CF}$ and $^{2}J_{CF}$ couplings in the $^{13}$C NMR spectrum, along with their relative chemical shifts enabled the assignment of *C*-7' ($^{1}J_{CF}$ = 175 Hz). The resonances at 52.5 and 36.5 ppm in the $^{13}$C NMR spectrum were assigned to *C*-3' and *C*-4' respectively through cross peaks with the triplets at 3.02 and 2.75 ppm of the $^{1}$H NMR spectrum. Of the remaining resonances in the $^{13}$C NMR spectrum, two exhibited distinctive couplings of 22.8 and 22.3 Hz at 61.4 and 33.5 ppm respectively, corresponding to $^{2}J_{CF}$ through bond coupling. Distinguishing between these resonances

was possible by referring to the $^{1}$H–$^{1}$H COSY spectrum (Figure 3.03), with the signal at 61.4 ppm corresponding to *C*-6' (Figure 3.04, purple line) and that at 33.5 ppm to *C*-8'. The remaining resonance, without any $J_{CF}$ coupling could be assigned to *C*-9'. The close proximity of the *C*-9' signal to the strongly correlating peak of *C*-3' (Figure 3.04, red line) obscured the *H*-9'$_a$ – *C*-9'correlation (Figure 3.04, green line), however, this could still be observed as a shoulder peak. These assignments were further supported by HMBC and $^{1}$H–$^{19}$F HMBC analyses. The aromatic quaternary carbons of the acridine ring were assigned based on DEPT-Q, HMBC and HSQC analyses. It was possible to assign the spectrum of (*R,R*)-**144** using the same combination of techniques detailed above. The spectra for diols (*R,R*)-**145** and (*S,S*)-**145**, were less complex and more readily assigned.

## 3.4 - Fluoropyrrolidine ring conformation in 144.HCl

To assess the conformation of the 3-fluoropyrrolidine ring in **144**, the HCl salts were prepared. Acridine (*S,S*)-**144** was dissolved in methanol and treated with HCl (1 M diethyl ether soln.), such that the nitrogen of the pyrrolidino rings were protonated (Scheme 3.06). This resulted in the precipitation of (*S,S*)-**144** as the hydrochloride salt, and thus the salt had to be dissolved in $d_6$-DMSO for NMR analysis.

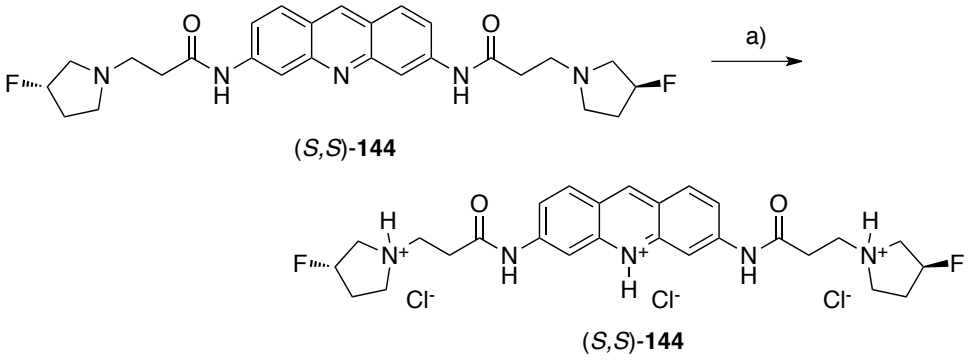


**Scheme 3.06**. *Reagents and conditions*: a) HCl (1 M in $Et_2O$), MeOH, rt.

The $^{1}$H NMR spectrum of (*S,S*)-**144**.HCl showed significantly broadened signals as a result of further coupling to the N–H of the pyrrolidino ring and no coupling constants could be extrapolated. Interestingly, the $^{19}$F NMR of (*S,S*)-**144**.HCl, split into two well-defined resonances at -171.9 ppm and -173.4 ppm, upfield from that of the free amine (Figure 3.05).

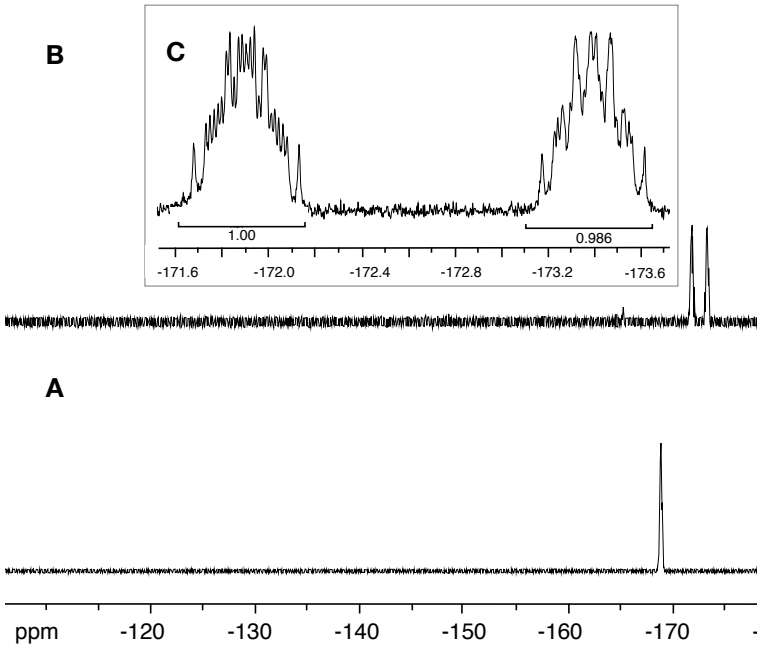


**Figure 3.05**. **A** -$^{19}$F NMR (470 MHz, $d_6$-DMSO) of (*S,S*)-**144**. **B** - $^{19}$F NMR of (*S,S*)-**144**.HCl & **C** - Expanded section of B.

The two resonances (Figure 3.05, C) must reasonably correspond to the formation of a diastereomeric pair, as protonation of the nitrogen can occur from either side of the rings, *syn* or *anti* to the axially orientated C–F bond (Figure 3.06). The equal distribution of protonation states was supported by DFT calculation, with the relative energy difference insignificant enough to influence the distribution of the two isomers (Figure 3.06).

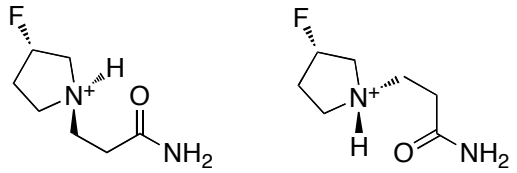


*syn*-**151**
$E_{rel}$ = 0 kJ/mol

*anti*-**151**
$E_{rel}$ = 0.218 kJ/mol

**Figure 3.06**. Protonation creates diastereomers of the pyrrolidine ring, which can be clearly observed in the $^{19}$F NMR. The relative energy difference was calculated by DFT (B3LYP/6-316(D)) by Dr Tomas Lebl, St Andrews. R = H.

The coupling constants from the two resonances (Figure 3.05, C) can be used to demonstrate an axial solution conformation of the C–F bond, consistent with the literature.[79-81] The $^2J_{FH}$ and $^3J_{FH}$ coupling constants could be extracted from the resonance at -171.9 ppm , although the $^4J_{FH}$ couplings are small and could not be

quantified (Figure 3.07, A). In (*S,S*)-**144**.HCl four $^{3}J_{FH}$ coupling constants at -171.9 ppm could be determined with values of 39.4, 33.0, 25.8 and 19.5 Hz. The experimental coupling constants were entered into a NMR simulation package (iNMR) and the simulated spectrum (Figure 3.07, B) provided a good fit with the experimental data (Figure 3.07, A). The same treatment could not be repeated with the resonance at -173.4 ppm, however this signal was of similar width.

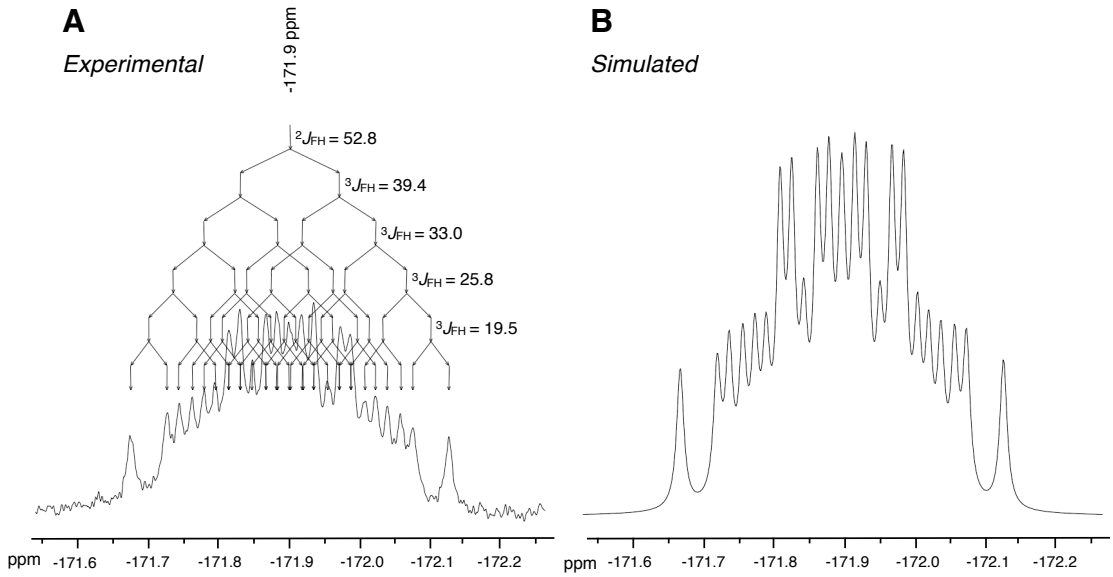


**Figure 3.07. A** - Expanded region of $^{19}$F NMR spectrum (470 MHz) for (*S,S*)-**144**.HCl & **B** - Simulated spectrum at 470 MHz.

A comparison of the coupling constants observed for (*S,S*)-**144**.HCl with the literature was made.[186] Thibaudeau *et al*., have reported *trans* $^{3}J_{HF}$ relationships (H–C–C–F torsion angles 160-180º) of between 30-45 Hz in ribose rings. In these systems, the size of the coupling constant is dependent on the substituents. The $^{3}J$ values of 39.4 and 33.0 Hz suggest an H–C–C–F torsional angle approaching 180º, indicative of a *pseudo*-axial/axial coupling. The remaining two $^{3}J_{FH}$ values correspond well with torsion angles in the range 0-60º respectively, suggesting a *pseudo*-axial/equatorial conformation. These large coupling constants support the view that the fluorine-ammonium interaction in (*S,S*)-**144**.HCl leads to a highly ordered conformation with the C–F bond orientating in axial conformation (Figure 3.08, A).

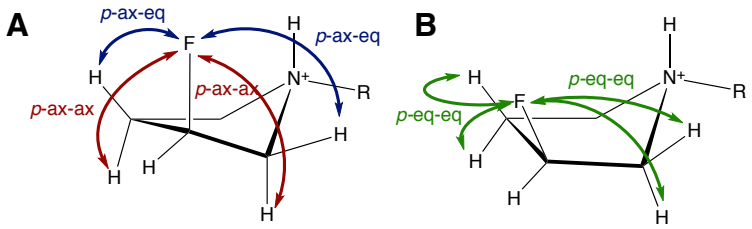


**Figure 3.08**. Representations for the *pseudo*-axial (A) and equatorial (B) orientation of the C–F bond.

If the C–F bond was orientated in a *pseudo*-equatorial conformation (Figure 3.08, B), for this particular signal, then the $^{3}J_{FH}$ coupling constants would be between 10-20 Hz. This is consistent with torsion angles approaching 60º, corresponding to a *pseudo*-equatorial-equatorial coupling. These coupling constants would result in a resonance with a smaller spectral width and less definition, similar to that of the non-protonated system (Figure 3.05, A).

## 3.5 - Co-crystallisation with quadruplex DNA

### *3.5.1 - Background and crystallisation*

Co-crystallisation trials with (*S,S*)- and (*R,R*)-**144** and **145** with quadruplex DNA were conducted in collaboration with Prof. Steven Neidle's laboratory at the UCL, School of Pharmacy. The approach used the hanging drop vapour-diffusion method (Figure 3.09).

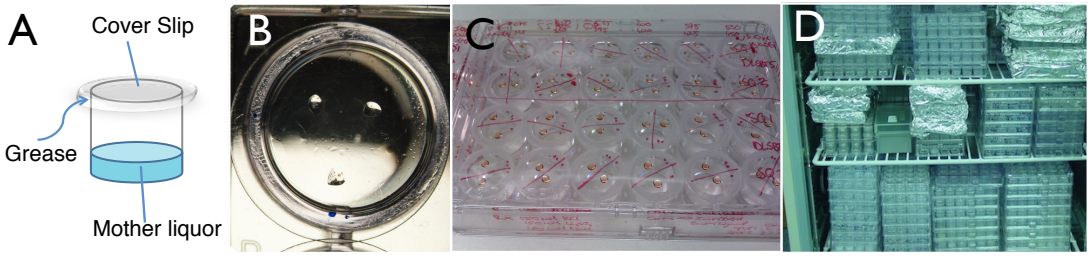


**Figure 3.09. A** - Hanging drop vapour diffusion method for growing crystals, **B** - Top view of crystals growing on the top cover slip, **C** - Crystal tray with various conditions attempted such as altering the mother liquor concentrations & **D** - Attempted trays stored at 16 ºC.

By this method the ligand and quadruplex DNA are added in various concentrations to a buffer solution, which is placed on a cover slip (Figure 3.09, A/B). This cover slip is then suspended over a concentrated salt solution, forming a closed system with grease

generating a tight seal. Evaporation of the buffer solution containing the ligand and quadruplex DNA results in super-saturation. Optimisation of this evaporation process by changing variables can result in the crystallisation of DNA-ligand crystals that are suitable for X-ray diffraction. The variables are: crystallisation temperature; buffer constituents; stock buffer concentrations; DNA to ligand ratio; and/or concentration relative to the buffer. Negative results such as DNA precipitation can be used to tune the crystal growing conditions.[157]

After an extensive exploration of variables by Dr. Nancy Campbell (School of Pharmacy) the optimal conditions for crystal growth were found, resulting in rhombohedral co-crystals of (*R,R*)-**144** and (*S,S*)-**144** with quadruplex DNA. The crystals (Figure 3.10) were subject to X-ray analysis on a synchrotron at the Diamond Light source (Oxfordshire, UK).

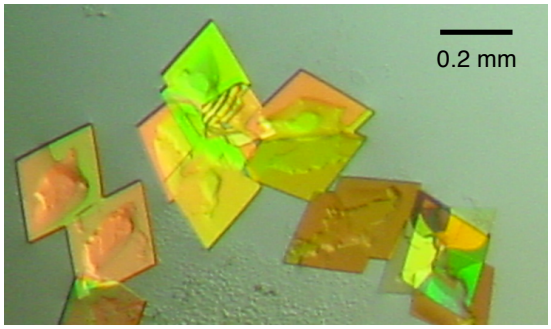


**Figure 3.10.** Photograph of diffracted ligand-DNA crystals.

The diffraction data was fitted and refined, providing crystal structures at a highly refined 1.18 Å and 1.10 Å resolution for (*R,R*)-**144** and (*S,S*)-**144** respectively. The resulting unit cell for crystals of (*R,R*)-**144** is shown in Figure 3.11.

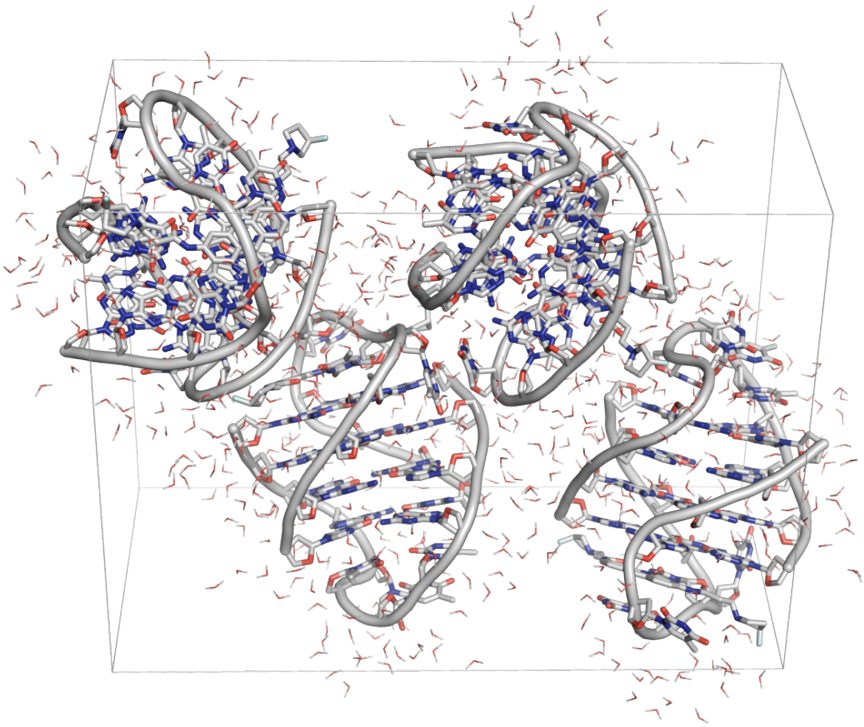

**Figure 3.11.** Unit cell of the co-crystal of (*R,R*)-**144** with *O. nova* bimolecular DNA.

This representation and that shown in subsequent figures were created from the files deposited in the Protein Data Bank (PDB) with file names 3NYP and 3NZ7 for (*R,R*)-and (*S,S*)-**144** respectively. Images were generated using the COOT[187] and PyMol[129] crystal visualisation packages.

The high level of resolution of these co-crystals enabled a detailed assessment of interactions of these ligands with *O. nova* DNA and they could be compared to the co-crystal structure previously solved with BSU6039 **141a** to 1.75 Å (Figure 2.16). Thus, the co-crystals with the fluorinated analogues (*R,R*)- and (*S,S*)-**144** were of particularly high quality.

While the fluorinated analogues (*R,R*)- and (*S,S*)-**144** provided suitable crystals for X-ray diffraction, the hydroxy compounds (*R,R*)- and (*S,S*)-**145** failed to crystallise under the same conditions Altering the conditions for crystallisation failed to produce any suitable crystals for diffraction (Nancy Campbell, UCL). These compounds would have enabled a useful comparison as an intermediate between hydrogen and fluorine in the pyrrolidine ring, however suitable co-crystals were not forthcoming.

### *3.5.2 - General observations in the co-crystals with (S,S)- and (R,R)-**144***

The topology observed within the unit cell for both enantiomers of **144** is the same. This corresponds to the quadruplex DNA assembling with the thymine bases forming a loop at either end of the quadruplex in an identical manner to the co-crystals BSU6039 **141a** discussed in Chapter 2.11 (Figure 3.12). The DNA and ligand are bound in a one to one ratio with the acridine ligand occupying the cavity between an upper guanine tetrad and the thymine base loop (Figure 3.13). Although the two structures are formally diastereomers this does not significantly change the G-quadruplex conformation.

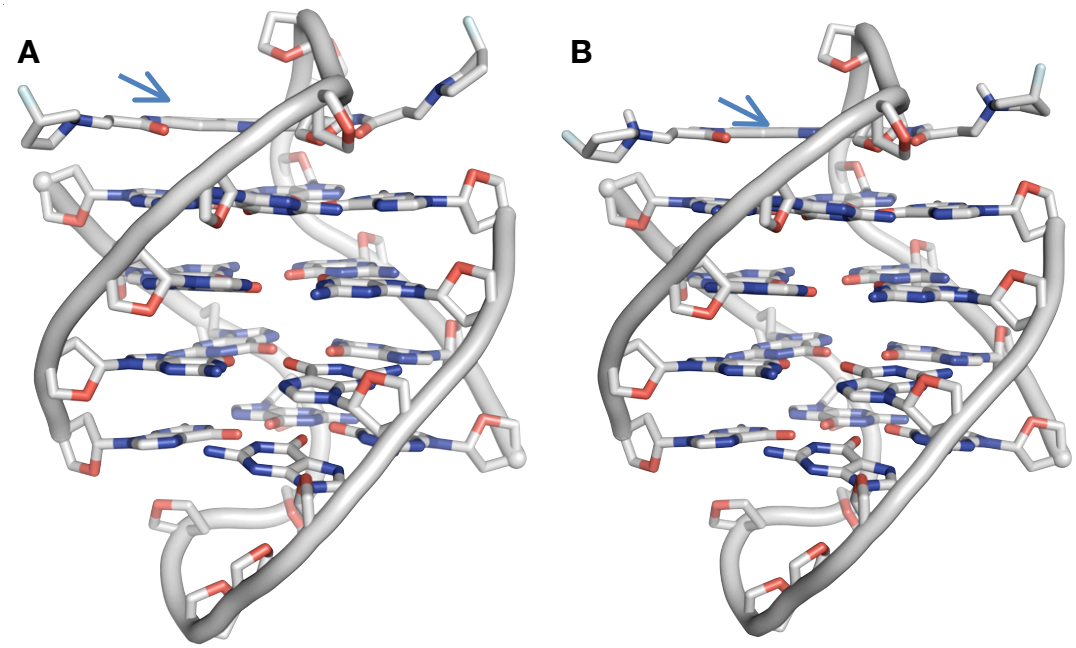


**Figure 3.12**. Co-crystal structures for fluorinated pyrrolidine analogues. **A** - (*S,S*)-**144** and **B** - (*R,R*)-**144** both with quadruplex DNA ($G_4T_4G_4$). The blue arrows highlight the ligand binding to the top face of the quadruplex. Representation created with PyMol.[129]

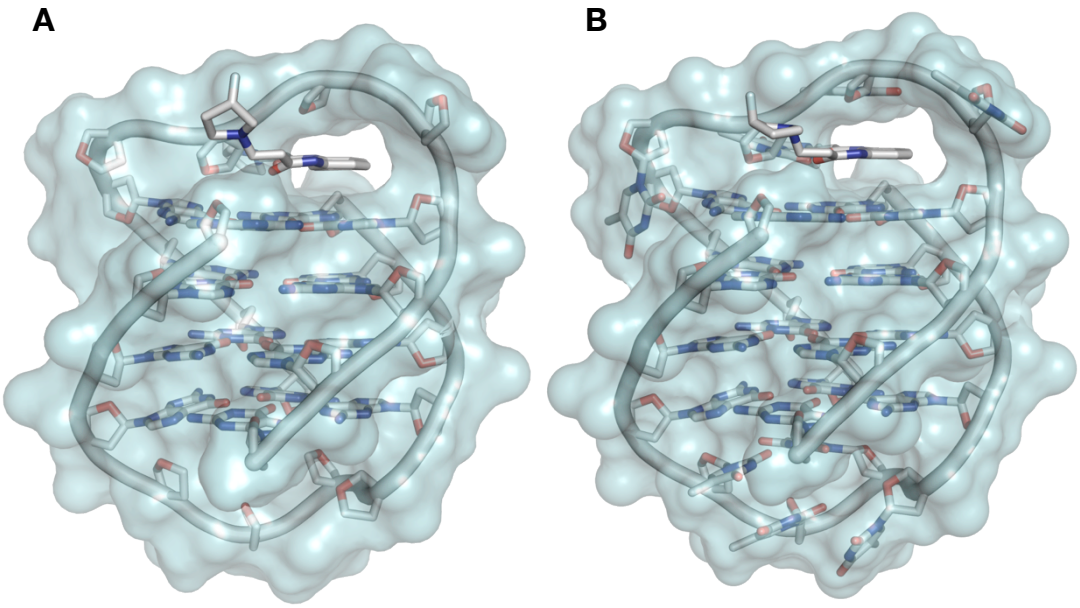


**Figure 3.13.** Surface representation in cyan with 50% transparency. The binding cleft of the fluorinated BSU6039 ligands can be clearly seen at the top of both structures. **A** - (*S,S*)-**144** & **B** - (*R,R*)-**144**. Generated with PyMOL. [129]

The unity of the electron density maps in structures (*R,R*)- and (*S,S*)-**144** correlates well with the resolution of the data, and enables a high degree of certainty in assigning atom coordinates (Figure 3.14 & 3.15). Where the electron density is poorly resolved, the crystallographer must use chemical intuition in fitting the structure. In Figures 3.14 & 3.15, the structures are represented according to the preset b-factor colours (COOT package), with cool (blue/green) and hot (yellow/red) representing low and high disorder of the atoms relative to one another. The b-factor is an important parameter of the solved data providing an appropriate measurement of the static/dynamic nature of the atoms within the crystal structure. It is intrinsically linked to the occupancy factor for each atom. The occupancy factor (0.10–1.00) is used in conjunction with the b-factor data to provide information about the precise geometry of substituents within the structure.

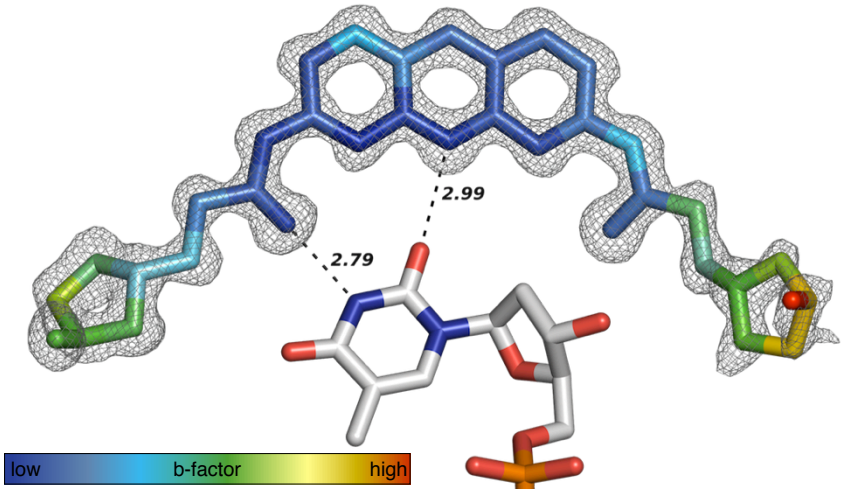


**Figure 3.14.** Electron density maps for (*S,S*)-**144** *Oxytricha nova* quadruplex DNA. Represented at the σ = 1 level using the COOT package.[187] Distances are in Å.

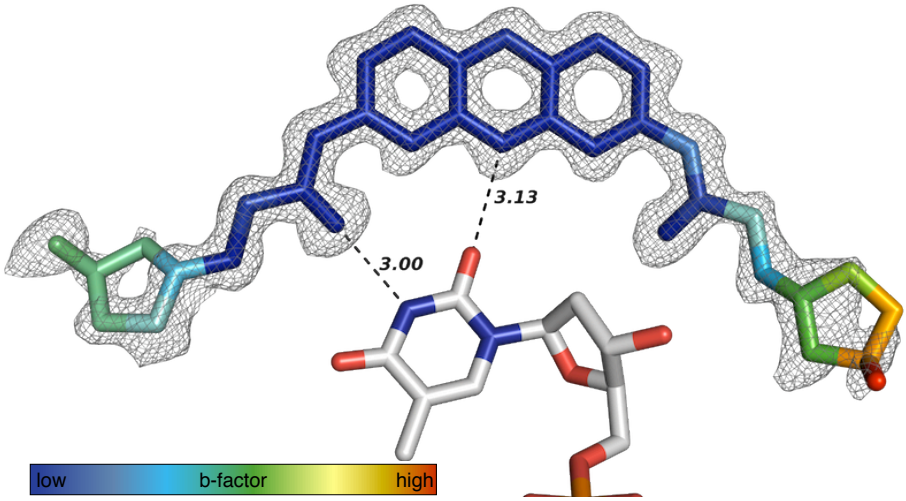


**Figure 3.15.** Electron density maps for (*R,R*)-**144** with *Oxytricha nova* quadruplex DNA. Represented at the σ = 1 level generated with the COOT package.[187] Distances are in Å.

The occupancy and b-factors (Table 3.01 and Figure 3.14/3.15) for each atom correlate well with the hydrogen bonding and electrostatic interactions, suggesting their contribution to structural stability.

| | Acridine nitrogen | Pyrrolidine-N (LHS/RHS) | C–F (LHS/RHS) | C–F (LHS/RHS) |
|---|---|---|---|---|
| BSU6039 (2.4 Å) | 9.04 | 33.96 / 25.65 | N/A | N/A |
| (*S,S*)-**144** (1.10 Å) | 6.73 | 11.03 / 18.65 | 17.21 / 37.35 | 11.03 / 18.65 |
| (*R,R*)-**144** (1.18 Å) | 8.05 | 17.54 / 25.77 | 23.56 / 56.09 | 17.54 / 25.77 |

**Table 3.01.** b-Factors for the crystal structures with BSU6039 **141a**, (*S,S*)-**144** and (*S,S*)-**144**

### *3.5.3 - Detailed assessment of the DNA co-crystal with (S,S)-144*

The structure of BSU6039 **141a**, discussed in Chapter 2.16 is reproduced for comparison (Figure 3.16). The (*S,S*)-**144** bound ligand is considered in Figure 3.17.

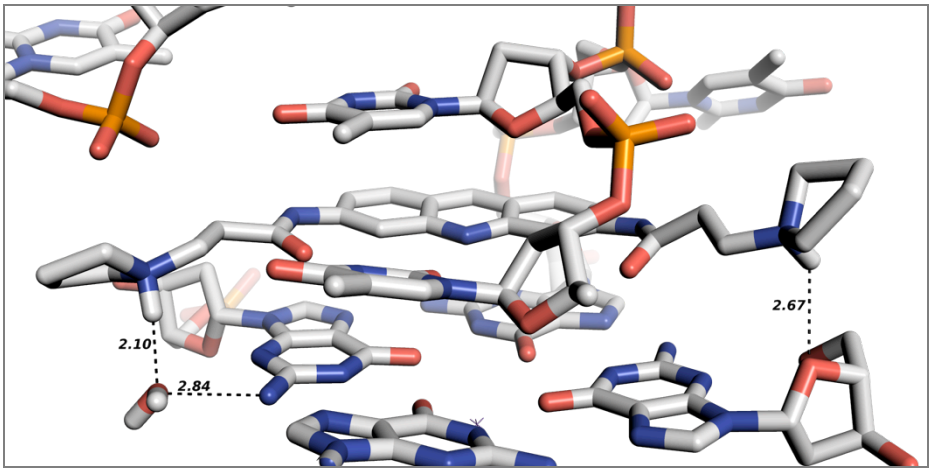


**Figure 3.16**. Hydrogen bonding and electrostatic interaction distances found in the BSU6039 **141a** crystal structure. Distances are in Å.

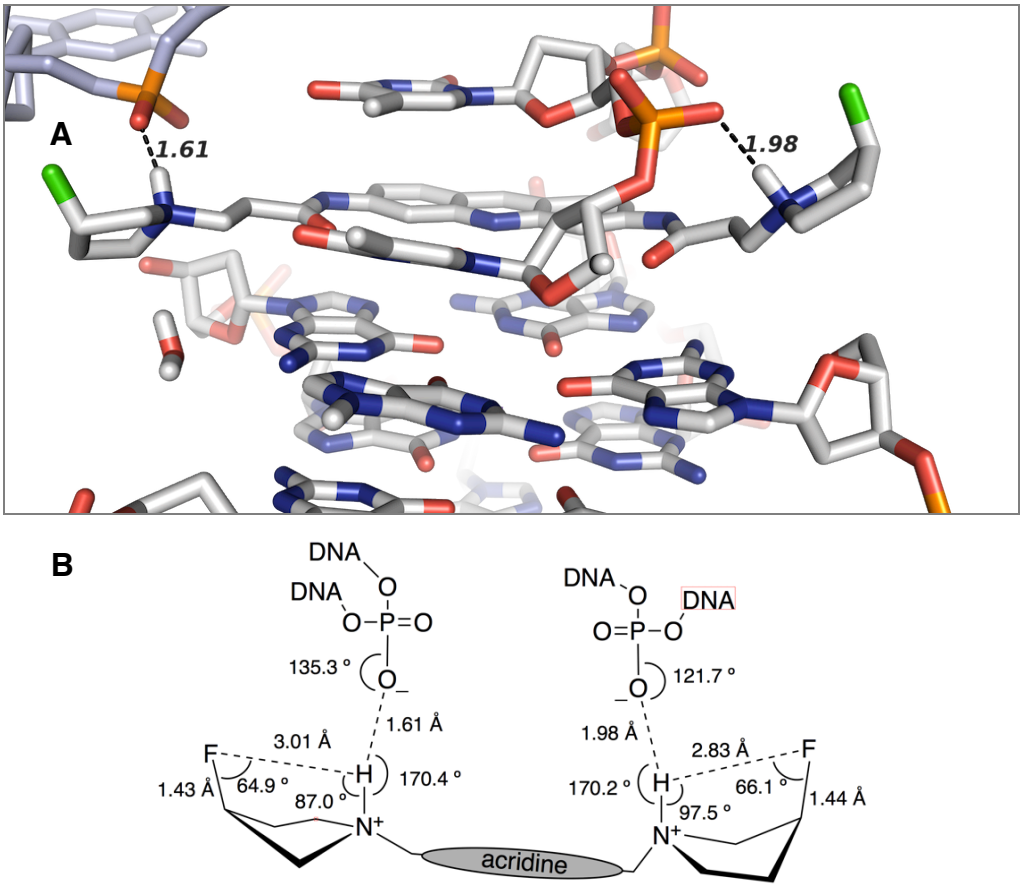


**Figure 3.17**. **A** - Expanded section of the mode of binding for ligand (*S,S*)-**144** with quadruplex DNA & **B** - graphical summary of angles and bond lengths. Distances are in Å.

The most notable difference in the binding of fluorinated (*S,S*)-**144** (Figure 3.17) over non-fluorinated BSU6039 **141a** (Figure 3.16) is that the fluoropyrrolidine rings have rotated by 180º and are forming new contacts within the crystal structure. Interestingly, in the left hand side (LHS) of the binding pocket (Figure 3.17), the N–H of the pyrrolidine is no longer forming a hydrogen bond with a crystallographically resolved water molecule. This water molecule is observed in all structures of this series and presumably plays an important role in the stabilisation of the guanine tetrad through a hydrogen-bonding network between the pyrrolidine and the guanine base (Figure 3.17). In fact, the pyrrolidine N–H of the structure with (*S,S*)-**144** now forms a hydrogen bond with a phosphate on a neighbouring quadruplex within the unit cell. It may be the change in the p$K_a$ of the pyrrolidine substituent, due to fluorine incorporation, is responsible for the change in hydrogen bonding partner. The trajectory of the $N^+$–H···$^-$O–P hydrogen bond is close to 180º and the H···O distance is short at <1.7 Å (Figure 3.17, B), correlating well with the more acidic hydrogen bonding to the basic

phosphate to result in a 'strong' hydrogen bond. The observed occupancy factors (F = 1.00 and N = 1.00) and a good fit with the electron density map (Figure 3.14), suggest high order and a stable hydrogen bonding interaction. The pyrrolidine ring is clearly puckered as a result of the C–F···N–$H^+$ dipole-charge interaction, with a F–C–C–N angle of approximately 90º.

A similar situation occurs at the RHS of the crystal structure (Figure 3.17) where again the pyrrolidine N–H directionality has rotated through 180º relative to BSU6039 **141a** (Figure 3.15) and a hydrogen bond forms now with the phosphate backbone, albeit with a longer N–H···O–P contact (Figure 3.17) of 1.98 Å. The b-factors for the atoms in this ring are lower (Table 3.01) perhaps suggesting a weaker hydrogen bond between this pyrrolidine ring and the phosphate. As with the LHS, the RHS pyrrolidine ring is also puckered, with the C–F bond occupying a dramatic axial orientation (fluorine occupancy = 1.00). The distance between the N–H and C–F bond (~3.0 Å) and the narrow angle (< 100º) in both of the rings in (*S,S*)-**144** preclude a reasonable hydrogen bond but are consistent with a charge-dipole interaction as discussed in Chapter 1.

### *3.5.4 - Detailed assessment of the DNA co-crystal with (R,R)-**144***

Examination of the binding mode of (*R,R*)-**144** (Figure 3.18) with the quadruplex, reveals a similar change in pyrrolidine ring orientation relative to BSU6039 **141a** (Figure 3.16). On the LHS of the structure (Figure 3.18, A) again the N–H of the pyrrolidine forms a hydrogen bond (Figure 3.18, B) with a phosphate group of a neighbouring quadruplex within the unit cell. The C–F bond is also axial (fluorine occupancy = 0.90), exhibiting a similar conformational bias to that observed for (*S,S*)-**144** (Figure 3.17).

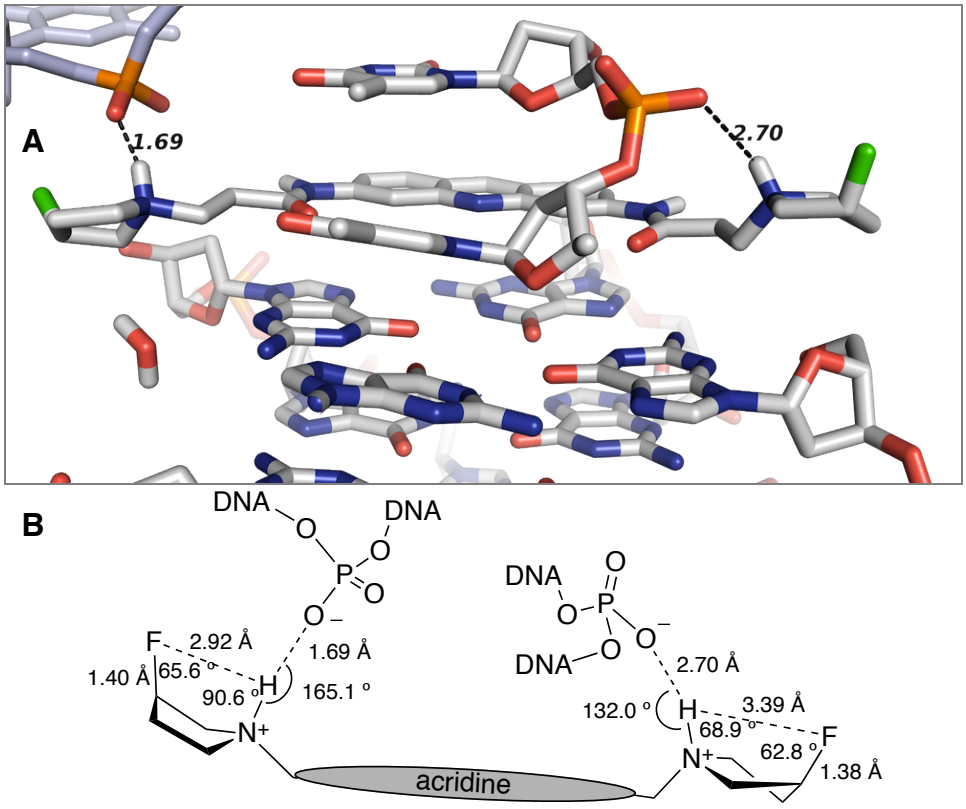


**Figure 3.18**. Expanded section of the mode of binding for ligand (*R,R*)-**144** with quadruplex DNA & **B** - graphical summary of angles and bond lengths. Distances are in Å.

The b-factors for the LHS of the X-ray structure of the co-crystalline (*R,R*)-**144** with DNA (Table 3.01) although slightly higher than for (*S,S*)-**144**, remain low compared to **141a** and indicate high resolution data. In the RHS binding pocket, it is clear that the co-crystalline DNA-(*R,R*)-**144** structure the interaction between the pyrrolidine ring and the phosphate group is more electrostatic in nature. This is deduced from the longer $N^{+}$–H···$^{-}$O–P contact distance and non-linear contact angle (Figure 3.18, B), which are out-with the topological parameters for a strong hydrogen bond. Based on this observation, it is anticipated that the tolerance of the RHS binding interaction is less favourable to accommodating the fluorine in the pyrrolidine ring. The orientation of the C–F bond, in the case of (*R,R*)-**144**, possibly positions the C–F bond closer to the phosphate resulting in a charge-dipole repulsion. The stereospecific incorporation of a C–F bond in this manner can lead to a diastereotopic difference in the topology of binding between the two enantiomers (*S,S*)- and (*R,R*)-**144**, altering their relative modes of binding.

## 3.6 - FRET studies with quadruplex DNA

The melting temperatures of co-complexes between the **144** and **145** series with quadruplex DNA were measured. This enabled the assessment of the relative stability of quadruplex DNA following addition of (*S,S*)- or (*R,R*)-**144** and **145**. For this application, the monomeric human quadruplex DNA sequence $G_3(T_2AG_3)_3$ with the donor and acceptor appendages TAMRA and FAM, as described in Chapter 2, were employed. These experiments were carried out in triplicate with 1 $\mu$M of (*S,S*)- or (*R,R*)-**144** and **145** (Table 3.02. By Tony Respka, UCL).

| Sample | Concentration | Run1 (ºC) | Run 2 (ºC) | Run 3 (ºC) | Average $T_m$ (ºC) | $dT_m$ (ºC) |
|---|---|---|---|---|---|---|
| DNA control | N/A | 58.6 | 58.7 | 58.7 | 58.7 | N/A |
| (*R,R*)-**144** | 1 $\mu$M | 62.8 | 63.4 | 63.3 | 63.2 | 4.5 ± 0.4 |
| (*S,S*)-**144** | 1 $\mu$M | 64.9 | 64.7 | 64.7 | 64.8 | 6.1 ± 0.2 |
| (*R,R*)-**145** | 1 $\mu$M | 71.0 | 71.1 | 71.2 | 71.1 | 12.4 ± 0.2 |
| (*S,S*)-**145** | 1 $\mu$M | 71.1 | 71.3 | 71.3 | 71.2 | 12.6 ± 0.2 |
| BSU6039 | 1 $\mu$M | - | - | - | - | 13.3 |

**Table 3.02.** Results from the FRET based assessment of (*R,R*)- and (*S,S*)-**144** and **145**. Errors by standard deviation of the mean and are reported to 1 DP.

Both types of ligands stabilised the quadruplex, however the fluorinated ligands (*S,S*)-and (*R,R*)-**144** resulted in a lower overall stabilisation of the fold relative to BSU6039 **141a**. This difference is difficult to quantify empirically, however it is likely that change in orientation of hydrogen bonding observed for the C–F ligands relative to BSU6039 **141a** weakens the structures. By contrast the hydroxyl compounds (*S,S*)- and (*R,R*)-**145** demonstrated a much better stabilisation compared to BSU6039 **142a**. These results show that the C–F bond in the peripheral pyrrolidines perturbs the mode of binding more than that of the C–OH bond.

## 3.7 - Conclusion

This chapter reports the synthesis of the (*S,S*)-/(*R,R*)-fluoro **144** and (*S,S*)-/(*R,R*)-hydroxy **145** analogues of BSU6039 **141a**. The fluoro analogues were successfully co-crystallised with the bimolecular *O. nova* quadruplex DNA and the X-ray structures were solved to high resolution. This data enabled a detailed assessment of the mode of binding between the two enantiomers of **144** and relative to BSU6039 **141a**. This analysis demonstrated that the C–F bond orientated in an axial position, consistent with the anticipated literature and that the hydrogen bonding network between the quadruplex DNA and ligand changed. In these structures with (*S,S*)- and (*R,R*)-**144** the pyrrolidine N–H had rotated by 180º and paired with the phosphate backbone to form new hydrogen bonding interactions. Further to this, FRET analysis indicates that the fluorinated derivatives increased the stability of the quadruplex fold, however to a lesser extent when compared to BSU6039 **141a**. This may be explained by the hydrogen-bond differences observed in the co-crystal structures. Overall, the incorporation of a C–F bond in the peripheral pyrrolidines leads to a ring pucker and perturbed the mode of binding to quadruplex DNA.

# Chapter 4

# Synthesis of C–F bond incorporated BRACO-19 analogues

## 4.1 - Introduction

This chapter describes the synthesis of an enantiomeric pair of 3- and 6- substituted di-fluorinated analogues (**152**) of BRACO-19 (**142a**) (Figure 4.01), to investigate if the C–F bonds can induce an improved binding conformation over BRACO-19 **142a** to quadruplex DNA.

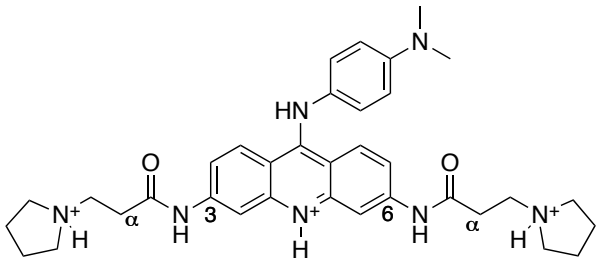

**142a**

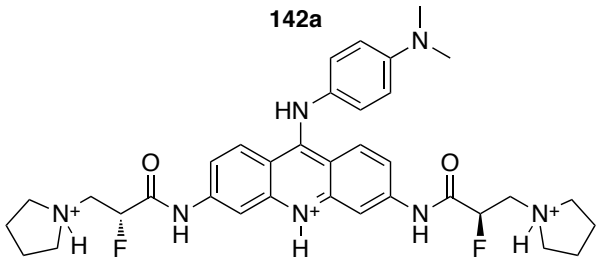

(*R,R*)-**152**

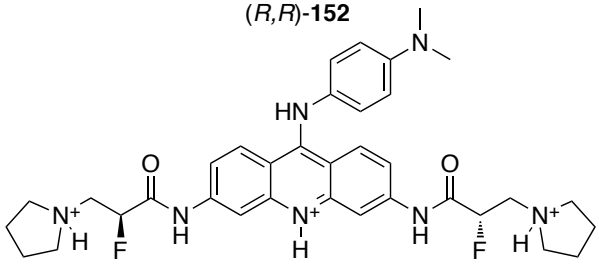

(*S,S*)-**152**

**Figure 4.01**. BRACO-19 **142a** & 3,6-C–F bond substituted BRACO-19 **152** analogues.

In BRACO-19 **142a**, the amino groups of the pyrrolidine substituents are protonated at physiological pH, thus stereospecific C–F bond incorporation in the $\alpha$-amide positions will exert a stereoelectronic influence to provide enantiomeric conformations of (*R,R*)- and (*S,S*)-**152**. This conformational bias is anticipated to arise for two reasons, charge-dipole compensation between C–F and $N^{+}$–H bonds and the $\alpha$-fluoroamide effect (Figure 4.01).

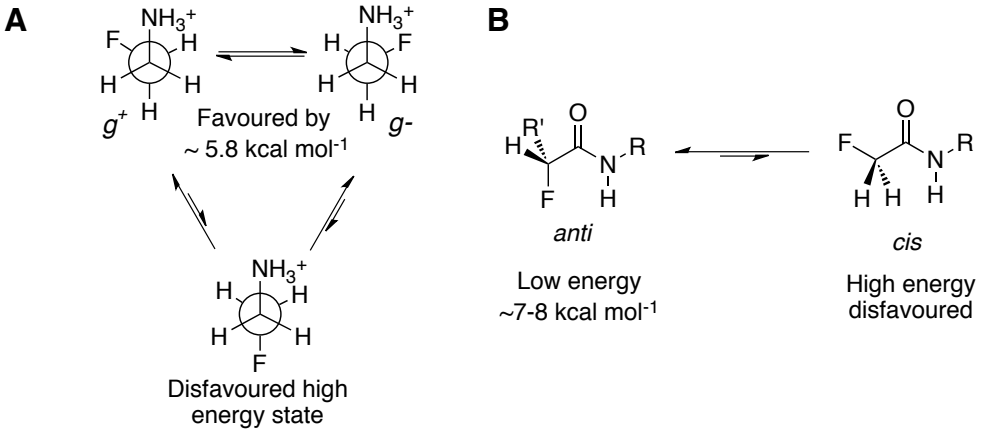


**Scheme 4.01**. The charge-dipole effect (**A**) and $\alpha$-fluoroamide effect (**B**). R/R' = H, $CH_3$.

Therefore, for each stereoisomer, the C–F bond will orientate *anti* to the carbonyl, extending the planarity of the amide bond (Figure 4.01). Also, the protonated ring amine will align $g^{+}$ or $g^{-}$ relative to the C–F bond through the charge-dipole effect (Chapter 1). Thus, the (*R,R*)-stereoisomer of **152** should have an enantiomeric twist relative to the (*S,S*)-stereoisomer (Figure 4.02).[19]

The conformational bias induced in **152** will force the charged pyrrolidine substituents to orientate towards the phosphate grooves of a quadruplex DNA fold. Thus, this conformation will be in contrast to the planar binding mode of BRACO-19 **142a** with quadruplex DNA (Figure 2.18). This conformational bias coupled with the change in $pK_a^H$ of the pyrrolidine nitrogen, as a result of C–F bond incorporation, will generate the potential for new hydrogen bonds between **152** and the phosphate backbone of quadruplex DNA structure. This altered binding conformation is hypothesised to result in a stronger complementary binding between **152** and quadruplex DNA and thus stabilise the DNA fold more than that of BRACO-19 **142a**.

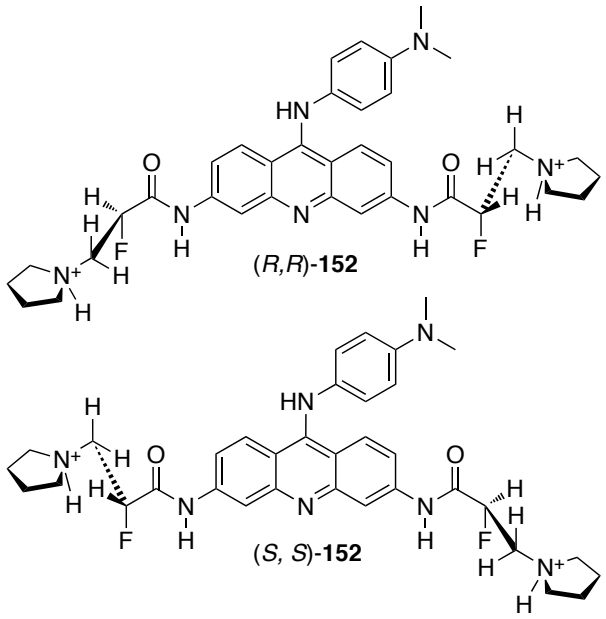


**Figure 4.02.** Conformational representations of the influence of the C–F bond in fluorinated BRACO-19 analogues **152**.

## 4.2 - Aims

It therefore became a research objective to prepare the (*R,R*)- and (*S,S*)- enantiomers of **152**. A retrosynthesis is shown in Scheme 4.02.

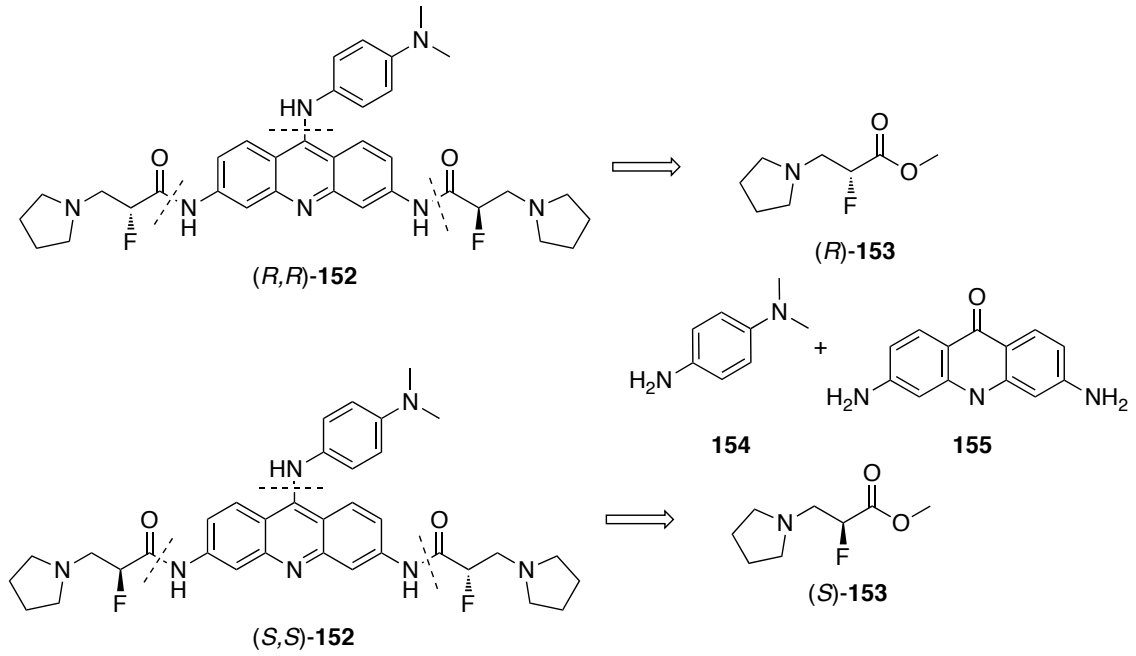


**Scheme 4.02**. Retrosynthetic approach to the synthesis of $\alpha$-fluorinated BRACO-19 **152** analogues.

A key step in the synthesis involved the preparation of each enantiomer of the fluorinated amino ester **153**.

## 4.3 - Synthesis of an $\alpha$-fluoro-$\beta$-amino acid

As highlighted in Chapter 1, Deniau *et al*., employed a DAST **32** mediated approach for the synthesis GABA analogues **110**.[87] Treating $\beta$-amino alcohol (*R*)-**157** with DAST **32** resulted in fluorination to furnish (*S*)-**158** in a stereospecific manner. The benzyl protected amine **158** could be further manipulated to 3-fluoro GABA (*S*)-**110** after oxidation of the aromatic ring and subsequent deprotection of the amine (Scheme 4.03).

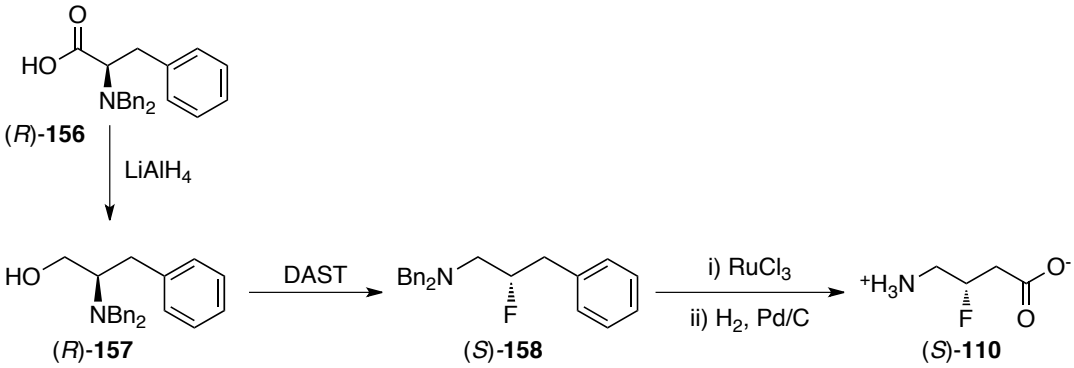


**Scheme 4.03**. *S*ynthesis of 3-fluoro GABA (*S*)-**110**.

The rearrangement and fluorination arise from the aziridinium intermediate **160** formed from $S_Ni$ attack of the nitrogen lone pair at the $\beta$-carbon following activation of the alcohol by DAST **159** (Scheme 4.04).[188] The transient intermediate **160** can either be fluorinated in the $\alpha$- or $\beta$-positions respectively by $S_N2$ attack of fluoride (Scheme 4.04).

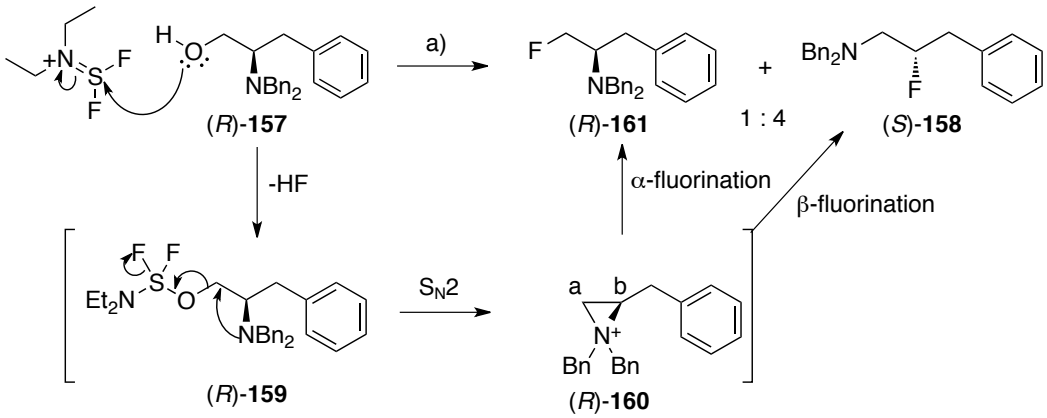


**Scheme 4.04**. Mechanism of DAST **32** mediated fluorination of $\beta$-amino alcohols

Nucleophilic attack of fluoride to the $\alpha$-position leads to the substitution product (*R*)-**161**, whereas attack at the $\beta$-position results in the rearranged product (*S*)-**158** and with an inversion of stereochemistry (Scheme 4.04). In this particular example the fluorination proceeds with a 4:1 selectivity in favour of the $\beta$-fluorinated product.

The fluorination of esters of the natural amino acid L-serine, with DAST **32**, also undergoes this rearrangement to furnish esters, (*R*)-**120** and (*S*)-**163** respectively (Scheme 4.05). This transformation typically proceeds with high $\alpha$-fluorination selectivity and with excellent enantiocontrol.[95]

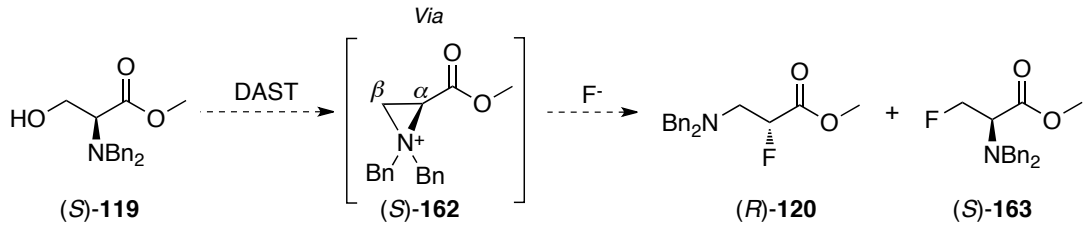


**Scheme 4.05**. Putative aziridinium intermediate formed during fluorination of benzyl protected (*S*)-serine methyl ester (*S*)-**119**.

The approach seemed appropriate for the synthesis of (*R*)- and (*S*)-**153**. The only concern was the tolerance of the functional groups on the nitrogen. Only benzyl protecting groups are reported in the literature for this transformation.[95]

The dialkyl amino acid **119** was first prepared from methyl ester **165**. Starting with racemic serine **164**, the methyl ester **165** could be synthesised on a gram scale by treatment with thionyl chloride in methanol (Scheme 4.06). Treatment of **165** with benzyl bromide and potassium carbonate enabled a straightforward preparation of **119** in good yield (94%) (Scheme 4.06), ready for fluorination with DAST **32**

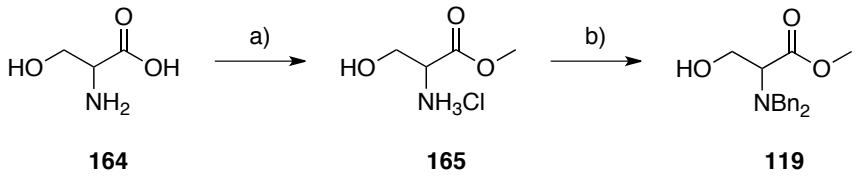


**Scheme 4.06.** *Reagents and conditions*: a) $SOCl_2$, MeOH, rt, 24 h and b) Benzyl bromide (2.2 eq), $K_2CO_3$ (4 eq), MeCN, rt, 24 h, 94%.

The reaction between alcohol **119** and DAST **32** in THF (Scheme 4.07) was monitored by $^{19}F$ NMR spectroscopy, which revealed the presence of the $\alpha$- and $\beta$-products, with signals at -190 ppm and -220 ppm.

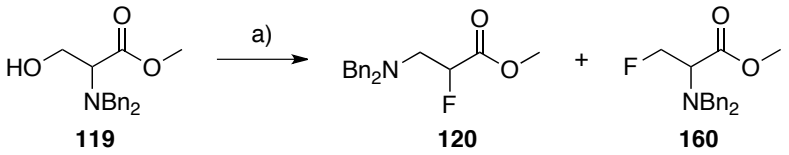


**119** **120** **160**

**Scheme 4.07.** *Reagents and conditions:* DAST **32** (1.1 eq), THF, 0 ºC, 1 h, 90%.

The major product was the $\alpha$-isomer **120,** which was formed with 95:5 selectivity over the $\beta$-isomer **163**. This reaction scaled well and the $\alpha$-isomer **120** was isolated in excellent yield (90%). This procedure was repeated with enantiopure D- and L-serine **164** and furnished the individual enantiomers (*S*)- and (*R*)-**120** in gram quantities with excellent enantiocontrol (>90% ee) as analysed by chiral HPLC (ChiralCel OD-H).

Debenzylation of methyl ester **120** was not straightforward. Classical hydrogenation conditions using 10% Pd/C in methanol or ethyl acetate under a hydrogen atmosphere was unsuccessful (Scheme 4.08).

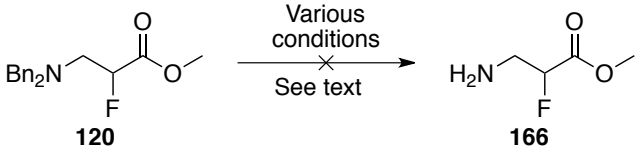


**120** **166**

**Scheme 4.08.** Hydrogenation of benzyl protected ester **120** gave multiple products.

In these reactions, analysis of the reaction product by $^{19}F$ NMR showed various fluorinated products, which could not be separated by standard reverse phase chromatography. These products could not be identified other than containing desired amine **166**. The addition of acid during the reaction resulted in elimination forming acrylate type products as confirmed by $^{19}F$ NMR. Successful debenzylation of **120** was achieved with $Pd(OH)_2/C$ in methanol, with ester **166** isolated in quantitative yield (Scheme 4.09). However, this reaction was unreliable and readily gave multiple products despite successful literature reports.[189,94,190]

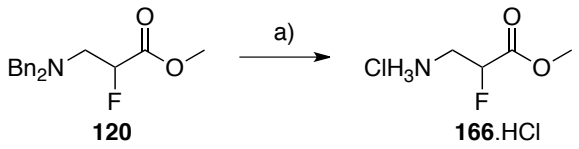


**120** **166**.HCl

**Scheme 4.09.** *Reagents and conditions:* a) $Pd(OH)_2/C$, $H_2$, MeOH, 24 h followed by HCl (1 M), 99%.

When the debenzylation was followed by $^{19}F\{^1H\}$ NMR, only one product at -200 ppm was observed, presumably the debenzylated material **166**. However, purification through Celite led to degradation. Thus, in an attempt to isolate amine **166** it was protected as its carbamate ester *in situ* following removal of the palladium catalyst by filtration, without addition of HCl to the mixture (Scheme 4.10).

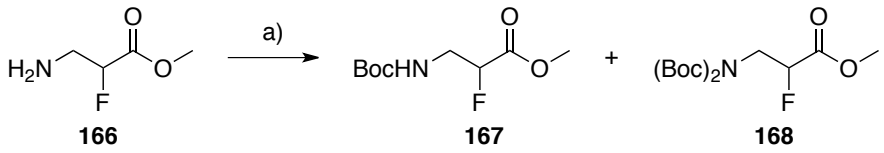


**166** **167** **168**

**Scheme 4.10**. *Reagents and conditions:* a) $Boc_2O$, $Et_3N$, aqueous dioxane (25% v/v), rt, 24 h.

The $^{19}F\{^1H\}$ NMR spectrum of this mixture again indicated a complex mixture from which both **167** and **168** could not be isolated cleanly as they co-eluted with multiple unidentifiable products, although the $^1H$ NMR spectrum had no evidence for aromatic residues. Due to the nature of this complex product mixture this approach proved unsuccessful and was discontinued.

### *4.3.1 - Pyrrolidine functionalisation of **166***

The double alkylation of **166**.HCl to form a pyrrolidine ring was next investigated. This involved treating the amine with 1,4-dibromobutane and a catalytic amount of TBAI (Scheme 4.11).

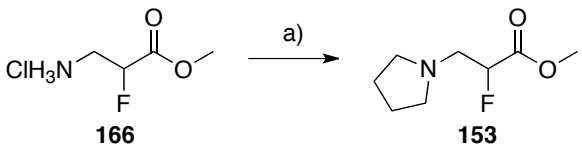


**166** **153**

**Scheme 4.11**. *Reagents and conditions:* 1,4-Dibromobutane (1.1 eq), TBAI (0.2 eq), $Na_2CO_3$ (4.0 eq), MeCN, reflux, 4 h, 77%.

Pyrrolidine **153** was isolated in good yield (77%) following purification by chromatography. However, this route was not practical for the synthesis of **153**, with the inefficient debenzylation step limiting the quantity of amine **166** available. Therefore an alternative approach was sought, which involved debenzylation after amide coupling to the acridone core (Scheme 4.12).

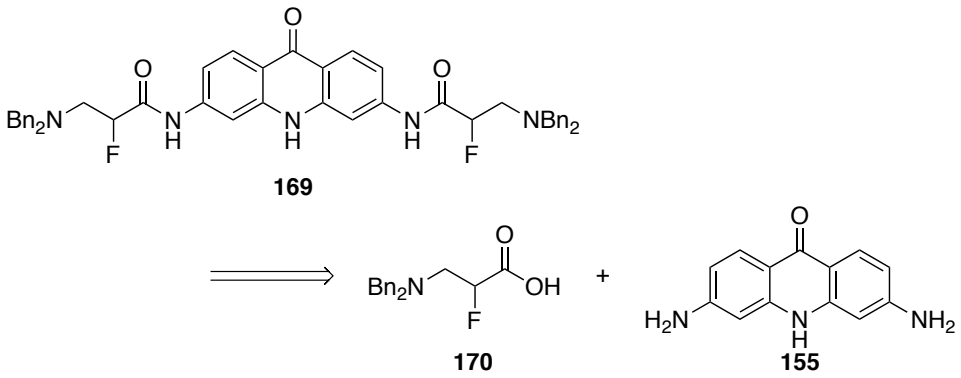


**Scheme 4.12**. Proposed amide coupling route to functionalise acridone **169**.

In order to investigate amide coupling to acridone **155**, the methyl ester **120** required hydrolysis to carboxylic acid **170**. This was achieved with KOH in methanol and generated (*R*)-**170** in 97% yield (Scheme 4.13).

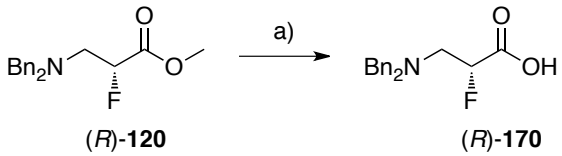


**Scheme 4.13.** *Reagents and conditions:* KOH, MeOH, rt, 36 h, 97%.

The reaction was repeated also for the (*S*)-**170** enantiomer. Thus with the carboxylic acids (*R*)- and (*S*)-**170** available, it was next required to synthesise acridone **155**.

## 4.4 - Acridone 155 synthesis

The synthesis of acridone **155**, the structural core of BRACO-19 **142a**, was carried out according to a literature method.[191,192] The tetranitro diphenylmethane **172** was prepared from diphenyl methane **171** in refluxing sulfuric acid with potassium nitrate (Scheme 4.14). The reaction product was recrystallised from acetic acid and furnished **172** in good yield (74%). Oxidation to benzophenone **173** was high yielding (95%) and

was achieved by refluxing **172** with chromium trioxide in acetic acid (Scheme 4.14).

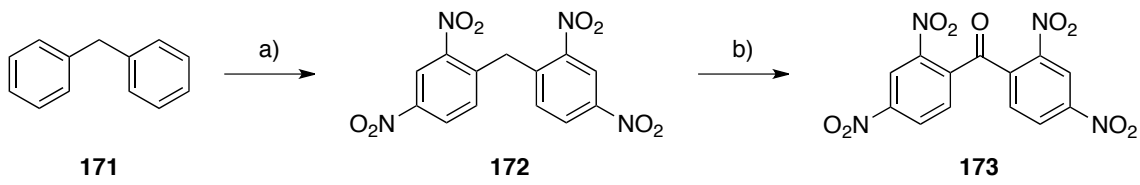


**171** **172** **173**

**Scheme 4.14.** *Reagents and conditions*: a) $KNO_3$, $H_2SO_4$ (conc), 70 °C, 2 h, 74%; b) $CrO_3$, acetic acid, 118 °C, 16 h, 95%.

The nitro-groups of the benzophenone derivative **173** were reduced by refluxing with a large excess of tin(II) chloride in hydrochloric acid. This also facilitated ring closure to form acridone **155** with the 3,6-diamino regiochemistry (Scheme 4.15).

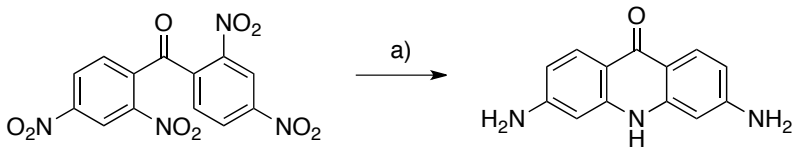


**173** **155**

**Scheme 4.15**. *Reagents and conditions:* a) $SnCl_2$, HCl (conc.), EtOH, reflux, 3 h, 63%.

Acridone **155** is a clay-like solid that was difficult to manipulate and had poor solubility in DMSO, DMF or DMAc. Despite this, it was possible to obtain an $^1$H NMR spectrum in $d_6$-DMSO where both $NH_2$ and NH resonances could be assigned in-line with the literature.[191]

## 4.5 - Coupling reactions with diaminoacridine 155

With suitable quantities of acridone **155** in hand, it was now possible to investigate coupling conditions with the fluorinated amino acid **170**. There is limited literature on the chemistry of acridone **155**. In the synthesis of BRACO-19 **142a**, 3-chloropropionyl chloride **148** is used as the reaction solvent under forcing conditions to prepare amide **174** (Scheme 4.16),[191] with a microwave irradiation approach also requiring a significant excess of the acid chloride **148**.[184] Another approach to form amides on acridone **155**, employed 1:1 mixtures of acid anhydrides under forcing conditions, to prepare acetamides such as **175** (Scheme 4.16).[193]

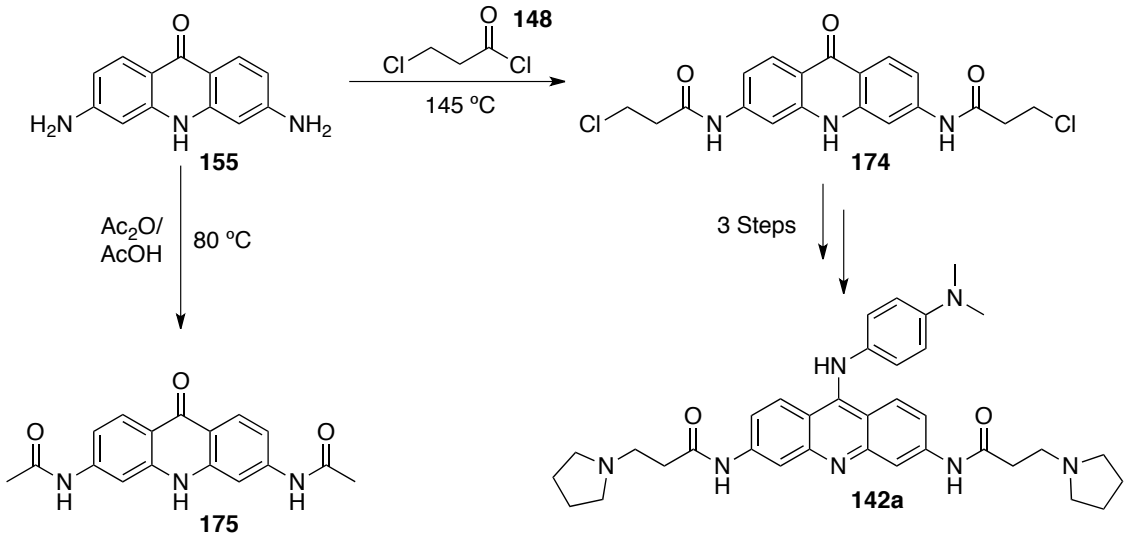


**Scheme 4.16**. Synthesis of bis-chloro and acetamide acridones.

From these examples it is clear that forcing conditions are required but in our case a large excess of fluorinated amino acid is not practical. Alternative efforts with practical equivalents of acid chloride **176** were investigated. Initially, 2.5 equivalents of the acid chloride **176**, which was formed *in situ* from with thionyl chloride and directly added to acridone **155** in DMAc, was explored (Scheme 4.17).

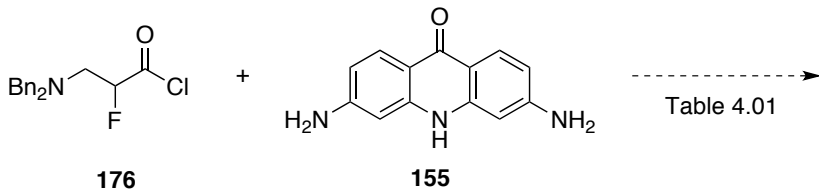


**Scheme 4.17**. Attempted coupling of acid chloride **176** to acridone **155**. Conditions are summarised in Table 4.01.

The use of $^{19}F\{^{1}H\}$ NMR with unquenched reaction aliquots was useful in following this reaction as both acid **170** and acid chloride **176** have characteristic chemical shifts. However, these reactions, which were heated over extended time periods, failed to give product as judged by TLC and $^{19}F\{^{1}H\}$ NMR. Alternative conditions with different equivalents of acid or with different reagents were attempted (Table 4.01), but in each case no product could be observed.

| Entry | Acid equiv. | Reagent | Base | Solvent | Temp (ºC) | Time (h) |
|---|---|---|---|---|---|---|
| 1 | 2.5 | $SOCl_2$ | $Na_2CO_3$ | DMAc | 100 | 24-48 |
| 2 | 2.5 | $SOCl_2$ | $Na_2CO_3$ | DMAc | 160 | 24 |
| 3 | 20 | $SOCl_2$ | - | DMAc | 160 | 24 |
| 4 | 20 | $SOCl_2$ | $Na_2CO_3$ | DMAc | 100 | 48 |
| 5 | 20 | $SOCl_2$ | pyridine | DMAc | 100 | 24 |
| 6 | 20 | $SOCl_2$ | DMAP | DMAc | 100 | 24 |
| 7 | 2.5 | cyanuric fluoride | pyridine | DMAc | 100 | 16 |
| 8 | 4 | Ethyl chloroformate | NMM | DMAc | rt | >24 |
| 9 | 4 | Benzyl chloroformate | NMM | DMAc | rt | >24 |
| 10 | 2.5 | EDC + HOBt | NMM | DMF | rt | >24 |
| 11 | 2.5 | EDC + HOBt | DiPEA | DMF | rt | 24 |
| 12 | 2.5 | EDC + HOBt | DiPEA + DMAP (cat.) | DMF | rt | 24 |
| 13 | 2.5 | EDC + HOBt | DiPEA | DMF | 60 | 24 |
| 14 | 2.5 | HBTU | DiPEA | DMF | rt | 24 |
| 15 | 2.5 | HATU | DiPEA | DMF | rt | 24 |

**Table 4.01**. Attempted conditions for the coupling of acid **170** with acridone **155**. In all cases there was no evidence for the formation of product **166**.

It was clear that the nucleophilicity of the amine in acridone **155** is insufficient for amide bond formation by classical means. An alternative literature approach employing metal amides, such as **178**, for the synthesis of aromatic amides such as **180** was subsequently explored (Scheme 4.18).[194,195]

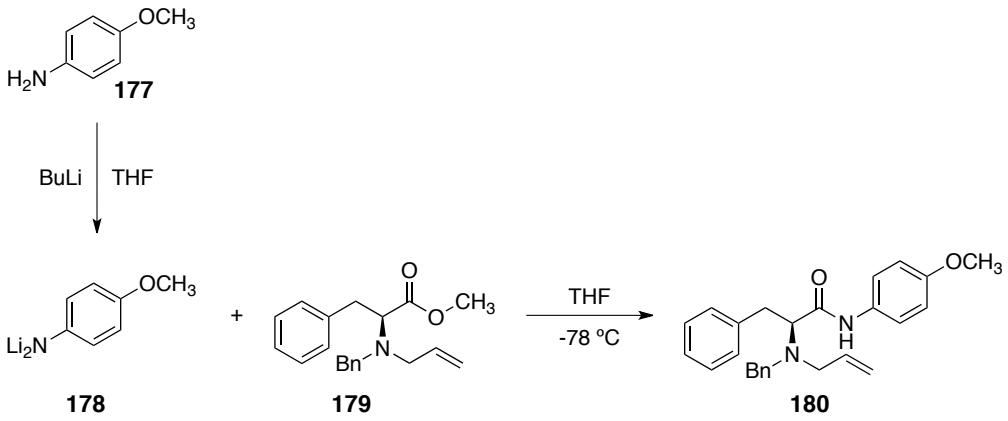


**Scheme 4.18.** Generation of the *bis*-lithium amide for the aminolysis reaction.

This was an attractive alternative for the construction of the desired acridone **169** (Scheme 4.19).

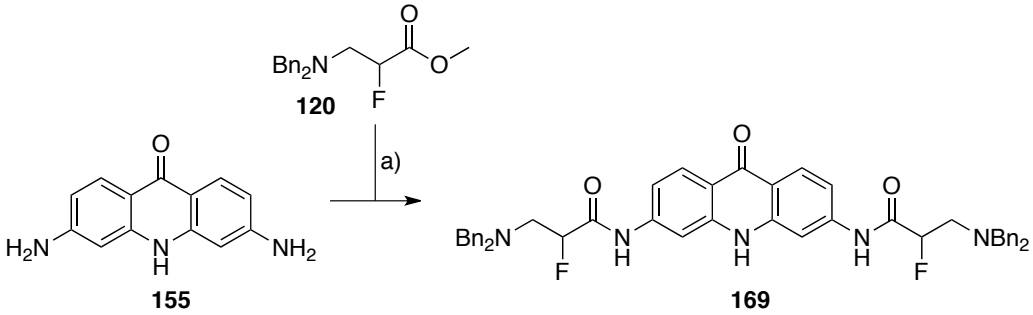


**Scheme 4.19.** *Reagents and conditions:* BuLi (4 eq), THF, -78 ºC, 1 h, followed by **120**, -78 ºC, 3 h, <10%.

The solubility of acridone **155** in THF was problematic, however the addition of BuLi brought the acridone into solution, resulting in a homogenous yellow solution. The addition of fluorinated ester **120** maintained this colour. Monitoring of the reaction by TLC and $^{19}F\{^{1}H\}$ NMR indicated multiple products. Separation of these products by column chromatography enabled the isolation of the coupled acridone **169**, although in low yield (<10%). The remaining products from the reaction, which were both non-fluorinated and fluorinated, could not be identified. Subsequent optimisation of the reaction conditions showed that treatment of acridone **155** with KHMDS followed by the addition of ester **120** in THF at -78 ºC *via* cannula, resulted in a modest improvement in the reaction yield (19%).

Treating acridone **169** with neat phosphorus oxychloride gave the 9-chloro intermediate **181**, which was reacted directly with *N*,*N*-dimethylaminoaniline **154** in chloroform (Scheme 4.20).

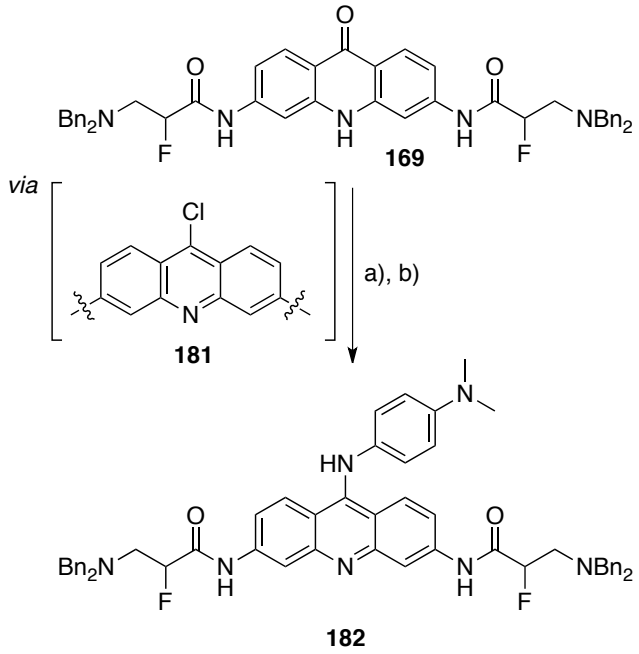


**Scheme 4.20.** *Reagents and conditions:* $POCl_3$ (neat), 105 ºC, 3 h and b) *N*,*N*-dimethylaminoaniline **154** (10 eq), $CHCl_3$, reflux, 2 h, 23% over two steps.

Decomposition of aniline **154** complicated both TLC analysis of the reaction and also the subsequent purification of racemic acridine **182**. Multiple columns were required to obtain a pure sample of the trisubstituted product **182**. The HCl salt of **182** was particularly insoluble and was not suitable for DNA quadruplex binding studies.

### *4.5.1 - Debenzylation of acridone **169***

It was evident that the benzyl groups of **182** gave an unsuitable non-drug like compound, thus removal of the benzyl groups of acridone **169** was explored. Various conditions (Table 4.02) were attempted (Scheme 4.21), however, multiple products were observed ($^{19}F\{^1H\}$ NMR analysis), similar to that obtained with ester **120**.

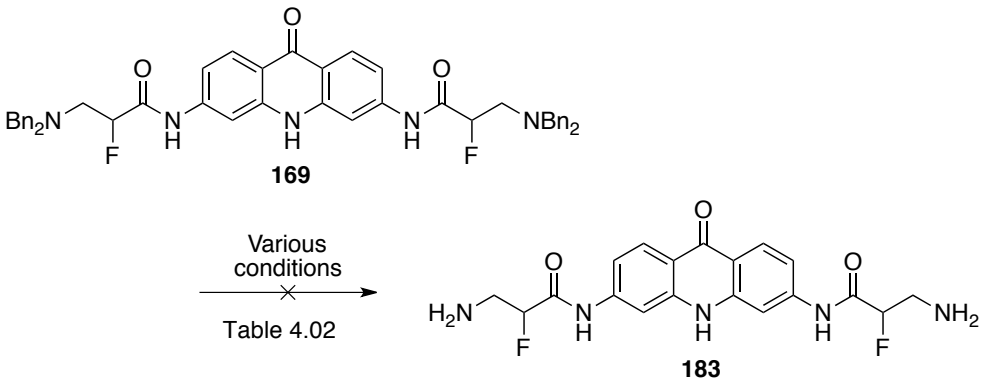


**Scheme 4.21**. Debenzylation of acridone **169**.

| Entry | Catalyst | Solvent | Temp. | Pressure |
|---|---|---|---|---|
| 1 | 10% Pd/C | $CH_3OH$ | rt | atm |
| 2 | 20% $Pd(OH)_2/C$ | $CH_3OH$ | rt | atm |
| 3 | 20% $Pd(OH)_2/C$ | $CH_3OH$ + Acetic acid | rt | atm |
| 4 | 20% $Pd(OH)_2/C$ | Ethyl Acetate | rt | atm |
| 5 | Pd black | $CH_3OH$ | rt | atm |
| 6 | (H-Cube®) Pd/C | MeOH | rt | 1 bar |
| 7 | (H-Cube®) 20% $Pd(OH)_2/C$ | MeOH | rt | 1 bar |
| 8 | (H-Cube®) 20% $Pd(OH)_2/C$ | MeOH | 40 ºC | 1 bar |
| 9 | (H-Cube®) 20% $Pd(OH)_2/C$ | MeOH | rt | 50 bar |

**Table 4.02.** Attempted hydrogenation conditions on tetra-benzylated **169**. All flow reactions were conducted on a 1 mmol scale with a flow rate of 1 mL/min. In all cases multiple products were observed.

## 4.6 - Alternative protecting groups

Alternative dialkyl protecting groups for serine were next explored. Cossy reported in 2010 that treating allyl protected **184** with DAST **32** resulted in fluorination and rearrangement, consistent with other amino alcohols, to furnish **185** with high selectivity and excellent enantiocontrol (99% ee). Deprotection of amine **185** was achieved to furnish **186** with a palladium based catalyst (Scheme 4.22).[196]

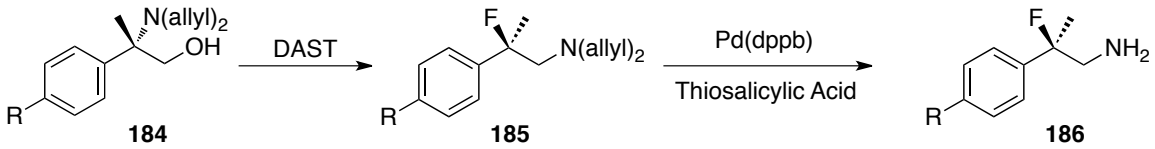


**Scheme 4.22.** Fluorination of quaternary-$\beta$-amino alcohols.

Thus, the route was investigated, with the potential for this motif to undergo RCM to form the 5-membered pyrrolidine ring. Starting from the respective serine methyl ester, both (*R*)- and (*S*)-**187** were prepared in good yields (62% and 57%) (Scheme 4.23).

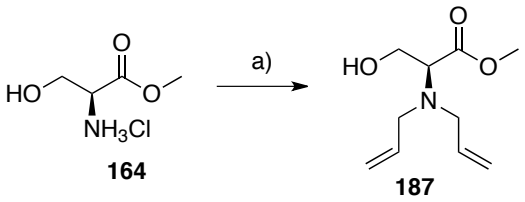


**Scheme 4.23.** *Reagents and conditions:* a) Allyl bromide (4 eq), $K_2CO_3$, MeCN, reflux, 16 h, 57%.

Fluorination of alcohols (*R*)- and (*S*)-**187** was achieved by treatment with DAST **32** and this gave their respective $\alpha$-fluorinated isomers (*S*)- and (*R*)-**188** in good yield (69% and 61% respectively, >95% ee) (Scheme 4.24). Analysis of the reaction mixture with $^{19}F\{^1H\}$ NMR showed that fluorination to the $\alpha$-product **188** proceeded with 95:5 regioselectivity over the $\beta$-product **189**, consistent with that found with the benzyl moiety.

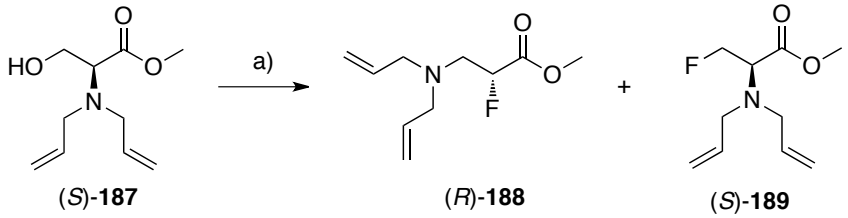


**Scheme 4.24**. *Reagents and conditions:* DAST **32** (1.1 eq), THF, 0 ºC, 1 h.

The removal of the allyl groups was next explored. Treatment of allyl protected **188** using various literature procedures (Table 4.03), failed to furnish free amine **166**.[197]

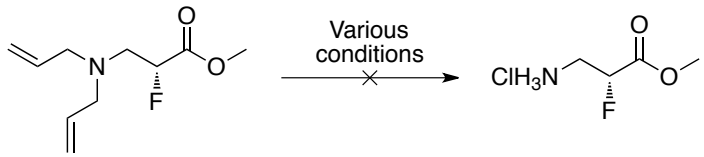


**Scheme 4.25**. Attempted de-allylation reaction with conditions summarised in Table 4.03

| Entry | Catalyst | Solvent | Temperature |
|---|---|---|---|
| 1 | $RhCl(PPh_3)_3$ | THF | reflux |
| 2 | $PdCl_2$ | THF | reflux |
| 3 | Pd(dppb) | THF | reflux |
| 4 | $PdCl_2$ | THF | rt |

**Table 4.03.** Summary of the conditions attempted for the cleavage of the allyl groups in **188**. In all cases multiple products were observed by TLC and NMR.

It was found that diallyl amine **188** exhibited a similar side-reactivity to hydrogenation of benzyl protected **120**, with multiple products observed in the $^{19}F\{^1H\}$ NMR spectrum. Thus an alternative approach was sought.

### *4.6.1 - Ring closing metathesis approach with **188***

The allyl groups in **188** offered the opportunity for ring-closing metathesis through to dehydropyrrolidine **190** (Scheme 4.26). Initial attempts of the RCM reaction of ester **188**, with 10 mol% of Grubbs 1$^{st}$ generation catalyst **191** failed to provide the desired cyclised product **190**, as judged by NMR and MS analyses.

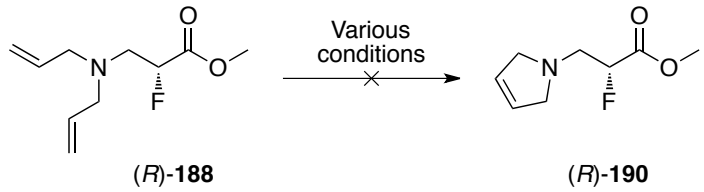


**Scheme 4.26.** Ring closing metathesis strategy to dehydropyrrolidine **190.**

The addition of $Ti(O^iPr)_4$ or acetic acid with the Grubbs I catalyst **191**, in $CH_2Cl_2$ or toluene at room temperature or reflux also failed to provide dehydropyrrolidine **190**.[198,199] Alternative catalysts such as Hoveyda-Grubbs **193** or the temperature stable

indenylidene based **194** at 1.0 mol% to 10 mol% catalytic loadings were also unsuccessful (Figure 4.03).[200] In each case multiple products were observed by $^{19}F\{^{1}H\}$ NMR analysis.

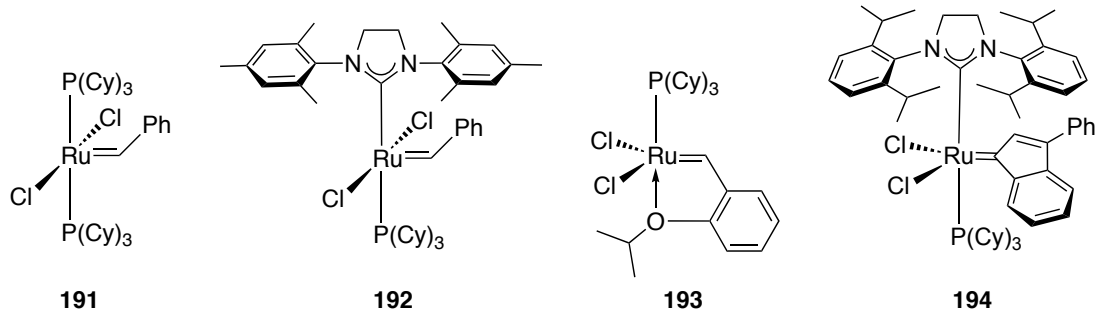


**191** **192** **193** **194**

**Figure 4.03**. Catalysts employed in the investigations of the RCM reaction of (*R*)-**188**.

## 4.7 - Acridone coupling with ester 188

As an alternative strategy, the diallyl ester **188** was coupled to acridone **155** and then chemistry on the side chains was subsequently explored. Thus (*S*)-**188** was treated with the optimised base mediated coupling procedure (Scheme 4.27) and diamide acridone (*S,S*)-**195** was isolated in a modest yield (23%).

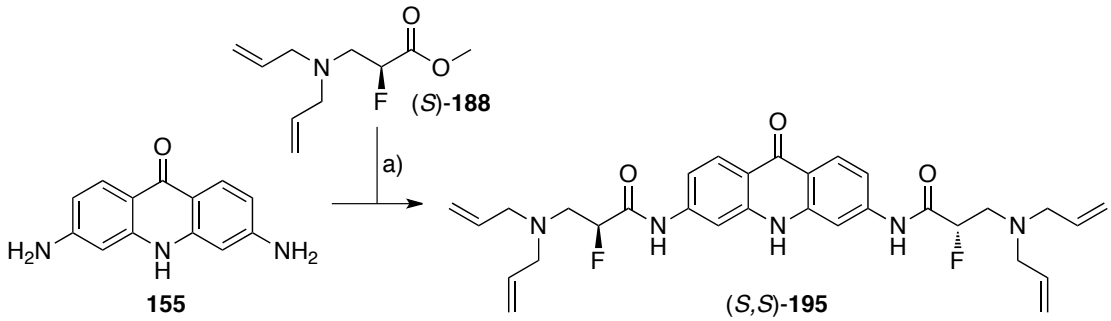


**Scheme 4.27.** *Reagents and conditions:* KHMDS, THF, -78 ºC 1 h, followed by (*S*)-**188**, 78 ºC to rt, 12 h, 23%.

The $^{1}H$ and $^{13}C$ NMR spectra of (*S,S*)-**195** were readily assigned with the overlapping terminal allyl resonance and C*H*F resonance confirmed by $^{1}H$-$^{19}F$ HMQC analysis (Figure 4.04**)**

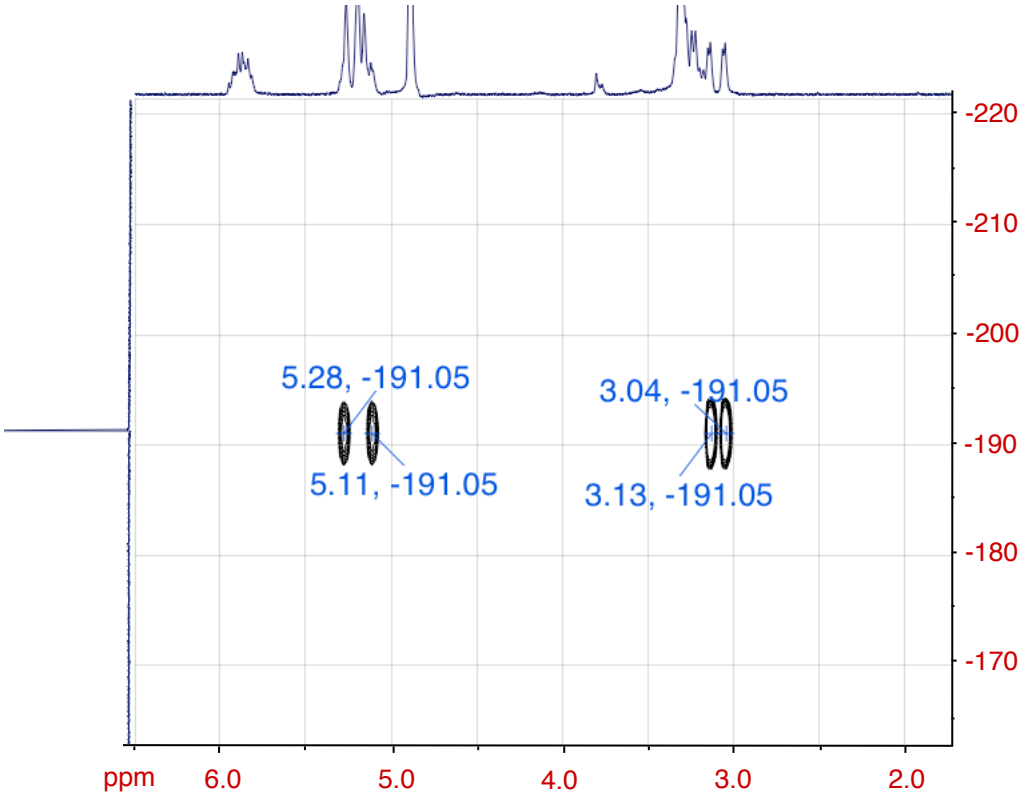


**Figure 4.04.** $^{1}H$-$^{19}F$ HMQC (300/282 MHz, $CD_3OD$) spectrum of acridone (*S,S*)-**195**.

Repeating the procedure starting from (*R*)-**188** enabled isolation of the enantiomeric (*R,R*)-**195**, which had identical spectroscopic characteristics.

### *4.7.1 - Allyl deprotection of acridone **195***

With suitable quantities of both stereoisomers of (*R,R*)- and (*S,S*)-**195** in hand, RCM and de-allylation of the allyl groups was explored. Ring closing metathesis failed again with the conditions previously attempted for ester **188**. This was presumably due to the lone pair of the secondary amine, but also to the insolubility of **195** in toluene or $CH_2Cl_2$. However, the de-allylation of acridone **195** to diamine **196** was achieved following a modification of a literature procedure. This used thiosalicylic acid **197** and a palladium phosphine based catalyst **198** (Scheme 4.28).

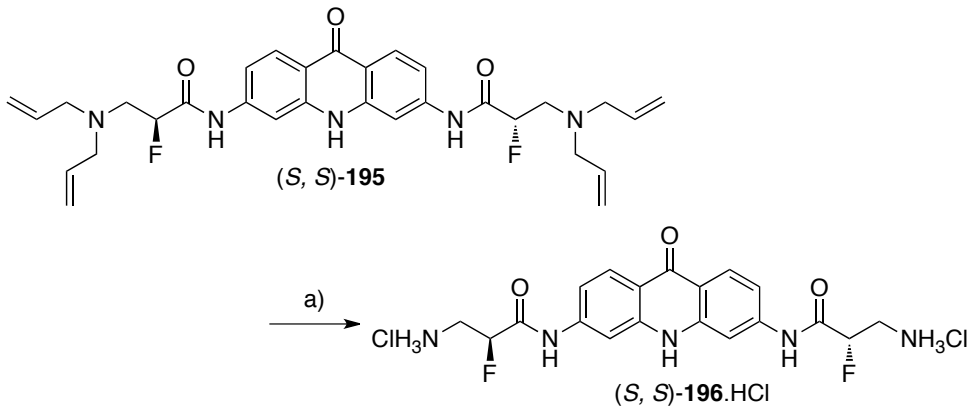


**Scheme 4.28.** *Reagents and conditions:* $Pd_2(dba)_3$ (10 mol%/allyl group), DPPB, thiosalicylic acid **197**, THF, reflux followed by HCl, 89%.

This reaction proceeds *via* the Pd-allyl cation **199** facilitating nucleophilic attack of thiosalicylic acid **197**, which acts as an allyl scavenger (Scheme 4.29).

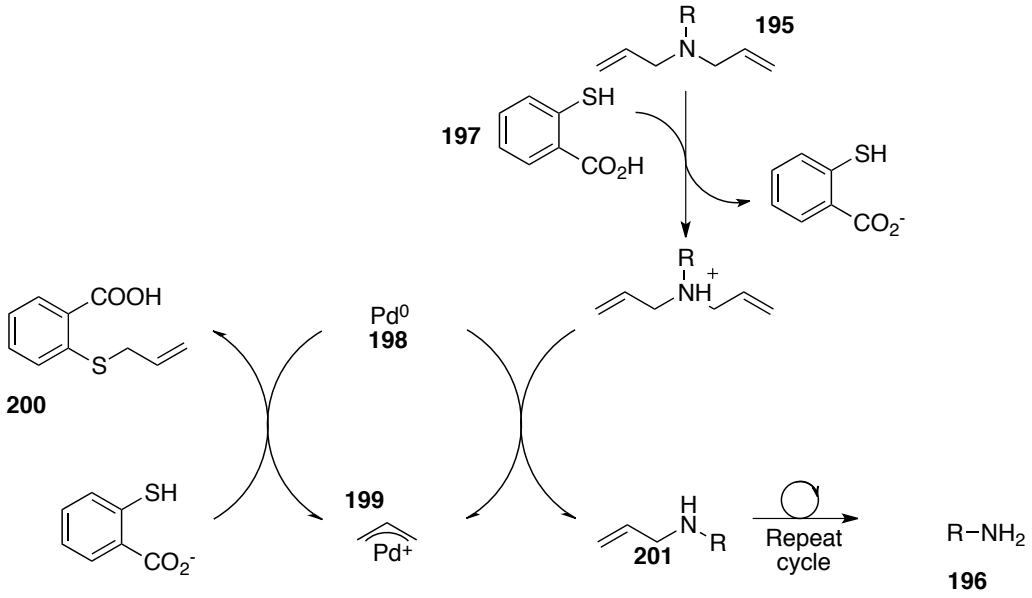


**Scheme 4.29**. Mechanism for Pd catalysed de-allylation with stoichiometric thiosalicylic acid. R/R' = alkyl, aryl.

This reaction proceeded smoothly, with an acidic work up enabling the isolation of amine (*S,S*)-**196**.HCl by aqueous extraction. Purification by reverse phase chromatography followed by freeze-drying provided amine (*S,S*)-**196**.HCl in an almost quantitative yield (95%). By contrast, when ester **188** had been treated under these conditions multiple products were observed. However, this post coupling strategy proved much more successful with acridone **195**. $^1$H NMR analysis confirmed that the

acridone core had remained intact and that the allyl groups were cleanly removed (Figure 4.05).

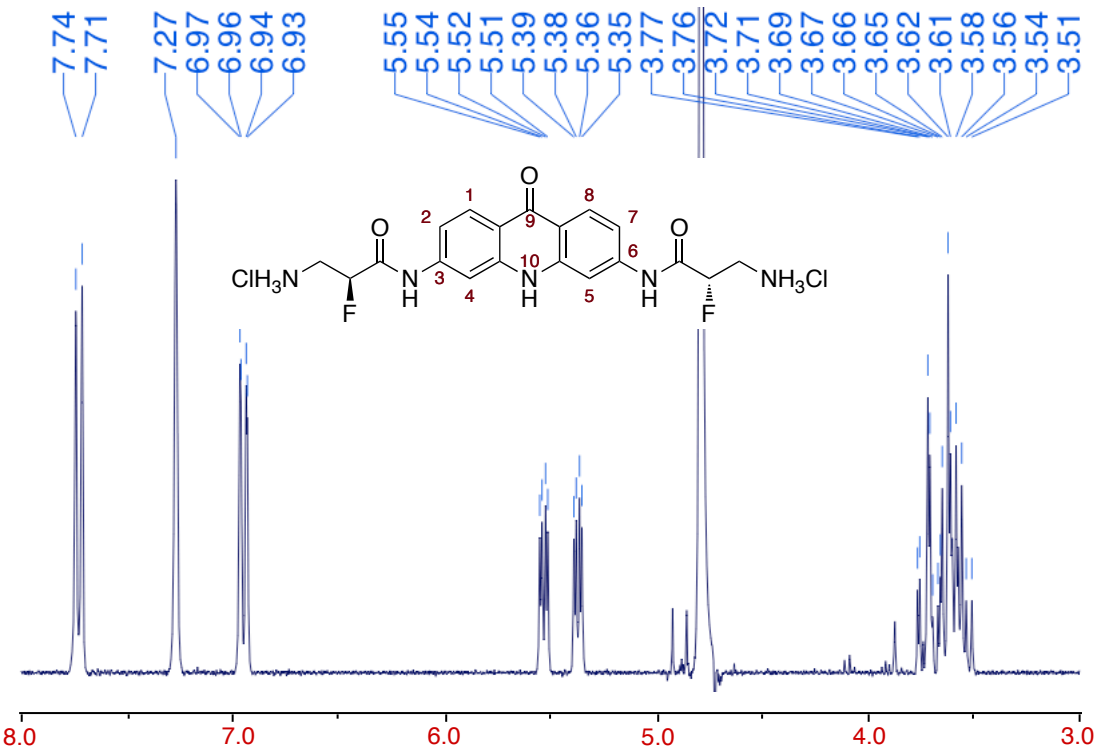


**Figure 4.05.** $^{1}$H NMR (300 MHz, $D_2O$) spectrum of acridone (*S,S*)-**196** after allyl deprotection.

Repeating the procedure with (*R,R*)-**195** enabled the isolation of the complementary diamine (*R,R*)-**196** (Figure 4.06). With both diamines available in suitable quantities, an investigation into the functionalisation of the terminal amines was now explored.

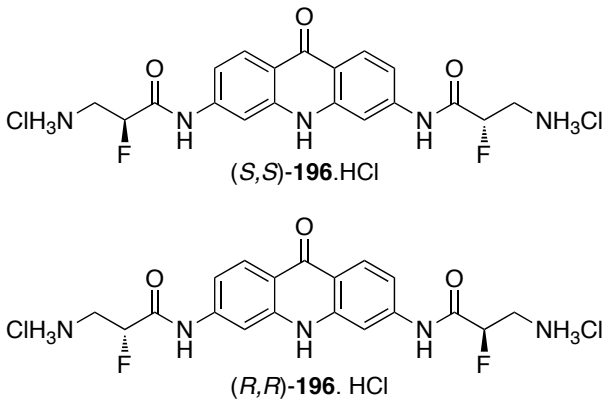


**Figure 4.06.** Both enantiomers of the deallylated acridone.

### *4.7.2 - Functionalisation of acridone **196***

Pyrrolidine formation of the terminal amines of **196** with 1,4-dibromobutane was explored (Scheme 4.30), however these reactions were unsuccessful despite trying a range of conditions (Table 4.04).

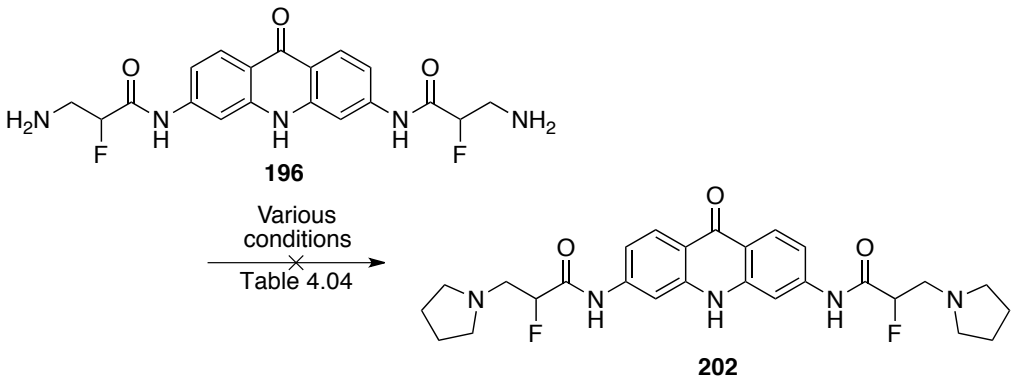


**Scheme 4.30.** Attempted functionalisation of the amino group in acridone **196**. Conditions tested are summarised in Table 4.04.

| 1,4-dihalobutane | Base | Solvent | Conditions | Time (h) | Outcome |
|---|---|---|---|---|---|
| Bromo- | DiPEA | MeCN | reflux | 48 | No Rx |
| Bromo- + TBAI (cat) | DiPEA | MeCN | reflux | 48 | Inconclusive |
| Bromo- | $K_2CO_3$ | THF | reflux | 48 | Inconclusive |
| Iodo- | $K_2CO_3$ | THF | reflux | 48 | No Rx |
| Iodo- | $K_2CO_3$ | DMF | 100 ºC | 24 | Cleavage of amide |
| Iodo- | $K_2CO_3$ | THF/MeCN (1:1) | Microwave, 120W | 0.5 | No Rx |
| Iodo- | $K_2CO_3$ | DMF | Microwave, 120W | 0.5 | Cleavage of amide |
| Iodo- | $K_2CO_3$ $Et_3N$ (2 eq) | THF/DMF (9:1) | rt | 48 | No Rx |
| Iodo- | $Et_3N$ (6 eq) | DMF | rt | 48 | No Rx |
| *cis*-1,4-dichloro-2-butene | $Et_3N$ (6 eq) | DMF | rt | 48 | No Rx |

**Table 4.04**. Attempted conditions for the reaction detailed in Scheme 4.30.

An alternative approach involved the double reductive amination of acridone **196** with 1,4-butanedial **204** (Scheme 4.32). The required succinate dialdehyde **204** was accessed by hydrolysis of 2,5-dimethoxytetrahydrofuran **203** (Scheme 4.31).

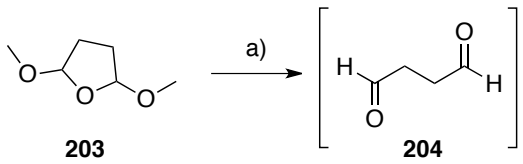


**Scheme 4.31.** *Reagents and conditions:* HCl (1 M), rt, 20 min, basified and distilled.[201]

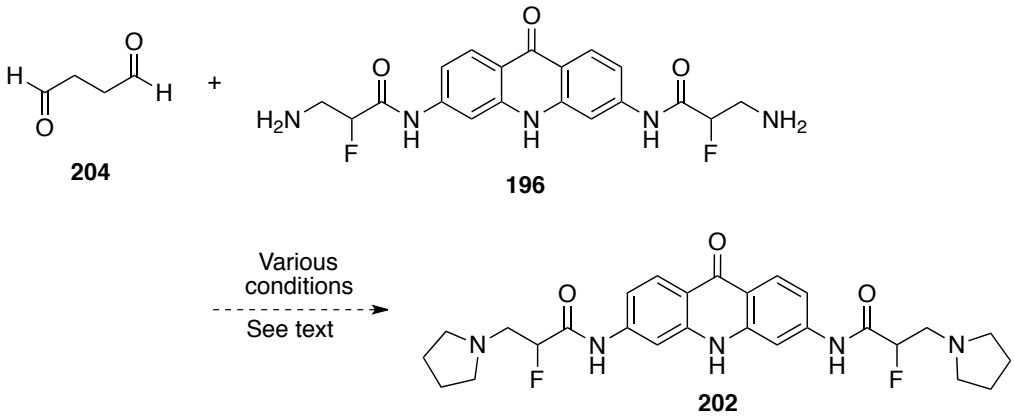


**Scheme 4.32.** Attempted route towards pyrrolidine functionalised acridone **202**.

Again, the solubility of acridone **196** was a limiting factor in this reaction (Scheme 4.32). Various borohydride reagents such as $NMe_4BH(OAc)_3$ and $NaBH(OMe)_3$ in THF were used with and without acetic acid.[202] However, the desired product was not identified.

## 4.8 - Trisubstituted acridine 206 synthesis

An alternative strategy where the acridone moiety in **195** was converted to the appropriately trisubstituted acridine was taken. This would enable the synthesis of analogues for DNA binding and telomerase assays. To achieve this, acridone **195** was treated with neat phosphorus oxychloride to access the 9-chloro intermediate **205** (Scheme 4.33). The use of elevated temperatures resulted in the elimination of diallyl amine as indicated by a resonance at -120 ppm in the $^{19}F$ NMR spectrum.

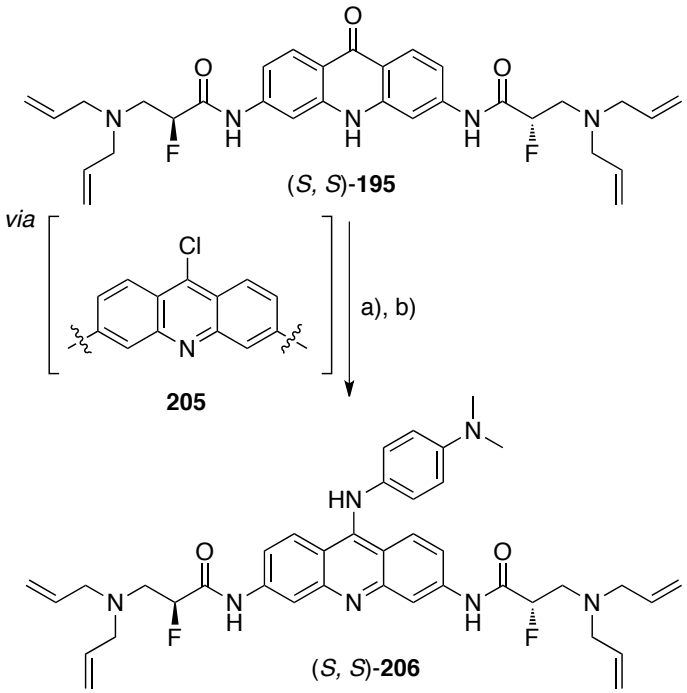


**Scheme 4.33.** *Reagents and conditions:* a) $POCl_3$ (neat), rt, 24 h & b) *N,N*-dimethylaminoaniline **154** (20 eq), $CHCl_3$, reflux, 5 h, 59%.

The intermediate was used straight away in a $S_NAr$ reaction with aniline **154**, using the stable monohydrochloride **207**, which was neutralised and used immediately to avoid decomposition (Scheme 4.34).

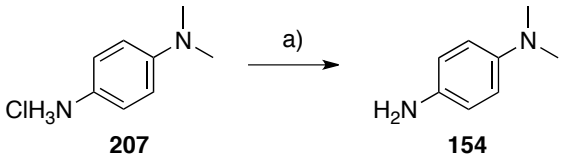


**Scheme 4.34**. *Reagents and conditions:* $Na_2CO_3$ (sat. aq. soln.), $Et_2O$, rt, quantitative.

Exclusion of light and air minimised the decomposition of the extracted aniline prior to the reaction. Refluxing aniline **154** with (*S,S*)-**195** in chloroform for 5 h enabled the formation of the desired acridine product in good yield over two steps (59%). The $^1$H NMR spectrum of (*S,S*)-**195** was readily assigned with the aniline substituent clearly defined (Figure 4.07). Starting from (*R,R*)-**195**, it was also possible to access the complementary (*R,R*)-**195** enantiomer, in a yield of 61%.

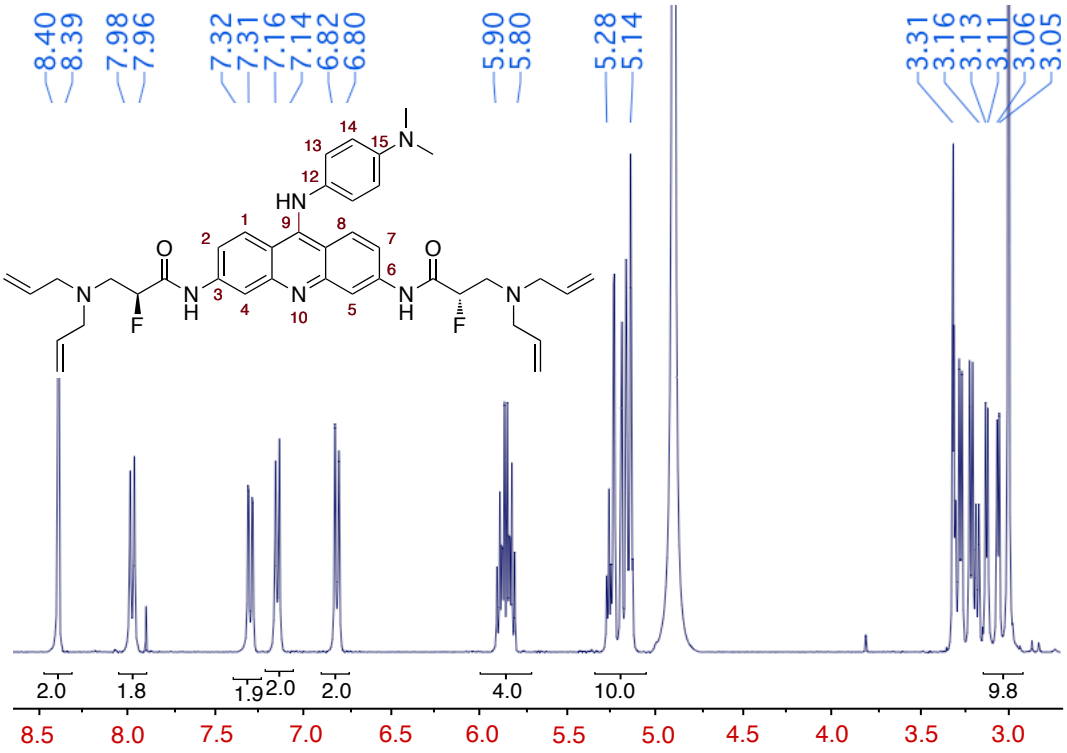


**Figure 4.07**. $^{1}$H NMR (400 MHz, $CD_3OD$) spectrum of trisubstituted acridine (*S,S*)-**206**.

The UV-vis absorption spectrum of acridine **206** (maxima at 268, 294, 365 and 425 nm) has a broad absorption extending up to 700 nm. This made it difficult to record an optical rotation value.

### *4.8.1 - Allyl deprotection of acridine **206***

With practical quantities of acridine (*R,R*)- and (*S,S*)-**206** in hand, allyl group deprotection was next investigated. This was successfully achieved following the protocol developed for the deallylation of acridone **195** (Scheme 4.35).

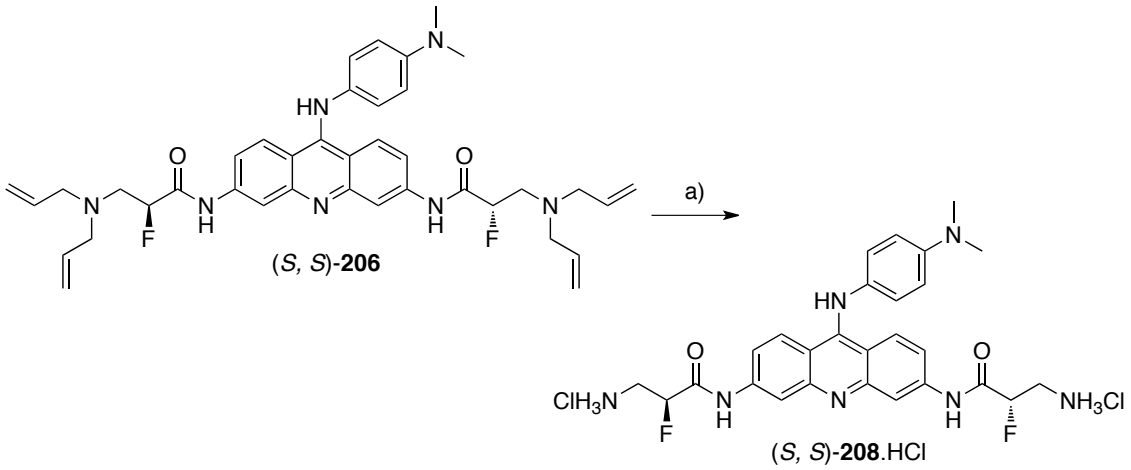


**Scheme 4.35.** *Reagents and conditions:* $Pd_2(dba)_3$ (10 mol%/allyl group), dppb, thiosalicylic acid, THF, reflux followed by HCl, 61%.

Analysis of the crude reaction product by NMR indicated that the acridine heterocyclic core was unaffected by the conditions and that the allyl groups were cleaved to furnish (*S,S*)-**208** as its HCl salt. This required careful purification by C-18 reverse phase chromatography. The $^1$H NMR confirmed cleavage of the allyl groups and the C*H*$_2$CHF, C*H*F and aromatic resonances were clearly resolved (Figure 4.08). The procedure was repeated for the other (*R,R*)-**206** enantiomer, to yield amine (*R,R*)-**208** in 51% yield.

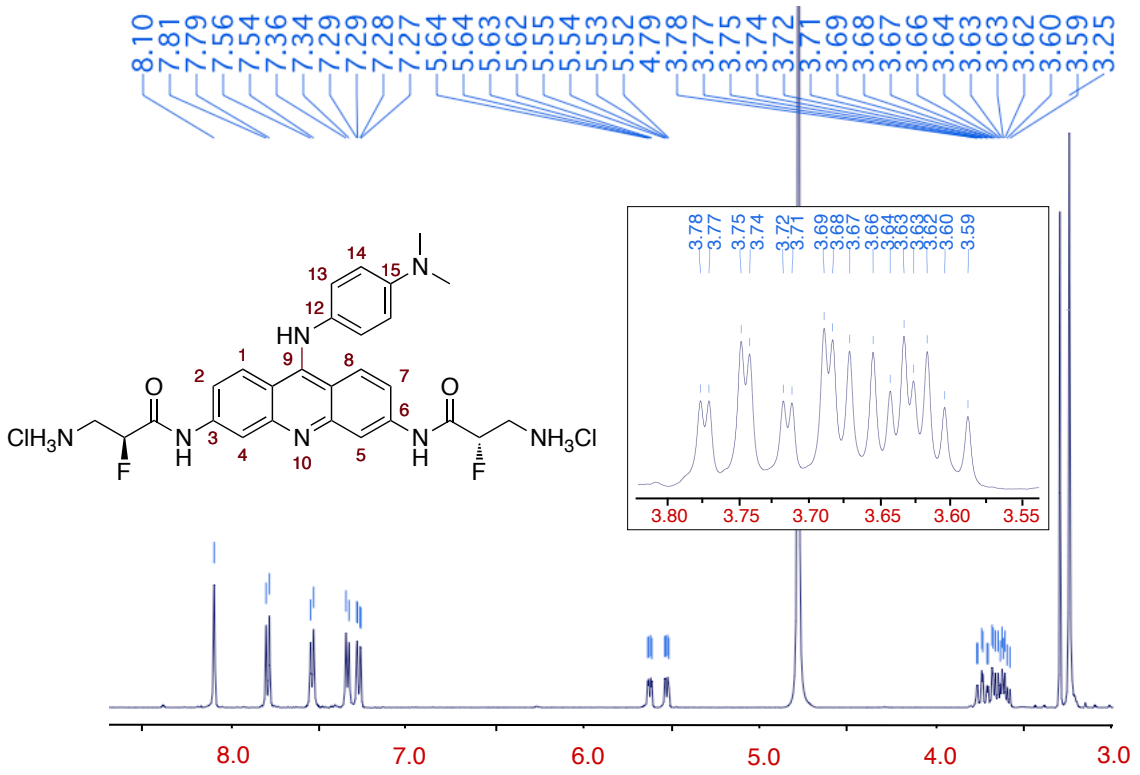


**Figure 4.08.** $^{1}$H NMR (500 MHz, $D_2O$) spectrum of acridine (*S,S*)-**208**.HCl after reverse phase chromatography.

The two stereoisomers (*R,R*)- and (*S,S*)-**208**.HCl are undergoing binding assays with human quadruplex DNA at the UCL School of Pharmacy (Figure 4.09). Co-crystallisation trials with the $G_3(T_2AG_3)_3$ telomeric sequence are also underway to enable a structural assessment of the influence of the C–F bond on ligand binding to quadruplex DNA.

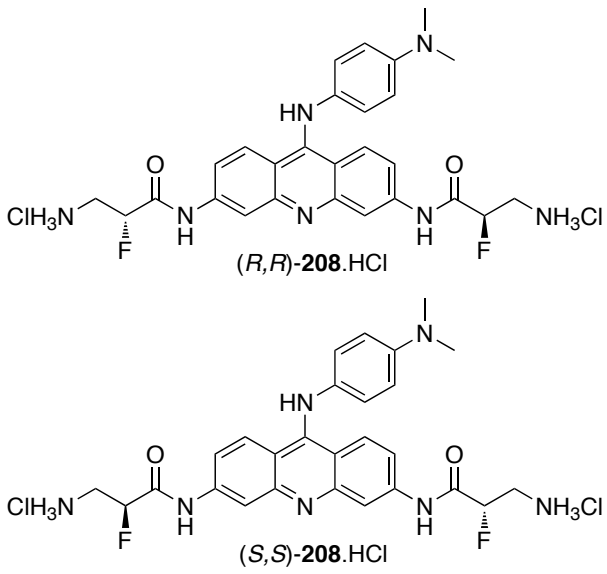


**Figure 4.09.** Selectively fluorinated acridines for studies with quadruplex DNA.

## 4.9 - Alternative side chain functionalisation

A hydrogenation reaction of the allyl groups of ester (*S*)-**188** was explored (Scheme 4.36). This proceeded smoothly with 10% Pd/C as a catalyst, and gave the *N*,*N*-dipropyl product (*S*)-**209** in good yield (61%)

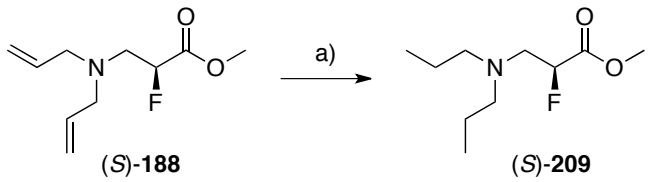


**Scheme 4.36.** *Reagents and conditions:* a) 10% Pd/C (20 mol%), $H_2$, EtOAc, 24 h, rt, 61%.

Repeating this reaction for (*R*)-**209** enabled the isolation of the other enantiomer in a yield of 51%.

### *4.9.1 - Acridone coupling with ester **209***

The *N*,*N*-dipropyl ester (*S*)-**209** was thus subject to the general coupling procedure described above, to generate acridone (*S,S*)-**210** (Scheme 4.37). This reaction went smoothly and purification of acridone (*S,S*)-**210** was relatively straightforward.

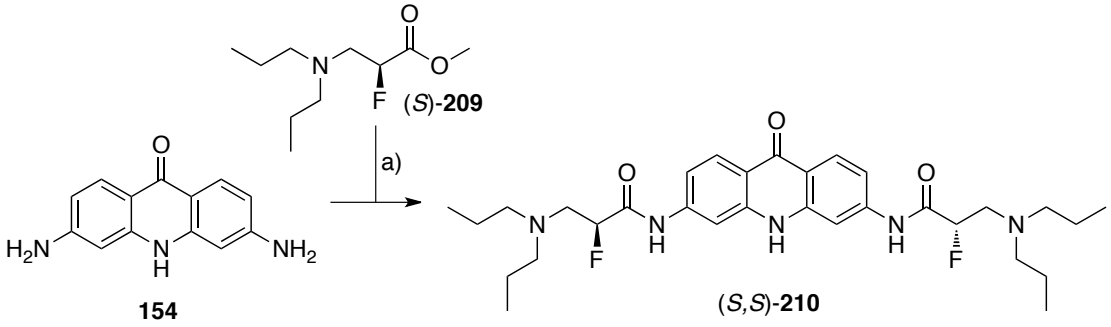


**Scheme 4.37**. *Reagents and conditions:* KHMDS, THF, -78 ºC, 1 h, followed by (*S*)-**209**, 78 ºC to rt, 12 h, 26%.

The propyl groups in (*S,S*)-**210** simplified the analysis of the $^{1}H$ (Figure 4.10) and $^{13}C$ NMR assignment, relative to the diallyl product **195**.

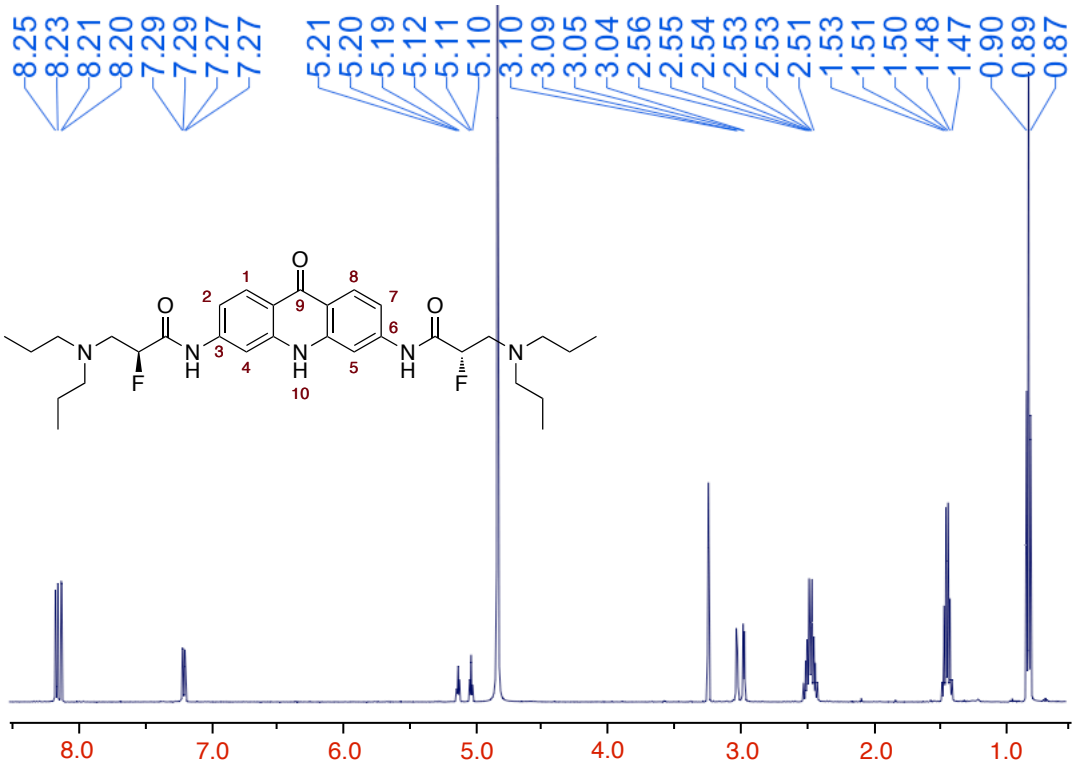


**Figure 4.10**. $^{1}$H NMR (300 MHz, $CD_3OD$) spectrum of acridone (*S,S*)-**210**.

This acridone coupling procedure was then carried out with the opposite enantiomer of ester (*R*)-**188** to furnish (*R,R*)-**210** acridone in 30% yield.

The *N,N*-dipropyl derivatised acridones (*S,S*)- and (*R,R*)-**210** were again treated with phosphorus oxychloride followed by the addition of aniline **154**. These reactions went smoothly to give the (*S,S*)- and (*R,R*)- enantiomers of acridine **212** (Scheme 4.38).

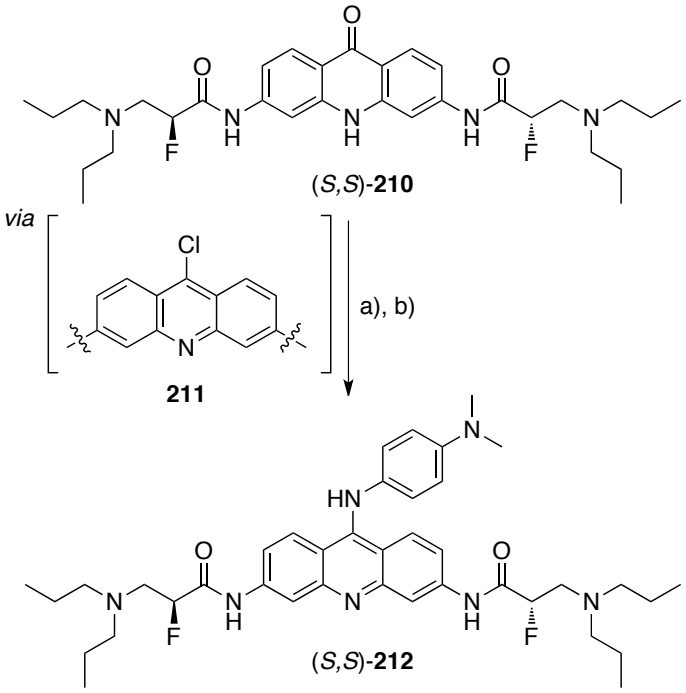


**Scheme 4.38**. *Reagents and conditions* a) $POCl_3$ (neat), rt, 24 h & b) *N,N*-dimethylaminoaniline **154** (20 eq), $CHCl_3$, reflux, 5 h, 21%.

In each case purification was achieved by silica gel chromatography, furnishing the (*S,S*)- and (*R,R*)-**212** enantiomers in reasonable yields (21% and 25% respectively) over two steps. The $^1$H NMR spectrum of (*R,R*)-**212** is shown in Figure 4.11 by way of example, with each resonance clearly resolved.

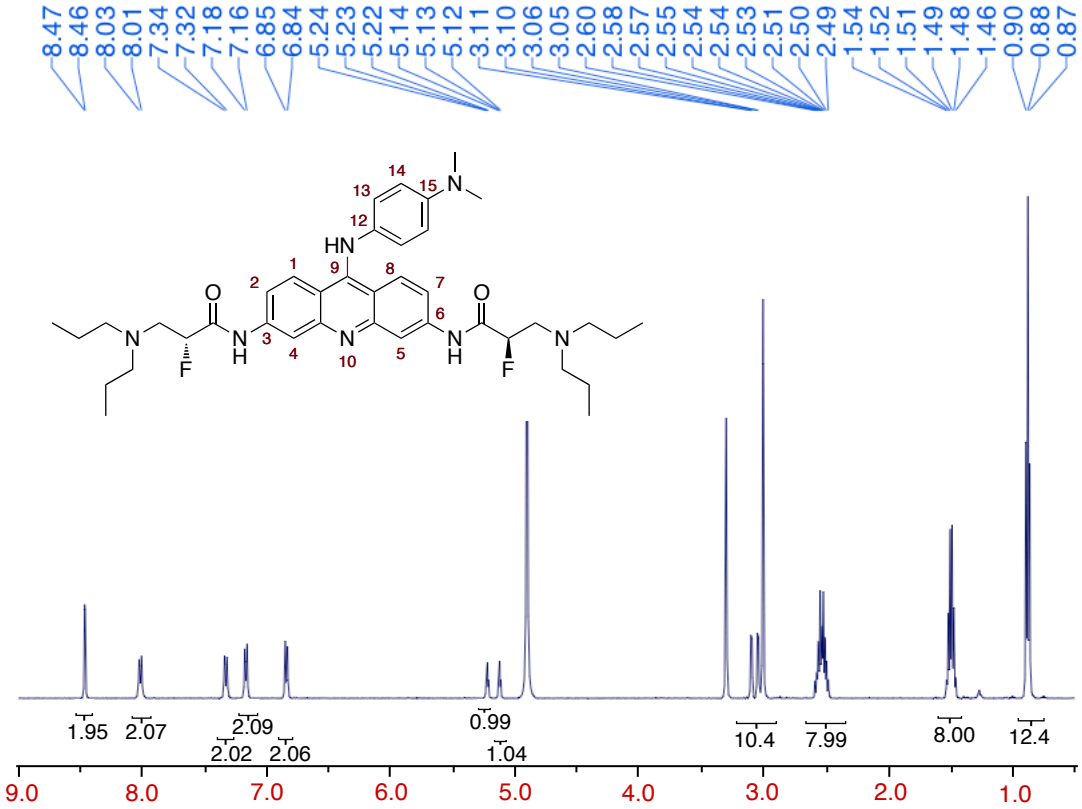


**Figure 4.11.** $^{1}$H NMR (400 MHz, $CD_3OD$) spectrum of trisubstituted acridine (*R,R*)-**212**.

The two enantiomers of the propyl functionalised acridines **212** (Figure 4.12) have also been submitted for binding assays to human telomeric DNA.

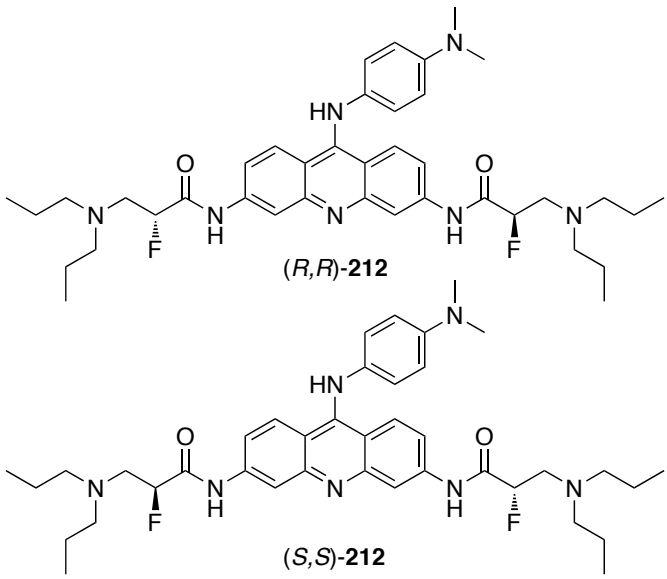


**Figure 4.12.** Selectively fluorinated enantiomers of BRACO-19 analogues.

### *4.9.2 - $^{1}H$-$^{19}F$ HOESY analysis of (S,S)-**212***

To investigate the solution conformation of the $\alpha$-fluoroamide moiety in **212** a 1D $^{1}H$-$^{19}F$ HOESY NMR of (*S,S*)-**212** was recorded. In this experiment, irradiation of the fluorine resonance strongly enhances the N*H* and the C*H*F resonances in the $^{1}H$ NMR spectrum (Figure 4.13). This is consistent with the C–F and N–H bonds orientated close in space, as expected for the anticipated $\alpha$-fluoroamide conformation (Figure 4.14).

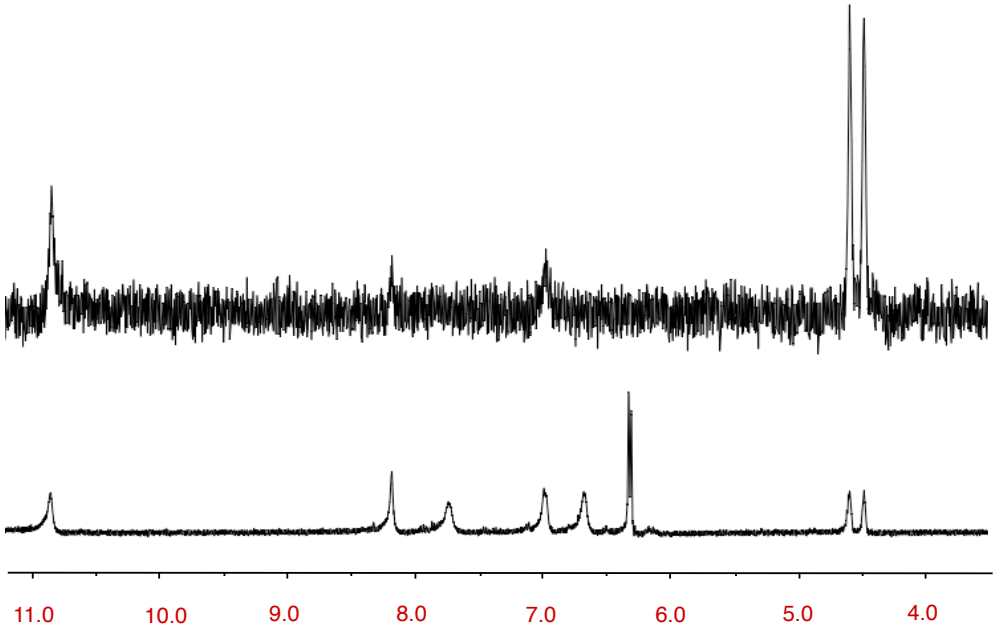


**Figure 4.13.** HOESY analysis of (*S,S*)-**212**. **Lower NMR**– $^{1}H$ NMR (500 MHz, $CDCl_3$) of acridine **212** with broad peaks as a result of $CDCl_3$ and **Top NMR** – $^{1}H$ NMR (500 MHz, $CDCl_3$) recorded during selective irradiation of the $^{19}F$ signal at -191.1 ppm.

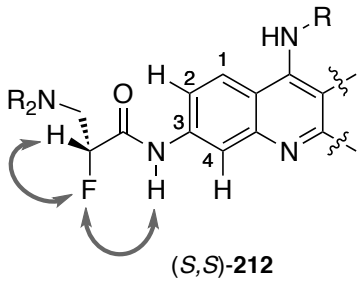


**Figure 4.14.** Simplified representation of acridine **212** with arrows detailing the main NOE enhancements in the HOESY spectrum in **Figure 4.14**. R = propyl, R' = *N,N*-dimethylaminoaniline.

## 4.10 - Non-fluorinated BRACO-19 142a analogues

The non-fluorinated compounds **213**.HCl and **214** have not been previously synthesised and were required as reference compounds to compare the effects of selective fluorination on the stabilisation of quadruplex DNA (Figure 4.16).

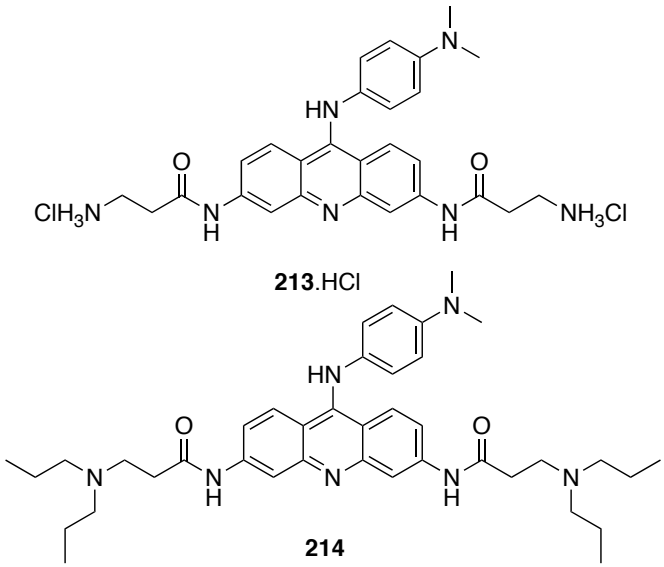


**Figure 4.15.** Non-fluorinated BRACO-19 analogues for comparative studies.

Initially, *bis*-chloro amide **174** was prepared by refluxing acridone **154** in neat 3-chloropropionyl chloride **148** (Scheme 4.39).

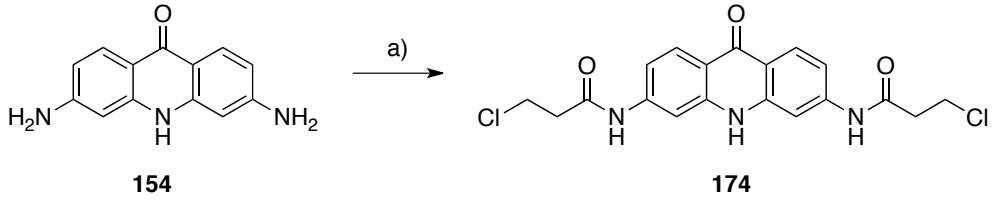


**Scheme 4.39**. *Reagents and conditions:* 3-Chloropropionyl chloride (neat), 145 ºC, 3 h, 27%

Acridone **174** proved difficult to isolate and purify, however gram scale reactions enabled the isolation of sufficient quantities for subsequent reactions. The resultant acridone **174** was then treated with either diallylamine (**215**) or dipropyl amine (**216**), and sodium iodide to furnish **140i** and **140j** respectively (Scheme 4.40).

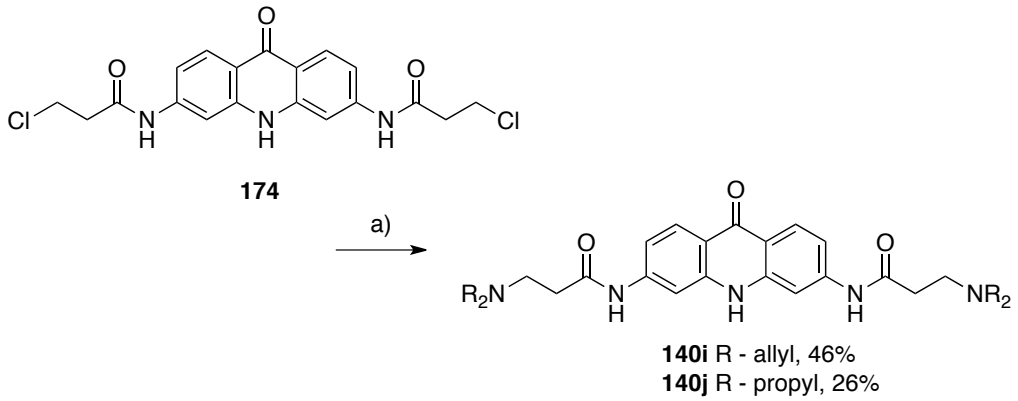


**Scheme 4.40**. *Reagents and conditions:* for **140i** a) Diallylamine, EtOH, 80 ºC, 3 h, 46% and for **140j** a) dipropylamine, EtOH, 80 ºC, 3 h, 26%.

The literature purification of similar acridone compounds calls for the recrystallisation from DMF and ethanol, however acridones **140i/j** were much more reasonably purified by column chromatography, albeit with the need to pre-basify the column with triethylamine.[191] In the event both **140i/j** were isolated in acceptable yields (46% & 26% respectively).

Treatment of acridones **140i/j** with neat phosphorus oxychloride at reflux afforded the corresponding 9-chloro intermediates **216** and **217** respectively. Again the chlorides were not purified but were reacted immediately, following a brief work-up, with aniline **154** (Scheme 4.41). Both of the trisubstituted acridines **219** and **214** were isolated in acceptable yields (37% & 29% respectively) following purification by column chromatography.

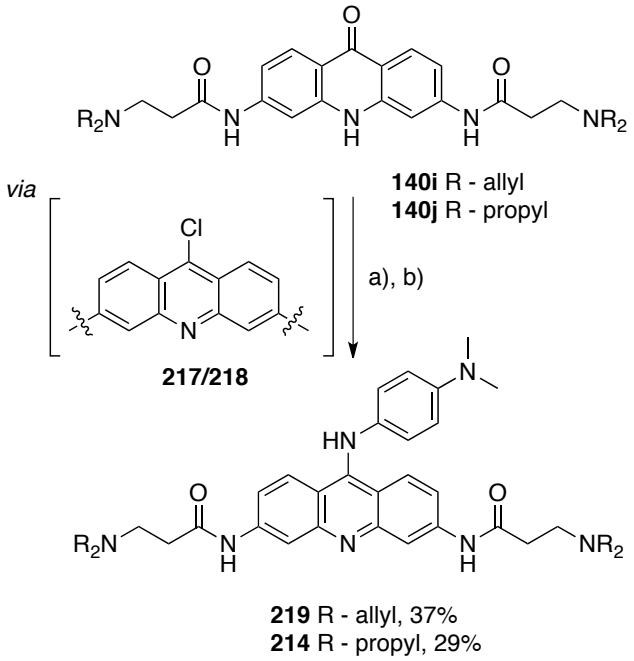


**Scheme 4.41**. *Reagents and conditions:* For both a) $POCl_3$ (neat), 140 ºC, 3 h, 37% & b) *N,N*-dimethylaminoaniline, $CHCl_3$, 80 ºC, 4 h, 29%.

The purification of **219** and **214** by column chromatography proved to be less straightforward than with the fluorinated analogues **206** and **212**. Acridines **219** and **214** were loaded on the column as their HCl salts and the column was flushed with chloroform and methanol (95:5) to remove any impurities. Addition of triethylamine to the eluant neutralised the salts, enabling the isolation of analytically pure tetra-allyl protected **219**. Repeated chromatography was required to provide a pure sample of the propyl functionalised acridine **214**.

Finally, removal of the allyl groups in **219** to furnish diamine **213** was achieved following the standard procedure using $Pd_2(dba)_3$ and thiosalicylic acid (Scheme 4.42).

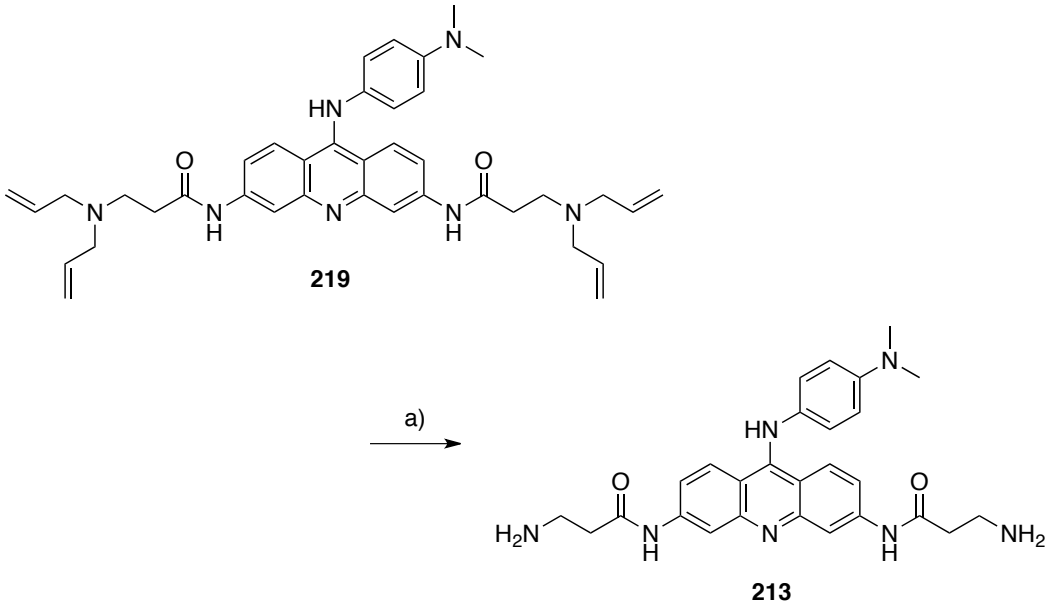


**Scheme 4.42**. *Reagents and conditions:* $Pd_2(dba)_3$ (10 mol%/allyl group), dppb, thiosalicylic acid, THF, reflux followed by HCl, 17%.

Purification of acridine **213** by reverse phase chromatography was particularly problematic and amine **213** could only be isolated in milligram quantities following the addition of formic acid to the eluant. Thus **213** was isolated as its formic acid salt and in a poor yield (17%). However, sufficient material was prepared for comparative biological assessment with the fluorinated analogues (*S,S*)- and (*R,R*)-**208**.

## 4.11 - Crystallographic assessment

To date, no suitable co-crystals of the fluorinated trisubstituted acridines have been achieved for X-ray diffraction despite repeated attempts to identify good crystallisation conditions. Crystals of (*R,R*)- and (*S,S*)-**212** with the human telomeric sequence have formed, however with poor morphology. Diffraction of these crystals has so far only provided low-resolution data (>6 Å). However this preliminary data demonstrated that the propyl functionalised acridine (*S,S*)-**212** does form a quadruplex fold with the DNA as highlighted by the characteristic $\pi$-$\pi$ stacking observed in the diffraction pattern. Studies have now focused on investigating conditions with the *O. nova* quadruplex

DNA sequence, which generally accommodates a wider variety of ligand substituents.[182]

Whole cell based assays and *in vitro* analysis by FRET are currently underway with our collaborators at the UCL School of Pharmacy in London.

## 4.12 - Conclusions

The chapter has demonstrated the successful synthesis of (*S,S*)-and (*R,R*)- stereoisomers of fluorinated **208** and **212**. In addition, the complementary non-fluorinated ligands **213** and **214** were also prepared for assessment by X-ray crystallography and *in vitro* based assays.

# Chapter 5

# Studies on the selective fluorination of dipeptides

## 5.1 - Introduction

In this chapter an alternative approach for the synthesis of $\alpha$-fluoroamides is explored. The fluorination of $\beta$-alcohol amino esters, as discussed in Chapters 1 and 4, with sulfur trifluoride reagents provides an efficient method for the generation of an array of fluorinated building blocks. The reaction of DAST **32** with peptides bearing the $\beta$-hydroxy functionality, such as in **220**, is commonly employed for the synthesis of oxazoles (**222**) and oxazolines (**223**) (Scheme 5.01) without incorporation of fluorine. The approach allows the synthesis of these heterocycles with various degrees of functionalisation and structural diversity.[203] Such activation with DAST **32** has even been employed in the synthesis of the telomerase inhibitor telomestatin **134** (Chapter 2.9.1), which contains repeating oxazole units.[162]

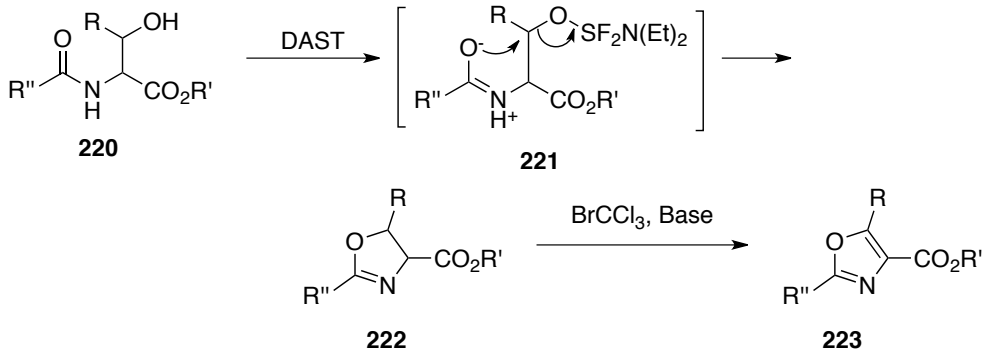


**Scheme 5.01.** Synthesis of oxazoles and oxazolines with sulfur trifluoride reagents. R,R', R'' = H, alkyl, aryl.

However, the use of dehydroxyfluorination reagents on $\alpha$-amino-$\beta$-hydroxyamides such as **224** has not been reported. At the outset the aim was to explore the scope and potential of the fluorination of dipeptides **224** with a terminal serine residue (Scheme 5.02).

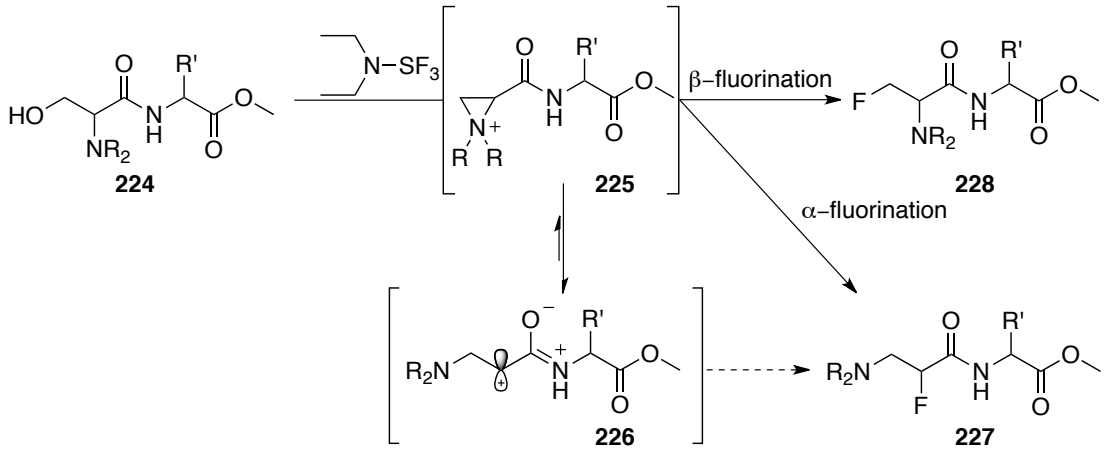


**Scheme 5.02.** Fluorination pathway for $\beta$-hydroxy amines bearing the amide functionality. The double bond character could support the intermediate or facilitate in the formation of an $\alpha$-carbocation leading to racemisation. R = allyl/benzyl & R' = H, alkyl, aryl.

The influence of the amide bond on the opening of the aziridinium ring in intermediate **225** and its effect on the distribution of $\alpha$- and $\beta$-fluorinated regioisomers **227** and **228** was a key consideration (Scheme 5.02). The amide resonance in **226** may also stabilise a carbocation at the $\alpha$-position and promote racemisation in the $\alpha$-fluorinated product **227**.

## 5.2 - Carboxylic acid synthesis for peptide couplings

The serine derivative (*S*)-**229** was first prepared (Scheme 5.03). *N*,*N*-Diallylation of L-serine methyl ester **165** was achieved by reaction with allyl bromide as summarised in Scheme 5.03. This proceeded straightforwardly generating gram quantities of alcohol (*S*)-**187**. The terminal hydroxyl group was then protected as its TBDMS ether (*S*)-**229** in preparation for peptide coupling (Scheme 5.03).

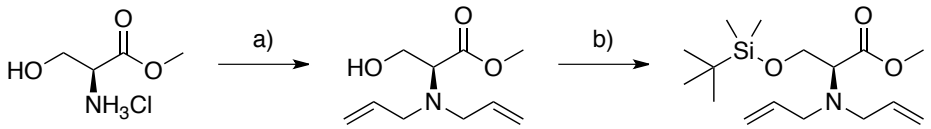


(*S*)-**165** (*S*)-**187** (*S*)-**229**

**Scheme 5.03**. *Reagents and conditions*: a) Allyl bromide (2.5 eq), $K_2CO_3$ (4.0 eq), $CH_3CN$, 60 ºC, 16 h, 57%; b) TBDMSOTf (1.1 eq), $Et_3N$ (5.0 eq), $CH_2Cl_2$, rt, 16 h, 83%.

Methyl ester (*S*)-**229** was hydrolysed using lithium hydroxide in methanol to give carboxylic acid (*S*)-**230** (Scheme 5.04). The purity of the extracted product was sufficient to be used directly in peptide coupling reactions.

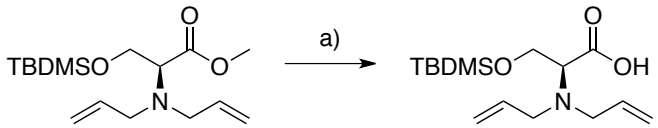


(*S*)-**229** (*S*)-**230**

**Scheme 5.04**. *Reagents and conditions*: a) LiOH (4.0 eq), $CH_3OH$:THF:$H_2O$ (3:1:1), 24 h, 90%.

## 5.3 - Peptide couplings

Peptides **323a-c** were prepared by coupling to a variety of commercially available amino acid methyl esters **231a-c** (Scheme 5.05).

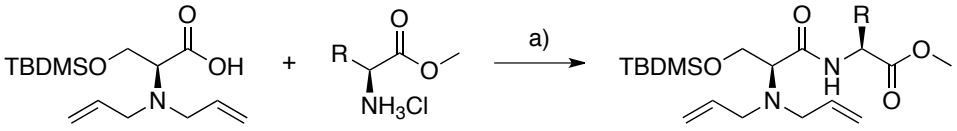


(*S*)-**230** **231a-c**

**232a** - 81%, R = $CH_2Ph$
**232b** - 85%, R = $CH_3$
**232c** - 79%, R = $CH(CH_3)_2$

**Scheme 5.05**. *Reagents and conditions*: a) T3P® (1.5 eq), amine **231a/b/c** (2.0 eq), diisopropylethylamine (4.0 eq), $CH_2Cl_2$, 0 ºC to rt, 1-12 h, 79-85%.

Both HBTU and T3P® were effective for the coupling reactions, although from a practical point of view, T3P® offered an advantage over HBTU. This was because the hydrolysis product is water-soluble and could be removed along with excess unreacted

amine by an acidic wash upon work-up (Scheme 5.05). More generally, T3P® mediated peptide couplings proceed in high yields with low levels of epimerisation.[204]

The synthesis of the L-phenylalanine dipeptide **232a** proved amenable to scale-up and was isolated in 81% yield. Dipeptides **232b/c** derived from L-alanine and L-valine, were synthesised in 85% and 79% yields respectively. All three dipeptides **232a-c**, were isolated with good diastereoselectivity, with only a very low level of epimerization at the $\alpha$-carbon (95:5 dr).

Fluorination of **232a-c** required that the silyl protecting group be removed to release alcohols **224a-c**. Initial silyl ether deprotection of **232a** with TBAF in THF cleaved the silyl ether to yield **224a** but also resulted in the hydrolysis of the methyl ester to give **233**. This gave rise to an unexpected cyclisation to the cyclic dimer **234** (Scheme 5.06).

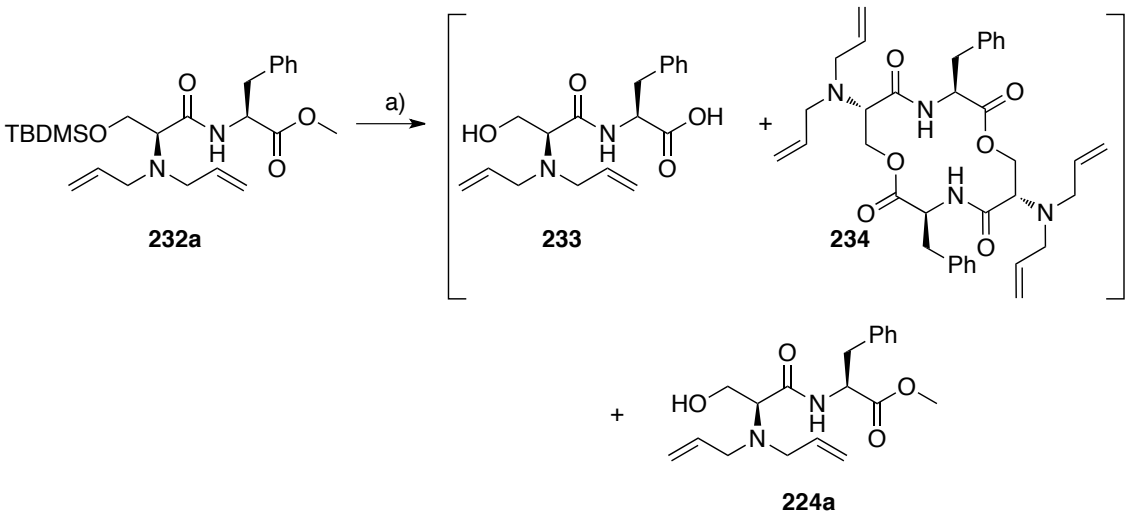


**Scheme 5.06.** *Reagents and conditions*: a) TBAF (2 eq), THF, 0 ºC to rt, 2 h.

Both carboxylic acid **233** and cyclic dimer **234** co-eluted during purification with the structure of the cyclic depsipeptide confirmed by single crystal X-ray crystallographic analysis (Figure 5.01). The formation of **234** is clearly a dimeric condensation, although the detailed sequence of events is not clear.

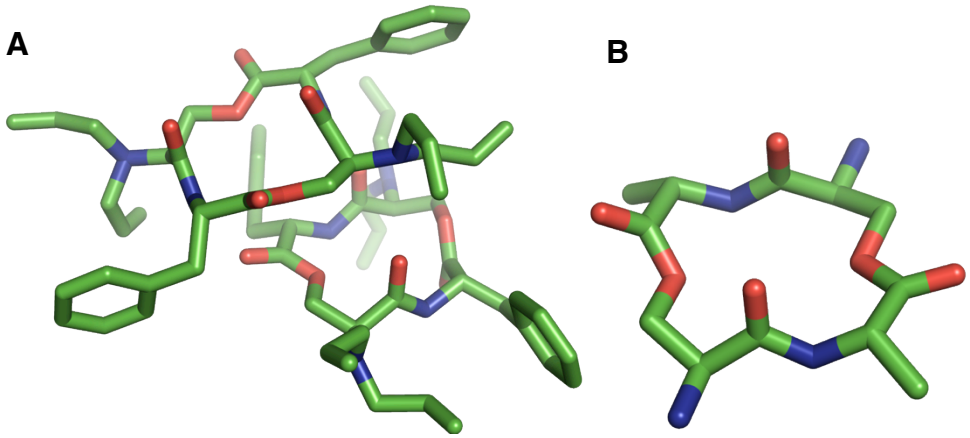


**Figure 5.01.** Crystal structure of the 14-membered cyclic (*R,R*) **234**. Structure **A** shows two cyclic dimers in the unit cell. The nature of the allyl groups results in some disorder. Structure **B** represents one ring with the peripheral benzyl and allyl groups removed so that both amide and ester bonds are clearly observed.

In order to circumvent the problematic methyl ester hydrolysis and cyclisation, the silyl ether was removed with an acetic acid buffered TBAF solution in dry THF, at rt (Scheme 5.07).

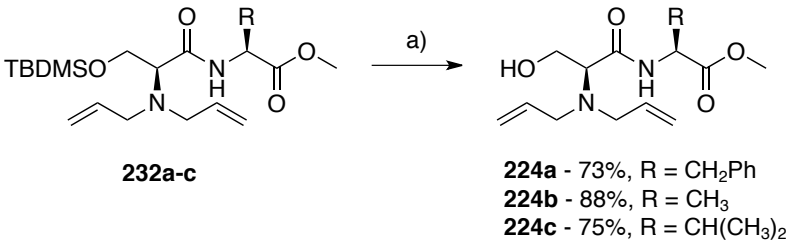


**Scheme 5.07.** *Reagents and conditions*: a) TBAF (4.0 eq, 1 M THF soln.), AcOH (5.0 eq), THF, rt, 12-24 h, 73-88%.

This gave an excellent conversion to the free alcohols **224a-c** (73-88%), which could then be purified by chromatography in a straightforward manner. Importantly, no further epimerisation was observed in the products.

### *5.3.1 - Fluorination reactions of dipeptides with DAST **32***

The fluorination of L-phenylalanine derived dipeptide **224a** with DAST **32** was initially explored (Scheme 5.08).

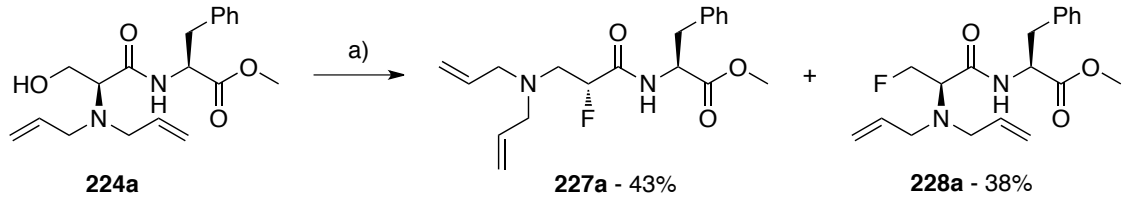


**Scheme 5.08.** *Reagents and conditions*: a) DAST **32**, THF, 0 ºC, 1 h, 81% (total fluorinated yield).

TLC analysis indicated that the starting material was consumed after 1 h stirring at 0 ºC showing a similar reactivity to the ester substrates **119**/**187** in Chapter 4. Analysis of the product mixture by $^{19}F$ and $^{1}H$ NMR indicated a ratio of 60:40 for the $\alpha$- and $\beta$-fluorinated products (**227a**:**228a**). The $\alpha$- and $\beta$- regioisomers could be distinguished by their distinctive coupling patterns in both the $^{19}F$ and $^{1}H$ NMR spectra and chemical shift in the $^{19}F$ NMR spectrum. This is a significant change in selectivity relative to the fluorination of esters **119**/**187** (Chapter 4). In those cases the $\alpha$-products were favoured in a 95:5 ($\alpha$:$\beta$) ratio (Table 5.1). However, despite the poorer selectivity in **224a**, the reaction proceeds cleanly, with the $^{1}H$ NMR and $^{19}F$ NMR spectra correlating accordingly.

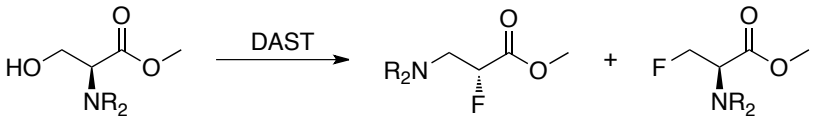


| Entry | R | $\alpha$-NMR ratio | $\beta$-NMR ratio |
|---|---|---|---|
| 1 | Benzyl (**119**) | 95 (**120**) | 5 (**160**) |
| 2 | Allyl (**187**) | 95 (**188**) | 5 (**189**) |

**Table 5.1.** Fluorination selectivity ratio for esters, **119** and **187** (Chapter 4.3/4.7).

The two fluorinated regioisomers **227a** and **228a** were readily separated by column chromatography. This is in contrast to the fluorinated esters **119**/**187**, which could not be easily separated. Both **227a** and **228a** were isolated in 43% and 38% representing an

efficient overall transformation. The diastereomeric ratio of the $\alpha$-fluorinated product **227a** was determined to be 95:5 from the $^{1}H$ and $^{19}F$ NMR spectra. This suggests that the reaction has good stereocontrol and does not proceed *via* substantial carbocation character at the $\alpha$-position.

The significant shift from high $\alpha$-selectivity in esters **119/187** to a poorer $\alpha$-selectivity for amide **224a** was unexpected. Accordingly, dipeptides **224b/c** were explored to assess the influence of less bulky amino acid side chain substituents on the outcome of the fluorination.

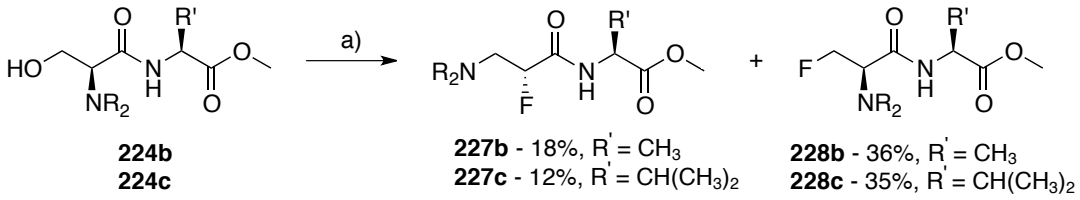


**Scheme 5.09.** *Reagents and conditions*: a) DAST **32**, THF, 0 ºC, 1 h, 47-54% (total fluorination). R = allyl

The reactions of **224b/c** with methyl and isopropyl side chains respectively, with DAST **32** demonstrated a shift towards the $\beta$-fluorinated product (Table 5.2, Entries 2/3) with an $\alpha$:$\beta$ ratio of 35:65 and 25:75 for **227b**/**228b** and **227c**/**228c** respectively. The fluorination ratios for **224a-c** are summarised in Table 5.2 along with their respective diastereomeric ratios.

| Entry | Substitution | $\alpha$:$\beta$ ratio | dr |
|---|---|---|---|
| 1 | Phe, **224a** | 60:40 | 95:5 |
| 2 | Ala, **224b** | 35:65 | 85:15 |
| 3 | Val, **224c** | 25:75 | 92:8 |

**Table 5.2.** Fluorination ratios and diastereomeric ratios of products **224a-c**.

An overlay and progressive offset display of the $^{19}F\{^{1}H\}$ NMR spectra of the crude reaction mixtures illustrates the $\alpha$:$\beta$ fluorination ratio of the three dipeptides **227**/**228a-c** products (Figure 5.02).

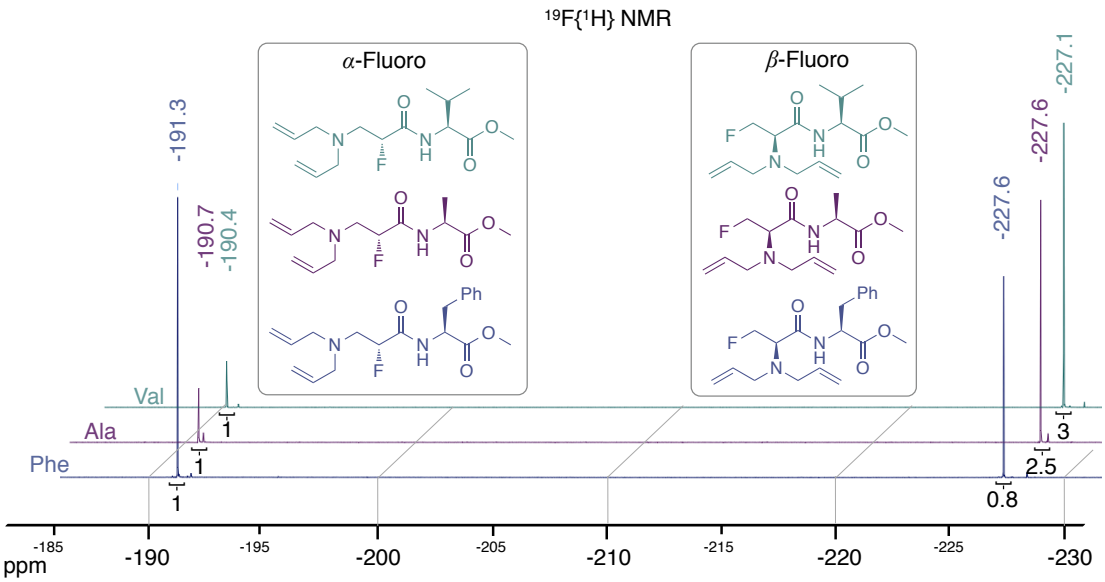


**Figure 5.02.** Overlay of the $^{19}F\{^{1}H\}$ NMR (376 MHz, $CDCl_3$) spectra of the crude products from the fluorination of amides **224a-c**.

These fluorination reactions proceed *via* an aziridinium intermediate with subsequent fluorination at either the *α*- or *β*-positions of **236a-c** (Scheme 5.10).[95] It is assumed that the *β*-product results from nucleophilic fluoride attack at the *β*-position of aziridinium **236a-c**, rather than by direct $S_N2$ attack of fluoride at the activated alcohol **235a-c**. It is not obvious that the *β* carbon will be significantly more electropositive in the aziridinium intermediate for the amides **224a-c** over that of the esters **119**/**187**. However, the product ratios observed for the fluorinations from **224a-c** suggest an increased *β*-reactivity (Scheme 5.10).

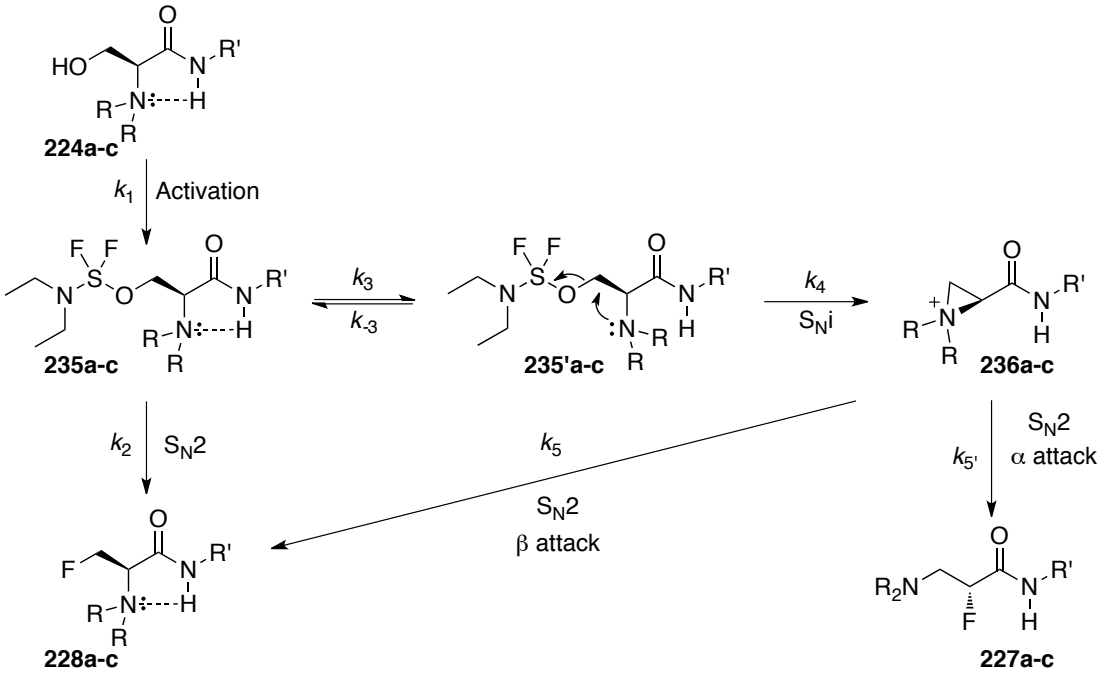


**Scheme 5.10**. Two proposed reaction pathways that could be occurring to explain the product distribution. R = allyl, R'= Phe (a), Ala (b), Val (c).

For the aziridinium intermediate **236a-c** to form, terminal alcohol **224a-c** requires to be activated (**235a-c**) such that the lone pair of the $\alpha$-amine nitrogen can undergo $S_Ni$ attack at the $\beta$-carbon. The rate at which this intramolecular $S_Ni$ reaction ($k_4$) occurs is governed by the availability of the nitrogen lone pairs of **235a-c** (Scheme 5.10). This will be compromised if the lone pairs form a hydrogen bond to the N–H of the amide. Such 5-membered hydrogen bonded rings are observed in the solid state within this structural class.[205] Therefore, the rate of aziridinium formation ($k_3$) over direct $S_N2$ substitution ($k_2$) at the $\beta$-carbon will be affected by this hydrogen bond (Scheme 5.10). On the other hand, if the nitrogen lone pair is free to form an aziridinium intermediate **236a-c** - as in the case of esters **119**/**187** - then the rate of this intramolecular reaction ($k_4$) will be significantly faster than the intermolecular fluoride ion attack ($k_2$) (Scheme 5.10). If $k_2 >> k_3$ then $\beta$-fluorination dominates, if $k_2 \geq k_3$ then this results in a mixture of $\alpha$- and $\beta$-products and if $k_3 >> k_2$ then $\alpha$-fluorination dominates. Fluoride attack of aziridinium intermediate **236** (Scheme 5.10) can either be at the $\alpha$- or $\beta$-position ($k_5$ or $k_{5'}$). Based on the observation with esters **119**/**187**, $k_{5'}$ is significantly faster than $k_5$ and so $\alpha$-fluorination will dominate as a result of the more electropositive $\alpha$-carbon.

Therefore, in the case of the L-phenylalanine dipeptide **224a** this analysis suggests that the benzyl group dictates a less favourable hydrogen bonding interaction than the methyl and isopropyl groups in **224b/c**. By comparing the chemical shift difference between the amide N*H* $^1$H NMR resonance of **224a-c**, a correlation between the fluorination ratios and the relative chemical shifts is apparent (Figure 5.03). A higher N*H* chemical shift and therefore a relatively stronger hydrogen bond, appears to correlate with a higher proportion of the *β*-product in the L-alanine and L-valine dipeptides.

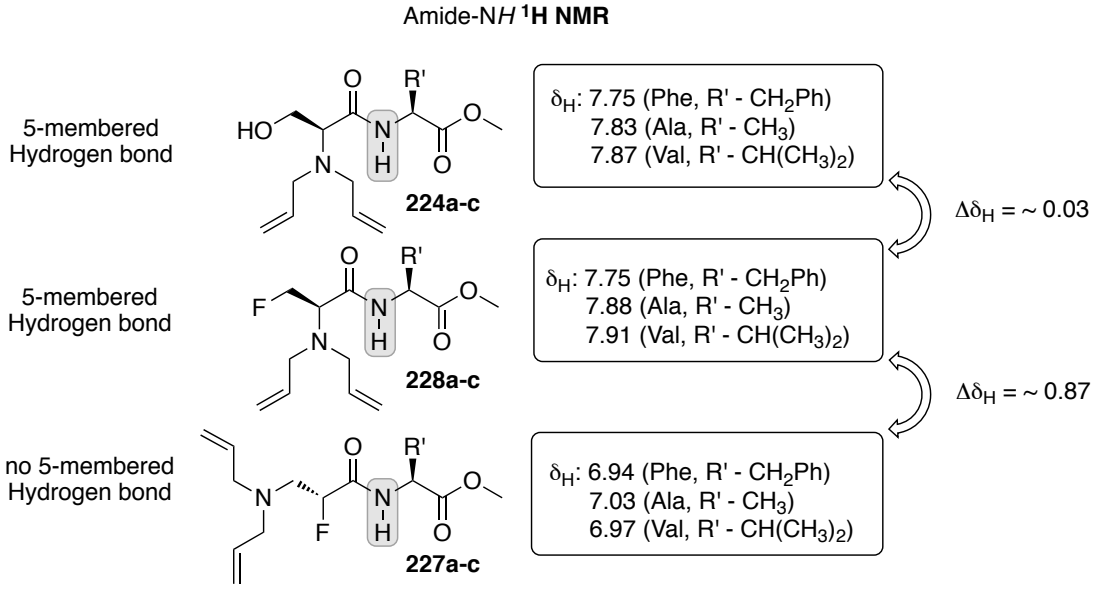


**Figure 5.03.** Analysis of the N*H* $^1$H NMR resonance between non-fluoro, *α* and *β* fluorinated products detailing the chemical shift disparities. Chemical shifts are reported in ppm and are quoted relative to $CDCl_3$.

The analysis of the amide N*H* chemical shifts in the $^1$H NMR spectrum in both the dipeptide starting materials **224a-c** and *α*/*β* fluorinated products **227**/**228a-c** provides further evidence of hydrogen bonding. In the *α*-fluorinated products **227a-c**, the N*H* resonance is approximately 0.9 ppm upfield relative to the respective starting materials **224a-c** and *β*-fluorinated products **228a-c**. Without the hydrogen bonding in these compounds, the direction of the chemical shift change of the *α*-fluorinated products may appear counter intuitive based on the electronegativity of the *α*-C–F bond. Thus these observations further support the evidence for a hydrogen bond in the alcohols **224a-c** resulting in a 5-membered ring.

To test this hypothesis further, the effect of temperature on the regioselectivity of the reaction was explored. It was anticipated at lower temperatures, that the selectivity for the *β*-fluorination in **224a** would increase relative to the *α*-fluorinated. Carrying out the reaction at -78 ºC gave rise to low levels of fluorination, however, the $^{19}$F NMR spectrum of the reaction mixture after 5 h showed only the *β*-fluorinated product. The reaction was then conducted at -20 ºC. After 2 h the $^{19}$F NMR spectrum showed a greater level of the *α*-fluorinated product, with an *α*:*β* ratio of 75:25. At ambient temperature, a black solution is immediately formed upon the addition of DAST **32**. After 20 minutes the $^{19}$F NMR spectrum of the crude mixture revealed an unexpected shift towards *β*-fluorinated product in a ratio of 50:50. The temperature profile was more complex than expected, but indicated a tendency to *β*-product at low temperature (-78 ºC).

### *5.3.2 - Dipeptide conformation in **227a***

$^{19}$F NMR analysis of *α*-fluorinated products **227a-c**, shows a through space $^{4}J_{FH}$ coupling constant, between the fluorine and the amide proton (Figure 5.04). These coupling constants are: 4.0, 3.7 and 4.3 Hz, corresponding to compounds **227a**, **227b** and **227c** respectively. This is indicative of an NMR solution structure with the expected ~180º relationship between the C–F bond and the amide (Chapter 1.11.2).[77]

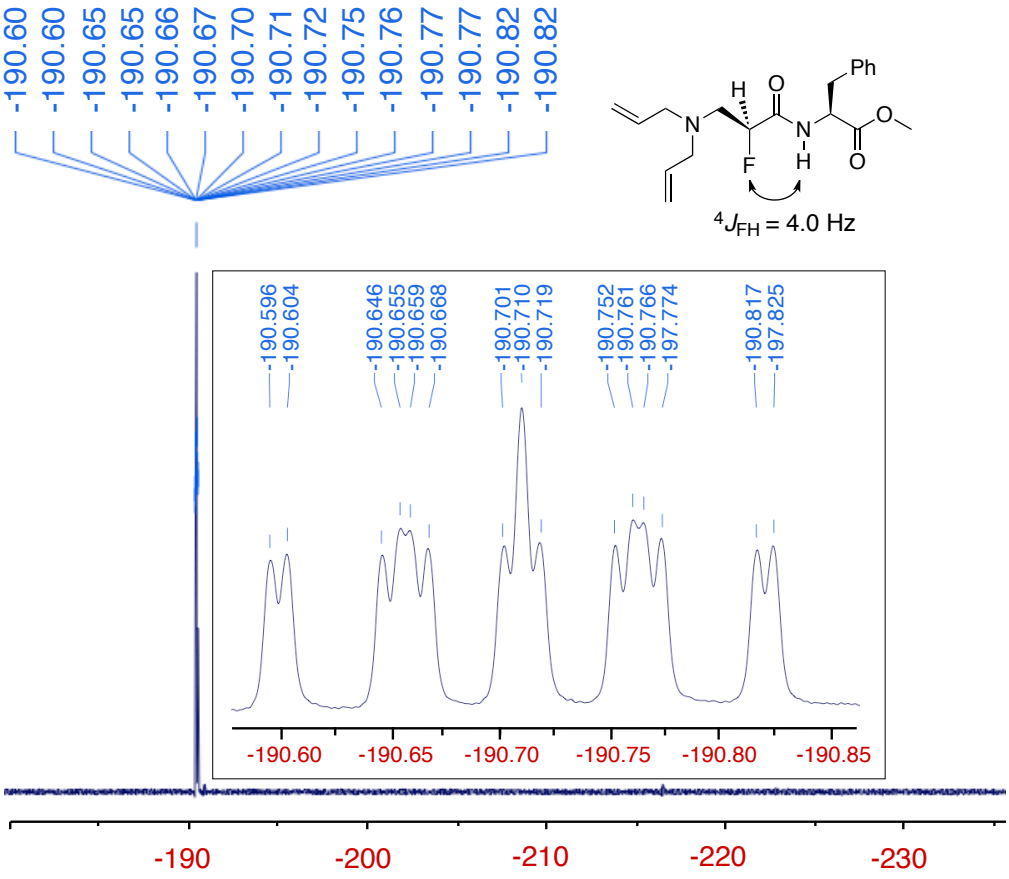


**Figure 5.04.** $^{19}F$ NMR (470 MHz, $CDCl_3$) of **227a** detailing the coupling pattern of the CHF resonance.

## 5.4 - Preparation of *α*-amino acid *N*–H and *N*–$CH_3$ amide derivatives

In order to study the effect of hydrogen bonding on the *α*/*β* fluorination ratio, incorporation of an *N*-methyl group on the amide nitrogen was explored. This removes any possibility of a hydrogen bond and may show an increase in *α*-fluorination selectivity. An initial effort to synthesise *N*-methylated **238** proved unsuccessful, even though a number of reported literature conditions were attempted (Scheme 5.11).[206,207] In our hands, the treatment of Boc protected L-phenylalanine with various bases and methyl iodide failed to furnish the desired *N*-methylated product **238** in suitable quantities and only complex mixtures resulted.

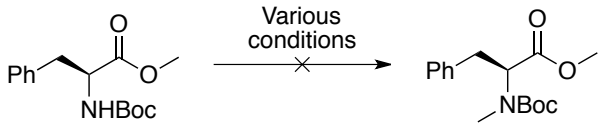


**237** **238**

**Scheme 5.11.** Attempted synthesis of *N*-methyl phenylalanine.

An alternative strategy was taken for the syntheses of appropriate *N*-methyl analogues and was achieved with secondary benzylamines **239a**/**b**. Starting from amine **239a** and following the same coupling procedure with T3P®, amide **240a** was synthesised in good yield (Scheme 5.12).

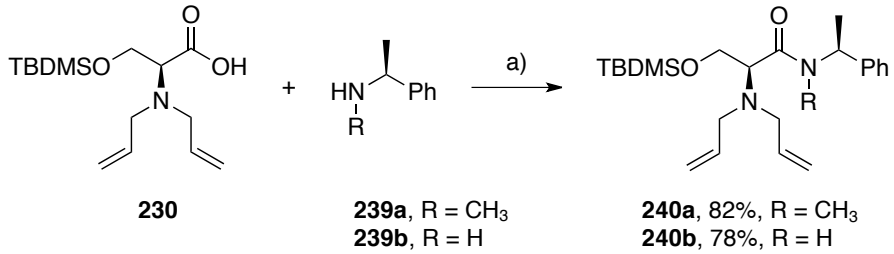


**230** **239a**, R = $CH_3$ **239b**, R = H **240a**, 82%, R = $CH_3$ **240b**, 78%, R = H

**Scheme 5.12**. *Reagents and conditions*: a) T3P® (1.5 eq), amine **239a/b** (2.0 eq), diisopropylethylamine (4.0 eq), $CH_2Cl_2$, 0 ºC to rt, 1-12 h.

Amide **240a** showed a significant *cis*-*trans* isomer ratio in the $^1$H NMR spectrum with a 75:25 preference for the *trans* isomer (Scheme 5.13). Isomerisation in this class of compound arises from the higher steric demand of the amide *N*′–$CH_3$ over that of an *N*–H in **232a-c**. The identification of the resonances attributed to both the *cis* and *trans* conformers in **240a** was possible by analysis of the $^1$H-$^1$H COSY spectrum. The resonance of the *N*′-$CH_3$ corresponding to the *trans* isomer was 0.2 ppm downfield of the *cis* resonance, with a ratio of 25:75 (*cis:trans*). This ratio was also observed for the $\alpha$-$CH_3$ resonance with the *trans* isomer 0.07 ppm upfield from that of the corresponding *cis* isomer. In 1D and 2D nOe experiments, irradiation of the $\alpha$-$CH_3$ (1.47 ppm) of the *trans* isomer resulted in a transfer of magnetization to both *cis* and *trans* conformers. This highlights that the two conformations are interconverting on the NMR timescale, complicating the unambiguous assignment of the *cis* and *trans* isomers.

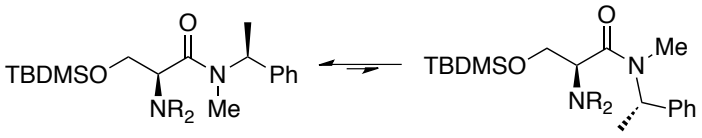


*trans* - **240a** *cis* - **240a**

**Scheme 5.13.** *Cis-trans* isomerisation of the tertiary amide **240a**. The *trans* conformation is preferred by 3:1 as indicated from integration of the $^1$H NMR signals. R = allyl.

For a direct comparison of the fluorination ratio between *N*′-Me and *N*-H amides, amide **240b** was synthesized from *α*-methylbenzylamine **239b** (Scheme 5.12). The amide **240b**, like the dipeptides **232a-c**, did not show any obvious *cis-trans* isomerisation by $^{1}$H NMR.

The silyl protecting groups of amides **240a/b** were removed using acetic acid buffered TBAF (Scheme 5.14), enabling the isolation of alcohols **241a/b** in good yields. The *cis-trans* isomer ratio in amide **241a** was also 25:75.

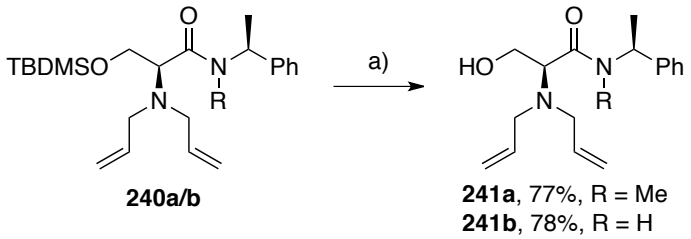


**Scheme 5.14**. *Reagents and conditions*: b) TBAF (4.0 eq, 1 M THF soln.), AcOH (5.0 eq), THF, rt, 12-24 h.

### *5.4.1 - Fluorination Reactions of amides 241a/b*

With the *N*′-alkylated substrates in hand, alcohols **241a**/**b** were treated with DAST **32** under the same conditions to that used previously, such that the *α*:*β* ratios could be directly compared (Scheme 5.15 & 5.16).

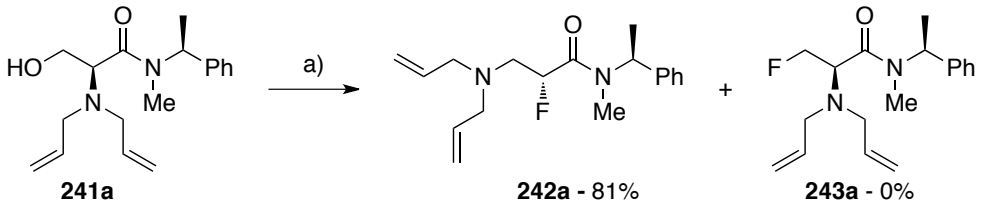


**Scheme 5.15.** *Reagents and conditions*: a) DAST **32** (1.1 eq), THF, 0 ºC, 1 h.

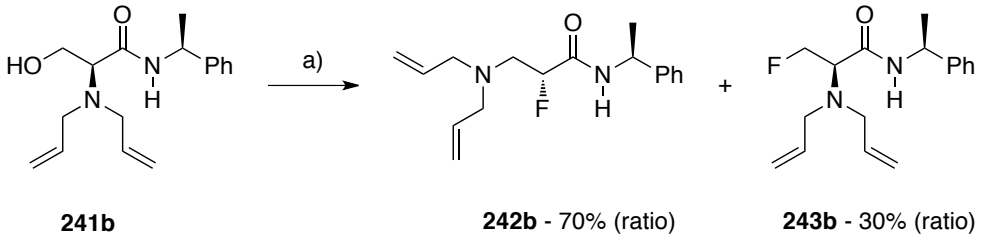


**Scheme 5.16.** *Reagents and conditions*: a) DAST **32** (1.1 eq), THF, 0 ºC, 1 h.

Direct analysis of the reaction mixture of N–H amide **241b**, which was still capable of forming a 5-membered intramolecular hydrogen bond, showed a 70:30 (*α*:*β*) bias for fluoride attack at the *α*–carbon (Figure 5.05, lower NMR). This reaction proceeded with a diastereomeric ratio of 92:8. Although the bias has shifted, it represents a significantly lower selectivity compared to esters **119** and **187**. This shift back to an *α*-fluorination preference suggests that the mechanism for selectivity may be more complex than anticipated. By contrast, analysis of the *α*:*β* ratio from *N*′-methylated amide **241a** was 99:1 in favour of *α*-fluorination (Figure 5.05, top NMR**)**. However, analysis of the crude $^{1}$H NMR indicated a diastereomeric ratio of 89:11. This represents a drop in diastereoselectivity for the fluorination of the *N*-substituted substrate **241b** compared to **224a-c**, suggesting that the reaction may have some $S_N1$ character. The $^{19}$F NMR of *α*-fluorinated **242a**, shows *cis* and *trans* products with resonances of -184.6 and -186.8 ppm respectively.

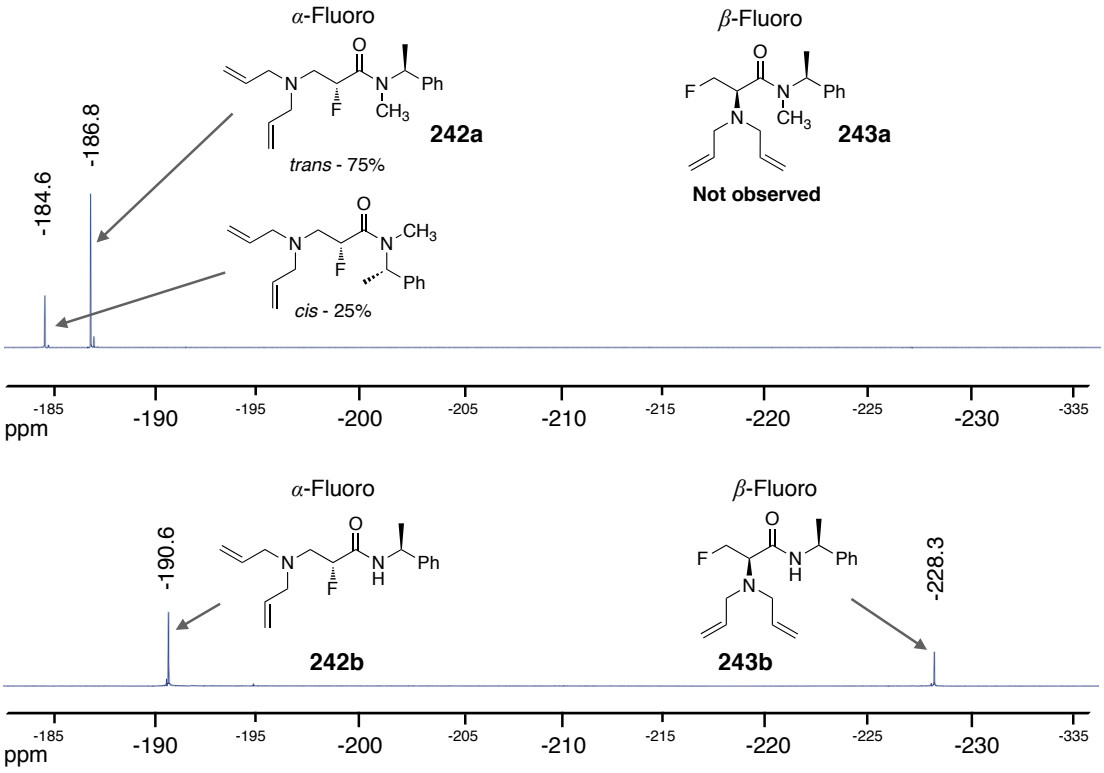


**Figure 5.05.** Overlay of the crude $^{19}$F{$^{1}$H} NMR (376 MHz, $CDCl_3$) from the fluorination of **241a/b** with DAST **32**.

The high fluorination selectivity for the *N*′-Me substrate for the *α*-product **242a** is greater than that observed for the fluorination of the amino esters **119** and **187** (Table 5.1). This is the first example of selective *α*-fluorination of an *N*′-substituted amide by deoxyfluorination. The difference in fluorination ratio between the *N*′-substituted amide **241a** and amide **241b** is consistent with the involvement of hydrogen bonding influencing the product profile.

It was possible to observe spin polarization in the 1D HOESY ($^{19}$F-$^{1}$H nOe) following selective irradiation of the fluorine signal in the two isomers of **242a**.[59] Selective irradiation of the *cis* isomer at -184.6 ppm in the $^{19}$F NMR (Figure 5.06, A) showed an enhancement of the *trans* $C_{\alpha+1}$–H proton.

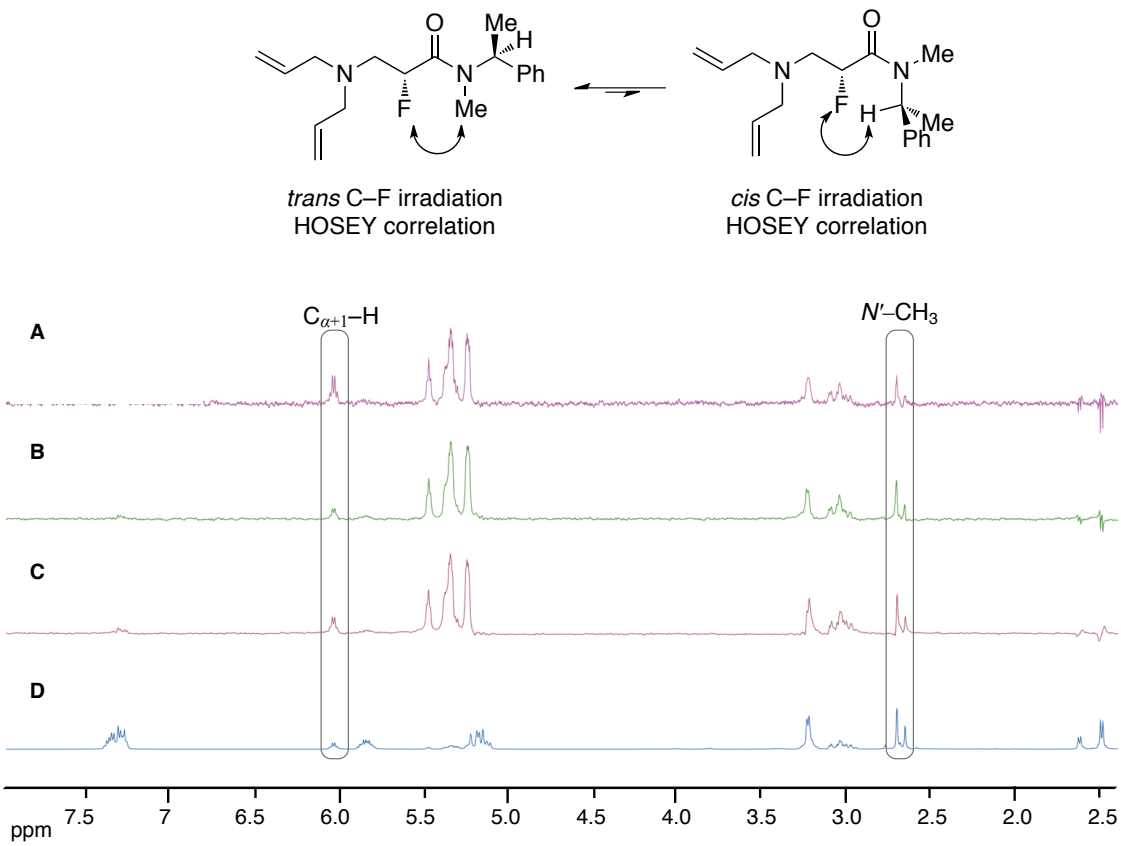


**Figure 5.06.** 1D HOESY (500 MHz, $d_6$-DMSO) of **242a**. **A** - Selective *cis* C–F irradiation at -184.6 ppm in **242a**; **B** - Selective *trans* C–F irradiation at -186.8 ppm in **242a**; **C** - Non-selective dual irradiation of *cis* and *trans* **242a**; **D** - standard $^{1}$H NMR.

This appears counterintuitive, however, this enhancement is observed as the amide is equilibrating on the NMR timescale, where during $\tau_m$ the spin polarization and enhancement is 'carried' over to the *trans* isomer. These is a strong enhancement of the allyl resonances, which overwhelms the *cis* $C_{\alpha+1}$–H resonance. Such an enhancement of the trans $C_{\alpha+1}$–H is not observed when selective irradiation of the signal at -186.8 ppm is carried out (Figure 5.06, B). An averaging of the enhancement is observed when a non-selective irradiation of the fluorine is conducted. The dynamic nature of the *cis*-*trans* isomerisation in **242a** clearly complicates the assignment.

## 5.5 - Extending the applicability to useful *N*-substituted amides

In order to extend the potential of this methodology, the *N*-allylamide **244** was prepared carrying non-orthogonal protecting groups. This protection strategy was designed to enable a one-pot deprotection to furnish a synthetically useful dipeptide for further peptide coupling through the free *β*-amine in **246** (Scheme 5.17).

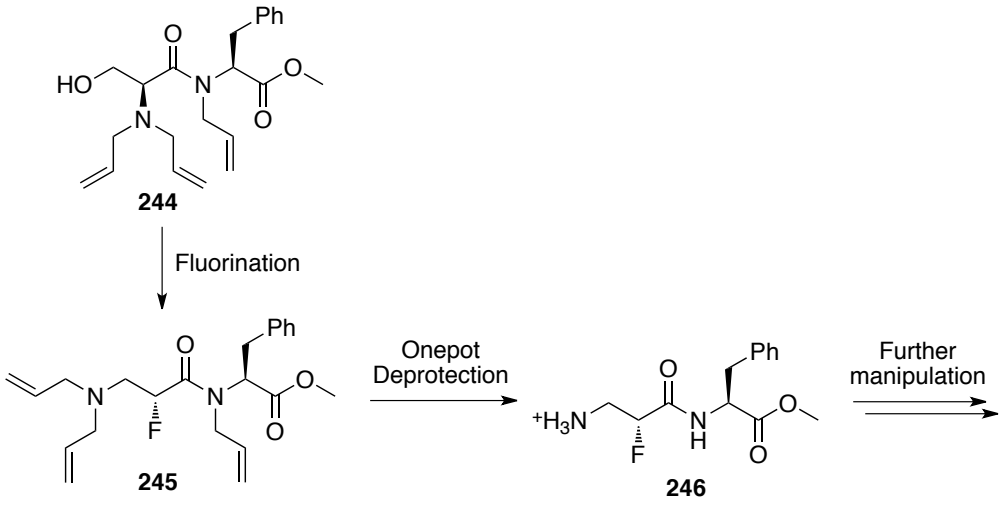


**Scheme 5.17.** Synthesis and deprotection strategy to peptide **246**.

The synthesis of *N*-allyl amine **247** was achieved by treating methyl ester **231a** with allyl bromide in DMF and diisopropylethylamine (Scheme 5.18). The addition of the reagents at 0 ºC and slow warming to room temperature enabled isolation of mono-allylated **247**, with no dialkylation observed. This method was efficient and gave

rise to sufficient quantities of allyl amine **247** for peptide coupling experiments to be conducted.

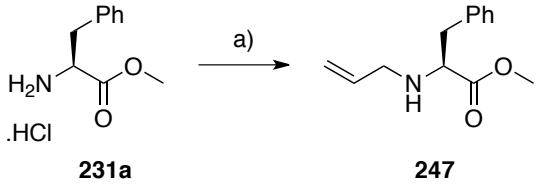


**231a** **247**

**Scheme 5.18.** *Reagents and conditions*: a) Allyl bromide (5.0 eq), diisopropylethylamine (4.0 eq), DMF, 0 ºC to rt, 24 h, 38%.

Initial efforts to prepare the allyl protected tertiary amide **248** utilising the conditions employed so far with T3P®, only provided a trace of the desired tertiary amide **248** (Table 5.3, Entry 1 & 2). Other peptide coupling reagents such as CDI, EDCI and HATU in either DMF or $CH_2Cl_2$ at room or elevated temperatures were also unsuccessful (Table 5.3, Entries 3-7 It is clear from these unsuccessful conditions that the *N*-allylated nitrogen is poorly nucleophilic as a result of the high steric hindrance from both the allyl and benzyl moieties in **230**.

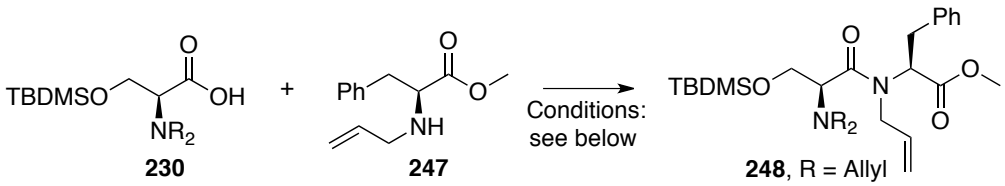


**230** **247** **248**, R = Allyl

| Entry | Reagent | Solvent | Temp (ºC) | Product |
|---|---|---|---|---|
| 1 | T3P® | $CH_2Cl_2$ | 20 | <5% (48 h) |
| 2 | T3P® | DMF | 20 | Trace |
| 3 | HATU | $CH_2Cl_2$ | 20 | No |
| 4 | HATU | DMF | 20 | No |
| 5 | HATU | DMF | 60 | No |
| 6 | CDI | $CH_2Cl_2$ | 20 | No |
| 7 | EDCI | $CH_2Cl_2$ | 20 | No |
| 8 | PyBrop | $CH_2Cl_2$ | 20 | No |
| 9 | PyBrop | DMF | 20 | No |
| 10 | PyBrop | DMF | 60 | No |
| 11 | $SOCl_2$ | $CH_2Cl_2$ | 20 | Multiple |

**Table 5.3**. Attempted peptide coupling conditions between **230** and **247**.

Entries 1 - 7 (Table 5.3) were also explored adding a catalytic amount of DMAP, however, this failed to generate the desired amide **248**. Alternative and more tailored peptide coupling reagents were explored. Attempts with the phosphonium salt, PyBrop[208] **249** (Figure 5.07) were also unsuccessful in the preparation of the coupled amide (Table 5.3, Entries 8-10). In each case starting materials were recovered from the reaction.

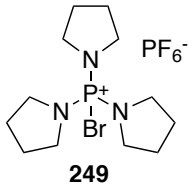


**249**

PyBroP

**Figure 5.07.** Tailored phosphonium salt for peptide coupling with sterically hindered substrates.

A final approach to prepare **248** was attempted using the acid chloride of **250** (Table 5.3, Entry 11) (Scheme 5.19).

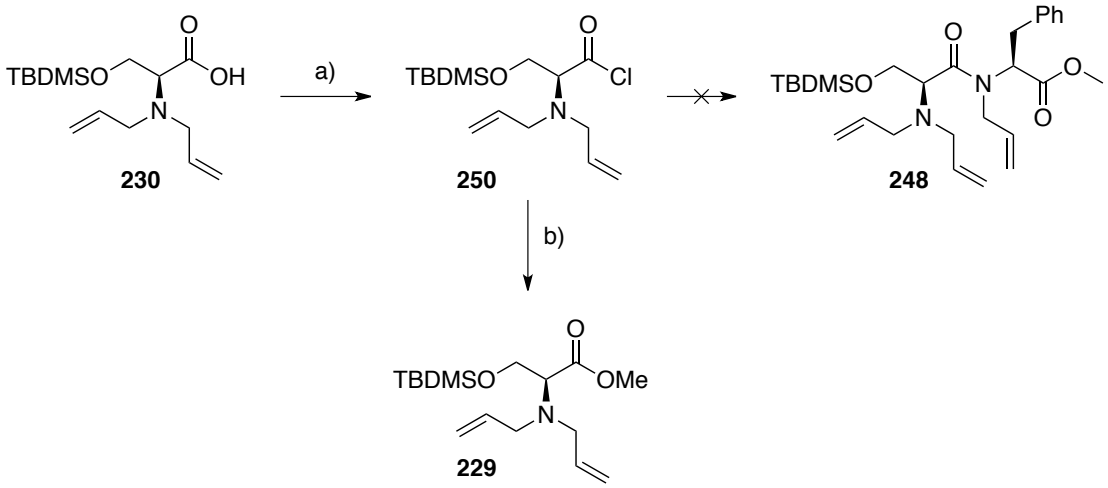


**230** **250** **248** **229**

**Scheme 5.19.** *Reagents and conditions*: a) $SOCl_2$, $CH_2Cl_2$, DMF (cat.), rt, 1 h followed by the addition of **247**; b) $CH_3OH$ quench.

Acid chloride **250** was prepared by treatment of the carboxylic acid **230** with thionyl chloride in $CH_2Cl_2$, and a catalytic amount of DMF. Its formation was confirmed by a methanol quench to furnish the corresponding methyl ester **229** (Scheme 5.19). Once the acid chloride was formed, secondary amine **247** was added. TLC analysis indicated

that multiple products had formed after 1 h, and a complex mixture was observed by $^{1}$H NMR analysis. In light of these results, this route was not investigated any further.

## 5.6 - Tertiary allylamide from secondary dipeptides

With the coupling between *N*-allyl amine **247**, and carboxylic acid **230**, failing to furnish the desired amide, attention turned to direct amide allylation (**251** to **252**). The tri-allylated dipeptide **232a**, could clearly be accessed using an appropriate base with an allyl halide or by the use of a transition metal catalysed allylation reaction (Scheme 5.20).

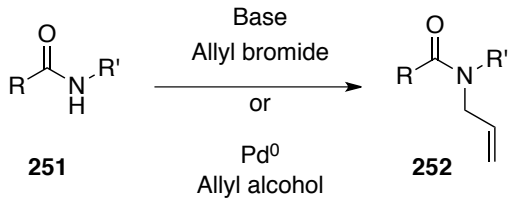


**Scheme 5.20.** Base and metal mediated approaches for the allylation of amides. R/R' = allyl/alkyl

Treatment of amide **232a** with NaH in THF . (Table 5.4, Entry 1 and 2) in the presence of an excess of allylbromide resulted in a complex product mixture, of which, the *β*-alanyl **253** species was one of the major side-products as judged by crude $^{1}$H NMR (Scheme 5.21).

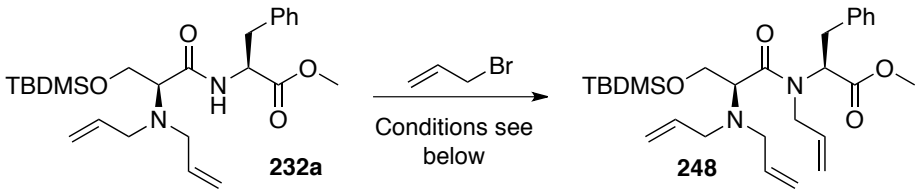


| Entry | Base | Equivalents | Solvent | Temp ºC | Products |
|---|---|---|---|---|---|
| 1 | NaH | 1 | THF | 20 | Multiple |
| 2 | NaH | 1 | DMF | 20 | Multiple |
| 3 | KHMDS | 1 | THF | -78 | Yes |
| 4 | KHMDS | 0.9 | THF | -78 | Yes |
| 5 | KHMDS | 1 | THF | -100 | Yes |
| 6 | KHMDS | 0.9 | THF | -100 | Yes |
| 7 | LiHMDS | 1 | THF | -78 | Yes |
| 8 | KO$^t$Bu | 1 | THF | 20 | No |
| 9 | $Cs_2CO_3$ | 4 | THF | 20 | Multiple |
| 10 | $Cs_2CO_3$ | 4 | THF | 60 | Multiple |
| 11 | $K_2CO_3$ | 4 | THF | 20 | Multiple |

**Table 5.4.** Reagents and conditions used for the attempted allylation of amide **248**.

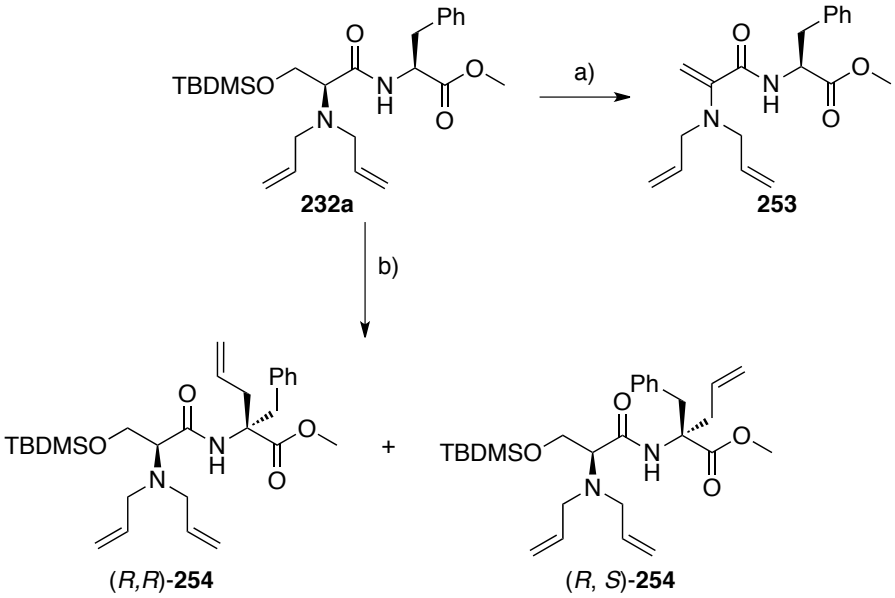


**Scheme 5.21**. *Reagents and conditions*: a) NaH (1.0 eq), allyl bromide (4.0 eq), DMF, 20 ºC; b) KHMDS (1.0 eq), allyl bromide (4.0 eq), THF, -78 ºC, 1-16 h, 53%.

When KHMDS and LiHMDS were used (Table 5.4, entries 3-7) at -78 ºC, the $C_{\alpha+1}$ allylated product **254** was formed (Scheme 5.21**)**. This product could also be observed even when a substoichiometric equivalent of KHMDS was employed at -78 ºC and -100 ºC (Table 5.5, entry 4 & 6).

The $C_{\alpha+1}$ product, an *α*-allyl phenylalanine dipeptide **254** was isolated as a diastereomeric pair, from the reaction with KHMDS and allyl bromide. The diastereomers could not be separated by column chromatography but were characterised as a mixture by 1D and 2D NMR. In the $^{1}$H NMR of **254**, the loss of the $C_{\alpha+1}$ proton resonance, and retention of the amide NH resonance were indicative of the formation of **254**. This was confirmed by DEPT and HMBC analyses of **254**, which identified the expected quaternary carbon. The fact that this is a 1:1 diastereomeric pair is consistent with *α*-proton abstraction and subsequent enolization. This diastereomer mixture was also observed when K$^{t}$OBu was used as a base (Table 5.4, entry 8). From these observations it is clear that the p$K_a$ of the $C_{\alpha+1}$ proton was similar or more acidic than that of the amide proton and that the bases were able to deprotonate this hindered proton, furnishing the $C_{\alpha+1}$ allylated product.

In an effort to circumvent this, the strong, hindered base *tert*-butyl P4 phosphazene **255** was explored (Figure 5.08). Developed in the late 90's by Reinhard Schwesinger, $^{t}$Bu P4 **255** has a $^{MeCN}pK_{BH^+}$ of 42.7 resulting form the potential large charge delocalisation available upon protonation (Figure 5.08). This class of base is well documented in the synthesis of *N*′-benzylated peptides.[209,210]

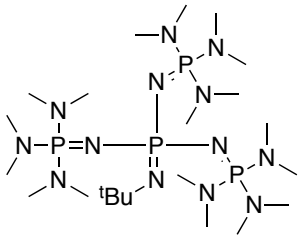


**255**

**Figure 5.08.** The strong hindered base $^{t}$Bu P4 **255**.

Initial treatment of **232** with of $^{t}$Bu P4 **255** at -78 ºC in THF with allyl bromide again gave rise to multiple products, of which both the $C_{\alpha+1}$ allylated product **254** and the desired *N*′-allyl amide **248** could be isolated (Scheme 5.22).

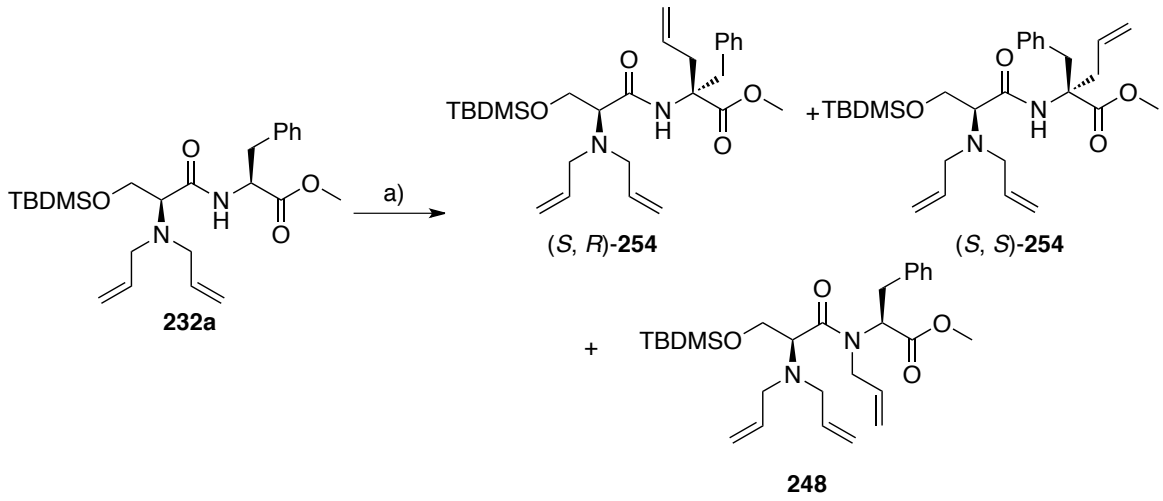


**Scheme 5.22.** *Reagents and conditions*: a) $^{t}$Bu P4 **255** (0.9 eq), allyl bromide (4.0 eq), THF, -78 ºC, 16 h, 30-50%.

The *N*′-allyl amide **248** was only isolated in a 10 % yield, however, interestingly, the $C_{\alpha+1}$ allylated product **254** was isolated again with a low but significantly improved selectivity for one diastereomer (2:1 from $^{1}$H NMR). The observation that **254** was still formed, even when using a particularly hindered base, highlights the similar p$K_a$ of both protons.

Using phosphazene base **255** with benzyl bromide in place of allyl bromide, three benzylated products could be isolated after chromatography. Analysis identified these as the $C_{\alpha+1}$ benzyl **256**, *N*′-benzyl **257**, and benzyl ester **258** (Scheme 5.23) which were isolated in yields of 20%, 18% and 15% respectively.

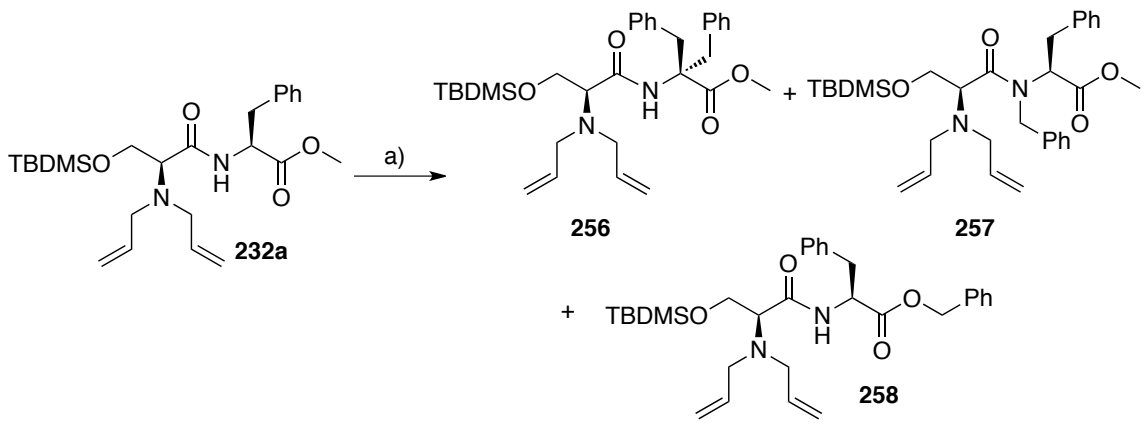


**Scheme 5.23.** *Reagents and conditions*: a) $^{t}$Bu P4 (0.9 eq), benzyl bromide (4.0 eq), THF, -78 ºC, 16 h, 15-20%.

*N*′-Benzylated amide **257** was formed in an improved yield (16%) compared to the *N*′-allyl amide **248** (10%). This protecting group is however not so attractive as deprotection of *N*′-benzyl amides involves the use of sodium metal in napthalene, a reagent combination incompatible with the functional groups in amide **257**.[197] The apparent hydrolysis of the methyl ester and subsequent carboxylate alkylation to generate an ester in **258**, was not observed with allyl bromide.

Optimisation of the reaction by increasing the scale and initial treatment of amide with $^{t}$Bu P4 at -100 ºC followed by gradual warming through to -78 ºC before the addition of allyl bromide, furnished amide **248** in a significantly improved yield of 53% (Scheme 5.24). This enabled sufficient quantities of the *N*′-allyl amide **248** to be isolated for subsequent transformations.

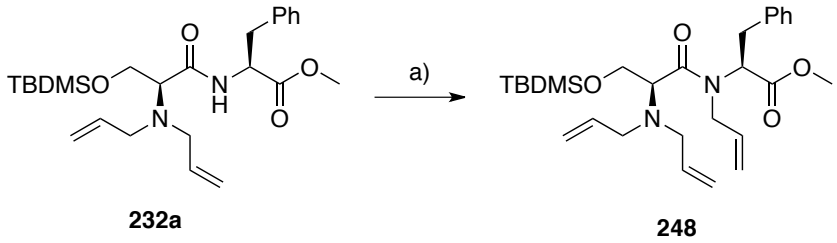


**Scheme 5.24**. *Reagents and conditions*: a) $^{t}$Bu P4 (0.93 eq), allyl bromide (5.0 eq), THF, -100 ºC to -78 ºC to rt, 20 h, 53%.

The $^{1}$H NMR spectrum of **248** clearly indicates two rotamers, designated here as the *cis* and *trans* allylic resonances for the *N*′-allyl group (Figure 5.09). The other resonances

were less easy to assign with confidence, however, from Figure 5.09 it would appear that the *trans* rotamer predominates in a ratio of 95:5.

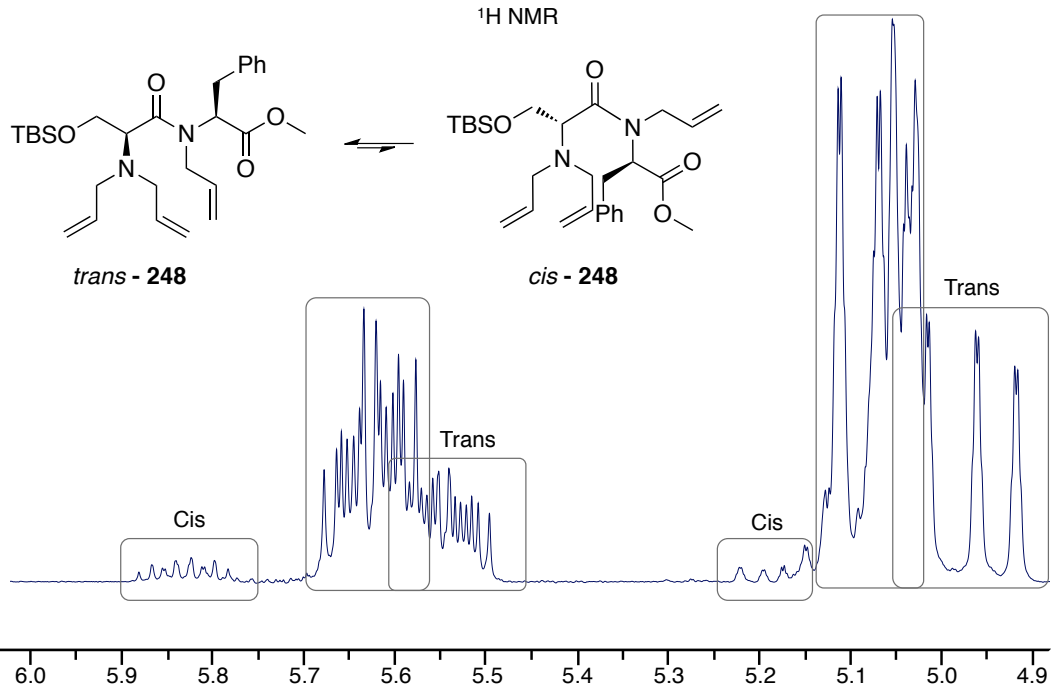


**Figure 5.09.** $^{1}$H NMR (400 MHz, $CDCl_3$) showing the allylic hydrogen spin system of **248** detailing the *cis*/*trans* resonances of the *N*′-allyl group.

The *cis*-*trans* relationship in **248** is significantly less than that observed in **240a**. It is likely that the steric demand of the *N*′-$CH_3$ in **240a** and the benzyl moiety are similar. Whereas in **248** the $CH_2$ of the *N*′-allyl group is significantly less demanding compared to phenylalanine. Thus, the *trans* isomer in **248** is likely to be the more stable conformation.

Silyl ether cleavage of amide **248** was achieved with acetic acid buffered TBAF to furnish alcohol **244** in good yield (Scheme 5.25). The nature of the *cis*-*trans* isomerism in the $^{1}$H NMR was similar to that of allyl amide **248**.

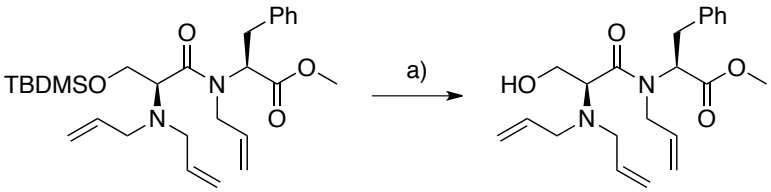


**248** **244**

**Scheme 5.25**. *Reagents and conditions*: a) TBAF (4.0 eq), AcOH (5.0 eq), THF, rt, 12 h, 84%.

### *5.6.1 - N-allyl amide dipeptide **244** fluorination with DAST **32***

Treatment of **244** with DAST **32** gave the expected $\alpha$-fluorinated rearranged product **245** and proved to be high yielding (73%) and also showed a high level of selectivity (Scheme 5.26), similar to that observed for fluorination of *N*′-methyl amide **241a**. Direct $^{19}$F NMR analysis of the reaction showed <1% $\beta$-fluorinated product **259** (Figure 5.10). However, amide **245** was isolated in a diastereomeric ratio of 90:10 suggesting a little $S_N1$ character, as observed with the *N*′-methyl amide **241a**. Presumably this arises from the steric bulk of the amide and perhaps some stabilisation of a carbocation intermediate by the amide bond.

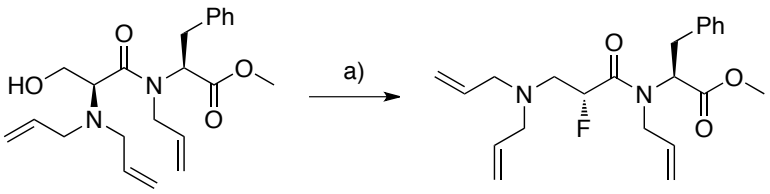


**244** **245**

**Scheme 5.26**. *Reagents and conditions*: a) DAST **32**, THF, rt, 1 h, 73%.

Purification of **245** from residual starting material was easily achieved by column chromatography. A combination of 1D and 2D NMR techniques were used to assign the resonances corresponding to the major *trans* isomer, which was favoured by 90:10 to the *cis* isomer.

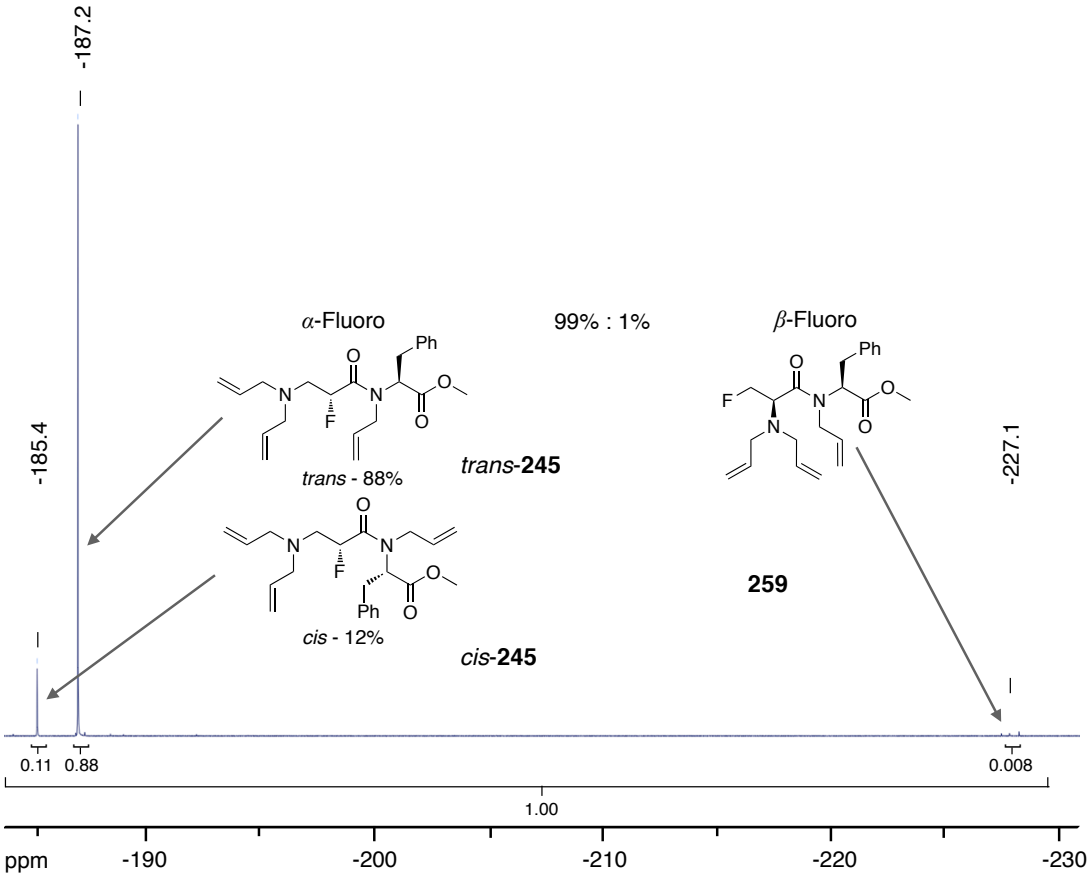


**Figure 5.10**. $^{19}F\{^{1}H\}$ NMR (470 MHz, $CDCl_3$) of tertiary amide **244** directly after reaction with DAST **32**. High selectivity for the $\alpha$- over the $\beta$-fluorinated product. Both *cis* and *trans* amide C–F resonances can be clearly observed, which were confirmed by VT.

## 5.7 - *N*-Allyl amide 245 deprotection

The next stage in the synthesis required complete *N*-deallylation of **245** by metal catalysis (Scheme 5.27).

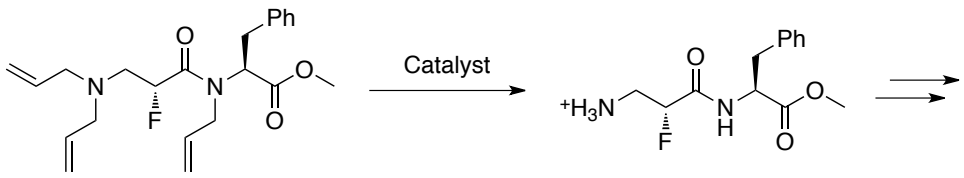


**245** **246**

**Scheme 5.27.** Proposed one pot de-allylation with a metal catalyst for further functionalisation.

Initially, deprotection of all three allyl protecting groups in one step was attempted following the procedure set out in Chapter 4. This involved $Pd_2(dba)_3$ as a catalyst and a stoichiometric amount of thiosalicylic acid in THF (Scheme 5.28).

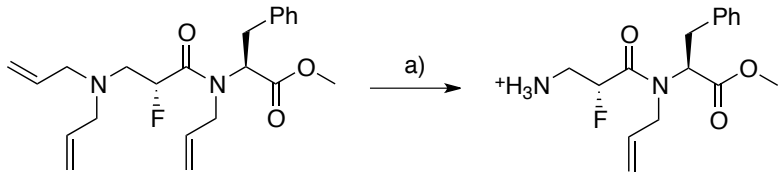


**Scheme 5.28**. *Reagents and conditions*: a) $Pd_2(dba)_3$ (25 mol%), dppb (30 mol%), thiosalicylic acid (3.3 eq), THF, reflux, 5 h, 93%.

This approach was only partially successful and led to the deprotection of the primary allyl groups, furnishing *N*-allyl amide **260**. Increasing the reaction time resulted in decomposition of the starting material and there was no evidence that the *N*′-allylamide could be cleaved by this approach. The lack of reactivity of the *N*′-allyl amide moiety can be rationalised as illustrated in Scheme 5.29. Protonation of the allyl amine nitrogen by the thiosalicylic acid enables a $\pi$-allyl Pd complex to be formed. Without protonation, cleavage of the allyl groups is not possible. The partial double bond character of the amide bond and subsequent partial positive charge on the amide nitrogen is not sufficiently activating for this purpose and does not enable the $\pi$-allyl Pd complex to form. Thus the *N*′-allyl amide is less reactive than the *N*,*N*-diallylamine towards this particular catalytic system.

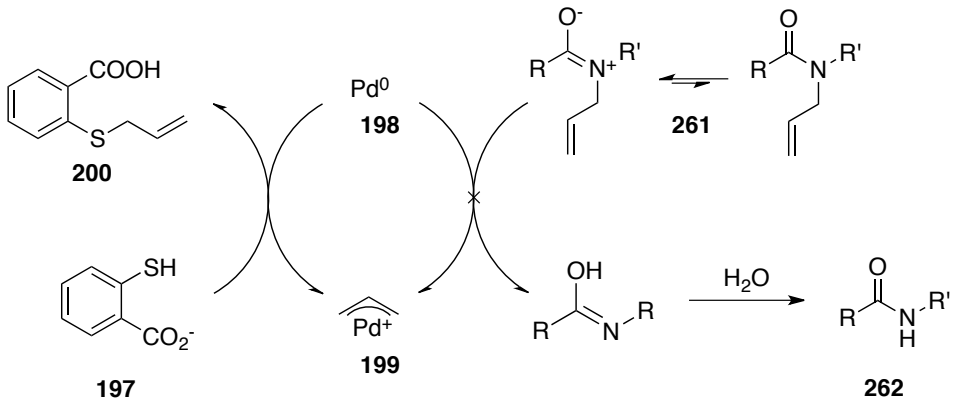


**Scheme 5.29**. Proposed mechanism for the unsuccesful cleavage of the allylamide protecting group.

The literature contains a wealth of methods for the removal of allyl ethers and amines, however there are few examples for the removal of *N*′-allyl amides.[211–213] The successful reports all use the same principal involving a metal mediated isomerisation of an allyl amide (**263**) to the enamide **264** (Scheme 5.30), followed by an oxidative cleavage, rather than direct cleavage of the *N*′-allyl amide.[214–217]

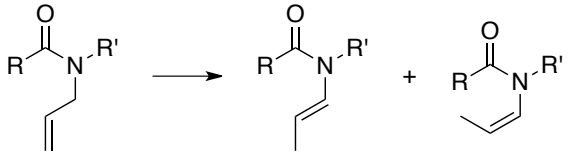

**263** *trans*-**264** *cis*-**264**

**Scheme 5.30.** Metal mediated isomerisation of an allylamide to *cis* and *trans* enamide. R/R′ = various alkyl and aryl substituents. M = metal catalyst

For this purpose the free amine of *N*-allyl amide **245** was protected as the *tert*-butyl carbamate ester **265** in aqueous dioxane with $Boc_2O$ and triethylamine (Scheme 5.32).

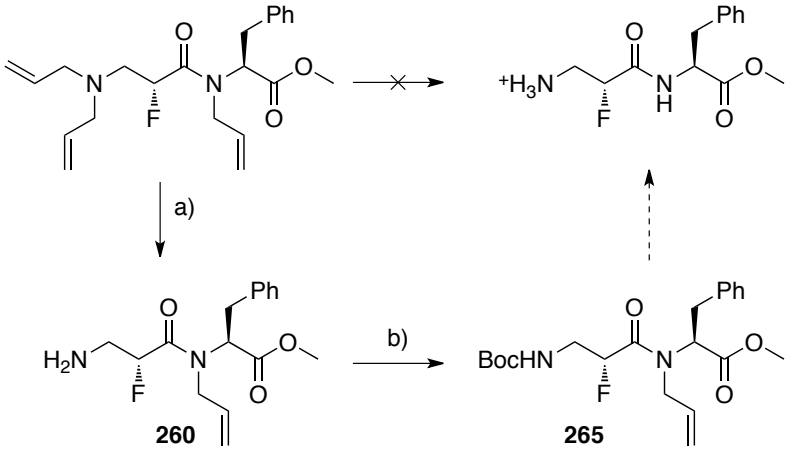

**260** **265**

**Scheme 5.32**. *Reagents and conditions*: a) $Pd_2(dba)_3$ (25 mol%), dppb (30 mol%), thiosalicylic acid (2.9 eq), THF, 60 ºC, 3 h, 93%; b) $Boc_2O$ (1.3 eq), diisopropylethylamine (3.0 eq), aqueous dioxane (25% *v*/*v*), rt, 24 h, 71%.

Purification of **265** was easily achieved by chromatography and the carbamate protected allyl amide **265** was isolated 71% yield. The $^1$H NMR was complex due to the N*H* carbamate proton coupling to the diastereotopic C$H_2$ protons and also the C*H*F group, resulting in signal broadening. With the amine protected, it was now possible to screen an array of catalysts for allylamide deprotection. Initial efforts with a variety of catalysts proved unsuccessful however the reaction with 10 mol% of $RuHCO(PPh_3)_2$ in toluene did generate the isomerised enamide **266** (Scheme 5.33) as indicated by direct $^1$H NMR analysis of the reaction product. The crude enamide and catalyst were then committed directly for oxidative cleavage by $RuCl_3$ and $NaIO_4$ (Scheme 5.33). TLC indicated that enamide **266** was consumed and then hydrolysis of the putative *N*-formyl intermediate was attempted by treatment with aqueous $NaHCO_3$ during work-up. However, this work

up was insufficient to cleave the formyl group with the *N*-formylamide **267** isolated after chromatography.

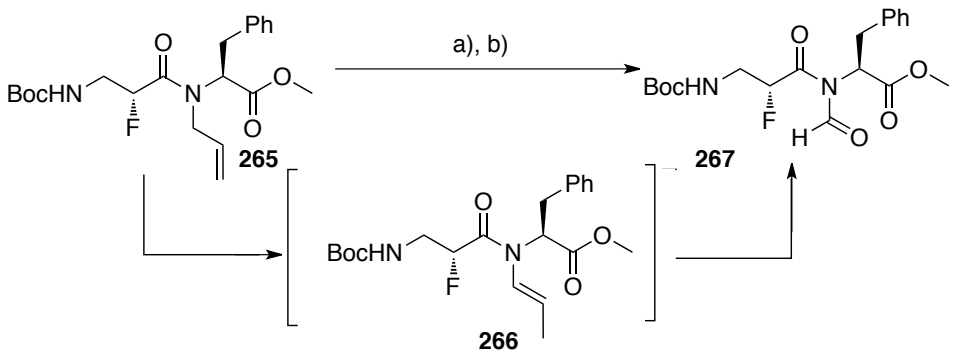


**Scheme 5.33.** *Reagents and conditions*: a) $RuHCO(PPh_3)_2$ (10 mol%), toluene, reflux, 3 h; b) $RuCl_3$, $NaIO_4$, 1,2-dichloroethane, water, rt, 12 h, 59%.

The distinctive chemical shift of the aldehyde proton (~9 ppm) and the carbonyl resonances observed in the $^{13}C$ NMR supported the structure of **267**. Subsequent hydrolysis of the formyl group in **267**, to yield amide **268** was achieved by stirring in basic aqueous acetone (Scheme 5.34).

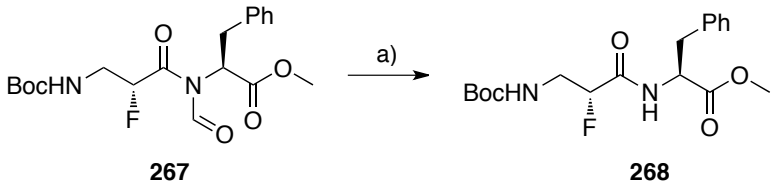


**Scheme 5.34.** *Reagents and conditions*: a) $NaHCO_3$ (1.0 eq), $Na_2CO_3$ (0.1 eq), acetone, water, 10 h, 46%.

Purification was achieved by column chromatography to furnish **268** in a yield of 46%. Amide **268**, did not show any *cis* isomer by NMR. The successful deprotection of the allyl amide in **265** demonstrates that it is possible to use this methodology to access synthetically useful peptides and demonstrates the applicability of selective fluorination of amides by DAST **32**.

## 5.8 - Conclusions

This chapter reports the scope and limitations of the fluorination of dipeptides and amide analogues bearing the hydroxy amine motif. Initial studies with amides **224a-c** demonstrated poor selectivity for $\alpha$-fluorination, however for *N*′-alkylated amides **241a** and **244** the selectivity for $\alpha$-fluorination returns. As discussed throughout the Chapter, this can be attributed to a hydrogen bond between the dialkylated amine and the amide *N*–H. With this methodology, it was possible to synthesize an $\alpha$-fluorinated *N*′-allylamide with high fluorination selectivity and satisfactory diastereomeric excess. It was also possible to demonstrate that this product could be successfully deprotected yielding a synthetically useful fluorinated dipeptide **268**.

# Chapter 6

# Future work

## 6.1 - Future Work for Chapter 3

Solving of the crystal structure with the hydroxy compounds (*S*,*S*)- and (*R*,*R*)-**145** would supplement the data presented in Chapter 3.5. This would enable a direct comparison to be made between the hydroxy-**145** and fluoro-**144** ligands. To achieve this it will be required to reconsider the conditions already attempted and to optimise these for suitable crystal growth. This process is timely, however careful optimisation should yield crystals that diffract at a suitable resolution.

## 6.2 - Future Work for Chapter 4

The key limitation of the chemistry in Chapter 4 was the amide bond synthesis between **155** and **120**/**188**/**209**, which typically returned poor yields of <30% (Chapter 4.5, 4.7 and 4.9.1). Alternative routes to access the coupled material may be possible through a copper or palladium mediated coupling between 3,6-dichloroacridone[218] **269** and fluoropropanamide **270** (Scheme 6.01).[219,220]

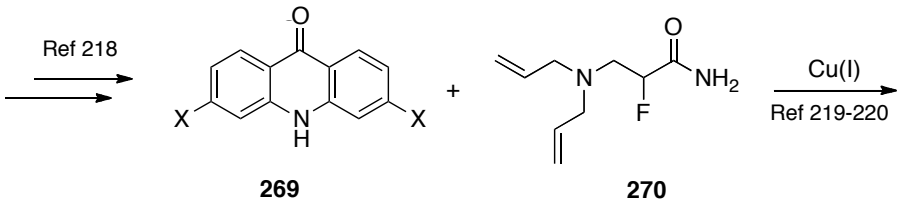


**269** **270**

**Scheme 6.01.** Proposed coupling route between 3,6-dichloroacridone **269** and primary amide **270**. X = halide

In addition to this, future work should be focused on the synthesis of a genuine BRACO-19 **142a** analogue. To achieve this, it may be required to re-assess the synthesis of the fluorinated amino acid. One promising route would be to treat methyl 3-chloropropanoate **271** with potassium phthalate **272** (Scheme 6.02) to form the protected β-amino acid **273** following simple functional group interconversions. This would be followed by a metal mediated asymmetric electrophilic fluorination of the acid chloride **273** to yield the α-fluoro product **274** as developed by Lectka (Scheme 6.02).[221] This reaction can be quenched by various nucleophiles to provide esters and amides in good yields with high enantiomeric excess. The quenching of the intermediate by the dianion of 3,6-diaminoacridone **155** may prove fruitful to explore.

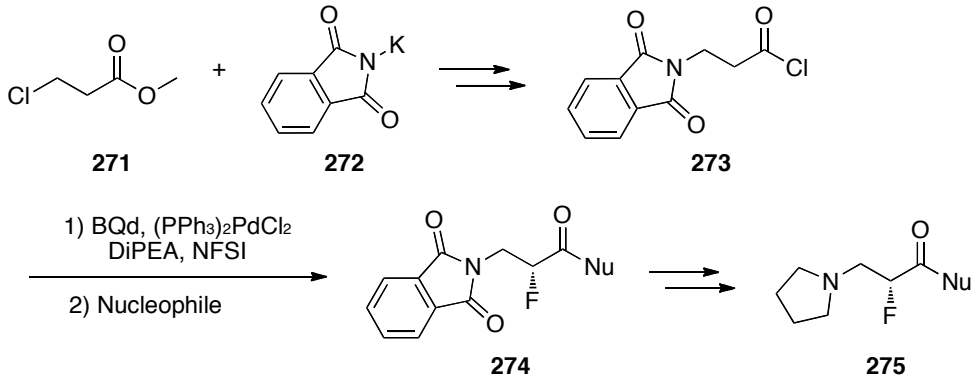


**Scheme 6.02.** Proposed alternative route to the synthesis of true BRACO-19 **142a** analogues. Nu = -OMe, -NHaryl, -$NH_2$

In addition to this, the incorporation of two C–F bonds into **208** and **212** may enable a useful NMR probe to study the interactions between **208** and **212** with quadruplex DNA. The investigation between quadruplex DNA stabilising ligands and DNA is a very complicated and multifaceted arena, however, 1D or 2D NMR experiments involving $^{19}F$ NMR may offer further information in addition to standard techniques employed.

## 6.3 - Future work for Chapter 5

In order to fully investigate the finer details of the reaction mechanism, the synthesis of an aziridine dipeptide such as **276** from **275** would be advantageous (Scheme 6.03). The synthesis of similar aziridine containing dipeptides has been previously reported in the literature.[222]

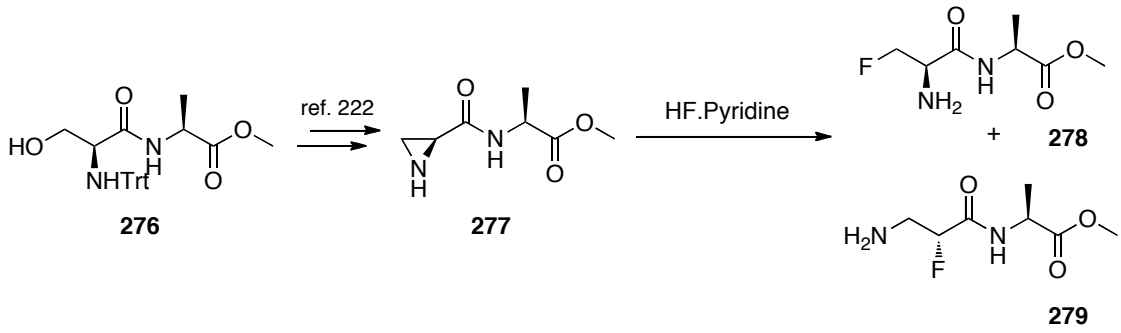


**Scheme 6.03.** Proposed synthesis of an aziridine containing dipeptide **276** to probe α/β-fluorination distribution.

Treatment of **276** with a nucleophilic source of fluorine, such as HF.pyridine, would enable the α/β-fluorination selectivity to be probed (Scheme 6.03). Further to this, the preparation of **276** as its $PF_6^-$ salt would allow for X-ray crystallographic evaluation of a *pseudo*-intermediate similar to that of **236** in the DAST pathway mechanism (Scheme 5.10). This would provide conformational information and thus allow for further assessment of the origin of α/β-selectivity in these systems.

In addition to the aforementioned investigations, the synthesis of the structures in Figure 6.01 followed by evaluation of the fluorination ratios by treating with DAST **32**. This would add to the overall quality of this work by providing a comprehensive evaluation, scope and limitation survey.

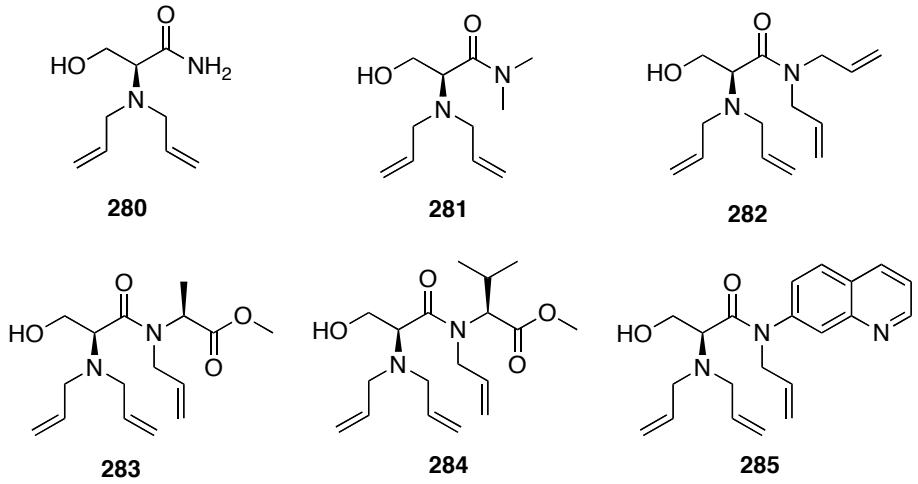


**Figure 6.01.** Target compounds to further understand the scope of the fluorination reaction.

The evaluation of other fluorinating reagents such as Deoxo-Fluor® or MOST would be of general interest, however, solvent investigations and work focused on improving the overall diastereomeric excess would vastly improve the synthetic use of this methodology.

# Chapter 7

# Experimental

## 7.1 - General experimental procedures

All glassware was flame dried under high vacuum other than in situations where aqueous solutions were employed. Reactions were carried out under an atmosphere of argon, unless otherwise noted. Compressed argon was passed through a drying column packed with 4 Å molecular sieves, potassium hydroxide and self-indicating desiccant, before reaching a double manifold. All reactions involving the use of organometallic reagents were conducted by standard air-free techniques in Schlenk tubes or flasks. Hydrogenations were conducted in multi-neck flasks and the atmosphere exchanged with hydrogen by a pump-purge method. Dry $CH_2Cl_2$, $Et_2O$, and THF were obtained from an mBRAUN SPS-800 solvent purification machine by passage through a drying column packed with 4Å molecular sieves and dispensed under an inert atmosphere when required. NOTE: THF from this purification system was unstabilised. Dry $CH_3OH$ was achieved by reflux over calcium hydride and collected in a still head when required. Where appropriate, solvents were degassed by the standard freeze-pump-thaw technique at least three times with freshly dispensed dry solvent.[223]

**$^1$H NMR** spectra were recorded on 300, 400 or 500 MHz Bruker Avance/Avance II spectrometers. All spectra were acquired in deuterated solvents, and calibrated to the chemical shift of that residual solvent. Proton assignments are made according to chemical shift, multiplicity and 2D NMR experiments. Coupling constants (*J*) are reported to 0.1 Hz and are averaged for coupling nuclei. Complex spectra are numbered for ease of interpretation. All other resonances are described based on their chemical environment. NMR spectra were interpreted using iNMR or TopSpin.

**$^{13}$C NMR** spectra were recorded at 75, 101, 126 MHz on Bruker Avance/Avance II spectrometers. Resonances were assigned by reference to DEPTQ, HMBC and HSQC spectra with coupling constants reported to 0.1 Hz, where appropriate.

**$^{19}$F NMR** spectra were recorded at 282, 376, 470 MHz on Bruker Avance/Avance II spectrometers. Resonances were assigned according to chemical shift, multiplicity, and reference to the literature. Coupling constants are reported to 0.1 Hz and are averaged for coupling nuclei. Dr Tomas Lebl recorded all HOESY spectra.

**NMR Multiplicities** are reported as follows: s - singlet; br s - broad singlet; m - multiplet; d - doublet; dd - doublet of doublets; ddd - doublet of doublet of doublets; dddd - doublet of doublet of doublet of doublets; dq - doublet of quartets; t - triplet; q - quartet; tq - triplet of quartets; qqd - quartet of quartet of doublets

***In vacuo*** refers to the use of a diaphragm vacuum pump to remove solvent under reduced pressure on a Büchi Rotavapor at 40 ºC. The bath temperature was reduced to 0 ºC with ice when removing solvents from volatile compounds. Drying under vacuum refers to the use of an Edwards RV-5 rotary-vane oil pump at a pressure of <0.1 mbar.

**Lypholisation** refers to the removal of water by sublimation on a Christ Alpha 1-2 LD Plus freeze dryer equipped with an Edwards RV3 rotary-vane oil pump.

**Optical rotations** were recorded on a Perkin Elmer optical rotation model 341 machine with a cell path length of 1 dm. The vast majority of samples were recorded at 589 nm (sodium D-line) at ambient temperature (20 ºC) and are denoted as $[\alpha]_D^{20}$. For acridone and acridine compounds the light source was maintained at either 365 nm, 436 nm, 546 nm or 578 nm in an attempt to achieve satisfactory beam transmission. Concentrations (*c*) are reported in g/dm and specific optical rotations are denoted as $[\alpha]_\lambda^{20}$ in the implied units of $10^{-1}$ deg cm$^3$ g$^{-1}$.

**HPLC analysis** was conducted on a Varian Prostar HPLC machine equipped with a Prostar Auto Sampler model 400 and a Prostar 240 solvent delivery system. Compound elution was monitored with a Prostar UV-Vis 325 module at a wavelength of 230 nm or 250 nm. Column for chiral analysis – Chiralcel OD (25 cm × 4.6mm, 10 $\mu$M), Chrialcel

OD-H (25 cm × 4.6mm, 5 $\mu$M) or Chiralcel AD-H (25 cm × 4.6mm, 5 $\mu$M). Reverse phase analysis – Nucleosil 100-5 C-18 RP column (25 mm × 3.2 mm, 5 $\mu$M). HPLC grade solvents were degassed prior to use and the column was preconditioned with the solvent system for at least 20 min before injection.

**Melting points** were measured using a Gallenkamp Griffin MPA350 or Electrothermal 9100 digital melting point apparatus and are uncorrected.

**Mass Spectroscopic** analyses at the Biomedical Sciences Research Complex (BSRC) were conducted by Mrs. Caroline Horsburgh on a Micromass LCT electrospray time of flight mass spectrometer by electrospray ionisation. Samples sent to the EPSRC mass spectrometry service in Swansea were analysed on a Thermofisher LTQ Orbitrap XL mass spectrometer using either electrospray ionisation (ES) or atmospheric solids analysis probe techniques (ASAP).

**X-ray** analysis of single crystals was conducted by Prof. Alexandra Slawin at the University of St Andrews on a Rigaku Cu MM007 high brilliance generator with Saturn 92 CCD and XStream LT accessories.

**IR** spectra were recorded a Perkin Elmer Spectrum GX FT-IR machine as either a KBr disc, neat on NaCl plates or on PTFE cards. Peptide samples were recorded neat on a Shimadzu Raffinity-1 FT-IR machine.

**UV-Vis** spectra were recorded on Perkin Elmer Lambda 35 UV/VIS spectrometer with a quartz cell with a 1 cm path length using spectrophotometric grade methanol. Samples were prepared at a concentration of 1 mg in 1 mL and diluted until suitable spectra could be obtained. Extinction coefficients ($\varepsilon$) were calculated using the Beer-Lambert law: $A = \varepsilon c \ell$ and are quoted as $\log_{10} \varepsilon$ values in $M^{-1}$ $cm^{-1}$.

**TLC** analysis was conducted on aluminium backed TLC silica gel 60 $F_{254}$ plates, and followed by visualisation with UV light (254 or 365 nm) and/or staining with the appropriate staining solution. Typical solutions used included: aqueous alkaline potassium permanganate; ninhydrin spray; vanillin solution; or ethanolic ceric ammonium molybdate. Flash column chromatography was achieved using Merck

Geduran Si-60 silica-gel (40-63 $\mu$M particle size).[224] Where required, reverse phase C-18 silica gel (2-10 $\mu$M particle size) aluminium backed TLC plates with 254nm indicator were used. Reverse phase flask chromatography was achieved with C-18 fully end-capped reverse phase silica gel (15-25 $\mu$M particle size).

***Miscellaneous*** - Brine referrers to a saturated solution of sodium chloride in deionised water. Reactions at -78 ºC were readily achieved with isopropanol and dry ice in a Dewar vacuum flask, -100 ºC was achieved with $CH_3OH$ and liquid nitrogen. Reactions that required a sustained low temperature were cooled with a LabPlant RP-60 Refrigerated Immersion Probe. Celite was washed with aqueous HCl (0.1 M), followed by water and $CH_3OH$ prior to use.

**Chemicals** - All chemicals were purchased from: Sigma-Aldrich, Alfa-Aesar, Fluorochem, TCI Europe or Fisher Scientific and were used as supplied unless otherwise noted. Triethylamine (distilled from KOH, stored over KOH), diisopropylethylamine (distilled from KOH, stored under $N_2$), diallylamine (distilled from NaOH, stored under inert atmosphere) and dipropylamine (distilled from KOH, stored under inert atmosphere) were distilled before use. Phosphorus oxychloride (distilled and stored in the dark under inert atmosphere), 3-chloropropionyl chloride (distilled under reduced pressure, stored in dark under inert atmosphere) and DMF (distilled from $CaH_2$ and stored over 3A molecular sieves under inert atmosphere) were distilled before use.[223]

## 7.2 - Experimental for Chapter 3

### 7.2.1 -

**3,6-Bis(3-chloropropionamido)acridine**[175] **146**

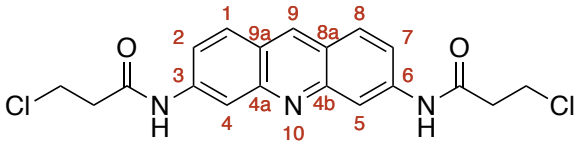


3,6-Diaminoacridine (1.00 g, 4.78 mmol, 1.0 eq) was heated under reflux in neat 3-chloropropionyl chloride (5 mL) for 3 h. The solution was cooled to rt and ice-cold $Et_2O$ (20 mL) was added, resulting in formation of a precipitate. The precipitate was isolated by filtration, washed with $Et_2O$ (2 × 10 mL) and dried under vacuum. This solid was recrystallized from ethanol and DMF (1:5), to yield 3,6-bis(3-chloropropionamido)acridine **146** (1.80 g, 4.30 mmol, 90%) as an orange amorphous solid: **mp** >300 °C (ethanol:DMF); **$^1$H NMR** (300 MHz, $d_6$-DMSO) $\delta_H$ 11.55 (2H, br s, N*H*CO), 9.61 (1H, s, Ar *H*-9), 8.91 (2H, d, *J* 1.6 Hz, Ar *H*-4,5), 8.37 (2H, d, *J* 9.2 Hz, Ar *H*-1,8), 7.92 (2H, dd, *J* 9.2, 1.6 Hz, Ar *H*-2,7), 4.00 (4H, t, *J* 6.2 Hz, 2 × COC$H_2$), 3.11 (4H, t, *J* 6.2 Hz, 2 × C$H_2$Cl).

### 7.2.2 -

**3,6-Bis(3-(3'-(*R*)-fluoropyrrolidin)propionamido)acridine** (*R,R*)-**144**

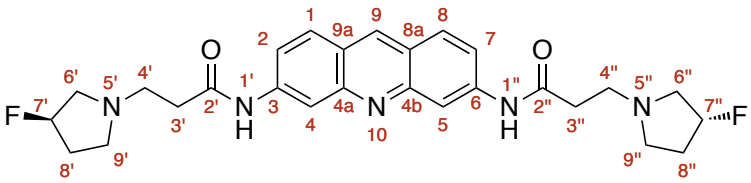

(3*R*)-Fluoropyrrolidine (340 mg, 3.8 mmol, 10.0 eq) in ethanol (1 mL) was added to a solution of 3,6-bis(3-chloropropionamido)acridine (150 mg, 0.38 mmol, 1.0 eq) and NaI (58 mg, 0.38 mmol 2.0 eq) in ethanol (5 mL) and the mixture was heated under reflux for 5 h. The reaction was cooled to 0 °C, resulting in formation of a precipitate, which was isolated by filtration and washed with $Et_2O$ (10 mL). The product was purified by silica gel column chromatography, eluting with $CH_2Cl_2$, $CH_3OH$ and $Et_3N$ (85:10:5), to yield *3,6-bis(3-(3'-(R)-fluoropyrrolindino)propionamido)acridine* (*R,R*)-**144** (121 mg, 0.24 mmol, 63%) as an orange amorphous solid: $R_f$ 0.1 ($CH_2Cl_2$:$CH_3OH$:$Et_3N$, 94:5:1); **IR** (film/$cm^{-1}$) 3689, 2958, 2918, 2780, 2310, 2315, 1644, 1445, 1304, 1215, 1154, 1084, 1026; **mp** >300 °C (dec.); $[\alpha]_{546}^{20}$ -8.0 (*c* 0.44, $CH_3OH$); **$^1$H NMR** (500 MHz, $CD_3OD$/$d_6$-DMSO) $\delta_H$ 8.82 (1H, s, Ar *H*-9), 8.54 (2H, d, *J* 1.9 Hz, Ar *H*-4,5), 8.01 (2H, d, *J* 9.1 Hz, Ar *H*-1,8), 7.64 (2H, dd, *J* 9.1, 1.9 Hz, Ar *H*-2,7), 5.36-5.23 (2H, m, 2 × C*H*F-7',7''), 3.20-3.10 (4H, m, 2 × C$H_a$ -6',6'' and 2 × C$H_a$-9',9''), 3.04 (4H, t, *J* 7.0 Hz, 2 × C$H_2$-3',3''), 2.89-2.79 (2H, m, 2 × C$H_b$-6',6''), 2.76 (4H, t, *J* 7.0 Hz, 2 × C$H_2$-4',4''), 2.68-2.63 (2H, m, 2 × C$H_b$-9',9''), 2.36-2.23 (2H, m, 2 × C$H_a$-8',8''), 2.16-2.05 (2H, m, 2 × C$H_b$-8',8''); **$^{13}$C NMR** (126 MHz, $CD_3OD$/$d_6$-DMSO) $\delta_C$ 172.6 (2 × *C*ONH), 150.7(2 × Ar *C*-8a,9a), 142.5 (2 × Ar *C*-4a,4b), 137.9 (Ar *C*H-9), 130.5 (2 × Ar *C*H-1,8), 124.5 (2 × Ar *C*-3,6),

121.6 (2 × Ar *C*H-2,7), 114.8 (2 × Ar *C*H-4,5), 94.3 (d, *J* 174.9 Hz, 2 × *C*HF-7',7''), 61.3 (d, *J* 22.8 Hz, 2 × $CH_2$-6',6''), 53.1 (2 × $CH_2$-9',9''), 52.5 (2 × $CH_2$-3',3''), 36.3 (2 × $CH_2$-4',4''), 33.4 (d, *J* 22.3 Hz, 2 × $CH_2$-8',8''); **$^{19}$F NMR** (470 MHz, $CD_3OD$/$d_6$-DMSO) $\delta_F$ -169.0 (2F, m, 2 × CH*F*); **HRMS** *m*/*z* ($ES^+$) calcd. for $C_{27}H_{32}F_2N_5O_2$ $[M+H]^+$ requires 496.2524, found 496.2540; ***m*/*z*** ($ES^+$) 496 ($[M+H]^+$, 100%).

### 7.2.3 -

**3,6-Bis(3-(3'-(*S*)-fluoropyrrolindino)propionamido)acridine** (*S*,*S*)-**144**

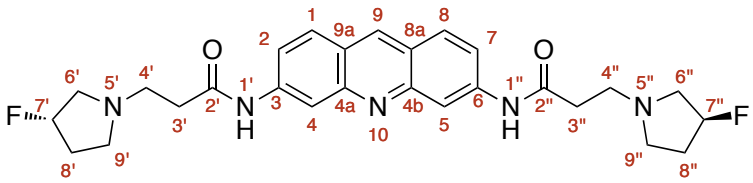


(3*S*)-Fluoropyrrolidine (340 mg, 3.8 mmol, 10.0 eq) in ethanol (1 mL) was added to a solution of 3,6-*bis*(3-chloropropionamido)acridine (150 mg, 0.38 mmol, 1.0 eq) and NaI (58 mg, 0.38 mmol 2.0 eq) in ethanol (5 mL) and the mixture was heated under reflux for 5 h. The reaction was cooled to 0 °C, resulting in formation of a precipitate, which was isolated by filtration and washed with $Et_2O$ (10 mL). The product was purified by silica gel column chromatography, eluting with $CH_2Cl_2$, $CH_3OH$ and $Et_3N$ (85:10:5), to yield *3,6-bis(3-(3'-(S)-fluoropyrrolindino)propionamido)acridine* (*S*,*S*)-**144** (123 mg, 0.26 mmol, 65%) as an orange amorphous solid: $R_f$ 0.1 ($CH_2Cl_2$:$CH_3OH$:$Et_3N$, 94:5:1); **IR** (film/$cm^{-1}$) 3689, 2958, 2918, 2780, 2310, 2315, 1644, 1445, 1304, 1304, 1215, 1154, 1084, 1038, 1026; **mp** >300 °C (dec.); $[\alpha]_{546}^{20}$ +8.1 (*c* 0.44, $CH_3OH$); **$^1$H NMR** (500 MHz, $CD_3OD$/$d_6$-DMSO) $\delta_H$ 8.85 (1H, s, Ar *H*-9), 8.56 (2H, d, *J* 1.9 Hz, Ar *H*-4,5), 8.04 (2H, d, *J* 9.1 Hz, Ar *H*-1,8), 7.66 (2H,

dd, *J* 9.1, 1.9 Hz, Ar *H*-2,7), 5.34-5.21 (2H, m, 2 × C*H*F-7',7''), 3.18-3.08 (4H, m, 2 × C$H_a$-6',6'' and 2 × C$H_a$-9',9''), 3.02 (4H, t, *J* 7.0 Hz, 2 × C$H_2$-3',3''), 2.89-2.79 (2H, m, 2 × C$H_b$-6',6''), 2.75 (4H, t, *J* 7.0 Hz, 2 × C$H_2$-4',4''), 2.64-2.59 (2H, m, 2 × C$H_b$-9',9''), 2.35-2.22 (2H, m, 2 × C$H_a$-8',8''), 2.15-2.04 (2H, m, 2 × C$H_b$-8',8''); **$^{13}$C NMR** (126 MHz, $CD_3OD$/$d_6$-DMSO) $\delta_C$ 172.6 (2 × *C*ONH), 150.8 (2 × Ar *C*-8a,9a), 142.5 (2 × Ar *C*-4a,4b), 137.8 (Ar *C*H-9), 130.5 (2 × Ar *C*H-1,8), 124.5 (2 × Ar *C*-3,6), 121.6 (2 × Ar *C*H-2,7), 114.9 (2 × Ar *C*H-4,5), 94.5 (d, *J* 174.9 Hz, 2 × *C*HF-7',7''), 61.4 (d, *J* 22.8 Hz, 2 × *C*$H_2$-6', 6''), 53.1 (2 × *C*$H_2$-9',9''), 52.5 (2 × *C*$H_2$-3',3''), 36.5 (2 × *C*$H_2$-4',4''), 33.5 (d, *J* 22.3 Hz, 2 × *C*$H_2$-8', 8''); **$^{19}$F NMR** (470 MHz, $CD_3OD$/$d_6$-DMSO) $\delta_F$ -168.5 (2F, m, 2 × CH*F*); **HRMS** *m*/*z* ($ES^+$) calcd. for $C_{27}H_{32}F_2N_5O_2$ $[M+H]^+$ requires 496.2524, found 496.2520; ***m*/*z*** ($ES^+$) 496 ($[M+H]^+$, 100%).

### 7.2.4 -

### 3,6-Bis(3-(3'-(*R*)-hydroxypyrrolindino)propionamido)acridine (*R*,*R*)-145

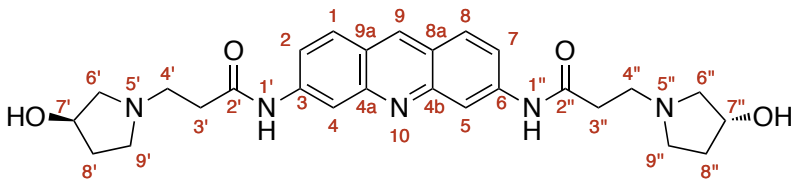


(3*R*)-Hydroxypyrrolidine hydrochloride (335 mg, 3.8 mmol, 10.0 eq) in ethanol (1 mL) was added to a solution of 3,6-bis(3-chloropropionamido)acridine (150 mg, 0.38 mmol, 1.0 eq) and NaI (58 mg, 0.38 mmol 2.0 eq) in ethanol (5 mL) and the mixture was heated under reflux for 5 h. The reaction was cooled to 0 °C, resulting in formation of a precipitate, which was isolated by filtration and washed with $Et_2O$ (10 mL). The product

was purified by silica gel column chromatography, eluting with $CH_2Cl_2$, $CH_3OH$ and $Et_3N$ (85:10:5), to yield *3,6-bis(3-(3'-(R)-hydroxypyrrolindino)propionamido)acridine* (*R*,*R*)-**145** (118 mg, 0.23 mmol, 59%) as an orange amorphous solid: **mp** >300 °C (dec.); **IR** (film/$cm^{-1}$) 3680, 2963, 2918, 2789, 2352, 1672, 1549, 1448, 1205, 1150, 1068, 1020; $[\alpha]_{578}^{20}$ +5.6 (*c* 0.53, $CH_3OH$); **$^1$H NMR** (500 MHz, $CD_3OD$/$d_6$-DMSO) $\delta_H$ 8.82 (1H, s, Ar *H*-9), 8.53 (2H, d, *J* 1.7 Hz, Ar *H*-4,5), 8.01 (2H, d, *J* 9.1 Hz, Ar *H*-1,8), 7.67 (2H, dd, *J* 9.0, 1.7 Hz, Ar *H*-2,7), 4.44-4.41 (2H, m, 2 × C*H*-7',7''), 3.03 (4H, t, *J* 6.9 Hz, 2 × C$H_2$-3',3''), 3.04-2.93 (4H, m, 2 × C$H_2$-6',6''), 2.73 (4H, t, *J* 6.9 Hz, 2 × C$H_2$-4',4''), 2.77-2.71 (4H, m, 2 × C$H_2$-9',9''), 2.24-2.17 (2H, m, 2 × C$H_a$-8',8''), 1.84-1.78 (2H, m, 2 × C$H_b$-8',8''); **$^{13}$C NMR** (126 MHz, $CD_3OD$/$d_6$-DMSO) $\delta_C$ 172.9 (2 × *C*ONH), 150.9 (2 × Ar *C*-8a,9a), 142.4 (2 × Ar *C*-4a,4b), 137.8 (Ar *C*H-9), 130.4 (2 × Ar *C*H-1,8), 124.7 (2 × Ar *C*-3,6), 121.7 (2 × Ar *C*H-2,7), 115.2 (2 × Ar *C*H-4,5), 71.4 (2 × *C*H-7',7''), 63.3 (2 × *C*$H_2$-6',6''), 53.5 (2 × *C*$H_2$-9',9''), 52.8 (2 × *C*$H_2$-3',3''), 36.2 (2 × *C*$H_2$-4',4''), 35.2 (2 × *C*$H_2$-5',5''); **HRMS** *m*/*z* ($ES^+$) calcd. for $C_{27}H_{34}N_5O_4$ $[M+H]^+$ requires 492.2611, found 492.2601; ***m*/*z*** ($ES^+$) 492 ($[M+H]^+$, 100%).

### 7.2.5 -

**3,6-Bis(3-(3'-(*S*)-hydroxypyrrolindino)propionamido)acridine** (*S*,*S*)-**145**

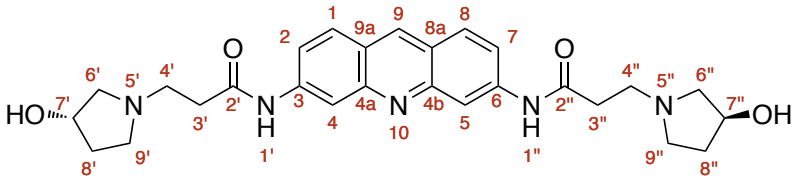


(3*S*)-Hydroxypyrrolidine hydrochloride (335 mg, 3.8 mmol, 10.0 eq) in ethanol (1 mL) was added to a solution of 3,6-bis(3-chloropropionamido)acridine (150 mg, 0.38 mmol,

1.0 eq) and NaI (58 mg, 0.38 mmol 2.0 eq) in ethanol (5 mL) and the mixture was heated under reflux for 5 h. The reaction was cooled to 0 °C, resulting in formation of a precipitate, which was isolated by filtration and washed with $Et_2O$ (10 mL). The product was purified by silica gel column chromatography, eluting with $CH_2Cl_2$, $CH_3OH$ and $Et_3N$ (85:10:5), to yield *3,6-bis(3-(3'-(S)-hydroxypyrrolindino)propionamido)acridine* (*S*,*S*)-**144** (110.9 mg, 0.225 mmol, 59%) as an orange amorphous solid: $[\alpha]_{578}^{20}$ -7.0 (*c* 0.44, $CH_3OH$); **$^1$H NMR** (500 MHz, $CD_3OD$/$d_6$-DMSO) $\delta_H$ 8.80 (1H, s, Ar *H*-9), 8.51 (2H, d, *J* 1.7 Hz, Ar *H*-4,5), 7.99 (2H, d, *J* 9.1 Hz, Ar *H*-1,8), 7.67 (2H, dd, *J* 9.0, 1.7 Hz, Ar *H*-2,7), 4.44-4.41 (2H, m, 2 × C*H*-7',7''), 2.99 (4H, t, *J* 6.9 Hz, 2 × C$H_2$-3',3''), 3.01-2.90 (4H, m, 2 × C$H_2$-6',6''), 2.71 (4H, t, *J* 6.9 Hz, 2 × C$H_2$-4',4''), 2.74-2.67 (4H, m, 2 × C$H_2$-9',9''), 2.24-2.17 (2H, m, 2 × C$H_a$-8',8''), 1.84-1.78 (2H, m, 2 × C$H_b$-8',8''); **$^{13}$C NMR** (126 MHz, $CD_3OD$/$d_6$-DMSO) $\delta_C$ 173.0 (2 × *C*ONH), 150.9 (2 × Ar *C*-8a,9a), 142.4 (2 × Ar *C*-4a,4b), 137.7 (Ar *C*H-9), 130.4 (2 × Ar *C*H-1,8), 124.7 (2 × Ar *C*-3,6), 121.7 (2 × Ar *C*H-2,7), 115.2 (2 × Ar *C*H-4,5), 71.4 (2 × *C*H-7',7''), 63.3 (2 × *C*$H_2$-6',6''), 53.5 (2 × *C*$H_2$-9',9''), 52.8 (2 × *C*$H_2$-3',3''), 36.4 (2 × *C*$H_2$-4',4''), 35.1 (2 × *C*$H_2$-5',5''); **HRMS** *m*/*z* ($ES^+$) calcd. for $C_{27}H_{34}N_5O_4$ $[M+H]^+$ requires 492.2611 found 492.2606; ***m*/*z*** ($ES^+$) 492 ($[M+H]^+$, 100%).

## 7.3 - Experimental for Chapter 4

### 7.3.1 -

**D-Serine methyl ester hydrochloride**[225] (*R*)-**164**

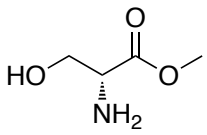


Thionyl chloride (13.7 mL, 192 mmol, 1.1 eq) was added dropwise to $CH_3OH$ (180 mL) over 30 min at rt followed by D-serine (18.0 g, 170 mmol, 1.0 eq) portion wise. Following consumption of the starting material as indicated by TLC, the solvent was removed *in vacuo* and the resulting solids were triturated with petroleum ether. Trituration and subsequent evaporation was repeated to remove excess thionyl chloride. The product was recrystallised from $CH_3OH$ to yield D-serine methyl ester hydrochloride (*R*)-**164** (21.0 g, 140 mmol, 80%) as a white crystalline solid: **mp** 163-165 °C ($CH_3OH$) [Lit.[225] 163-166 ºC]; $[\alpha]_D^{20}$ -4.2 (*c* 4.0, $CH_3OH$) [Lit.[225] $[\alpha]_D^{23}$ -3.7 (*c* 4.0, $CH_3OH$)]; **$^1$H NMR** (400 MHz, $CD_3OD$) $\delta_H$ 4.91 (1H, br s, O*H*), 4.19 (1H, dd, *J* 4.4, 3.5 Hz, C*H*N), 4.04 (1H, dd, *J* 11.9, 4.4 Hz, C$H_a$H$_b$OH), 3.98 (1H, dd, *J* 11.9, 3.5 Hz, CH$_a$$H_b$OH), 3.88 (3H, s, C$H_3$).

### 7.3.2 -

**L-Serine methyl ester hydrochloride**[225] (*S*)-**164**

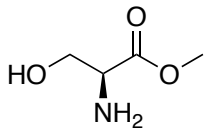


Thionyl chloride (13.7 mL, 190 mmol, 1.1 eq) was added dropwise to $CH_3OH$ (180 mL) over 30 min at rt followed by L-serine (18.0 g, 170 mmol, 1.0 eq) in a portion wise manner. Following consumption of the starting material as indicated by TLC, the solvent was removed *in vacuo* and the solids were triturated with petroleum ether. Trituration and subsequent evaporation was repeated to remove excess thionyl chloride. The product was recrystallised from $CH_3OH$ to yield L-serine methyl ester hydrochloride (*S*)-**164** (21.3 g, 140 mmol, 80%) as a white crystalline solid: **mp** 162-165 ºC [Lit.[225] 163-166 ºC]; $[\boldsymbol{\alpha}]_{\mathbf{D}}^{\mathbf{20}}$ +4.3 (*c* 4.0, $CH_3OH$), [Lit.[225] $[\boldsymbol{\alpha}]_{\mathbf{D}}^{\mathbf{23}}$ +3.7 (*c* 4.0, $CH_3OH$)]; **$^1$H NMR** (400 MHz, $CD_3OD$) $\delta_H$ 4.91 (1H, br s, O*H*), 4.19 (1H, dd, *J* 4.4, 3.5 Hz, C*H*N), 4.04 (1H, dd, *J* 11.9, 4.4 Hz, C$H_a$H$_b$OH), 3.98 (1H, dd, *J* 11.9, 3.5 Hz, CH$_a$$H_b$OH), 3.88 (3H, s, C$H_3$).

### 7.3.3 -

**Methyl (±)-2-(dibenzylamino)-3-hydroxypropanoate[226] 119**

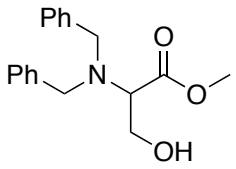


Benzyl bromide (19.3 mL, 162 mmol, 2.5 eq) was added to a solution of DL-serine methyl ester hydrochloride (10.0 g, 64.0 mmol, 1.0 eq) and $K_2CO_3$ (44.7 g, 323 mmol, 5.0 eq) in acetonitrile. This mixture was stirred for 24 h at rt and quenched by the addition of water (300 mL). The aqueous phase was extracted with ethyl acetate (3 × 300 mL) and the combined organic fractions were dried over $Na_2SO_4$, filtered and concentrated *in vacuo*. The product was purified by silica gel column chromatography, eluting with hexane and ethyl acetate (80:20), to yield methyl 2-(dibenzylamino)-3-hydroxypropanoate **119** (18.1 g, 60.0 mmol, 94%) as a colorless oil: **$^1$H NMR** (400 MHz, $CD_3OD$) $\delta_H$ 7.40-7.22 (10H, m, 10 × Ar *H*), 3.94 (1H, dd, *J* 10.9, 7.8 Hz, C$H_a$H$_b$OH), 3.88 (2H, d, *J* 13.8 Hz, 2 × NC$H_a$H$_b$-benzyl), 3.80 (3H, s, OC$H_3$), 3.75 (1H, dd, *J* 10.9, 5.9 Hz, CH$_a$$H_b$OH), 3.61 (2H, d, *J* 13.8 Hz, 2 × NCH$_a$$H_b$-benzyl), 3.47 (1H, dd, *J* 7.8, 5.9 Hz, C*H*N); ***m/z*** (ES$^+$) 300 ([M+H]$^+$, 100%).

### 7.3.4 -

**Methyl (+)-(2*R*)-(dibenzylamino)-3-hydroxypropanoate**[226] (*R*)-**119**

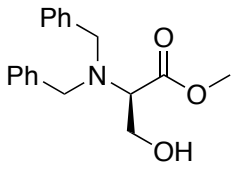


Following the procedure set out for methyl 2-(dibenzylamino)-3-hydroxypropanoate **119**, starting from D-serine methyl ester hydrochloride (*R*)-**164** (10.0 g, 64.0 mmol), methyl (2*R*)-(dibenzylamino)-3-hydroxypropanoate (*R*)-**119** (18.3 g, 61.0 mmol, 95%) was obtained as a colourless oil: $[\boldsymbol{\alpha}]_{\mathbf{D}}^{\mathbf{20}}$ +144 (*c* 1.0, $CHCl_3$), [Lit.[226] $[\boldsymbol{\alpha}]_{\mathbf{D}}^{\mathbf{23}}$ +147 (*c* 0.96, $CHCl_3$)]; **$^1$H NMR** (400 MHz, $CD_3OD$) $\delta_H$ 7.40-7.22 (10H, m, 10 × Ar *H*), 3.94 (1H, dd, *J* 10.9, 7.8 Hz, C$H_a$H$_b$OH), 3.88 (2H, d, *J* 13.8 Hz, 2 × NC$H_a$H$_b$-benzyl), 3.80 (3H, s, OC$H_3$), 3.75 (1H, dd, *J* 10.9, 5.9 Hz, CH$_a$$H_b$OH), 3.61 (2H, d, *J* 13.8 Hz, 2 × NCH$_a$$H_b$-benzyl), 3.47 (1H, dd, *J* 7.8, 5.9 Hz, C*H*N); ***m/z*** ($ES^+$) 300 ($[M+H]^+$, 100%).

### 7.3.5 -

**Methyl (–)-(2*S*)-(dibenzylamino)-3-hydroxypropanoate**[227] (*S*)-**119**

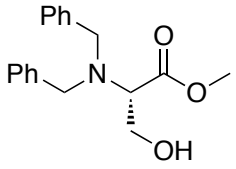


Following the procedure set out for methyl 2-(dibenzylamino)-3-hydroxypropanoate **119**, starting from L-serine methyl ester hydrochloride (*S*)-**164** (10.0 g, 64.0 mmol),

methyl (2*S*)-(dibenzylamino)-3-hydroxypropanoate (*S*)-**119** (18.0 g, 60.0 mmol, 94%) was obtained as a colourless oil: $[\alpha]_D^{20}$ -140 (*c* 1.0, $CHCl_3$) [Lit.[221] $[\alpha]_D^{26}$ -105 (*c* 1.21, $CH_3OH$)]; **$^1$H NMR** (300 MHz, $CD_3OD$) $\delta_H$ 7.37-7.19 (10H, m, 10 × Ar *H*), 3.91 (1H, dd, *J* 10.9, 7.8 Hz, C*H*$_a$H$_b$CHN), 3.85 (2H, d, *J* 13.8 Hz, 2 × C*H*$_a$H$_b$-benzyl), 3.77 (3H, s, OC*H*$_3$), 3.72 (1H, dd, *J* 10.9, 5.9 Hz, CH$_a$*H*$_b$CHN), 3.58 (2H, d, *J* 13.8 Hz, 2 × CH$_a$*H*$_b$-benzyl), 3.47 (1H, dd, *J* 7.8, 5.9 Hz, C*H*N); ***m/z*** (ES$^+$) 300 ([M+H]$^+$, 100%).

### 7.3.6 -

### Methyl (±)-3-(dibenzylamino)-2-fluoropropanoate 120

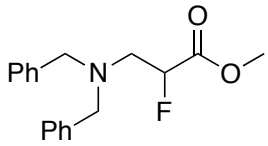


Diethylaminosulfur trifluoride **32** (4.20 mL, 32.0 mmol, 1.2 eq) was added to a solution of methyl 2-(dibenzylamino)-3-hydroxypropanoate **119** (8.00 g, 26.7 mmol, 1.0 eq) in THF (45 mL) and the reaction was cooled to 0 °C. This solution was stirred for 1 h at 0 °C before being quenched by the addition of cold water (90 mL), followed by an excess of solid $K_2CO_3$ and $Et_2O$ (90 mL). The organic phase was separated and the aqueous mixture re-extracted with $Et_2O$ (2 × 90 mL). The organic fractions were combined, dried over $Na_2SO_4$ and concentrated *in vacuo.* The product was purified by silica gel column chromatography, eluting with hexane and ethyl acetate (80:20), to yield *methyl 3-(dibenzylamino)-2-fluoropropanoate* **120** (7.25 g, 24.1 mmol, 90%) as a colourless oil: **IR** $\nu_{max}$ (film, cm$^{-1}$) 3027, 2802, 1763, 1494, 1438, 1352, 1368, 1291, 1207, 1150, 1066; **$^1$H NMR** (400 MHz, $CDCl_3$) $\delta_H$ 7.25-7.15 (10H, m, 10 × Ar-*H*), 4.98 (1H, ddd, *J* 49.3, 5.8, 3.3 Hz, C*H*F), 3.76 (2H, d, *J* 13.6 Hz, 2 × NC*H*$_a$H$_b$-benzyl),

3.61 (3H, s, $OCH_3$), 3.45 (2H, d, *J* 13.6 Hz, 2 × $NCH_aH_b$-benzyl), 3.03-2.85 (2H, m, $CH_2CHF$); **$^{13}$C NMR** (101 MHz, $CDCl_3$) $\delta_C$ 169.3 (d, *J* 24.2 Hz, $CO_2CH_3$), 138.9 (2 × Ar-*C*), 129.1 (4 × Ar-*C*H), 128.4 (4 × Ar-*C*H), 127.2 (2 × Ar-*C*H), 89.5 (d, *J* 186.1 Hz, *C*HF), 58.9 (2 × $CH_2Ar$), 54.3 (d, *J* 20.1 Hz, $NCH_2$), 52.3 ($OCH_3$); **$^{19}$F NMR** (283 MHz, $CDCl_3$) $\delta_F$ -192.2 (ddd, *J* 49.3, 29.2, 22.1 Hz, CH*F*); **HRMS** *m*/*z* ($ES^+$) calcd. for $C_{18}H_{20}NO_2FNa$ $[M+Na]^+$ requires 324.1376, found 324.1369; ***m*/*z*** ($ES^+$) 324 ($[M+Na]^+$, 100%).

### 7.3.7 -

**Methyl (–)-(2*S*)-3-(dibenzylamino)-2-fluoropropanoate** (*S*)-**120**

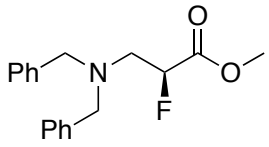


Following the procedure set out for methyl 3-(dibenzylamino)-2-fluoropropanoate **120**, starting from methyl (2*R*)-(dibenzylamino)-3-hydroxypropanoate (*R*)-**119** (8.00 g, 26.7 mmol) with diethylaminosulfur trifluoride **32** (4.20 mL, 32.0 mmol, 1.2 eq) in THF (45 mL), furnished *methyl (2S)-3-(dibenzylamino)-2-fluoropropanoate* (*S*)-**120** (7.19 g, 23.9 mmol, 89%) as a colourless oil: $[\alpha]_D^{20}$ -19.0 (*c* 2.0, $CH_3OH$); **$^1$H NMR** (300 MHz, $CDCl_3$) $\delta_H$ 7.26-7.14 (10H, m, 10 × Ar *H*), 4.97 (1H, ddd, *J* 49.5, 5.7, 3.3 Hz, C*H*F), 3.75 (2H, d, *J* 13.6 Hz, 2 × $CH_aH_bPh$), 3.61 (3H, s, $OCH_3$), 3.44 (2H, d, *J* 13.6 Hz, 2 × $CH_aH_bPh$), 2.97 (1H, ddd, *J* 26.9, 14.7, 5.7 Hz, 2 × $CH_aH_bCHF$), 2.90 (1H, ddd, *J* 24.3, 14.7, 3.3 Hz, 2 × $CH_aH_bCHF$); **$^{13}$C NMR** (75 MHz, $CDCl_3$) $\delta_C$ 169.3 (d, *J* 24.2 Hz, $CO_2CH_3$), 138.9 (2 × Ar *C*), 129.1 (4 × Ar *C*H), 128.4 (4 × Ar *C*H), 127.2 (2 × Ar *C*H), 89.5 (d, *J* 186.1 Hz, *C*HF), 58.9 (2 × $CH_2Ph$),

54.3 (d, *J* 20.1 Hz, *C*$H_2$CHF), 52.3 (O*C*$H_3$); **$^{19}$F NMR** (282 MHz, $CDCl_3$) $\delta_F$ -191.0 (ddd, *J* 49.5, 26.9, 24.3 Hz, CH*F*); **HRMS** *m*/*z* ($ES^+$) calcd. for $C_{18}H_{20}NO_2FNa$ $[M+Na]^+$ requires 324.1376, found 324.1375; ***m*/*z*** ($ES^+$) 324 ($[M+Na]^+$, 100%). Enantiomeric excess determined by chiral HPLC (Chiralcel OD 5% $^i$PrOH in hexane, 0.25 mL/min, $t_{r\ maj}$ = 14.51 min >95%, $t_{r\ min}$ = 15.70 min <5%).

### 7.3.8 -

**Methyl (+)-(2*R*)-3-(dibenzylamino)-2-fluoropropanoate** (*R*)-**120**

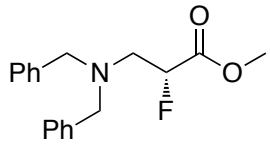


Following the procedure set out for methyl 3-(dibenzylamino)-2-fluoropropanoate **120**, starting from methyl (2*S*)-(dibenzylamino)-3-hydroxypropanoate (*S*)-**119** (8.00 g, 26.7 mmol) with diethylaminosulfur trifluoride **32** (4.20 mL, 32.0 mmol, 1.2 eq) in THF (45 mL), furnished *methyl (2R)-3-(dibenzylamino)-2-fluoropropanoate* (*R*)-**120** (7.23 g, 24.0 mmol, 90%) as a colourless oil: $[\alpha]_D^{20}$ +19.1 (*c* 2.0, $CH_3OH$); **$^1$H NMR** (300 MHz, $CDCl_3$) $\delta_H$ 7.29-7.12 (10H, m, 10 × Ar *H*), 4.97 (1H, ddd, *J* 49.5, 5.7, 3.3 Hz, C*H*F), 3.75 (2H, d, *J* 13.6 Hz, 2 × C$H_a$$H_b$Ph), 3.61 (3H, s, OC$H_3$), 3.44 (2H, d, *J* 13.6 Hz, 2 × C$H_a$$H_b$Ph), 2.97 (1H, ddd, *J* 26.9, 14.7, 5.7 Hz, 2 × C$H_a$$H_b$CHF), 2.90 (1H, ddd, *J* 24.3, 14.7, 3.3 Hz, 2 × C$H_a$$H_b$CHF); **$^{13}$C NMR** (75 MHz, $CDCl_3$) $\delta_C$ 169.3 (d, *J* 24.2 Hz, *C*$O_2CH_3$), 138.9 (2 × Ar *C*), 129.1 (4 × Ar *C*H), 128.4 (4 × Ar *C*H), 127.2 (2 × Ar *C*H), 89.5 (d, *J* 186.1 Hz, *C*HF), 58.9 (2 × $CH_2$Ph), 54.3 (d, *J* 20.1 Hz, *C*$H_2$CHF), 52.3 (O*C*$H_3$); **$^{19}$F NMR** (282 MHz, $CDCl_3$) $\delta_F$ -191.0 (ddd, *J* 49.5, 26.9, 24.3 Hz, CH*F*); **HRMS** *m*/*z* ($ES^+$) calcd. for

$C_{18}H_{21}NO_2F$ $[M+H]^+$ requires 302.1556, found 302.1548; ***m/z*** ($ES^+$) 324 ($[M+Na]^+$, 100%), 302 ([M+H], 80%). Enantiomeric excess determined by chiral HPLC (Chiralcel OD-H 5% $^i$PrOH in hexane, 0.25 mL/min, $t_{r\ maj}$ = 15.70 min >95%, $t_{r\ min}$ = 14.51 min <5%).

### 7.3.9 -

**Methyl (±)-3-amino-2-fluoropropanoate hydrochloride 166**.HCl

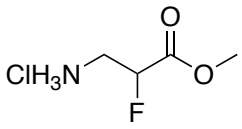


A solution of methyl (±)-3-(dibenzylamino)-2-fluoropropanoate **120** (200 mg, 0.66 mmol, 1.0 eq) and 20% $Pd(OH)_2/C$ (40.0 mg, 10 mol%) in $CH_3OH$ (10 mL) was stirred under an $H_2$ atmosphere. This suspension was stirred vigorously until TLC/$^{19}$F NMR analysis had indicated complete debenzylation and HCl (0.5 M, 1.5 mL) was added. The mixture was filtered through a pad of Celite and the residue was washed with $CH_3OH$ (30 mL). The filtrate was concentrated *in vacuo* to yield *methyl (±)-3-amino-2-fluoropropanoate* hydrochloride **166**.HCl (80 mg, 99%) as a colourless solid, which was used without purification: **$^1$H NMR** (400 MHz, $CD_3OD$) $\delta_H$ 5.37 (1H, ddd, *J* 47.6, 7.5, 3.4 Hz, C*H*F), 3.86 (3H, s, OC$H_3$), 3.61-3.42 (2H, m, C$H_2$); **$^{13}$C NMR** (101 MHz, $CD_3OD$) $\delta_C$ 171.2 (d, *J* 22.9 Hz, *C*$O_2CH_3$), 86.7 (d, *J* 185.9 Hz, *C*HF), 53.6 (O*C*$H_3$), 41.1 (d, *J* 21.4 Hz, *C*$H_2$); **$^{19}$F NMR** (376 MHz, $CD_3OD$) $\delta_F$ -200.3 (ddd, *J* 48.0, 25.0, 23.0 Hz, CH*F*); **HRMS** *m/z* ($ES^+$) calcd. for $C_4H_9NO_2F$ $[M+H]^+$ requires 122.0614, found 122.0621; ***m/z*** ($ES^+$) 122 ($[M+H]^+$, 100%).

### 7.3.10 -

**Methyl (±)-3-(pyrrolidin-1-yl)-2-fluoropropanoate 153**

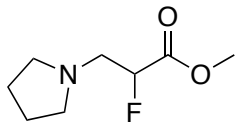


1,4-Dibromobutane (85 $\mu$L, 712 $\mu$mol, 1.1 eq) was added to a solution of tetrabutylammonium iodide (45 mg, 146 $\mu$mol, 0.2 eq), sodium carbonate (270 mg, 2.55 mmol, 4.0 eq) and methyl (±)-3-amino-2-fluoropropanoate **166** (100 mg, 634 $\mu$mol, 1.0 eq) in THF. The resulting solution was heated under reflux for 4 hr, cooled to rt and quenched with water (2 mL) and ethyl acetate (4 mL). The organics were separated and the aqueous layer further extracted with ethyl acetate (4 mL). The organic phases were combined, washed with brine (5 mL), dried over sodium sulfate, filtered and the solvent removed *in vacuo*. The product was purified by silica gel column chromatography eluting with $CH_2Cl_2$ and $CH_3OH$ (100:0, 99:1), to furnish *methyl (±)-3-(pyrrolidin-1-yl)-2-fluoropropanoate* **153** (85 mg, 485 $\mu$mol, 77%) as a colourless oil: $\boldsymbol{R_f}$ 0.13 ($CH_2Cl_2$:$CH_3OH$, 99:1); **$^1$H NMR** (400 MHz, $CDCl_3$) $\delta_H$ 5.09 (1H, ddd, *J* 49.5, 6.8, 2.8 Hz, C*H*F), 3.81 (3H, s, OC$H_3$), 3.02 (1H, ddd, *J* 26.2, 14.0, 6.8 Hz, C$H_a$H$_b$CHF), 2.95 (1H, ddd, *J* 28.6, 14.0, 2.8 Hz, CH$_a$$H_b$CHF), 2.67-2.56 (4H, m, 2 × C$H_2$), 1.79-1.76 (4H, m, 2 × C$H_2$); **$^{13}$C NMR** (101 MHz, $CDCl_3$) $\delta_C$ 169.5 (d, *J* 24.0 Hz, *C*$O_2$$CH_3$), 89.5 (d, *J* 187.0 Hz, *C*HF), 57.2 (d, *J* 20.3 Hz, *C*$H_2$CHF), 54.9 (2 × *C*$H_2$), 52.5 (O*C*$H_3$), 23.8 (2 × *C*$H_2$); **$^{19}$F{$^1$H} NMR** (376 MHz, $CDCl_3$) $\delta_F$ -192.2 (s, CH*F*); **HRMS** *m*/*z* (ES$^+$) calcd. for $C_8H_{15}NO_2F$ $[M+H]^+$ requires 176.1087, found 176.1087; ***m*/*z*** (ES$^+$) 194 ($[M+Na]^+$, 10%), 176 ($[M+H]^+$, 100%).

### 7.3.11 -

**(+)-(2*S*)-3-(Dibenzylamino)-2-fluoropropanoic acid**[228] (*S*)-**170**

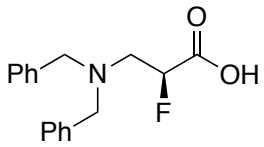


Methyl (2*S*)-3-(dibenzylamino)-2-fluoropropanoate (*S*)-**120** (1.00 g, 3.32 mmol, 1.0 eq) was added to a solution of KOH (3.20 g, 57.1 mmol, 10.0 eq) in $CH_3OH$ (10 mL). The resulting solution was stirred for 36 h at rt. The reaction was diluted with HCl (1 M, 10 mL) and the aqueous phase extracted with ethyl acetate (3 × 5 mL). The combined organic fractions were dried over $Na_2SO_4$, filtered and the solvent removed *in vacuo* to furnished (2*S*)-3-(dibenzylamino)-2-fluoropropanoic acid (*S*)-**170** (0.91 g, 98%) as a colourless oil, which was used without any further purification: $[\alpha]_D^{20}$ +0.8 (*c* 2.5, $CHCl_3$); **$^1$H NMR** (400 MHz, $CD_3OD$) $\delta_H$ 7.31 (10H, m, 10 × Ar-*H*), 4.98 (1H, ddd, *J* 49.5, 7.3, 3.3 Hz, C*H*F), 3.79 (2H, d, *J* 13.8 Hz, 2 × NC$H_aH_b$), 3.66 (2H, d, *J* 13.8 Hz, 2 × NC$H_aH_b$), 3.01 (2H, m, C$H_2$CHF); **$^{19}$F NMR** (282 MHz, $CD_3OD$) $\delta_F$ -189.0 (ddd, *J* 49.5, 22.5, 22.5 Hz, CH*F*); ***m/z*** ($ES^+$) 310 ($[M+Na]^+$, 80%), 288 ($[M+H]^+$, 100%).

### 7.3.12 -

**(–)-(2*R*)-3-(Dibenzylamino)-2-fluoropropanoic acid**[228,229] (*R*)-**170**

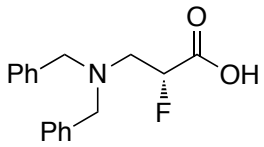


Methyl (2*R*)-3-(dibenzylamino)-2-fluoropropanoate (*R*)-**120** (1.00 g, 3.32 mmol, 1.0 eq) was added to a solution of KOH (3.20 g, 57.1 mmol, 10.0 eq) in $CH_3OH$ (10 mL). The resulting solution was stirred for 36 h at rt. The reaction was diluted with HCl (1 M, 10 mL) and the aqueous phase extracted with ethyl acetate (3 × 5 mL). The combined organic fractions were dried over $Na_2SO_4$, filtered and the solvent removed *in vacuo* to furnish (2*R*)-3-(dibenzylamino)-2-fluoropropanoic acid (*R*)-**170** (0.90 g, 97%) as a colourless oil which was used without any further purification: $[\boldsymbol{\alpha}]_{\mathbf{D}}^{\mathbf{20}}$ -0.8 (*c* 2.5, $CHCl_3$); **$^1$H NMR** (300 MHz, $CD_3OD$) $\delta_H$ 7.44-7.33 (10H, m, 10 × Ar-*H*), 5.08 (1H, ddd, *J* 49.5, 7.3, 3.3 Hz, C*H*F), 4.09 (2H, d, *J* 13.4 Hz, 2 × C$H_aH_b$Ph), 3.95 (2H, d, *J* 13.4 Hz, 2 × C$H_aH_b$Ph), 3.31-3.19 (2H, m, C$H_2$CHF); **$^{19}$F NMR** (282 MHz, $CD_3OD$) $\delta_F$ -189.0 (ddd, *J* 49.5, 22.5, 22.5 Hz, CH*F*); ***m/z*** ($ES^+$) 288 ($[M+H]^+$, 100%).

### 7.3.13 -

### 2,2',4,4'-Tetranitrodiphenylmethane[191, 230] 172

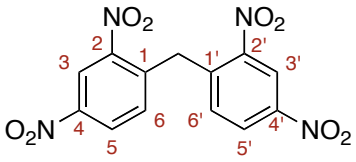


Finely powdered potassium nitrate (27.7 g, 270 mmol, 4.5 eq) was added to a solution of aqueous sulfuric acid (200 mL, 15 M) over 0.5 h at 30 °C. Diphenylmethane (10.0 mL, 60 mmol, 1.0 eq) was added dropwise over 1 h, with the temperature maintained below 30 °C. After stirring for a further 0.5 h at rt, the solution was heated to 70 °C for 1 h, cooled to rt before iced water (1.5 L) was added, which resulted in the immediate precipitation of yellow solid that was isolated by filtration. This solid was suspended in ethanol (75 mL) and was heated under reflux for 5 min, after which the solid was re-collected by hot filtration and recrystallised from acetic acid (~75 mL), to yield 2,2',4,4'-tetranitrodiphenylmethane **172** (15.3 g, 44 mmol, 74%) as large yellow crystals: **mp** 172-173 °C (acetic acid) [Lit. [191, 230] 173 ºC]; **$^1$H NMR** (300 MHz, $d_6$-DMSO) $\delta_H$ 8.85 (2H, d, *J* 2.5 Hz, Ar *H*-3,3′), 8.52 (2H, dd, *J* 8.6, 2.5 Hz, Ar *H*-5,5′), 7.62 (2H, d, *J* 8.6 Hz, Ar *H*-6,6′), 3.36 (2H, s, C$H_2$); ***m/z*** (ASAP) 349 ($[M+H]^+$, 100%), 348 ($[M]^+$, 55%).

### 7.3.14 -

### 2,2',4,4'-Tetranitrobenzophenone[230] 173

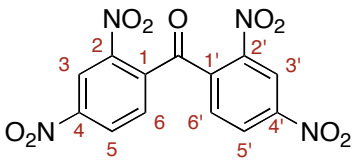


Chromium trioxide (6.90 g, 68.9 mmol, 2.0 eq) was slowly added to a solution of 2,2',4,4'-tetranitrodiphenylmethane **172** (12.0 g, 34.5 mmol, 1.0 eq) in acetic acid (100 mL) under reflux. The resulting dark green solution was stirred under reflux for 16 h, cooled to rt with the precipitate isolated by filtration and washed with acetic acid (20 mL). The precipitate was further washed with ethanol (200 mL), water (200 mL). and was re-crystallised from acetic acid to yield 2,2',4,4'-tetranitrobenzophenone **173** (11.8 g, 32.7 mmol, 95%) as small light yellow crystals: **mp** 235-238 °C (acetic acid) [lit.[230] 232 °C]; **$^1$H NMR** (300 MHz, $d_6$-DMSO) $\delta_H$ 8.98 (2H, d, *J* 2.1 Hz, Ar *H*-3,3′), 8.67 (2H, dd, *J* 8.5, 2.1 Hz, Ar *H*-5,5′), 8.05 (2H, d, *J* 8.5 Hz, Ar *H*-6,6′); ***m/z*** (ASAP) 363 ($[M+H]^+$, 100%).

### 7.3.15 -

### 3,6-Diamino-9-(10*H*)-acridone[230, 231] 155

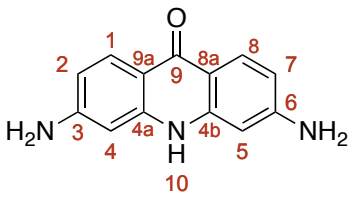


A solution of stannous chloride (69.1 g, 360 mmol, 12 eq) in concentrated HCl (200 mL, 1.18 specific gravity) was heated under reflux for 0.5 h while a steady flow of argon removed HCl gas evolved from the reaction [NOTE: Evolved HCl was neutralised by passing through double Drechsel flask set up containing a solution of NaOH (30% w/v)]. 2,2',4,4'-tetranitrobenzophenone **174** (11.0 g, 30.4 mmol) and ethanol (30 mL) were added, followed by a further portion of concentrated HCl (30 mL, 1.18 specific gravity). This mixture was heated under reflux for 3 h, cooled to rt and concentrated HCl (50 mL, 1.18 specific gravity) was added. The mixture was stirred for 16 h at rt resulting in precipitation of the hydrochloride salt of **155**, which was isolated by filtration. This salt was dissolved in hot aqueous HCl (0.1 M, 200 mL) and heated under reflux for 1 h before activated carbon was added. This suspension was heated under reflux for 1 h, filtered and the filtrate was basified (pH 13) with NaOH (30% *w*/*v*). The resulting precipitate was isolated by hot filtration, washed with hot aqueous NaOH (50 mL, 2 M) and hot water (200 mL), until the filtrate was neutral, to furnish 3,6-diamino-9-(10*H*)-acridone **155** (4.30 g, 19.0 mmol, 63%) as a light brown solid: **mp** >300 °C [lit. [230, 231] >300 ºC]; **$^1$H NMR** (300 MHz, $d_6$-DMSO) $\delta_H$ 10.85 (1H, s, N*H*), 7.83 (2H, d, *J* 8.7 Hz, Ar *H*-1,8), 6.45 (2H, dd, *J* 8.7, 2.0 Hz, Ar *H*-2,7),

6.40 (2H, d, *J* 2.0 Hz, Ar *H*-4,5), 4.00 (4H, br s, 2 × N$H_2$); ***m/z*** ($ES^+$) 289 ($[M+Na+MeCN]^+$, 20%), 226 ($[M+H]^+$, 80%).

### 7.3.16 -

### (±)-3,6-Bis(3-*N*,*N*-dibenzylamino-2-fluoropropionamido)-9-(10*H*)-acridone *rac*-169

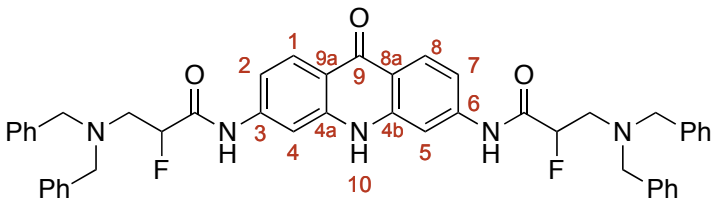


Potassium hexamethyldisilazide (1.8 mL, 1 M in THF, 4.0 eq) was added dropwise to a suspension of 3,6-diaminoacridone **155** (102 mg, 0.45 mmol, 1.0 eq) in THF (5.0 mL) over 0.5 h at -78 °C and the mixture stirred for a further 1 h at -78 ºC. Methyl (±)-3-dibenzylamino-2-fluoropropanoate *rac*-**120** (300 mg, 1.0 mmol, 2.2 eq) in THF (5.0 mL) was added and the mixture was stirred for 16 h whist warming to rt. The reaction was quenched by the addition of saturated aqueous $NH_4OH$ (20 mL) and ethyl acetate (20 mL) resulting in significant precipitation. The organic phase was separated and the solids were isolated from the aqueous phase by filtration. The aqueous filtrate was extracted with ethyl acetate (3 × 10 mL) and the combined organic phases were washed with brine (30 mL), dried over $Na_2SO_4$, filtered and solvent removed *in vacuo* to yield a dark orange solid. This solid was absorbed onto $Na_2SO_4$ for purification by silica gel column chromatography, eluting with ethyl acetate and hexane (60:40, 90:10, 100:0) to furnish *(±)-3,6-bis(3-N,N-dibenzylamino-2-fluoropropionamido)-9-(10H)-acridone* *rac*-**169** (64.0 mg, 83.8 μmol, 19%) as a pale yellow solid: **$^1$H NMR** (400 MHz, $d_6$-DMSO) $\delta_H$ 11.84 (1H, s, N*H*-10), 10.45 (2H, s, 2 × CON*H*),

8.23 (2H, d, *J* 1.7 Hz, Ar *H*-4/5), 8.15 (2H, d, *J* 8.8 Hz, Ar *H*-1/8), 7.39-7.16 (22H, m, 20 × Ar*H,* Ar *H*-2/7), 5.38 (2H, ddd, *J* 49.2, 5.9, 3.6 Hz, 2 × C*H*F), 3.78 (4H, d, *J* 13.9 Hz, 4 × C$H_a$$H_b$Ph), 3.58 (4H, d, *J* 13.9 Hz, 4 × CH$_a$*H*$_b$Ph), 3.10-2.94 (4H, m, 2 × C$H_2$CHF); **$^{19}$F{$^{1}$H} NMR** (376 MHz, $d_6$-DMSO) $\delta_F$ -187.9 (2F, dt, *J* 49.2, 24.9 Hz, 2 × CH*F*); **HRMS** *m/z* (ES$^-$) calcd. for $C_{47}H_{42}F_2N_5O_3$ [M-H]$^-$ 762.3256, found 762.3246; ***m/z*** (ES$^-$) 762 ([M-H]$^-$, 100%).

### 7.3.17 -

**(±)-3,6-Bis(3-*N,N*-dibenzylamino-2-fluoropropionamido)-9-(4-dimethylaminophenylamino)acridine *rac*-182**

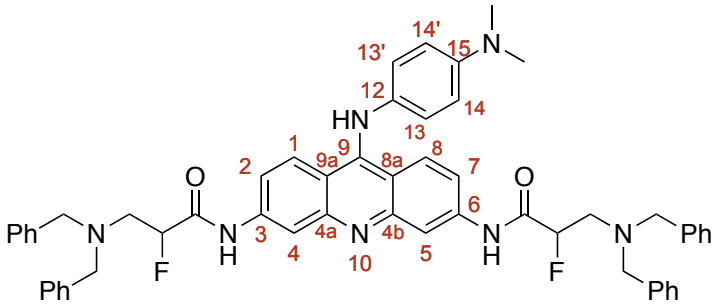


Phosphorous oxychloride (5.0 mL) was added to (±)-3,6-bis(3-*N,N*-dibenzylamino-2-fluoropropionamido)-9-(10*H*)-acridone *rac*-**169** (20.0 mg, 26.2 $\mu$mol, 1.0 eq), with the resulting suspension stirred at reflux for 3 hr. The solution was cooled to 0 °C and cold $Et_2O$ (10 mL) was added, resulting in formation of a precipitate. The precipitate was isolated by filtration and washed with further $Et_2O$ (2 × 5 mL) and dissolved in $CHCl_3$ (5 mL). The organic phase was washed with aqueous $NH_4OH$ (1 M, 5 mL), and brine (5 mL), dried over $Na_2SO_4$, filtered and the solvent removed *in vacuo* to yield *(±)-3,6-bis(3-N,N-dibenzylamino-2-fluoropropionamido)-9-chloroacridine* (18.2 mg) as a red brown solid, which was used in the next step without further purification.

*N,N*-dimethylaminoaniline (63.0 mg, 466 mmol, 20 eq) in $CHCl_3$ (2 mL) was added dropwise to a refluxing solution of (±)-3,6-*bis*((3-*N,N*-dibenzylamino-2-fluoropropionamido)-9-chloroacridine in $CHCl_3$ (2 mL). The mixture was heated under reflux until TLC analysis had indicated the consumption of the chloride, at which point the solvent was removed *in vacuo* to yield a black oil. Cold $Et_2O$ (excess) was added, resulting in the precipitation of a red-brown solid. The solids were isolated by filtration and washed with further $Et_2O$ (5 mL), dissolved in $CHCl_3$ (5 mL) and washed with aqueous $NH_4OH$ (1 M, 5 mL) followed by brine (5 mL). The organic phase was dried over $Na_2SO_4$, filtered and the solvent removed *in vacuo* to yield a red solid. The solid was purified by silica gel column chromatography, eluting with $CHCl_3$ and $CH_3OH$ (95:5), to yield *(±)-3,6-bis(3-N,N-dibenzylamino-2-fluoropropionamido)-9-(4-dimethylaminophenylamino)acridine rac*-**182** (4.9 mg, 5.5 $\mu$mol, 23%) as a dark red solid: **$^1$H NMR** (500 MHz, $CD_3OD$) $\delta_H$ 8.28 (2H, s, Ar *H*-4/5), 7.93 (2H, d, *J* 9.0 Hz, Ar *H*-1/8), 7.29-7.00 (24H, m, 20 × Ar-*H*, Ar *H*-2/7, Ar *H*-14/14′), 6.77 (2H, d, *J* 8.9 Hz, Ar *H*-13/13′), 5.13 (2H, ddd, *J* 49.1, 5.3, 3.7 Hz, 2 × C*H*F), 3.73 (4H, d, *J* 13.7 Hz, 4 × C$H_a$H$_b$Ph), 3.50 (4H, d, *J* 13.7 Hz, 4 × CH$_a$$H_b$Ph), 3.07-2.95 (4H, m, 2 × C$H_2$CHF), 2.89 (6H, s, 2 × NC$H_3$); **$^{19}$F{$^1$H} NMR** (470 MHz, $CD_3OD$) -187.5 (2F, s, 2 × CH*F*); **HRMS** *m/z* ($ES^+$) calcd. for $C_{55}H_{54}F_2N_7O_2$ $[M+H]^+$ 882.4307, found 882.4299; ***m/z*** ($ES^+$) 882 ($[M+H]^+$, 100%).

### 7.3.18 -

**Methyl (+)-(2*R*)-(diallylamino)-3-hydroxypropanoate** (*R*)-**187**

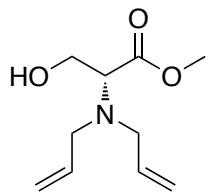


Allyl bromide (12.2 mL, 141 mmol, 2.2 eq) was added to a suspension of D-serine methyl ester hydrochloride (*R*)-**164** (10.0 g, 64.8 mmol, 1.0 eq) and $K_2CO_3$ (35.6 g, 258 mmol, 4.0 eq) in acetonitrile (300 mL) and the resulting suspension was heated under reflux for 24 h. The reaction was cooled to rt, diluted with water (300 mL) and extracted with ethyl acetate (3 × 100 mL). The organic fractions were combined, washed with brine (100 mL), dried over $Na_2SO_4$, filtered and the solvent removed *in vacuo*. The resulting oil was purified by silica gel column chromatography, eluting with hexane and ethyl acetate (95:5 to 90:10), to yield *methyl (2R)-3-hydroxy-2-N,N-bisallylaminopropanoate* (*R*)-**187** (7.66 g, 39.8 mmol, 62%) as a colourless oil: $\boldsymbol{R_f}$ 0.1 (hexane:ethyl acetate, 90:10); $[\boldsymbol{\alpha}]_{\mathbf{D}}^{\mathbf{20}}$ +80.3 (*c* 3.0, $CHCl_3$); **IR** $\nu_{max}$ (neat, $cm^{-1}$) 3446 (OH), 2953 (C=CH), 1730 (C=O), 1645, 993, 920; **$^1$H NMR** (400 MHz, $CDCl_3$) $\delta_H$ 5.75 (2H, dddd, *J* 17.2, 10.1, 7.9, 4.8 Hz, 2 × =C*H*), 5.20 (2H, dddd, *J* 17.2, 1.8, 1.1, 1.1 Hz, 2 × C$H_a$H$_b$=), 5.14 (2H, dddd, *J* 10.1, 1.8, 0.9, 0.9 Hz, 2 × CH$_a$$H_b$=), 3.75 (1H, dd, *J* 9.2, 4.6 Hz, C*H*N), 3.70 (3H, s, OC$H_3$), 3.67-3.64 (2H, m, OC$H_2$), 3.36 (2H, dddd, *J* 14.3, 4.8, 1.1, 0.9 Hz, 2 × NC$H_a$H$_b$), 3.20-3.14 (2H, dddd, *J* 14.3, 7.9, 1.1, 0.9 Hz, 2 × NCH$_a$$H_b$), 2.63 (1H, br s, O*H*); **$^{13}$C NMR** (101 MHz, $CDCl_3$) $\delta_c$ 171.8 (*C*$O_2$$CH_3$), 135.9 (2 × =*C*H), 118.1 (2 × *C*$H_2$=), 62.5 (*C*HN), 59.1 (*C*$H_2$OH), 53.7 (2 × N*C*$H_2$-allyl), 51.5 (O*C*$H_3$); **HRMS** *m*/*z* (ES$^+$) calcd. for $C_{10}H_{17}NO_3Na$ [M+Na]$^+$ 222.1106, found 222.1100; ***m*/*z*** (ES$^+$) 222 ([M+Na]$^+$, 100%).

### 7.3.19 -

**Methyl (–)-(2*S*)-(diallylamino)-3-hydroxypropanoate** (*S*)-**187**

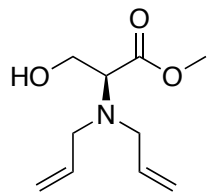


Allyl bromide (12.2 mL, 141 mmol, 2.2 eq) was added to a suspension of L-serine methyl ester hydrochloride (*S*)-**164** (10.0 g, 64.8 mmol, 1.0 eq) and $K_2CO_3$ (35.6 g, 258 mmol, 4.0 eq) in acetonitrile (300 mL) and the resulting suspension was heated under reflux for 24 h. The reaction was cooled to rt, diluted with water (300 mL) and extracted with ethyl acetate (3 × 100 mL). The organic fractions were combined, washed with brine (100 mL), dried over $Na_2SO_4$, filtered and the solvent removed *in vacuo*. The resulting oil was purified by silica gel column chromatography, eluting with hexane and ethyl acetate (95:5 to 90:10), to yield *methyl (2S)-3-hydroxy-2-N,N-bisallylaminopropanoate* (*S*)-**187** (7.02 g, 36.5 mmol, 57%) as a colourless oil: $\boldsymbol{R_f}$ 0.1 (hexane:ethyl acetate, 90:10); $[\boldsymbol{\alpha}]_{\mathbf{D}}^{\mathbf{20}}$ -81.3 (*c* 2.9, $CHCl_3$); **IR** $\nu_{max}$ (neat, $cm^{-1}$) 3446 (OH), 2926 (C=CH), 1730 (C=O), 1645, 993, 920; **$^1$H NMR** (400 MHz, $CDCl_3$) $\delta_H$ 5.75 (2H, dddd, *J* 17.2, 10.1, 7.9, 4.8 Hz, 2 × =C*H*), 5.20 (2H, dddd, *J* 17.2, 1.8, 1.1, 1.1 Hz, 2 × C$H_a$$H_b$=), 5.14 (2H, dddd, *J* 10.1, 1.8, 0.9, 0.9 Hz, 2 × CH$_a$$H_b$=), 3.70 (3H, s, OC$H_3$), 3.75 (1H, dd, *J* 9.2, 4.6 Hz, C*H*N), 3.67 (1H, dd, *J* 14.3, 4.6 Hz, OC$H_a$$H_b$), 3.64 (1H, d, *J* 14.3, 9.2 Hz, OCH$_a$$H_b$), 3.36 (2H, dddd, *J* 14.3, 4.8, 1.1, 0.9 Hz, 2 × NC$H_a$$H_b$-allyl), 3.20-3.14 (2H, m, 2 × NCH$_a$$H_b$-allyl), 2.63 (1H, br s, O*H*); **$^{13}$C NMR** (101 MHz, $CDCl_3$) $\delta_C$ 171.8 (*C*$O_2$$CH_3$), 135.9 (2 × =*C*H), 118.1 (2 × *C*$H_2$=),

62.5 (*C*HN), 59.1 (*C*$H_2$OH), 53.7 (2 × *C*$H_2$N), 51.5 (O*C*$H_3$); **HRMS** *m*/*z* ($ES^+$) calcd. for $C_{10}H_{18}NO_3$ $[M+H]^+$ 200.1276, found 200.1277; ***m*/*z*** ($ES^+$) 200 ($[M+H]^+$, 100%).

### 7.3.20 -

**Methyl (–)-(2*S*)-3-diallylamino-2-fluoropropanoate** (*S*)-**188**

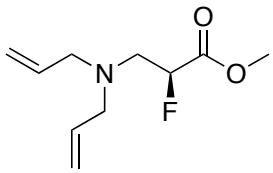


Diethylaminosulfur trifluoride **32** (2.2 mL, 18.1 mmol, 1.2 eq) was added to a solution of methyl (2*R*)-(diallylamino)-3-hydroxypropanoate (*R*)-**187** (3.00 g, 15.1 mmol, 1.0 eq) in THF (80 mL) over a period of 5 min at 0 ºC. The resulting solution was stirred at 0 °C for 1 h and the reaction was quenched by the addition of solid $K_2CO_3$ (excess) and water (1 mL). As the effervescence subsided, the solution was diluted further with water (20 mL) and the organic fractions extracted with diethyl ether (3 × 20 mL). The organic fractions were combined and washed with brine (20 mL), dried over $Na_2SO_4$, filtered and the solvent removed *in vacuo*. The resulting oil was purified by silica gel column chromatography, eluting with hexane:ethyl acetate (95:5), to yield *methyl (2S)-3-diallylamino-2-fluoropropanoate* (*S*)-**188** (2.06 g, 9.2 mmol, 61%) as a colourless oil: $\boldsymbol{R_f}$ 0.15 (hexane:ethyl acetate, 95:5); $[\boldsymbol{\alpha}]_{\mathbf{D}}^{\mathbf{20}}$ -9.7 (*c* 0.97, $CHCl_3$); **IR** $\nu_{max}$ (neat, $cm^{-1}$) 2956, 2814, 1767 (C=O), 1643, 1440, 1213, 922; **$^1$H NMR** (500 MHz, $CDCl_3$) $\delta_H$ 5.80 (2H, dddd, *J* 16.9, 10.4, 6.9, 5.9 Hz, 2 × =C*H*), 5.20-5.13 (4H, m, 2 × C$H_2$=), 5.05 (1H, ddd, *J* 49.7, 6.4, 3.2 Hz, C*H*F), 3.79 (3H, s, OC$H_3$), 3.28-3.24 (2H, m, 2 × NC$H_a$$H_b$-allyl), 3.14-3.10 (2H, m, 2 × NC$H_a$$H_b$-allyl),

2.99 (1H, ddd, *J* 25.8, 14.7, 6.4 Hz, C$H_a$$H_b$CHF), 2.96 (1H, ddd, *J* 26.6, 14.7, 3.2 Hz, CH$_a$$H_b$CHF); **$^{13}$C NMR** (101 MHz, $CDCl_3$) $\delta_C$ 169.5 (d, *J* 23.5 Hz, *C*$O_2$$CH_3$), 135.3 (2 × =*C*H), 118.0 (2 × *C*$H_2$=), 89.5 (d, *J* 187.1 Hz, *C*HF), 57.6 (2 × N*C*$H_2$-allyl), 54.2 (d, *J* 20.2 Hz, *C*$H_2$), 52.4 (O*C*$H_3$); **$^{19}$F NMR** (470 MHz, $CDCl_3$) $\delta_C$ -191.4 (ddd, *J* 49.7, 26.6, 25.8 Hz, CH*F*); **HRMS** *m*/*z* ($ES^+$) calcd. for $C_{10}H_{16}NO_2FNa$ $[M+Na]^+$ 224.1058, found 224.1064; ***m*/*z*** ($ES^+$) 224 ($[M+Na]^+$, 100%), 202 ($[M+H]^+$, 20%). Enantiomeric excess determined by chiral HPLC (Chiralcel OD-H 5% $^i$PrOH in hexane, 0.5 mL/min, $t_{r\ maj}$ = 9.57 min >95%, $t_{r\ min}$ = 9.33 min <5%).

### 7.3.21 -

**Methyl (+)-(2*R*)-3-diallylamino-2-fluoropropanoate** (*R*)-**188**

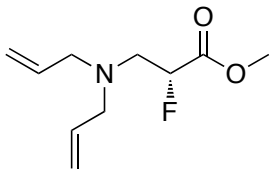


Following the procedure set out for methyl (2*S*)-3-diallylamino-2-fluoropropanoate (*S*)-**188**, starting from methyl 2-(*S*)-3-hydroxypropanoate (*S*)-**187** (3.10 g, 15.6 mmol, 1.0 eq) with diethylaminosulfur trifluoride **32** (2.3 mL, 18.7 mmol, 1.2 eq) in THF (80 mL), the reaction yielded *methyl (2R)-3-diallylamino-2-fluoropropanoate* (*R*)-**188** (2.19 g, 10.9 mmol, 69%) as a colourless oil: $\boldsymbol{R_f}$ 0.15 (hexane:ethyl acetate, 95:5); **IR** $\nu_{max}$ (neat, $cm^{-1}$) 2956, 2815, 1767 (C=O), 1643, 1440, 1214, 1069, 923; $\boldsymbol{[\alpha]_D^{20}}$ +9.8 (*c* 0.97, $CHCl_3$); **$^1$H NMR** (400 MHz, $CDCl_3$) $\delta_H$ 5.80 (2H, dddd, *J* 17.2, 10.2, 7.0, 6.0 Hz, 2 × =C*H*), 5.20-5.13 (4H, m, 2 × C$H_2$=), 5.05 (1H, ddd, *J* 49.7, 6.3, 3.2 Hz, C*H*F), 3.73 (3H, s, OC$H_3$), 3.29-3.23 (2H, m, 2 × NC$H_a$$H_b$-allyl),

3.15-3.09 (2H, m, 2 × $NCH_aH_b$-allyl), 2.99 (1H, ddd, *J* 25.8, 14.7, 6.3 Hz, $CH_aH_bCHF$), 2.97 (1H, ddd, *J* 26.6, 14.7, 3.2 Hz, $CH_aH_bCHF$); **$^{13}$C NMR** (101 MHz, $CDCl_3$) $\delta_C$ 169.5 (d, *J* 23.5 Hz, *C*ONH), 135.3 (2 × =*C*H), 118.0 (2 × $CH_2$=), 89.5 (d, *J* 186.1 Hz, *C*HF), 57.6 (2 × $NCH_2$-allyl), 54.2 (d, *J* 20.2 Hz, $CH_2CHF$), 52.4 ($OCH_3$); **$^{19}$F NMR** (376 MHz, $CDCl_3$) $\delta_F$ -191.9 (ddd, *J* 49.7, 26.6, 25.8 Hz, CH*F*); **HRMS** *m/z* ($ES^+$) calcd. for $C_{10}H_{17}NO_2F$ $[M+H]^+$, 202.1233, found 202.1235; ***m/z*** ($ES^+$) 202 ($[M+H]^+$, 100%). Enantiomeric excess determined by chiral HPLC (Chiralcel OD-H 5% $^i$PrOH in hexane, 0.5 mL/min, $t_{r\ maj}$ = 9.33 min >95%, $t_{r\ min}$ = 9.57 min <5%).

### 7.3.22 -

**3,6-Bis((2*R*)-3-*N,N*-diallylamino-2-fluoropropionamido)-9-(10*H*)-acridone (*R,R*)-195**

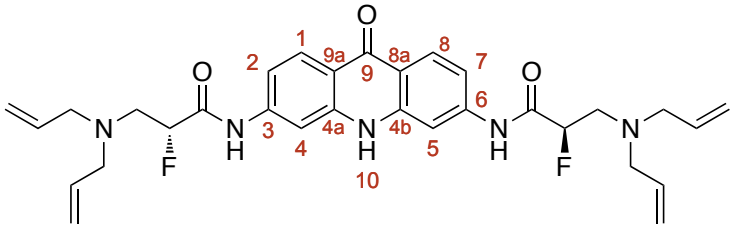


Potassium hexamethyldisilazide (4.4 mL, 1M in THF, 5.0 eq) was added dropwise to a suspension of 3,6-diaminoacridone **155** (200 mg, 0.88 mmol, 1.0 eq) in THF (10 mL) over 0.5 h at -78 °C and the mixture stirred for a further 1 h at -78 ºC. Methyl (2*R*)-3-diallylamino-2-fluoropropanoate (*R*)-**188** (450 mg, 2.2 mmol, 2.5 eq) in THF (10 mL) was gradually added *via* cannula to the homogeneous orange solution and the mixture was stirred for 16 h whist warming to rt. The reaction was quenched by the addition of saturated aqueous $Na_2CO_3$ (20 mL) resulting in significant precipitation. The

solids were removed by filtration and the filtrate was extracted with ethyl acetate (3 × 20 mL). The combined organic phases were washed with brine (30 mL), dried over $Na_2SO_4$, filtered and solvent removed *in vacuo* to yield a dark orange solid. This solid was absorbed onto $Na_2SO_4$ for purification by silica gel column chromatography, eluting with ethyl acetate and hexane (60:40, 90:10, 100:0) to furnish *3,6-bis((2R)-3-N,N-diallylamino-2-fluoropropionamido)-9-(10H)-acridone* (*R*,*R*)-**195** (132 mg, 0.19 mmol, 22%) as a pale yellow solid: $\boldsymbol{R_f}$ 0.31 (ethyl acetate:hexane, 80:20); **mp** 240 ºC (dec.) ; $[\alpha]_{546}^{20}$ 3.7 (*c* 0.9, $CH_3OH$); **IR** $\nu_{max}$ (KBr, $cm^{-1}$) 3271, 3200, 2851, 1688, 1629, 1599, 1462, 1300, 1269, 1190, 1118, 997, 921; **$^1$H NMR** (400 MHz, $CD_3OD$) $\delta_H$ 8.14 (2H, d, *J* 8.9 Hz, Ar *H*-1,8), 8.08 (2H, d, *J* 1.8 Hz, Ar *H*-4,5), 7.17 (2H, dd, *J* 8.9, 1.8 Hz, Ar *H*-2,7), 5.77 (4H, dddd, *J* 17.0, 10.4, 6.6, 6.6 Hz, 4 × =C*H*), 5.15-5.03 (10H, m, 4 × C$H_2$=, 2 × C*H*F), 3.21-3.08 (8H, m, 4 × NC$H_2$-allyl), 2.99 (4H, dd, *J* 25.8, 5.0 Hz, 2 × C$H_2$CHF); **$^{13}$C NMR** (101 MHz, $CD_3OD$) $\delta_C$ 178.5 (Ar *C*-9), 170.1 (d, *J* 20.6 Hz, 2 × *C*ONH), 143.7 (2 × *C*-8a,9a & 2 × Ar *C*-4a,4b), 136.5 (4 × =*C*H), 128.2 (2 × Ar *C*H-1,8), 118.8 (4 × *C*$H_2$=), 118.6 (2 × Ar *C*-3,6), 115.9 (2 × Ar *C*H-2,7), 107.7 (2 × Ar *C*H-4,5), 92.1 (d, *J* 187.9 Hz, 2 × *C*HF), 58.5 (4 × NC$H_2$-allyl), 55.5 (d, *J* 20.4 Hz, 2 × *C*$H_2$CHF); **$^{19}$F NMR** (376 MHz, $CD_3OD$) $\delta_F$ -191.2 (2F, dt, *J* 49.5, 24.7 Hz, 2 × CH*F*); **HRMS** *m*/*z* ($ES^-$) calcd. for $C_{31}H_{34}F_2N_5O_3$ $[M-H]^-$ requires 562.2630, found 562.2637; ***m*/*z*** ($ES^-$) 562 ($[M-H]^-$, 100%).

### 7.3.23 -

**3,6-Bis((2*S*)-3-*N*,*N*-diallylamino-2-fluoropropionamido)-9-(10*H*)-acridone** (*S*,*S*)-**195**

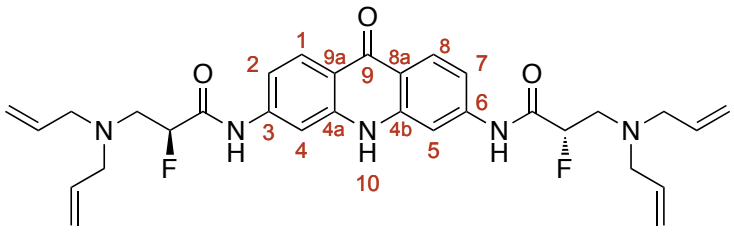


Following the procedure set out for 3,6-bis((2*R*)-3-*N*,*N*-diallylamino-2-fluoropropionamido)-9-(10*H*)-acridone (*R*,*R*)-**195**, starting from methyl (2*S*)-3-diallylamino-2-fluoropropanoate (*S*)-**188** (450 mg, 2.2 mmol, 2.5 eq) the reaction furnished *3,6-bis((2S)-3-N,N-diallylamino-2-fluoropropionamido)-9-(10H)-acridone* (*S*,*S*)-**195** (138 mg, 0.20 mmol, 23%) as a pale yellow solid: $\boldsymbol{R_f}$ 0.31 (ethyl acetate:hexane, 80:20); **mp** 240 ºC (dec.); $[\boldsymbol{\alpha}]_{546}^{20}$ -3.6 (*c* 1.1, $CH_3OH$); **IR** $\nu_{max}$ (KBr, $cm^{-1}$) 3269, 3200, 2850, 1691, 1628, 1598, 1462, 1299, 1268, 1190, 1118, 997, 922; **$^1$H NMR** (400 MHz, $CD_3OD$) $\delta_H$ 8.24 (2H, d, *J* 8.9 Hz, Ar *H*-1,8), 8.17 (2H, d, *J* 2.0 Hz, Ar *H*-4,5), 7.27 (2H, dd, *J* 8.9, 2.0 Hz, Ar *H*-2,7), 5.92-5.82 (4H, m, 4 × =C*H*), 5.26-5.11 (10H, m, 4 × C$H_2$= and 2 × C*H*F), 3.32-3.17 (8H, m, 4 × NC$H_2$-allyl), 3.09 (4H, dd, *J* 25.9, 5.0 Hz, 2 × C$H_2$CHF); **$^{13}$C NMR** (101 MHz, $CD_3OD$) $\delta_C$ 178.5 (Ar *C*-9), 170.0 (d, *J* 20.6 Hz, 2 × *C*ONH), 143.7 (2 × Ar *C*-8a,9a & 2 × Ar *C*-4a,4b), 136.1 (4 × =*C*H), 128.2 (2 × Ar *C*H-1,8), 118.7 (4 × *C*$H_2$=), 118.6 (2 × Ar *C*-3,6), 115.9 (2 × Ar *C*H-2,7), 107.7 (2 × Ar *C*H-4,5), 92.1 (d, *J* 187.9 Hz, 2 × *C*HF), 58.4 (4 × NC$H_2$-allyl), 55.6 (d, *J* 20.4 Hz, 2 × *C*$H_2$CHF); **$^{19}$F NMR** (376 MHz, $CD_3OD$) $\delta_F$ -191.2 (2F, dt, *J* 49.5, 24.7 Hz, 2 × CH*F*); **HRMS** *m*/*z* ($ES^+$) calcd. for $C_{31}H_{36}F_2N_5O_3$ $[M+H]^+$ requires 564.2786, found 564.2789; ***m*/*z*** ($ES^+$) 564 ($[M+H]^+$, 100%), 586 ($[M+H]^+$, 50%).

### 7.3.24 -

**3,6-Bis((2*R*)-3-amino-2-fluoropropionamido)-9-(10*H*)-acridone** (*R*,*R*)-**196**.HCl

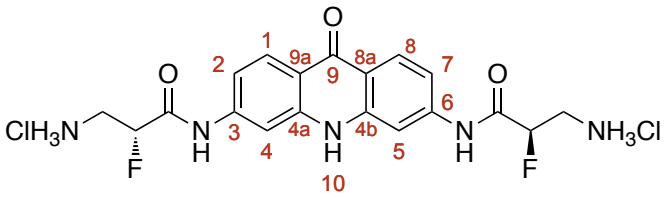


1,4-Di(phenylphosphino)butane (30 mg, 71 µmol, 10 mol%/allyl group) was added to a solution of palladium acetylacetonate (33 mg, 36 µmol, 5 mol%/allyl group) in degassed THF (5.0 mL) and the resulting solution was stirred at rt for 15 min. 3,6-Bis((2*R*)-3-*N,N*-diallylamino-2-fluoropropionamido)-9-(10*H*)-acridone (*R*,*R*)-**195** (100 mg, 0.18 mmol, 1.0 eq) and 2-mercaptosalicylic acid (137 mg, 890 mmol, 5.0 eq) in THF (5.0 mL) were added *via* cannula to the catalyst solution and the reaction was heated under reflux for 3 h. The reaction was cooled to rt and water (10 mL) and HCl (1 M, 60 µL) were added, resulting in precipitation of a yellow solid. The precipitate was isolated by filtration and the residue was washed repeatedly with water (3 × 10 mL). The filtrate was reduced *in vacuo* to furnish a yellow solid. This solid was reconstituted in water, filtered and the filtrate was lyophilised to yield *3,6-bis(3-amino-(2R)-fluoropropionamido)-9-(10H)-acridone dihydrochloride* (*R*,*R*)-**196**.HCl (81 mg, 0.17 mmol, 95% based on dichloride salt) as a pale yellow amorphous solid: **mp** 160 ºC (dec.); $[\alpha]_{436}^{20}$ 27.8 (*c* 0.9, $CH_3OH$); **IR** (KBr, $cm^{-1}$) 2960, 2921, 1677, 1563, 1416, 1207, 1149, 1063, 1042, 741; **$^1$H NMR** (300 MHz, $D_2O$) $\delta_H$ 7.73 (2H, d, *J* 9.0 Hz, Ar *H*-1,8), 7.27 (2H, d, *J* 1.9 Hz, Ar *H*-4,5), 6.95 (2H, dd, *J* 9.0, 1.9 Hz, Ar *H*-2,7), 5.45 (2H, ddd, *J* 48.5, 8.1, 3.2 Hz, 2 × CH*F*), 3.77-3.51 (4H, m, 2 × C$H_2$CHF); **$^{13}$C NMR** (126 MHz, $D_2O$/$d_6$-DMSO) $\delta_C$ 178.3 (Ar *C*-9), 167.4 (d,

*J* 19.6 Hz, 2 × *C*ONH), 142.6 (2 × Ar *C*-8a,9a), 142.5 (2 × Ar *C*-4a,4b), 128.3 (2 × Ar *C*H-1,8), 118.2 (2 × Ar *C*-3,6), 116.3 (2 × Ar *C*H-2,7), 107.9 (2 × Ar *C*H-4,5), 88.7 (d, *J* 188.2 Hz, 2 × *C*HF), 41.9 (d, *J* 20.6, 2 × *C*$H_2$CHF); **$^{19}$F NMR** (286 MHz, $D_2O$/$d_6$-DMSO) $\delta_F$ -196.9 (2F, ddd, *J* 48.5, 29.1, 19.3 Hz, 2 × C*H*F); **HRMS** *m*/*z* ($ES^+$) calcd. for $C_{19}H_{20}F_2N_5O_3$ $[M+H]^+$ requires 404.1529, found 404.1530; ***m*/*z*** ($ES^+$) 404 ($[M+H]^+$, 100%).

### 7.3.25 -

**3,6-Bis((2*S*)-3-amino-2-fluoropropionamido)-9-(10*H*)-acridone** (*S*,*S*)-**196**.HCl

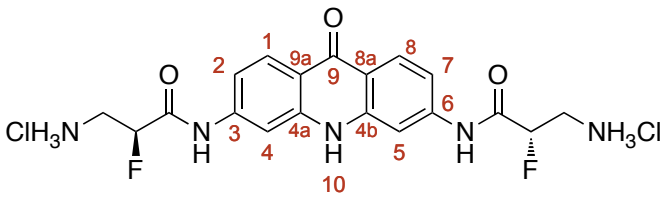


Following the procedure set out for 3,6-bis((2*S*)-3-amino-2-fluoropropionamido)-9-(10*H*)-acridone dihydrochloride (*R*,*R*)-**196**, starting from 3,6-bis((2*S*)-3-*N*,*N*-diallylamino-2-fluoropropionamido)-9-(10*H*)-acridone (*S*,*S*)-**195** (51 mg, 0.09 mmol) the reaction yielded *3,6-bis((2S)-3-amino-2-fluoropropionamido)-9-(10H)-acridone dihydrochloride* (*S*,*S*)-**196**.HCl (38 mg, 0.08 mmol, 89%) as a pale yellow amorphous solid: **mp** 160 ºC (dec.); $[\alpha]_{546}^{20}$ -22.5 (*c* 1.1, $CH_3OH$); **$^1$H NMR** (300 MHz, $D_2O$) $\delta_H$ 7.73 (2H, d, *J* 9.0 Hz, Ar *H*-1,8), 7.27 (2H, d, *J* 1.6 Hz, Ar *H*-4,5), 6.95 (2H, dd, *J* 9.0, 1.6 Hz, Ar *H*-2,7), 5.45 (2H, ddd, *J* 48.4, 8.1, 3.1 Hz, 2 × C*H*F), 3.68 (2H, ddd, *J* 29.0, 14.4, 3.1 Hz, 2 × C$H_a$$H_b$CHF), 3.58 (2H, ddd, *J* 19.4, 14.4, 8.1 Hz, 2 × C$H_a$$H_b$CHF); **$^{13}$C NMR** (126 MHz, $D_2O$) $\delta_C$ 178.3 (Ar *C*-9), 167.4 (d, *J* 19.7 Hz, 2 × *C*ONH), 142.6 (2 × Ar *C*-8a,9a), 142.5 (2 × Ar *C*-4a,4b), 128.3 (2 × Ar *C*H-1,8),

118.2 (2 × Ar *C*-3,6), 116.3 (2 × Ar *C*H-2,7), 107.9 (2 × Ar *C*H-4,5), 88.7 (d, *J* 188.2 Hz, 2 × *C*HF), 41.9 (d, *J* 20.7 Hz, 2 × C*H*$_2$CHF); **$^{19}$F NMR** (282 MHz, $D_2O$) $\delta_F$ -195.5 (2F, ddd, *J* 48.4, 29.0, 19.4 Hz, 2 × CH*F*); **HRMS** *m*/*z* ($ES^+$) calcd. for $C_{19}H_{20}F_2N_5O_3$ $[M+H]^+$ requires 404.1529, found 404.1528; ***m*/*z*** ($ES^+$) 404 ($[M+H]^+$, 100%).

### 7.3.26 -

**3,6-Bis((2*R*)-3-*N*,*N*-bisallylamino-2-fluoropropionamido)-9-(4-dimethylamino phenylamino)acridine** (*R*,*R*)-**206**

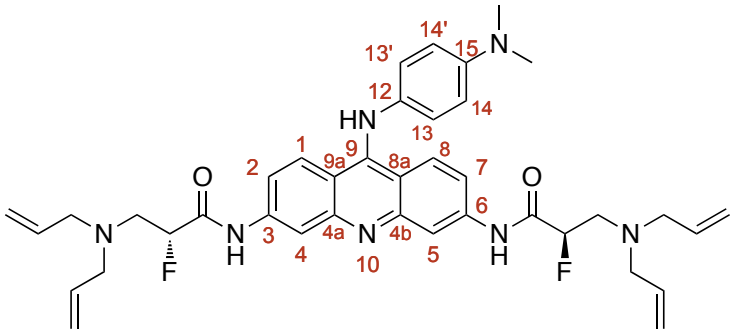


Phosphorous oxychloride (10 mL) was added to 3,6-bis((2*R*)-3-amino-2-fluoropropionamido)-9-(10*H*)-acridone (*R*,*R*)-**195** (100 mg, 0.18 mmol, 1.0 eq). The resulting bright orange suspension was stirred at rt until TLC analysis had indicated consumption of the starting material. The solution was cooled to 0 °C and cold $Et_2O$ (20 mL) was added, resulting in formation of a precipitate. The precipitate was isolated by filtration and washed with further $Et_2O$ (2 × 10 mL) and dissolved in $CHCl_3$ (10 mL). The organic phase was washed with aqueous $NH_4OH$ (1 M, 10 mL), and brine (10 mL), dried over $Na_2SO_4$, filtered and the solvent removed *in vacuo* to yield *3,6-bis((2R)-3-N,N-diallylamino-2-fluoropropionamido)-9-chloro*

*acridine* (74 mg, 72%) as a red brown solid, which was used in the next step without further purification. *N*,*N*-dimethylaminoaniline monohydrochloride (445 mg, 2.60 mmol, 20 eq) was dissolved in saturated aqueous $Na_2CO_3$ and extracted with $Et_2O$ (3 × 20 mL). The organic fractions were combined, washed with brine (20 mL), dried over $Na_2SO_4$, filtered and the solvent was removed *in vacuo* to yield *N*,*N*-dimethylaminoaniline as a light brown oil. This oil was dissolved in $CHCl_3$ (10 mL) and the solution was gradually added *via* cannula to a refluxing solution of 3,6-bis((2*R*)-3-*N,N*-diallylamino-2-fluoropropionamido)-9-chloroacridine (74 mg, 0.13 mmol, 1.0 eq) in $CHCl_3$ (10 mL) over 30 min. The mixture was heated under reflux until TLC analysis had indicated the consumption of the chloride, at which point the solvent was removed *in vacuo* to yield a purple oil. Cold $Et_2O$ (excess) was added, resulting the precipitation of a red-brown solid. The solids were isolated by filtration and washed with further $Et_2O$ (20 mL), dissolved in $CHCl_3$ (20 mL) and washed with aqueous $NH_4OH$ (1 M, 10 mL) followed by brine (10 mL). The organic phase was dried over $Na_2SO_4$, filtered and the solvent removed *in vacuo* to yield a red solid. The solid was purified by silica gel column chromatography, eluting with $CHCl_3$ and $CH_3OH$ (95:5), to yield *3,6-bis((2R)-3-N,N-bisallylamino-2-fluoropropionamido)-9-(4-dimethylamino phenylamino)acridine* (*R*,*R*)-**206** (53 mg, 0.08 mmol, 61%) as a dark red solid: $\boldsymbol{R_f}$ 0.09 ($CHCl_3$:$CH_3OH$, 95:5); **mp** 195 ºC (dec.); **IR** $\nu_{max}$ (KBr disc, $cm^{-1}$) 3428, 3077, 1700 (C=O), 1633 (C=O), 1521, 1469, 1446, 1359, 1257, 1065, 922; **$^1$H NMR** (400 MHz, $CD_3OD$) $\delta_H$ 8.37 (2H, d, *J* 1.9 Hz, Ar *H*-4,5), 7.96 (2H, d, *J* 9.4 Hz, Ar *H*-1,8), 7.27 (2H, dd, *J* 9.4, 1.9 Hz, Ar *H*-2,7), 7.10 (2H, d, *J* 8.9 Hz, Ar *H*-14,14'), 6.78 (2H, d, *J* 8.9 Hz, Ar *H*-13,13'), 5.85 (4H, dddd, *J* 17.0, 10.4, 6.5, 6.5 Hz, 4 × =C*H*), 5.24-5.14 (8H, m, 4 × C$H_2$=), 5.20 (2H, dt, *J* 49.3, 5.0 Hz, 2 × C*H*F), 3.31-3.25 (4H, m, 4 × NC$H_a$$H_b$-allyl), 3.24-3.19 (4H, m, 4 × NCH$_a$$H_b$-allyl), 3.09 (4H,

dd, *J* 26.0, 5.0 Hz, 2 × C*H*$_2$CHF), 3.00 (6H, s, 2 × NC*H*$_3$); **$^{13}$C NMR** (101 MHz, $CD_3OD$) $\delta_C$ 170.3 (d, *J* 20.9 Hz, 2 × *C*ONH), 153.9 (Ar *C*-9), 151.0 (Ar *C*-15), 144.3 (2 × Ar *C*-4a,4b), 143.8 (2 × Ar *C*-8a,9a), 136.2 (4 × =*C*H), 132.0 (Ar *C*-12), 127.7 (2 × Ar *C*H-1,8), 126.2 (2 × Ar *C*H-14,14'), 118.7 (4 × *C*H$_2$=), 117.9 (2 × Ar *C*H-2,7), 114.4 (2 × Ar *C*H-13,13'), 112.2 (2 × Ar *C*-3,6), 109.0 (2 × Ar *C*H-4,5), 92.2 (d, *J* 187.9 Hz, 2 × *C*HF), 58.4 (4 × NCH$_2$-allyl), 55.5 (d, *J* 20.0 Hz, 2 × *C*H$_2$CHF), 40.9 (2 × NC*H*$_3$); **$^{19}$F NMR** (376 MHz, $CD_3OD$) $\delta_F$ 191.2 (2F, dt, *J* 49.3, 26.0 Hz, 2 × CH*F*); **HRMS** *m/z* (ES$^+$) calcd. for $C_{39}H_{46}F_2N_7O_2$ $[M+H]^+$ requires 682.3676, found 682.3670; ***m/z*** (ES$^+$) 682 ($[M+H]^+$, 100%).

### 7.3.27 -

**3,6-Bis((2*S*)-3-*N,N*-bisallylamino-2-fluoropropionamido)-9-(4-dimethylamino phenylamino) acridine** (*S,S*)-**206**

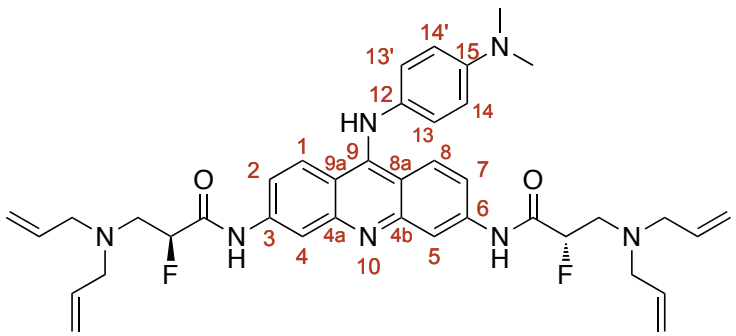


Following the procedure set out for 3,6-bis((2*R*)-3-bisallylamino-2-fluoropropionamido)-9-(4-dimethylaminophenylamino) acridine (*R,R*)-**206**, starting from 3,6-bis((2*S*)-3-*N,N*-diallylamino-2-fluoropropionamido)-9-(10*H*)-acridone (*S,S*)-**195** (100 mg, 0.18 mmol), the reaction yielded *3,6-bis((2S)-3-N,N-bisallylamino-*

*2-fluoropropionamido)-9-(4-dimethylaminophenylamino) acridine* (*S*,*S*)-**206** (41.7 mg, 0.063 mmol, 48%) as a red solid: $\boldsymbol{R_f}$ 0.09 ($CHCl_3$:$CH_3OH$, 95:5); **mp** 195 ºC (dec.); **IR** $\nu_{max}$ (KBr disc, $cm^{-1}$) 3453, 3077, 1697 (C=O), 1633 (C=O), 1521, 1469, 1446, 1359, 1257, 1064, 922; **UV-vis** ($CH_3OH$) $\lambda_{max}$ 268 nm ($\log_{10} \varepsilon$ 11.34), 293 nm ($\log_{10} \varepsilon$ 8.04), 364 nm ($\log_{10} \varepsilon$ 4.00), 425 nm ($\log_{10} \varepsilon$ 1.63); **$^1$H NMR** (400 MHz, $CD_3OD$) $\delta_H$ 8.39 (2H, d, *J* 1.9 Hz, Ar *H*-4,5), 7.97 (2H, d, *J* 9.4 Hz, Ar *H*-1,8), 7.31 (2H, dd, *J* 9.4, 1.9 Hz, Ar *H*-2,7), 7.15 (2H, d, *J* 9.0 Hz, Ar *H*-14,14'), 6.81 (2H, d, *J* 9.0 Hz, Ar *H*-13,13'), 5.85 (4H, dddd, *J* 17.0, 10.4, 6.5, 6.5 Hz, 4 × =C*H*), 5.28-5.13 (8H, m, 4 × C$H_2$=), 5.20 (2H, dt, *J* 49.4, 4.9 Hz, 2 × C*H*F), 3.32-3.16 (8H, m, 4 × NC$H_2$-allyl), 3.09 (4H, dd, *J* 26.0, 4.9 Hz, C$H_2$CHF), 3.00 (6H, s, 2 × NC$H_3$); **$^{13}$C NMR** (101 MHz, $CD_3OD$) $\delta_C$ 170.3 (d, *J* 20.9 Hz, 2 × *C*ONH), 154.4 (Ar *C*-9), 151.3 (Ar *C*-15), 144.2 (2 × Ar *C*-4a,4b), 143.8 (2 × Ar *C*-8a,9a), 136.2 (4 × =*C*H), 131.2 (Ar *C*-12), 127.8 (2 × Ar *C*H-1,8) 126.6 (2 × Ar *C*H-14,14'), 118.7 (4 × *C*$H_2$=), 118.0 (2 × Ar *C*H-2,7), 114.3 (2 × Ar *C*H-13,13´), 111.8 (2 × Ar *C*-3,6), 108.4 (2 × Ar *C*H-4,5), 92.2 (d, *J* 187.9 Hz, 2 × *C*HF), 58.4 (4 × NC$H_2$-allyl), 55.5 (d, *J* 20.0 Hz, 2 × *C*$H_2$CHF), 40.8 (2 × N*C*$H_3$); **$^{19}$F NMR** (376 MHz, $CD_3OD$) $\delta_F$ 191.4 (2F, dt, *J* 49.4, 26.0 Hz, 2 × CH*F*); **HRMS** *m*/*z* ($ES^+$) calcd. for $C_{39}H_{46}F_2N_7O_2$ $[M+H]^+$ requires 682.3676, found 682.3666; ***m*/*z*** ($ES^+$) 682 ($[M+H]^+$, 100%).

### 7.3.28 -

**3,6-Bis((2*R*)-3-amino-2-fluoropropionamido)-9-(4-dimethylaminophenylamino) acridine dihydrochloride** (*R*,*R*)-**208**.HCl

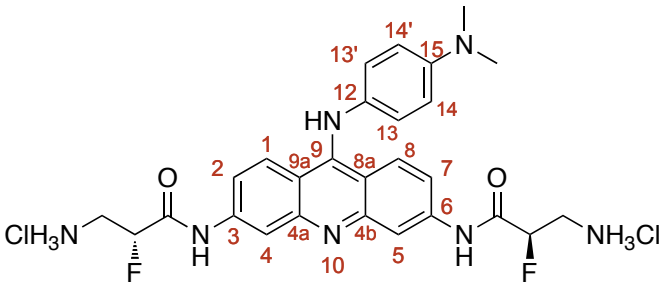


1,4-Di(phenylphosphino)butane (25.2 mg, 59 µmol, 20 mol%/allyl group) was added to a solution of tris(dibenzylideneacetone)dipalladium (26.5 mg, 29 µmol, 10 mol%/allyl group) in THF (8 mL) and stirred for 15 min until the solution turned yellow. The solution was added to a solution of 3,6-bis((2*R*)-3-*N,N*-bisallylamino-2-fluoropropionamido)-9-(4-dimethylaminophenylamino) acridine (*R*,*R*)-**206** (48.8 mg, 72 µmol, 1.0 eq) and 2-mercaptosalicylic acid (55.0 mg, 0.356 mmol, 5.0 eq) in THF (5.0 mL) *via* cannula. The resulting solution was heated under reflux for 3 h before being cooled to rt and diluted with distilled water (5 mL) and HCl (1 M, 60 µL), which caused precipitation of a solid. The precipitate was isolated by filtration and the residue was washed repeatedly with distilled water (3 × 10 mL). The water/THF filtrate was concentrated *in vacuo* to yield a yellow solid. The solid was redissolved in water and filtered. The filtrate was lyophilised to yield *3,6-bis((2R)-3-amino-2-fluoropropionamido)-9-(4-dimethylaminophenylamino)acridine dihydrochloride* (*R*,*R*)-**208**.HCl (25.2 mg, 42 µmol, 59% based on dichloride salt) as a red amorphous solid: **IR** $\nu_{max}$ (KBr disc, $cm^{-1}$) 3424, 1700 (C=O), 1633 (C=O), 1610, 1594, 1546, 1516, 1467, 1447, 1386, 1257; **$^1$H NMR** (500 MHz, $D_2O$) $\delta_H$ 8.01 (2H, s, Ar *H*-4,5),

7.70 (2H, d, *J* 9.4 Hz, Ar *H*-1,8), 7.45 (2H, d, *J* 8.7 Hz, Ar *H*-14,14′), 7.25 (2H, d, *J* 8.7 Hz, Ar *H*-13,13′), 7.19 (2H, d, *J* 9.4 Hz, Ar *H*-2,7), 5.49 (2H, ddd, *J* 48.3, 8.3, 3.0 Hz, 2 × C*H*F), 3.63 (2H, ddd, *J* 29.3, 14.4, 3.0 Hz, 2 × C$H_a$$H_b$CHF), 3.53 (2H, ddd, *J* 19.1, 14.4, 8.3 Hz, 2 × CH$_a$$H_b$CHF), 3.15 (6H, s, 2 × N C$H_3$); **$^{13}$C NMR** (126 MHz, $D_2O$) $\delta_C$ 166.8 (d, *J* 20.0 Hz, 2 × *C*ONH), 153.2 (Ar *C*-9), 152.0 (Ar *C*-15), 142.1 (2 × Ar *C*-4a,4b), 140.7 (2 × Ar *C*-8a,9a), 133.1 (Ar *C*-12), 126.5 (2 × Ar *C*H-1,8), 125.5 (2 × Ar *C*H-14,14'), 117.5 (2 × Ar *C*H-2,7), 110.3 (2 × Ar *C*-3,6), 106.9 (2 × Ar *C*H-4,5), 87.4 (d, *J* 189.2 Hz, 2 × *C*HF), 65.9 (2 × N*C*H$_3$), 40.5 (d, *J* 20.6 Hz, 2 × *C*H$_2$CHF); **$^{19}$F NMR** (470 MHz, $D_2O$) $\delta_F$ -195.7 (2F, ddd, *J* 48.3, 29.3, 19.1 Hz, 2 × CH*F*); **HRMS** *m*/*z* (ES$^+$) calcd. for $C_{27}H_{30}F_2N_7O_2$ $[M+H]^+$ requires 522.2429, found 522.2421; ***m*/*z*** (ES$^+$) 522 ($[M+H]^+$, 100%).

### 7.3.29 -

**3,6-Bis((2*S*)-3-amino-2-fluoropropionamido)-9-(4-dimethylaminophenylamino) acridine dihydrochloride** (*S*,*S*)-**208**.HCl

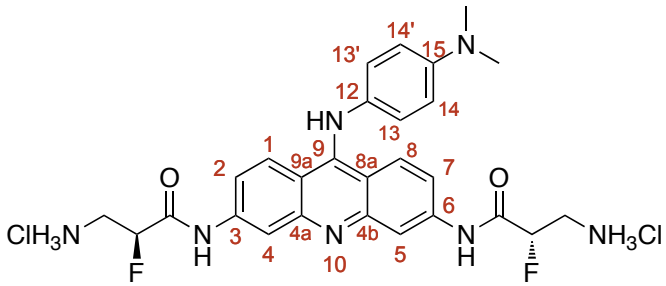


Following the procedure set out for 3,6-bis((2*R*)-3-amino-2-fluoropropionamido)-9-(4-dimethylaminophenylamino) acridine dihydrochloride (*R*,*R*)-**208**.HCl, starting from 3,6-bis((2*S*)-3-*N*,*N*-bisallylamino-2-fluoropropionamido)-9-(4-dimethylaminophenyl

amino)acridine (*S*,*S*)-**206** (41.7 mg, 61 μmol), the reaction yielded *3,6-bis((2S)-3-amino-2-fluoropropionamido)-9-(4-dimethylaminophenylamino)acridine dihydrochloride* (*S*,*S*)-**208**.HCl (19.3 mg, 33 μmol, 53%) as a red solid: **IR** $\nu_{max}$ (KBr disc, $cm^{-1}$) 3424, 2927, 1700 (C=O), 1633 (C=O), 1610, 1595, 1517, 1446, 1257; **$^{1}$H NMR** (500 MHz, $D_2O$) $\delta_H$ 8.01 (2H, d, *J* 1.9 Hz, Ar *H*-4,5), 7.70 (2H, d, *J* 9.4 Hz, Ar *H*-1,8), 7.45 (2H, d, *J* 8.7 Hz, Ar *H*-14,14'), 7.25 (2H, d, *J* 8.7 Hz, Ar *H*-13,13'), 7.19 (2H, dd, *J* 9.4, 1.9 Hz, Ar *H*-2,7), 5.49 (2H, ddd, *J* 48.3, 8.2, 3.0 Hz, 2 × C*H*F), 3.63 (2H, ddd, *J* 29.3, 14.4, 3.0 Hz, 2 × C$H_a$$H_b$CHF), 3.53 (2H, ddd, *J* 19.2, 14.4, 8.2 Hz, 2 × CH$_a$$H_b$CHF), 3.15 (6H, s, 2 × N*C*H$_3$); **$^{13}$C NMR** (126 MHz, $D_2O$) $\delta_C$ 166.8 (d, *J* 20.0 Hz, 2 × *C*ONH), 153.2 (Ar *C*-9), 152.0 (Ar *C*-15), 142.1 (2 × Ar *C*-4a,4b), 140.7 (2 × Ar *C*-8a,9a), 133.1 (Ar *C*-12), 126.5 (2 × Ar *C*H-14,14′), 125.5 (2 × Ar *C*H-1,8), 117.5 (2 × Ar *C*H-2,7), 110.3 (2 × Ar *C*-3,6), 106.9 (2 × Ar *C*H-4,5), 87.4 (d, *J* 189.2 Hz, 2 × *C*HF), 65.9 (2 × N*C*H$_3$), 40.5 (d, *J* 20.6 Hz, 2 × *C*H$_2$CHF); **$^{19}$F NMR** (470 MHz, $D_2O$) $\delta_F$ -195.7 (2F, ddd, *J* 48.3, 29.3, 19.2 Hz, 2 × CH*F*); **HRMS** *m*/*z* ($ES^+$) calcd. for $C_{27}H_{30}F_2N_7O_2$ $[M+H]^+$ requires 522.2429, found 522.2440; ***m*/*z*** ($ES^+$) 522 ($[M+H]^+$, 100%).

### 7.3.30 -

**Methyl (–)-(2*R*)-3-dipropylamino-2-fluoropropanoate** (*R*)-**209**

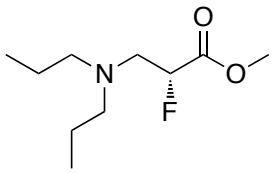

Palladium on carbon (20%, 205 mg, 10 mol%) was added to a solution of methyl (2*R*)-3-diallylamino-2-fluoropropanoate (*R*)-**188** (755 mg, 3.88 mmol, 1.0 eq) in ethyl acetate (10 mL). The resulting suspension was stirred vigorously under a hydrogen atmosphere at rt for 24 h. The solids were removed by filtration and the residue was washed repeatedly with ethyl acetate (3 × 20 mL). The filtrate was made deliberately wet with water (1 mL) followed by the addition of $MgSO_4$ to remove any remaining fine particulate. The solvent was removed *in vacuo* to yield a oil that was purified by silica gel column chromatography, eluting with ethyl acetate and hexane (20:80), to yield *methyl (2R)-3-dipropylamino-2-fluoropropanoate* (*R*)-**209** (393 mg, 1.91 mmol, 51%) as a colourless oil: $\boldsymbol{R_f}$ 0.16 (hexane:ethyl acetate, 95:5); $\boldsymbol{[\alpha]_D^{20}}$ -23.0 (*c* 1.0, $CHCl_3$); **IR** $\nu_{max}$ (neat, $cm^{-1}$) 2960, 1769 (C=O), 1462, 1212, 1074; **$^1$H NMR** (400 MHz, $CDCl_3$) $\delta_H$ 4.95 (1H, ddd, *J* 49.8, 5.5, 5.5 Hz, C*H*F), 3.72 (3H, s, OC$H_3$), 2.90-2.88 (2H, m, C$H_2$CHF), 2.47-2.33 (4H, m, 2 × NC$H_2$CH$_2$), 1.41-1.32 (4H, m, 2 × NCH$_2$C$H_2$), 0.79 (6H, t, *J* 7.4 Hz, 2 × CH$_2$C$H_3$); **$^{13}$C NMR** (101 MHz, $CDCl_3$) $\delta_C$ 169.8 (d, *J* 23.9 Hz, *C*O$_2$CH$_3$), 89.6 (d, *J* 186.5 Hz, *C*HF), 57.0 (2 × NCH$_2$CH$_2$), 55.8 (d, *J* 20.2 Hz, *C*H$_2$CHF), 52.3 (O*C*H$_3$), 20.5 (2 × NCH$_2$*C*H$_2$), 11.8 (2 × CH$_2$*C*H$_3$); **$^{19}$F NMR** (376 MHz, $CDCl_3$) $\delta_F$ -192.0 (ddd, *J* 49.8, 25.9, 25.9 Hz, CH*F*); **HRMS** *m*/*z* ($ES^+$) calcd. for $C_{10}H_{21}FNO_2$ $[M+H]^+$, requires 206.1551, found 206.1550; ***m*/*z*** ($ES^+$) 206 ($[M+H]^+$, 100%).

### 7.3.31 -

**Methyl (+)-(2*S*)-3-dipropylamino-2-fluoropropanoate** (*S*)-**209**

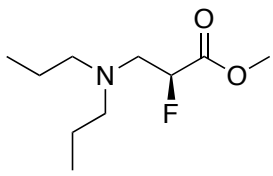


Following the procedure set out for methyl 3-dipropylamino-(2*R*)-fluoropropanoate (*R*)-**209**, starting from methyl (2*S*)-3-diallylamino-2-fluoropropanoate (*S*)-**188** (830 mg, 414 mmol) the reaction yielded *methyl (2S)-3-dipropylamino-2-fluoropropanoate* (*S*)-**209** (520 mg, 2.25 mmol, 61%) as a colourless oil: $R_f$ 0.16 (hexane:ethyl acetate, 95:5); $[\alpha]_D^{20}$ +22.5 (*c* 1.0, $CHCl_3$); **IR** $\nu_{max}$ (neat, $cm^{-1}$) 2959, 1769 (C=O), 1461, 1212, 1073; **$^1$H NMR** (300 MHz, $CDCl_3$) $\delta_H$ 5.01 (1H, ddd, *J* 49.7, 5.4, 5.4 Hz, C*H*F), 3.79 (3H, s, $OCH_3$), 3.01-2.92 (2H, m, C$H_2$CHF), 2.55-2.38 (4H, m, 2 × NC$H_2$CH$_2$), 1.43 (4H, tq, *J* 7.4, 7.4 Hz, 2 × NCH$_2$C$H_2$), 0.86 (6H, t, *J* 7.4 Hz, 2 × CH$_2$C$H_3$); **$^{13}$C NMR** (75 MHz, $CDCl_3$) $\delta_C$ 169.8 (d, *J* 23.8, *C*$O_2CH_3$), 89.7 (d, *J* 187.1, *C*HF), 57.0 (2 × NC$H_2$CH$_2$), 55.8 (d, *J* 20.2, *C*$H_2$CHF), 52.3 (O*C*$H_3$), 20.5 (2 × CH$_2$*C*H$_2$CH$_3$), 11.8 (2 × CH$_2$*C*H$_3$); **$^{19}$F NMR** (282 MHz, $CDCl_3$) $\delta_F$ -191.9 (ddd, *J* 49.7, 26.0, 26.0 Hz, CH*F*); **HRMS** *m*/*z* ($ES^+$) calcd. for $C_{10}H_{21}FNO_2$ $[M+H]^+$, requires 206.1551, found 206.1550; ***m*/*z*** ($ES^+$) 206 ($[M+H]^+$, 100%).

### 7.3.32 -

**3,6-Bis((2*R*)-3-*N,N*-dipropylamino-2-fluoropropionamido)-9-(10*H*)-acridone**

(*R,R*)-**210**

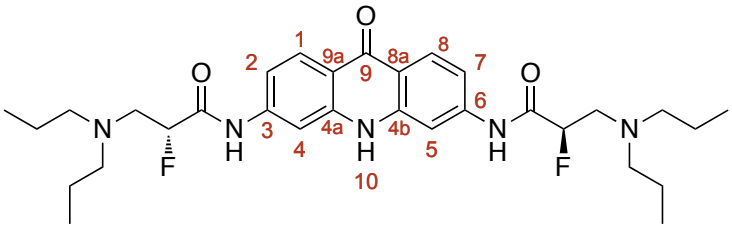


Potassium hexamethyldisilazide (4.1 mL, 1 M in THF, 5.0 eq) was added dropwise to a suspension of 3,6-diaminoacridone (188 mg, 0.83 mmol, 1.0 eq) in THF (10 mL) at -78 °C over 30 min and stirred for a further 1 h at -78 ºC. Methyl (2*R*)-3-dipropylamino-2-fluoropropanoate (*R*)-**209** (375 mg, 1.83 mmol, 2.2 eq) in THF (10 mL) was gradually added *via* cannula to the homogeneous orange solution and the mixture was stirred for 16 h while gently warming through to rt. The reaction was quenched by the addition of saturated aqueous $Na_2CO_3$ (20 mL), resulting in significant precipitation, which was removed by filtration. The filtrate was extracted with ethyl acetate (3 × 20 mL). The organic phases were combined and washed with brine (30 mL), dried over $Na_2SO_4$, filtered and solvent removed *in vacuo* to yield a dark orange solid. The solids were absorbed onto $Na_2SO_4$ for purification by silica gel column chromatography, eluting with ethyl acetate and hexane (30:70, 90:10, 100:0) to furnish *3,6-bis((2R)-3-N,N-dipropylamino-2-fluoropropionamido)-9-(10H)-acridone* (*R,R*)-**210** (142 mg, 0.14 mmol, 30%) as a pale yellow solid: $\boldsymbol{R_f}$ 0.17 (ethyl acetate:hexane, 80:20); **mp** 215 ºC (dec.); $[\alpha]_{546}^{20}$ +3.7 (*c* 0.88, $CH_3OH$), $[\alpha]_{578}^{20}$ +4.0 (*c* 0.88, $CH_3OH$); **IR** $\nu_{max}$ (KBr, $cm^{-1}$) 3286, 2961, 1685 (C=O), 1633 (C=O), 1600, 1536, 1464; **$^1$H NMR** (300 MHz, $CD_3OD$) $\delta_H$ 8.25 (2H, d, *J* 8.9 Hz,

Ar *H*-1,8), 8.21 (2H, d, *J* 1.9 Hz, Ar *H*-4,5), 7.29 (2H, dd, *J* 8.9, 1.9 Hz, Ar *H*-2,7), 5.16 (2H, dt, *J* 49.4, 4.9 Hz, 2 × C*H*F), 3.07 (4H, dd, *J* 27.9, 4.9 Hz, 2 × C$H_2$CHF), 2.62-2.47 (8H, m, 4 × C$H_2$N), 1.54-1.48 (8H, m, 4 × $CH_3CH_2CH_2$), 0.89 (12H, t, *J* 7.4 Hz, 4 × $CH_3CH_2$); **$^{13}$C NMR** (75.5 MHz, $CD_3OD$) $\delta_C$ 178.6 (Ar *C*-9), 170.3 (d, 20.6 Hz, 2 × *C*ONH), 143.7 (2 × Ar *C*-8a,9a & 2 × Ar *C*-4a,4b), 128.2 (2 × Ar *C*H-1,8), 118.8 (2 × Ar *C*-3,6), 115.6 (2 × Ar *C*H-2,7), 107. (2 × Ar *C*H-4,5), 92.1 (d, *J* 187.8 Hz, 2 × *C*HF), 58.0 (4 × $CH_2N$), 56.9 (d, *J* 20.6 Hz, 2 × $CH_2CHF$), 21.2 (4 × $CH_3CH_2CH_2$), 12.1 (4 × $CH_2CH_3$); **$^{19}$F NMR** (282 MHz, $CD_3OD$) $\delta_F$ 191.2 (2F, dt, *J* 49.4, 27.9 Hz, 2 × CH*F*); **HRMS** *m/z* ($ES^-$) calcd. for $C_{31}H_{42}F_2N_5O_3$ $[M-H]^-$ requires 570.3251, found 570.3242; ***m/z*** ($ES^-$) 570 ($[M-H]^-$, 100%).

### 7.3.33 -

**3,6-Bis((2*S*)-3-*N*,*N*-dipropylamino-2-fluoropropionamido)-9-(10*H*)-acridone** (*S*,*S*)-**210**

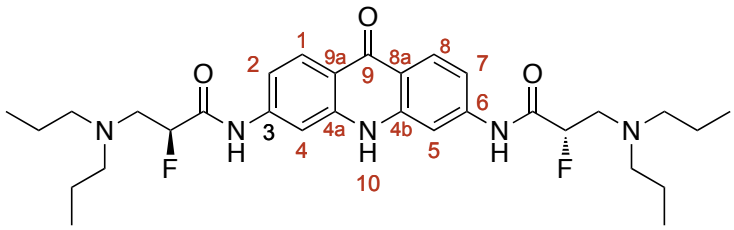


Following the procedure set out for 3,6-bis((2*R*)-3-*N*,*N*-dipropylamino-2-fluoropropionamido)-9-(10*H*)-acridone (*R*,*R*)-**210** starting from methyl 2(*S*)-fluoropropanoate (*S*)-**209** (370 mg, 1.8 mmol), the reaction yielded *3,6-bis((2S)-3-N,N-dipropylamino-2-fluoropropionamido)-9-(10H)-acridone* (*S*,*S*)-**210** (124 mg, 0.22 mmol, 26%) as a pale yellow solid: ***R$_f$*** 0.17 (ethyl acetate:hexane, 80:20);

**mp** 215 ºC (dec.); $[\alpha]_{436}^{20}$ -11.7 (*c* 1.02, $CH_3OH$), $[\alpha]_{546}^{20}$ -5.4 (*c* 1.02, $CH_3OH$), $[\alpha]_{578}^{20}$ -4.1 (*c* 1.02, $CH_3OH$); **IR** $\nu_{max}$ (KBr, $cm^{-1}$) 3283, 2959, 1687 (C=O), 1637 (C=O), 1600, 1537, 1464; **$^1$H NMR** (300 MHz, $CD_3OD$) $\delta_H$ 8.25 (2H, d, *J* 8.9 Hz, Ar *H*-1,8), 8.21 (2H, d, *J* 1.9 Hz, Ar *H*-4,5), 7.29 (2H, dd, *J* 8.9, 1.9 Hz, Ar *H*-2,7), 5.16 (2H, dt, *J* 49.4, 4.9 Hz, 2 × C*H*F), 3.07 (4H, dd, *J* 27.9, 4.9 Hz, 2 × C$H_2$CHF), 2.62-2.47 (8H, m, 4 × C$H_2$N), 1.54-1.48 (8H, m, 4 × $CH_3CH_2CH_2$), 0.89 (12H, t, *J* 7.4 Hz, 4 × C$H_3CH_2$); **$^{13}$C NMR** (75.5 MHz, $CD_3OD$) $\delta_C$ 178.5 (Ar *C*-9), 170.3 (d, *J* 20.6 Hz, 2 × *C*ONH), 143.7 (2 × Ar *C*-8a,9a & 2 × Ar *C*-4a,4b), 128.2 (2 × Ar *C*H-1,8), 118.6 (2 × Ar *C*-3,6), 115.9 (2 × Ar *C*H-2,7), 107.7 (2 × Ar *C*H-4,5), 92.1 (d, *J* 187.8-Hz, 2 × *C*HF), 58.0 (4 × *C*$H_2$N), 57.0 (d, *J* 20.6 Hz, 2 × *C*$H_2$CHF), 21.2 (4 × $CH_3CH_2CH_2$), 12.1 (4 × *C*$H_3CH_2$); **$^{19}$F NMR** (282 MHz, $CD_3OD$) $\delta_F$ -191.2 (2F, dt, *J* 49.4, 27.9 Hz, 2 × CH*F*); **HRMS** *m*/*z* ($ES^-$) calcd. for $C_{31}H_{42}F_2N_5O_3$ $[M-H]^-$ requires 570.3251, found 570.3263; ***m*/*z*** ($ES^-$) 570 ($[M-H]^-$, 100%).

### 7.3.34 -

**3,6-Bis((2*R*)-3-*N*,*N*-bispropylamino-2-fluoropropionamido)-9-(4-dimethylamino phenylamino)acridine** (*R*,*R*)-**212**

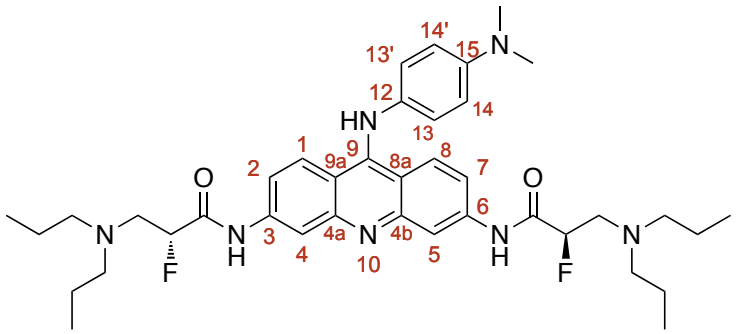


Phosphorous oxychloride (5 mL) was added to 3,6-bis((2*R*)-3-dipropylamino-2-fluoropropionamido)-9-(10*H*)-acridone (*R*,*R*)-**210** (115 mg, 0.20 mmol, 1.0 eq). The resulting bright orange suspension was stirred at rt until TLC analysis indicated consumption of the starting material. The solution was cooled to 0 °C and cold $Et_2O$ (10 mL) was added, resulting in formation of a precipitate. The precipitate was isolated by filtration and washed with further $Et_2O$ (2 × 10 mL) and dissolved in $CHCl_3$ (10 mL). The organic phase was washed with aqueous $NH_4OH$ (1 M, 10 mL) and brine (10 mL), dried over $Na_2SO_4$, filtered and the solvent removed *in vacuo* to yield 3,6-bis((2*R*)-3-*N*,*N*-dipropylamino-2-fluoropropionamido)-9-chloroacridine (*R*,*R*)-**211** as a red brown solid, which was used directly in the next step without further purification. *N*,*N*-dimethylaminoaniline monohydrochloride (700 mg, 4.05 mmol, 20 eq) was dissolved in saturated aqueous $Na_2CO_3$ and extracted with $Et_2O$ (3 × 20 mL). The organic fractions were combined, washed with brine, dried over $Na_2SO_4$, filtered and the solvent removed *in vacuo* to yield *N*,*N*-dimethylaminoaniline as a light brown oil. This oil was dissolved in $CHCl_3$ (20 mL) and added *via* cannula to

a refluxing solution of 3,6-bis((2*R*)-3-*N,N*-dipropylamino-2-fluoropropionamido)-9-chloroacridine in $CHCl_3$ (10 mL) over 30 min. This mixture was heated under reflux until TLC analysis indicated the consumption of the chloride, at which point the solvent was removed *in vacuo* to yield a purple oil. Cold $Et_2O$ (excess) was added, resulting in the precipitation of a red-brown solid. The solid was isolated by filtration and washed with further $Et_2O$ (excess). The residue was dissolved in $CHCl_3$ (20 mL) and washed with aqueous $NH_4OH$ (1 M, 10 mL) followed by brine (10 mL). The organic phase was dried over $Na_2SO_4$, filtered and the solvent removed *in vacuo* to yield a red solid, which was purified by silica gel column chromatography, eluting with $CHCl_3$ and $CH_3OH$ (95:5), to yield *3,6-bis((2R)-3-bispropylamino-2-fluoropropanamide)-9-(4-dimethylamino phenylamino) acridine* (*R*,*R*)-**212** (34.6 mg, 50.6 μmol, 25% over two steps) as a dark red solid: $\boldsymbol{R_f}$ 0.06 ($CHCl_3$:$CH_3OH$, 95:5); **mp** 190 ºC (dec.); **IR** $\nu_{max}$ (KBr disc, $cm^{-1}$) 3421, 2960, 1701 (C=O), 1611 (C=O), 1518, 1277; **$^1$H NMR** (500 MHz, $CD_3OD$) $\delta_H$ 8.46 (2H, d, *J* 1.5 Hz, Ar C*H*-4,5), 8.02 (2H, d, *J* 9.4 Hz, Ar C*H*-1,8), 7.33 (2H, dd, *J* 9.4, 1.5 Hz, Ar C*H*-2,7), 7.17 (2H, d, *J* 8.8 Hz, Ar C*H*-14,14′), 6.85 (2H, d, *J* 8.8 Hz, Ar C*H*-13,13′), 5.18 (2H, dt, *J* 49.5, 4.8 Hz, 2 × C*H*F), 3.08 (4H, dd, *J* 26.0, 4.8 Hz, 2 × C$H_2$CHF), 2.97 (6H, s, 2 × NC$H_3$), 2.60-2.49 (8H, m, 4 × $CH_2$C$H_2$N), 1.54-1.46 (8H, m, 4 × $CH_3$C$H_2$$CH_2$), 0.88 (12H, t, *J* 7.3 Hz, 4 × C$H_3$$CH_2$); **$^{13}$C NMR** (126 MHz, $CD_3OD$) $\delta_C$ 170.7 (d, *J* 20.8 Hz, *C*ONH), 154.5 (Ar *C*-9), 151.3 (Ar *C*-15), 144.2 (2 × Ar *C*-4a,4b), 144.0 (2 × Ar *C*-8a,9a), 131.2 (Ar *C*-12), 127.8 (2 × Ar *C*H-1,8), 126.5 (2 × Ar *C*H-14,14′), 118.0 (2 × Ar *C*H-2,7), 114.5 (2 × Ar *C*H-13,13′), 112.0 (2 × Ar *C*-3,6), 108.7 (2 × Ar *C*H-4,5), 92.3 (d, *J* 188.4 Hz, 2 × *C*HF), 58.0 (4 × $CH_2$*C*$H_2$N), 56.9 (d, *J* 19.9 Hz, 2 × *C*$H_2$CHF), 40.8 (2 × N*C*$H_3$), 21.3 (4 × $CH_3$*C*$H_2$$CH_2$), 12.1 (4 × *C*$H_3$$CH_2$); **$^{19}$F NMR** (470 MHz, $CD_3OD$) $\delta_F$ -191.2 (2F, dt, *J* 49.5, 26.0 Hz,

2 × CH*F*); **HRMS** *m/z* ($ES^+$) calcd. for $C_{39}H_{54}F_2N_7O_2$ $[M+H]^+$ requires 690.4302, found 690.4309; ***m/z*** ($ES^+$) 690 ($[M+H]^+$, 100%).

### 7.3.35 -

**3,6-Bis((2*S*)-3-bispropylamino-2-fluoropropanamide)-9-(4-dimethylamino phenylamino)acridine** (*S*,*S*)-**212**

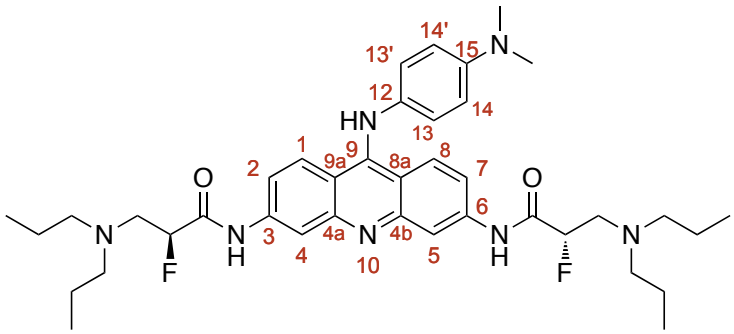


Following the procedure set out for 3,6-bis((2*R*)-3-bispropylamino-2-fluoropropanamide)-9-(4-dimethylaminophenylamino)acridine (*R*,*R*)-**212** , starting from 3,6-bis((2*S*)-3-*N*,*N*-dipropylamino-2-fluoropropionamido)-9-(10*H*)-acridone (*S*,*S*)-**210** (118 mg, 0.209 mmol), the reaction yielded *3,6-bis((2S)-3-bispropylamino-2-fluoropropanamide)-9-(4-dimethylaminophenylamino) acridine* (*S*,*S*)-**212** (29.7 mg, 44 µmol, 21% over two steps) as a dark red solid: ***R*$_f$** 0.06 ($CHCl_3$:$CH_3OH$, 95:5); **mp** 190 ºC (dec.); **IR** $\nu_{max}$ (KBr disc, $cm^{-1}$) 3420, 2959, 1701 (C=O), 1610 (C=O), 1520, 1276; **$^1$H NMR** (400 MHz, $CD_3OD$) $\delta_H$ 8.33 (2H, d, *J* 2.1 Hz, Ar *H*-4,5), 7.92 (2H, d, *J* 9.4 Hz, Ar *H*-1,8), 7.27 (2H, dd, *J* 9.4, 2.1 Hz, Ar *H*-2,7), 7.11 (2H, d, *J* 9.0 Hz, Ar *H*-14,14′), 6.77 (2H, d, *J* 9.0 Hz, Ar *H*-13,13′), 5.16 (2H, dt, *J* 49.4, 4.9 Hz, 2 × C*H*F), 3.09-3.02 (4H, m, 2 × C$H_2$CHF), 2.97 (6H, s, 2 × NC$H_3$), 2.58-2.46 (8H, m, 4 × $CH_2CH_2$N), 1.54-1.44 (8H, m, 4 × $CH_3CH_2CH_2$), 0.87 (12H, t, *J* 7.4 Hz,

4 × C*H*$_3$CH$_2$); **$^{13}$C NMR** (101 MHz, CD$_3$OD) $\delta_C$ 170.5 (d, *J* 20.1 Hz, 2 × *C*ONH), 154.1 (Ar *C*-9), 151.1 (Ar *C*-15), 144.0 (2 × Ar *C*-4a,4b), 143.9 (2 × Ar *C*-8a,9a), 131.1 (Ar *C*-12), 127.7 (2 × Ar *C*H-1,8), 126.4 (2 × Ar *C*H-14,14′), 117.9 (2 × Ar *C*H-2,7), 114.3 (2 × Ar *C*H-13,13′), 111.8 (2 × Ar *C*-3,6), 108.5 (2 × Ar *C*H-4,5), 92.1 (d, *J* 188.4 Hz, 2 × *C*HF), 57.9 (4 × CH$_2$*C*H$_2$N), 56.9 (d, *J* 19.9 Hz, 2 × *C*H$_2$CHF), 40.8 (2 × N*C*H$_3$), 21.2 (4 × CH$_3$*C*H$_2$CH$_2$), 12.1 (4 × *C*H$_3$CH$_2$); **$^{19}$F NMR** (376 MHz, CD$_3$OD) $\delta_F$ -191.1 (2F, dt, *J* 49.4, 26.2 Hz, 2 × CH*F*); **HRMS** *m/z* (ES$^+$) calcd. for $C_{39}H_{54}F_2N_7O_2$ $[M+H]^+$ requires 690.4302, found 690.4294; ***m/z*** (ES$^+$) 690 ($[M+H]^+$, 100%).

### 7.3.36 -

### 3,6-Bis(3-chloropropionamido)-9-(10*H*)-acridone[191] 174

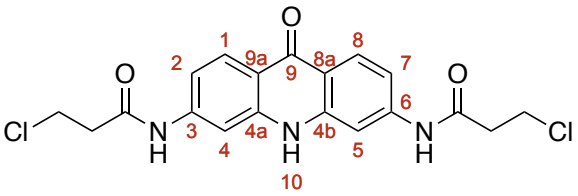


3,6-Diamino-9-(10*H*)-acridone **155** (500 mg, 2.2 mmol, 1.0 eq) was heated under reflux in neat 3-chloropropionyl chloride (5.0 mL) for 5 h. The solution was cooled to rt and ice-cold Et$_2$O (30 mL) was added, resulting in formation of a precipitate. The precipitate was isolated by filtration, washed with Et$_2$O (2 × 30 mL) and dried under vacuum to yield 3,6-bis(3-chloropropionamido)-9(10*H*)-acridone **174** (241 mg, 0.59 mmol, 27%) as an orange amorphous solid which was used without further purification: **mp** 295-297 ºC [Lit.[191] 300 ºC]; **$^1$H NMR** (300 MHz; *d*$_6$-DMSO) $\delta_H$ 11.48 (2H, s, 2 × CON*H*), 9.58 (1H, s, N*H*-10), 8.88 (2H, d, *J* 1.7 Hz, Ar *H*-4/5), 8.35 (2H, d,

*J* 9.1 Hz, Ar *H*-1/8), 7.87 (2H, dd, *J* 9.1, 1.7 Hz, Ar *H*-2/7), 3.96 (4H, t, *J* 6.2 Hz, 2 × C*H*$_2$CH$_2$Cl), 3.06 (4H, t, *J* 6.2 Hz, 2 × CH$_2$C*H*$_2$Cl); ***m/z*** (ES$^-$) 404 ([M[$^{35}$Cl]-H], 100%).

### 7.3.37 -

### 3,6-Bis(3-*N,N*-bisallylaminopropionamido)-9-(10*H*)-acridone 140i

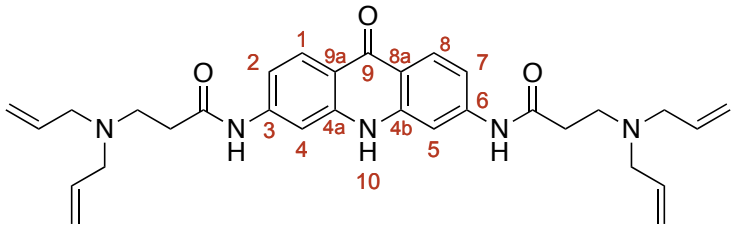


Diallylamine (320 $\mu$L, 2.6 mmol, 10 eq) was added dropwise to a refluxing solution of 3,6-bis(3-chloropropionamido)-9-(10*H*)-acridone **174** (100 mg, 0.25 mmol, 1.0 eq) and NaI (96 mg, 0.64 mmol, 2.5 eq) in EtOH (10 mL) and the resulting mixture was stirred for 3 h at reflux. The solution was cooled to rt and the solvent removed *in vacuo* and Et$_2$O (20 mL) was added, resulting in the formation of a precipitate. The precipitate was isolated by filtration, and washed with further Et$_2$O (2 × 10 mL) and dissolved in ethyl acetate (20 mL). The organic phase was washed with NH$_4$OH (1 M, 2 × 10 mL) and brine (10 mL), dried over Na$_2$SO$_4$, filtered and the solvent removed *in vacuo*. The material was purified by silica gel chromatography, eluting with CHCl$_3$, CH$_3$OH and triethylamine (90:9:1), to yield *3,6-bis(3-N,N-bisallylaminopropionamido)-9-(10H)-acridone* **140i** (62 mg, 0.12 mmol, 46%) as a yellow solid: **mp** 300 ºC dec.; **IR** $\nu_{max}$ (NaCl plate, cm$^{-1}$) 3417, 2928, 1600 (C=O), 1554, 1493, 1458; **$^1$H NMR** (500 MHz, CDCl$_3$) $\delta_H$ 11.17 (1H, br s, Ar*H*-10), 11.05 (2H, br s, 2 × CON*H*),

8.20 (2H, d, *J* 8.8 Hz, Ar*H*-1/8), 8.06 (2H, d, *J* 1.6 Hz, Ar*H*-4/5), 6.82 (2H, dd, *J* 8.8, 1.6 Hz, Ar*H*-2/7), 5.81-5.76 (4H, m, 4 × =C*H*), 5.19-5.15 (8H, m, 4 × C$H_2$=), 3.14 (8H, s, 4 × NC$H_2$-allyl), 2.77 (4H, t, *J* 6.3 Hz, 2 × C$H_2$C$H_2$), 2.50 (4H, t, *J* 6.3 Hz, 2 × C$H_2$N); **$^{13}$C NMR** (126 MHz, $CD_3OD$) $\delta_C$ 178.5 (Ar*C*-9), 173.5 (2 × *C*ONH), 144.6 (Ar*C*-8a/9a), 143.9 (Ar*C*-4a/4b), 135.6 (4 × =*C*H), 128.2 (Ar*C*H-1/8), 119.2 (4 × *C*$H_2$=), 118.1 (Ar*C*-3/6), 115.3 (Ar*C*H-2/7), 106.6 (Ar*C*H-4/5), 57.5 (4 × NC$H_2$-allyl), 50.0 (2 × *C*$H_2$C$H_2$), 35.1 (2 × C$H_2$*C*$H_2$N); **HRMS** *m/z* (ES$^+$ calcd. for $C_{31}H_{38}N_5O_3$ $[M+H]^+$ requires 528.2975, found 528.2963; ***m/z*** (ES$^+$) 528 ($[M+H]^+$, 100%), 550 ($[M+Na]^+$, 20%).

### 7.3.38 -

### 3,6-Bis(3-*N,N*-bispropylaminopropionamido)-9-(10*H*)-acridone 140j

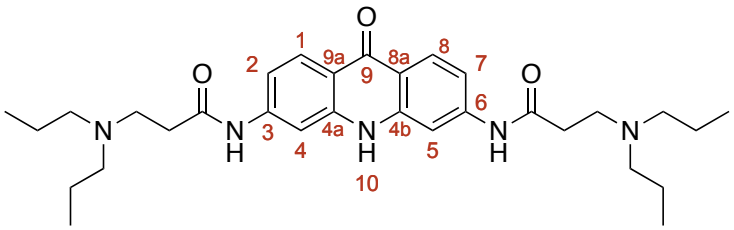


Following the proceedure set out for 3,6-bis(3-*N,N*-bisallylamino-propionamido)-9-(10*H*)-acridone **140i**, starting from diproplyamine (350 $\mu$L, 2.5 mmol, 10 eq) with 3,6-bis(3-chloropropionamido)-9-(10*H*)-acridone **174** (103 mg, 0.25 mmol, 1.0 eq) and NaI (95 mg, 0.63 mmol, 2.5 eq), the reacton yielded *3,6-bis(3-N,N-bispropylaminopropionamido)-9-(10H)-acridone* **140j** (35.8 mg, 0.067 mmol, 26%) as a yellow solid: **mp** 320 ºC (dec.); **IR** $\nu_{max}$ (NaCl plate, cm$^{-1}$) 3420, 2930, 1602 (C=O), 1545, 1459; **$^1$H NMR** (500 MHz, $CDCl_3$) $\delta_H$ 11.72 (1H, s, Ar*H*-10), 10.83 (2H, s, 2 × CONH), 8.49 (2H, d, *J* 1.6 Hz, Ar*H*-4/5), 8.35 (2H, d, *J* 8.7 Hz, Ar*H*-1/8), 6.73 (2H,

dd, *J* 8.7, 1.6 Hz, Ar*H*-2/7), 2.81 (4H, t, *J* 5.6 Hz, 2 × C$H_2$N), 2.68 (4H, t, *J* 5.6 Hz, 2 × C$H_2$CH$_2$), 2.56-2.53 (8H, m, 4 × NC$H_2$CH$_2$), 1.62-1.55 (8H, m, 4 × C$H_2$CH$_3$), 0.92 (12H, t, *J* 7.3 Hz, 4 × CH$_2$C$H_3$); **$^{13}$C NMR** (126 MHz, CDCl$_3$) $\delta_C$ 176.9 (Ar*C*-9), 172.3 (2 × CONH), 142.7 (Ar*C*-8a/9a), 142.5 (Ar*C*-4a/4b), 127.9 (Ar*C*H-1/8), 117.7 (Ar*C*-3/6), 113.6 (Ar*C*H-2/7), 106.2 (Ar*C*H-4/5), 55.3 (4 × NCH$_2$), 50.3 (2 × *C*H$_2$CH$_2$), 33.5 (2 × CH$_2$*C*H$_2$N) , 19.9 (4 × *C*H$_2$CH$_3$), 12.1 (4 × CH$_2$*C*H$_3$); **HRMS** *m/z* (ES$^+$) calcd. for $C_{31}H_{45}N_5O_2$ [M+H]$^+$ requires 536.3601, found 536.3594; ***m/z*** (ES$^+$) 536 ([M+H]$^+$, 100%).

### 7.3.39 -

**3,6-Bis(3-*N*,*N*-diallylamino-propanamide)-9-(4-dimethylaminophenylamino) acridine 219**

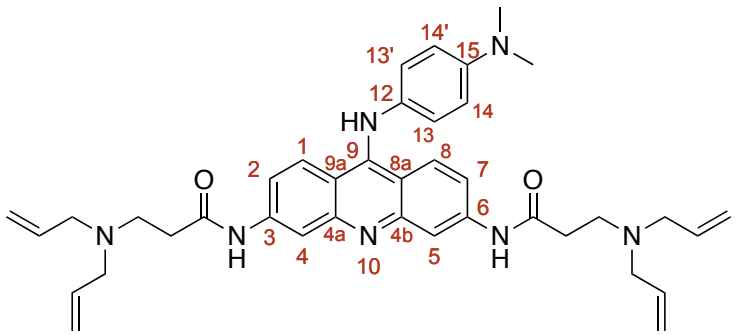


Phosphorous oxychloride (5.0 mL) was added to 3,6-bis(3-*N,N*-diallylamino-propionamido)-9-(10*H*)-acridone **140i** (30.0 mg, 0.20 mmol, 1.0 eq). The resulting suspension was stirred at rt until TLC analysis indicated consumption of the starting material. The solution was cooled to 0 °C and cold Et$_2$O (10 mL) was added, resulting in formation of a precipitate. The precipitate was isolated by filtration and washed with further Et$_2$O (2 × 10 mL) and dissolved in CHCl$_3$ (10 mL). The organic phase was

washed with aqueous $NH_4OH$ (1 M, 10 mL) and brine (10 mL), dried over $Na_2SO_4$, filtered and the solvent removed *in vacuo* to yield 3,6-bis(3-*N*,*N*-diallylamino-propionamido)-9-chloroacridine as a red brown solid, which was used directly in the next step without further purification. *N*,*N*-dimethylaminoaniline monohydrochloride (200 mg, 1.16 mmol, 20 eq) was dissolved in saturated aqueous $Na_2CO_3$ (10 mL) and extracted with $Et_2O$ (3 × 5 mL). The organic fractions were combined, washed with brine, dried over $Na_2SO_4$, filtered and the solvent removed *in vacuo* to yield *N*,*N*-dimethylaminoaniline as a light brown oil. This oil was dissolved in $CHCl_3$ (5 mL) and added *via* cannula to a refluxing solution of 3,6-bis(3-*N,N*-diallylamino-propionamido)-9-chloroacridine in $CHCl_3$ (5 mL) over 30 min. This mixture was heated under reflux until TLC analysis indicated the consumption of the chloride, at which point the solvent was removed *in vacuo* to yield a purple oil. Cold $Et_2O$ (20 mL) was added, resulting in the precipitation of a red-brown solid. The solid was isolated by filtration and washed with further $Et_2O$ (excess). The residue was dissolved in $CHCl_3$ (10 mL) and washed with aqueous $NH_4OH$ (1 M, 10 mL) followed by brine (10 mL). The organic phase was dried over $Na_2SO_4$, filtered and the solvent reduced *in vacuo* to yield a dark red solution. The material was prepared as its HCl salt by the addition of HCl (1 M, diethyl ether), which resulted in precipitation. This salt solution was loaded onto silica gel and purified by column chromatography, eluting with $CHCl_3$, $CH_3OH$ and triethylamine (100:0:0, 95:5:0, 90:5:5). The desired fractions were collected and washed with $NH_4OH$ (1.0 M, 2 × 10 mL), brine (10 mL), dried over $Na_2SO_4$, filtered and the solvent was removed *in vacuo* to yield *3,6-bis(3-N,N-diallylamino-propanamide)-9-(4-dimethylamino phenylamino) acridine* **219** (13.5 mg, 20.9 $\mu$mol, 37%) as a dark red solid: $\boldsymbol{R_f}$ 0.09 ($CHCl_3$:$CH_3OH$:$Et_3N$, 90:8:2); **mp** >320 ºC; **IR** $\nu_{max}$ (NaCl plate, $cm^{-1}$) 3419,

2930, 1603, 1548, 1488, 1398; **$^{1}$H NMR** (500 MHz, $CD_3OD$) $\delta_H$ 8.37 (2H, s, Ar*H*-4/5), 8.00 (2H, d, *J* 8.5, Ar*H*-1/8), 7.28 (2H, d, *J* 8.5, Ar*H*-2/7), 7.22 (2H, d, *J* 8.7, Ar*H*-14/14′), 6.85 (2H, d, *J* 8.7, Ar*H*-13/13′), 6.03-6.11 (4H, m, 4 × =C*H*), 5.59-5.69 (8H, m, 4 × C$H_2$=), 3.85 (8H, s, 4 × NC$H_2$-allyl), 3.50 (4H, t, *J* 6.7 Hz, 2 × C$H_2$CH$_2$), 3.07 (4H, t, *J* 6.7 Hz, 2 × CH$_2$C$H_2$N), 3.03 (6H, s, 2 × NC$H_3$); **$^{13}$C NMR** (75 MHz, $CDCl_3$) $\delta_C$ 171.9 (2 × *C*ONH), 153.9 (Ar *C*-9), 150.3 (Ar *C*-15), 145.7 (2 × Ar *C*-4a/4b), 143.4 (2 × Ar *C*-8a/9a), 134.0 (4 × =*C*H), 133.2 (Ar *C*-12), 127.3 (2 × Ar *C*H-1/8), 123.7 (2 × Ar *C*H-14/14′), 119.4 (4 × *C*H$_2$=), 116.4 (2 × Ar *C*H-2/7), 115.9 (2 × Ar *C*H-13/13′), 113.6 (2 × Ar *C*-3/6), 107.5 (2 × Ar *C*H-4/5), 48.8 (2 × *C*H$_2$CH$_2$), 46.2 (4 × NCH$_2$-allyl), 40.9 (2 × NCH$_3$), 33.7 (2 × CH$_2$*C*H$_2$N); **HRMS** *m/z* (ES$^+$) calcd. for $C_{39}H_{47}N_7O_2$ [M+H]$^+$ requires 646.3869, found 646.3870; ***m/z*** (ES$^+$) 646 ([M+H]$^+$, 100%).

### 7.3.40 -

**3,6-Bis(3-*N,N*-dipropylamino-propionamido)-9-(4-dimethylaminophenylamino) acridine 214**

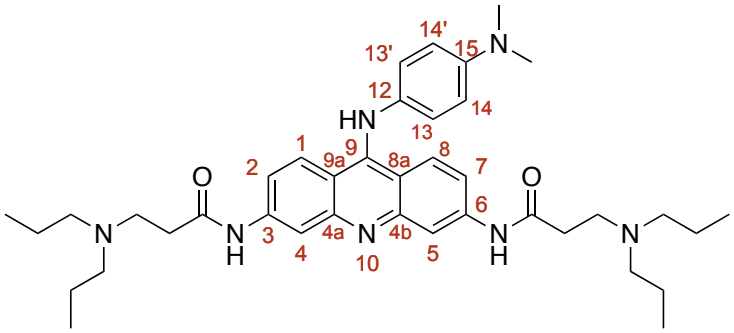


Following the proceedure set out for 3,6-bis(3-*N,N*-diallylamino-propanamide)-9-(4-dimethylaminophenylamino) acridine **219**, starting from 3,6-bis(3-*N,N*-bispropylamino-

propionamido)-9-(10*H*)-acridone **140j** (25.0 mg, 46.9 $\mu$mol, 1.0 eq) and *N*,*N*-dimethylaminoaniline monohydrochloride (160 mg, 0.93 mmol, 20 eq), the reacton yielded *3,6-bis(3-N,N-dipropylamino-propanamide)-9-(4-dimethylaminophenylamino) acridine* **214** (8.9 mg, 13.6 $\mu$mol, 29%) as a red solid: **IR** $\nu_{max}$ (NaCl plate, $cm^{-1}$) 3401, 2928, 1601, 1491, 1454, 1405; **$^{1}$H NMR** (500 MHz, $CD_3OD$) $\delta_H$ 8.47 (2H, d, *J* 1.8 Hz, Ar*H*-4/5), 8.05 (2H, d, *J* 9.3 Hz, Ar*H*-1/8), 7.23 (2H, dd, *J* 9.3, 1.8 Hz, Ar*H*-2/7), 7.22 (2H, d, *J* 9.0 Hz, Ar*H*-14/14′), 6.87 (2H, d, *J* 9.0 Hz, Ar*H*-13/13′), 3.07 (4H, t, *J* 6.8 Hz, C$H_2$$CH_2$N), 3.03 (6H, s, 2 × NC$H_3$), 2.73 (4H, t, *J* 6.8 Hz, 2 × $CH_2$C$H_2$N), 2.68-2.65 (8H, m, 4 × NC$H_2$$CH_2$), 1.66-1.58 (8H, m, 4 × C$H_2$$CH_3$), 0.95 (12H, t, *J* 7.4 Hz, 4 × $CH_2$C$H_3$); **$^{13}$C NMR** (126 MHz, $CDCl_3$) $\delta_C$ 173.6 (2 × *C*ONH), 154.9 (Ar *C*-9), 151.5 (Ar *C*-15), 145.4 (2 × Ar *C*-4a/4b), 143.8 (2 × Ar *C*-8a/9a), 130.5 (Ar *C*-12), 127.9 (2 × Ar *C*H-1/8), 126.9 (2 × Ar *C*H-14/14′), 117.6 (2 × Ar *C*H-2/7), 114.3 (2 × Ar *C*H-13/13′), 111.0 (2 × Ar *C*-3/6), 106.8 (2 × Ar *C*H-4/5), 56.7 (4 × N$CH_2$$CH_2$), 50.6 (2 × *C*$H_2$$CH_2$), 40.7 (2 × N$CH_3$), 34.5 (2 × $CH_2$*C*$H_2$N), 20.5 (4 × *C*$H_2$$CH_3$), 12.1 (4 × $CH_2$*C*$H_3$); **HRMS** *m*/*z* ($ES^+$) calcd. for $C_{39}H_{56}N_7O_2$ $[M+H]^+$ requires 654.4495, found 654.4513; ***m*/*z*** ($ES^+$) 654 ($[M+H]^+$, 100%).

### 7.3.41 -

### 3,6-Bis(3-amino-propionamido)-9-(4-dimethylaminophenylamino) acridine diformate 213

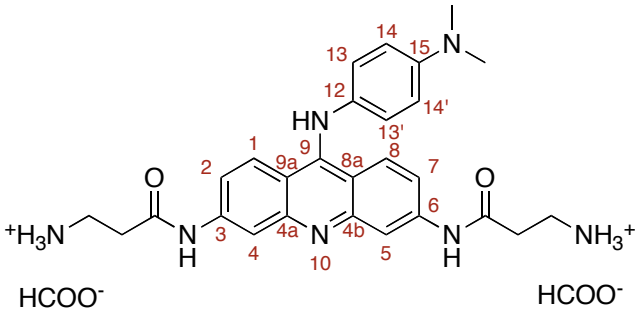


1,4-Di(phenylphosphino)butane (4.2 mg, 9.8 µmol, 20 mol%/allyl group) was added to a solution of tris(dibenzylideneacetone)dipalladium (4.5 mg, 4.9 µmol, 10 mol%/allyl group) in THF (1.0 mL) and stirred for 15 min until the solution turned yellow. The solution was added to a solution of 3,6-bis(3-*N,N*-diallylamino-propionamido)-9-(4-dimethylaminophenylamino) acridine **219** (8.1 mg, 13 µmol, 1.0 eq) and 2-mercaptosalicylic acid (9.8 mg, 64 µmol, 5.0 eq) in THF (1.0 mL). The resulting solution was heated under reflux for 3 h before being cooled to rt and diluted with distilled water (2.0 mL) and HCl (0.1 M, 250 µL), which caused precipitation of a solid. The precipitate was isolated by filtration and the residue was washed repeatedly with distilled water (3 × 1.0 mL). The water/THF filtrate was concentrated *in vacuo* to yield a yellow solid, which was purified by reverse phase silica gel chromatography eluting with water and $CH_3OH$ (90:10 with 1% formic acid) to yield *3,6-bis(3-amino-propionamido)-9-(4-dimethylaminophenylamino) acridine* **213** as its diformic acid salt (1.2 mg, 2.1 µmol, 17%) as a red powder: $R_f$ 0.12 ($H_2O$:$CH_3OH$:$HCO_2H$, 90:9:1); **$^1$H NMR** (500 MHz, $D_2O$) $\delta_H$ 8.14 (2H, s, Ar *H*-4,5), 7.91 (2H, d, *J* 9.2 Hz, Ar *H*-1,8), 7.23 (2H, d, *J* 8.9 Hz, Ar *H*-14/14'),

7.15 (2H, d, *J* 9.2 Hz, Ar *H*-2,7), 7.02 (2H, d, *J* 8.9 Hz, Ar *H*-13,13'), 3.36 (4H, t, *J* 6.5 Hz, 2 × C$H_2$), 2.94 (4H, t, *J* 6.5 Hz, 2 × C$H_2$), 2.92 (6H, s, 2 × NC$H_3$); **HRMS** *m*/*z* ($ES^+$) calcd. for $C_{27}H_{32}N_7O_2$ $[M+H]^+$ requires 486.2617, found 486.2621; ***m*/*z*** ($ES^+$) 486 ($[M+H]^+$, 100%).

## 7.4 - Experimental for Chapter 5

### *7.4.1 - General proceedures*

**General procedure (GP) 1** - The appropriate quantities of (–)-(2*S*)-3-[(*tert*-butyldimethylsilyl)oxy]-2-diallylamino-propanoic acid (*S*)-**230** (1.0 eq), diisopropylethylamine (4.0 eq) and amino ester (2.0 eq) in $CH_2Cl_2$ (1.0 mL $mmol^{-1}$) were cooled to 0 ºC and propylphosphonic anhydride (T3P) (50% *w*/*w* in ethyl acetate, 2.0 eq) was added dropwise. The solution was maintained at 0 ºC for a further 30 min before being warmed to rt and stirred until TLC analysis indicated consumption of the starting material. The reaction mixture was quenched by the addition of HCl (1 M, 10 mL) and the aqueous phase was extracted with ethyl acetate (2 × 10 mL). The combined organic phases were washed sequentially with HCl (1 M, 3 × 10 mL), saturated aqueous $Na_2CO_3$ (3 × 10 mL), brine (20 mL) and dried over $Na_2SO_4$. The solvent was removed *in vacuo* and the product purified by silica gel chromatography, eluting with mixtures of ethyl acetate and hexane.

**General Procedure (GP) 2 -** Tetrabutylammonium fluoride (1 M in THF, 4.0 eq) was added dropwise to the appropriate silyl protected dipeptide **232a-c** (1.0 eq) and acetic acid (5.0 eq) in THF (8.0 mL $mmol^{-1}$) and the resulting reaction mixture stirred at rt. The reaction was quenched by the addition of water (5 mL) followed by ethyl acetate (10 mL). The organic phases were washed successively with water (2 × 5 mL) and brine (10 mL), dried over $Na_2SO_4$ and the solvent removed *in vacuo*. The product was purified by silica gel column chromatography, eluting with mixtures of ethyl acetate and hexane.

**General procedure (GP) 3 -** Diethylaminosulfur trifluoride **32** (1.5 eq) was added dropwise to a solution of the appropriate amino alcohol dipeptide **224a-c** (1.0 eq) in THF (5.0 mL $mmol^{-1}$) at 0 ºC. The resulting solution was stirred at 0 ºC for 1 h before being quenched by the addition of $NaHCO_3$ (solid) and water until the solution was basic (pH >9) and effervescence subsided. The aqueous phase was extracted with diethyl ether (3 × 10 mL) and the combined organic phases were washed with brine, dried over $Na_2SO_4$, filtered and the solvent removed *in vacuo*. The product mixtures were purified by silica gel column chromatography, eluting with mixtures of ethyl acetate and hexane, separating the α- and *β*-fluorinated regioisomers where applicable.

### 7.4.2 -

**Methyl (–)-(2*S*)-3-[(*tert*-butyldimethylsilyl)oxy]-2-diallylamino-propanoate** (*S*)-**229**

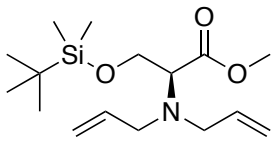

Triethylamine (16.0 mL, 115 mmol, 4.5 eq) was added dropwise over 30 min to a solution of methyl (2*S*)-2-diallylamino-3-hydroxy-propanoate (*S*)-**187** (5.00 g, 25.1 mmol, 1.0 eq) and *tert*-butyldimethylsilyl trifluoromethanesulfonate (9.00 mL, 39.1 mmol, 1.8 eq) in $CH_2Cl_2$ (230 mL) at 0 ºC. The mixture was brought to rt and stirred for 16 h, quenched by the addition of $CH_3OH$ (40 mL) followed by saturated aqueous $Na_2CO_3$ (100 mL). The organic phase was separated and the aqueous phase was extracted with $CH_2Cl_2$ (3 × 100 mL). The organic phases were combined, dried over $Na_2SO_4$ and the solvent removed *in vacuo*. The oil was purified by silica gel chromatography, eluting with hexane and ethyl acetate (95:5), to yield *methyl (–)-(2S)-3-[(tert-butyldimethylsilyl)oxy]-2-diallylamino-propanoate* (*S*)-**229** (6.52 g, 20.8 mmol, 83%) as a colourless oil: $\boldsymbol{R_f}$ 0.5 (hexane:ethyl acetate, 90:10); $[\boldsymbol{\alpha}]_{\mathbf{D}}^{\mathbf{20}}$ -18.1 (*c* 0.6, $CHCl_3$); **IR** $\nu_{max}$ (neat, $cm^{-1}$) 2951, 2929, 1735 (C=O), 1251 (Si–C), 1103, 918 (Si–C); **$^1$H NMR** (400 MHz, $CDCl_3$) $\delta_H$ 5.78 (2H, dddd, *J* 17.2, 10.1, 7.0, 5.4 Hz, 2 × =C*H*), 5.21-5.09 (4H, m, 2 × C$H_2$=), 3.93 (1H, dd, *J* 9.9, 7.0 Hz, OC$H_a$H$_b$), 3.82 (1H, dd, *J* 9.9, 5.6 Hz, OCH$_a$$H_b$), 3.61 (1H, dd, *J* 7.0, 5.6 Hz, C*H*N), 3.38-3.32 (4H, m, 2 × NC$H_2$), 3.15 (3H, OC$H_3$), 0.86 (9H, s, (C$H_3$)$_3$), 0.03 (3H, s, SiC$H_3$), 0.03 (3H, s, SiC$H_3$); **$^{13}$C NMR** (101 MHz, $CDCl_3$) $\delta_C$ 172.4 (*C*$O_2$CH$_3$), 136.7 (2 × =*C*H), 117.2 (2 × *C*$H_2$=), 64.2 (*C*HN), 62.9 (*C*$H_2$), 54.6 (2 × NC$H_2$-allyl), 51.2 (O*C*H$_3$), 25.9 (C(*C*H$_3$)$_3$), 18.3 (Si*C*), -5.4 (Si*C*H$_3$), -5.4 (Si*C*H$_3$); **HRMS** *m*/*z* (ES$^+$) calcd.

for $C_{16}H_{32}NO_3Si$ $[M+H]^+$ requires 314.2151, found 314.2156; ***m/z*** ($ES^+$) 314 ($[M+H]^+$, 100%). Enantiomeric excess determined by chiral HPLC (Chiralcel OD-H, 5% $^i$PrOH in hexane, 0.25 mL/min, $t_{r\ maj}$ = 7.08 min).

### 7.4.3 -

### (–)-(2*S*)-3-[(*tert*-butyldimethylsilyl)oxy]-2-diallylamino-propanoic acid (*S*)-230

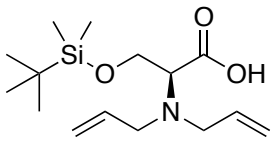


Lithium hydroxide monohydrate (3.37 g, 80.4 mmol, 4.0 eq) was added portionwise to a solution of methyl (–)-(2*S*)-3-[(*tert*-butyldimethylsilyl)oxy]-2-diallylamino-propanoate (*S*)-**229** (6.30 g, 20.1 mmol, 1.0 eq) in THF:$H_2O$:$CH_3OH$ (20:20:60, 150 mL) and was stirred for 24 h at rt. The reaction was quenched by neutralisation with HCl (1 M, 60 mL) and the aqueous phase extracted with $CH_2Cl_2$ (3 × 50 mL). The combined organics were dried with $Na_2SO_4$, filtered and the solvent removed *in vacuo* to yield *(–)-(2S)-3-[(tert-butyldimethylsilyl)oxy]-2-diallylamino-propanoic acid* (*S*)-**230** (5.41 g, 18.1 mmol, 90%) as a colourless gum, which was used without any further purification: $[\boldsymbol{\alpha}]_{\boldsymbol{D}}^{\boldsymbol{20}}$ -3.1 (*c* 1.7, $CH_3OH$); **IR** $\nu_{max}$ (neat, $cm^{-1}$) 2927, 2856, 1635 (C=O), 1417, 1257 (Si–C), 1087, 918 (Si–C); **$^1$H NMR** (300 MHz, $CD_3OD$) $\delta_H$ 5.90 (2H, dddd, *J* 17.0, 10.3, 6.6, 6.6 Hz, 2 × =C*H*), 5.27-5.12 (4H, m, 2 × C$H_2$=), 4.01 (1H, dd, *J* 10.7, 5.2 Hz, OC$H_a$H$_b$), 3.92 (1H, dd, *J* 10.7, 6.8 Hz, OCH$_a$$H_b$), 3.47 (1H, dd, *J* 6.8, 5.2 Hz, C*H*N), 3.40 (4H, m, NC$H_2$-allyl), 0.91 (9H, s, C(C$H_3$)$_3$), 0.08 (3H, s, SiC$H_3$), 0.08 (3H, s SiC$H_3$); **$^{13}$C NMR** (75 MHz, $CD_3OD$) $\delta_C$ 178.3 (*C*$O_2$H), 135.0 (2 × =*C*H), 118.5 (2 × *C*$H_2$=), 68.5 (*C*HN), 64.4 (O*C*$H_2$), 55.5 (2 × N*C*$H_2$-allyl), 26.5 (C(*C*$H_3$)$_3$),

19.2 (Si*C*), -5.1 (2 × Si*C*H$_3$); **HRMS** *m/z* (ES$^+$) calcd. for $C_{15}H_{30}NO_3Si$ $[M+H]^+$ requires 300.1995, found 300.2004; ***m/z*** (ES$^+$) 322 ($[M+Na]^+$, 100%), 300 ($[M+H]^+$, 5%).

### 7.4.4 -

**Methyl (+)-*N*-[*O*-(*tert*-butyldimethyl)silyl-*N′*,*N′*-diallyl-(*S*)-seryl]-(*S*)-phenylalaninate 232a**

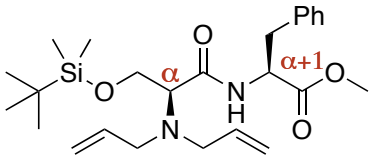


**Following GP1**: Starting with (–)-(2*S*)-3-[(*tert*-butyldimethylsilyl)oxy]-2-diallylamino-propanoic acid (*S*)-**230** (1.00 g, 3.34 mmol), L-phenylalanine methyl ester hydrochloride **231a** (1.44 g, 6.68 mmol), diisopropylethylamine (2.30 mL, 13.2 mmol) and T3P (50% *w/w* in ethyl acetate, 2.33 mL), the reaction yielded *methyl (+)-N-[O-(tert-butyldimethyl)silyl-N',N'-diallyl-(S)-seryl]-(S)-phenylalaninate* **232a** (1.25 g, 2.71 mmol, 81%) as a colourless oil: $R_f$ 0.35 (hexane:ethyl acetate, 90:10); $[\alpha]_D^{20}$ +15.0 (*c* 0.6, $CHCl_3$); **IR** $\nu_{max}$ (neat, cm$^{-1}$) 3361 (NH), 2953, 1747 (C=O), 1670 (C=O), 1496 (NH), 1093, 920 (Si–C); **$^1$H NMR** (400 MHz, $CDCl_3$) $\delta_H$ 7.90 (1H, d, *J* 7.9 Hz, CON*H*), 7.28-7.08 (5H, m, 5 × Ar-*H*), 5.61 (2H, dddd, *J* 17.0, 10.4, 6.4, 6.4 Hz, 2 × =C*H*), 5.14-5.04 (4H, m, 2 × C$H_2$=), 4.80 (1H, dt, *J* 7.9, 6.2 Hz, C$_{\alpha+1}H$), 4.14 (1H, dd, *J* 11.1, 4.0 Hz, OC$H_a$H$_b$), 3.90 (1H, dd, *J* 11.1, 8.3 Hz, OCH$_a$$H_b$), 3.71 (3H, s, OC$H_3$), 3.53 (1H, dd, *J* 8.3, 4.0 Hz, C$_\alpha H$), 3.21 (4H, m, 2 × NC$H_2$-allyl), 3.17-3.02 (2H, m, C$H_2$Ph), 0.86 (9H, s, C(C$H_3$)$_3$), 0.03 (3H, s, SiC$H_3$), 0.03 (3H, s, SiC$H_3$); **$^{13}$C NMR** (101 MHz, $CDCl_3$) $\delta_C$ 172.1 (*C*ONH), 171.9 (*C*O$_2$CH$_3$),

136.4 (Ar-*C*), 136.2 (2 × =*C*H), 129.3 (2 × Ar-*C*H), 128.6 (2 × Ar-*C*H), 127.1 (Ar-*C*H), 117.3 (2 × $CH_2$=), 63.9 ($C_\alpha$H), 61.3 (O$CH_2$), 53.9 (2 × N$CH_2$-allyl), 53.0 ($C_{\alpha+1}$H), 52.3 (O$CH_3$), 38.1 ($CH_2$Ph), 26.0 (C($CH_3$)$_3$), 18.2 (Si*C*), -5.5 (Si$CH_3$), -5.5 (Si$CH_3$); **HRMS** *m*/*z* (ES$^+$) calcd. for $C_{25}H_{40}N_2O_4SiNa$ [M+Na]$^+$ requires 483.2655, found 483.2643; ***m*/*z*** (ES$^+$) 483 ([M+Na]$^+$, 30%), 461 ([M+H]$^+$, 100%).

### 7.4.5 -

### Methyl (–)-*N*-[*O*-(*tert*-butyldimethyl)silyl-*N'*,*N'*-diallyl-(*S*)-seryl]-(*S*)-alaninate 232b

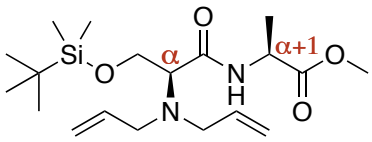


**Following GP1**: Starting with (–)-(2*S*)-3-[(*tert*-butyldimethylsilyl)oxy]-2-diallylamino-propanoic acid (*S*)-**230** (198 mg, 0.661 mmol), L-alanine methyl ester hydrochloride **231b** (185 mg, 1.32 mmol), diisopropylethylamine (460 μL, 2.64 mmol) and T3P (460 μL, 50% *w*/*w* in ethyl acetate), *methyl (–)-N-[O-(tert-butyldimethyl)silyl-N',N'-diallyl-(S)-seryl]-(S)-alaninate* **232b** (215 mg, 0.559 mmol, 85%) was isolated as a colourless oil: $R_f$ 0.2 (hexane:ethyl acetate 90:10); $[\alpha]_D^{20}$ -7.5 (*c* 0.4, $CHCl_3$); **$^1$H NMR** (400 MHz, $CDCl_3$) $\delta_H$ 7.94 (1H, d, *J* 7.6 Hz, CON*H*), 5.83 (2H, dddd, *J* 17.1, 10.3, 6.8, 5.6 Hz, 2 × =C*H*), 5.24-5.13 (4H, m, 2 × $CH_2$=), 4.54 (1H, dq, *J* 7.6, 7.2 Hz, $C_{\alpha+1}H$), 4.17 (1H, dd, *J* 11.1, 4.1 Hz, OC$H_aH_b$), 3.97 (1H, dd, *J* 11.1, 7.6 Hz, OC$H_aH_b$), 3.72 (3H, s, O$CH_3$), 3.53 (1H, dd, *J* 7.6, 4.1 Hz, $C_\alpha H$), 3.39-3.29 (4H, m, 2 × N$CH_2$), 1.37 (3H, d, *J* 7.2 Hz, CH$CH_3$), 0.89 (9H, s, C($CH_3$)$_3$), 0.06 (6H, s, 2 × Si$CH_3$); **$^{13}$C NMR** (101 MHz, $CDCl_3$) $\delta_C$ 173.5 (*C*ONH), 171.8 ($CO_2CH_3$), 136.2 (2 × =*C*H),

117.5 (2 × $CH_2$=), 64.1 ($C_\alpha H$), 61.3 ($OCH_2$), 54.0 (2 × $NCH_2$-allyl), 52.5 ($OCH_3$), 47.7 ($C_{\alpha+1}H$), 25.9 ($C(CH_3)_3$), 18.7 ($CHCH_3$), 18.2 (Si*C*), -5.4 ($SiCH_3$), -5.5 ($SiCH_3$); **HRMS** *m*/*z* ($ES^+$) calcd. for $C_{19}H_{36}N_2O_4NaSi$ $[M+Na]^+$ requires 407.2342, found 407.2339; ***m*/*z*** ($ES^+$) 407 ($[M+Na]^+$, 50%), 385 ($[M+H]^+$, 100%).

### 7.4.6 -

### Methyl (–)-*N*-[*O*-(*tert*-butyldimethyl)silyl-*N'*,*N'*-diallyl-(*S*)-seryl]-(*S*)-valinate 232c

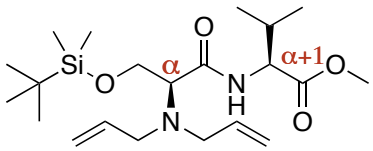


**Following GP1**: starting with (–)-(2*S*)-3-[(*tert*-butyldimethylsilyl)oxy]-2-diallylamino-propanoic acid (*S*)-**230** (205 mg, 0.685 mmol), L-valine methyl ester hydrochloride **231c** (330 mg, 1.37 mmol), diisopropylethylamine (480 μL, 2.76 mmol) and T3P (480 μL, 50% *w*/*w* in ethyl acetate), the reaction yielded *methyl (–)-N-[O-(tert-butyldimethyl)silyl-N',N'-diallyl-(S)-seryl]-(S)-valinate* **232c** (224 mg, 0.590 mmol, 79%) as a colourless oil: $R_f$ 0.3 (hexane:ethyl acetate, 90:10); $[\alpha]_D^{20}$ -37.0 (*c* 0.8, $CHCl_3$); **IR** $\nu_{max}$ (neat, $cm^{-1}$) 3365 (NH), 2954, 1745 (C=O), 1680 (C=O), 1496 (NH), 920 (Si–C); **$^1$H NMR** (400 MHz, $CDCl_3$) $\delta_H$ 8.01 (1H, d, *J* 9.3 Hz, CON*H*), 5.83 (2H, dddd, *J* 17.2, 10.2, 7.0, 4.8 Hz, 2 × =C*H*), 5.26-5.14 (4H, m, 2 × $CH_2$=), 4.49 (1H, dd, *J* 9.3, 4.7 Hz, $C_{\alpha+1}H$), 4.20 (1H, dd, *J* 11.1, 4.0 Hz, $OCH_aH_b$), 4.00 (1H, dd, *J* 11.1, 8.0 Hz, $OCH_aH_b$), 3.75 (3H, s, $OCH_3$), 3.59 (1H, dd, *J* 8.0, 4.0 Hz, $C_\alpha H$), 3.43-3.30 (4H, m, $NCH_2$-allyl), 2.21-2.13 (1H, m, $CH(CH_3)_2$), 0.92-0.86 (15H, m, $C(CH_3)_2$ and $C(CH_3)_3$), 0.06 (6H, s, 2 × $SiCH_3$); **$^{13}$C NMR** (101 MHz, $CDCl_3$) $\delta_C$ 172.4 (*C*ONH), 172.0 ($CO_2CH_3$), 136.2 (2 × =*C*H), 117.4 (2 × $CH_2$=), 64.0 ($C_\alpha H$), 61.3 ($OCH_2$),

56.9 ($C_{\alpha+1}$H), 54.0 (2 × N$CH_2$-allyl), 52.1 (O$CH_3$), 31.3 (*C*H), 26.0 (C($CH_3$)$_3$), 19.3 ($CH_3$), 18.2 (Si*C*), 17.8 ($CH_3$), -5.5 (Si$CH_3$), -5.5 (Si$CH_3$); **HRMS** *m*/*z* ($ES^+$) calcd. for $C_{21}H_{40}N_2O_4SiNa$ $[M+Na]^+$ requires 435.2655, found 435.2654; ***m*/*z*** ($ES^+$) 435 ($[M+Na]^+$, 5%), 413 ($[M+H]^+$, 100%).

### 7.4.7 -

### Cyclo-(*N*,*N*-bisallyl-(*S*)-seryl-(*S*)-phenylalanine) 234

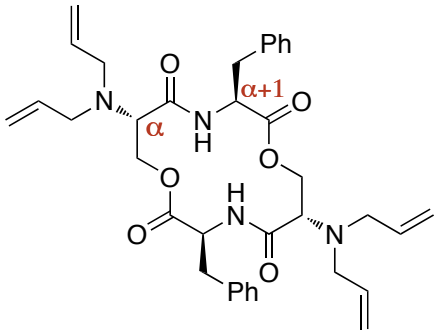


Tetrabutylammonium fluoride (870 $\mu$L, 1 M in THF, 4.0 eq) was added dropwise to methyl (+)-*N*-[*O*-(*tert*-butyldimethyl)silyl-*N*′,*N*′-diallyl-(*S*)-seryl]-(*S*)-phenylalaninate **232a** (100 mg, 0.217 mmol, 1.0 eq) in dry THF (1.5 mL) and was stirred at rt for 2 h. The reaction was quenched by the addition of water (5 mL) followed by ethyl acetate (10 mL). The organic phases were washed successively with water (2 × 5 mL) and brine (10 mL), dried over $Na_2SO_4$ and the solvent removed *in vacuo*. The product was purified by silica gel column chromatography, eluting with ethyl acetate and hexane (20:80), to yield *cyclo-(N,N-bisallyl-(S)-seryl-(S)-phenylalanine)* **234** (18.4 mg, 0.029 mmol, 27%) as a colourless solid: **mp** 170-172 ºC (ethyl acetate); $[\alpha]_D^{20}$ -83.9 (*c* 0.3, $CH_3OH$); **IR** $\nu_{max}$ (NaCl plate, $cm^{-1}$) 3359 (NH), 3303, 2928, 1716 (C=O), 1663 (C=O), 1551 (NH), 1261 (C–O–C); **$^1$H NMR** (400 MHz,

$CDCl_3$) $\delta_H$ 7.31-7.14 (10H, m, 10 × Ar-*H*), 6.65 (2H, d, *J* 7.5 Hz, 2 × N*H*), 5.57 (4H, dddd, *J* 17.0, 10.4, 6.6, 5.7 Hz, 4 × =C*H*), 5.12-5.06 (8H, m, 4 × C$H_2$=), 4.52 (2H, dd, *J* 11.1, 3.3 Hz, 2 × C$H_a$H$_b$CHN), 4.54-4.38 (2H, m, 2 × C$_{\alpha+1}$*H*), 4.40 (2H, dd, *J* 11.1, 6.2 Hz, 2 × CH$_a$*H*$_b$CHN), 3.39 (2H, dd, *J* 6.2, 3.3 Hz, 2 × C$_\alpha$*H*), 3.30 (2H, dd, *J* 14.3, 4.8 Hz, 2 × C$H_a$H$_b$Ph), 3.16 (2H, dd, *J* 14.3, 10.0 Hz, 2 × CH$_a$*H*$_b$Ph), 3.10-3.05 (4H, m, 4 × NC$H_a$H$_b$-allyl), 2.99-2.93 (4H, m, 4 × NCH$_a$*H*$_b$-allyl); **$^{13}$C NMR** (101 MHz, $CDCl_3$) $\delta_C$ 170.6 (2 × *C*O$_2$CH$_2$), 170.1 (2 × *C*ONH), 137.5 (2 × Ar *C*), 135.8 (4 × =*C*H), 129.3 (4 × Ar *C*H), 128.8 (4 × Ar *C*H), 127.0 (2 × Ar *C*H), 117.9 (4 × *C*H$_2$=), 61.4 (2 × *C*$_\alpha$H), 60.1 (2 × *C*H$_2$CHN), 53.9 (2 × *C*$_{\alpha+1}$H), 53.7 (4 × NC*H*$_2$-allyl), 35.7 (2 × *C*H$_2$Ph); **HRMS** *m/z* (ES$^+$) calcd. for $C_{36}H_{44}N_4O_6Na$ [M+Na]$^+$ requires 651.3153, found 651.3154; ***m/z*** (ES$^+$) 667 ([M+K]$^+$, 40%), 651 ([M+Na]$^+$, 100%).

### 7.4.8 -

**Methyl (+)-(*N*,*N*-bisallyl-(*S*)-seryl)-(*S*)-phenylalaninate 224a**

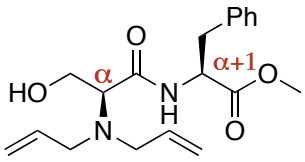


**Following GP2**: Starting with methyl (+)-*N*-[*O*-(*tert*-butyldimethyl)silyl-*N*′,*N*′-diallyl-(*S*)-seryl]-(*S*)-phenylalaninate **232a** (220 mg, 0.478 mmol), acetic acid (140 μL, 2.45 mmol) and TBAF (1.88 mL, 1 M in THF), the reaction yielded *methyl (+)-(N,N-bisallyl-(S)-seryl)-(S)-phenylalaninate* **224a** (121 mg, 0.349 mmol, 73%) as a colourless oil: $R_f$ 0.10 (hexane:ethyl acetate, 70:30); $[\alpha]_D^{20}$ +28.1 (*c* 1.15, $CHCl_3$); **IR** $\nu_{max}$ (neat, cm$^{-1}$) 3349 (OH), 2955, 1744 (C=O), 1659 (C=O), 1513, 1254, 1032;

**$^1$H NMR** (500 MHz, $CDCl_3$) $\delta_H$ 7.75 (1H, d, *J* 7.7 Hz, CON*H*), 7.31-7.09 (5H, m, 5 × Ar-*H*), 5.57 (2H, dddd, *J* 17.3, 10.0, 7.5, 4.5 Hz, 2 × =C*H*), 5.16-5.10 (4H, m, 2 × $CH_2$=), 4.85 (1H, ddd, *J* 7.7, 7.3, 5.7 Hz, $C_{\alpha+1}H$), 3.85 (1H, dd, *J* 11.2, 7.6 Hz, $OCH_aH_b$), 3.76 (3H, s, $OCH_3$), 3.75 (1H, dd, *J* 11.2, 4.1 Hz, $OCH_aH_b$), 3.41 (1H, dd, *J* 7.6, 4.1 Hz, $C_\alpha H$), 3.25 (1H, dd, *J* 14.0, 5.7 Hz, $CH_aH_bPh$), 3.15-3.11 (3H, m, 2 × $NCH_aH_b$-allyl and $CH_2OH$), 3.06 (1H, dd, *J* 14.0, 7.3 Hz, $CH_aH_bPh$), 2.96-2.92 (2H, m, 2 × $NCH_aH_b$-allyl); **$^{13}$C NMR** (126 MHz, $CDCl_3$) $\delta_C$ 174.3 (*C*ONH), 172.0 ($CO_2CH_3$), 135.9 (Ar-*C*), 135.5 (2 × =*C*H), 129.2 (2 × Ar-C*H*), 128.8 (2 × Ar-*C*H), 127.3 (Ar-*C*H), 118.1 (2 × $CH_2$=), 62.9 ($C_\alpha H$), 58.5 ($OCH_2$), 53.5 (2 × $NCH_2$-allyl), 52.9 ($C_{\alpha+1}H$), 52.6 ($OCH_3$), 38.0 ($CH_2Ph$); **HRMS** *m*/*z* ($ES^+$) calcd. for $C_{19}H_{26}N_2O_4Na$ $[M+Na]^+$ requires 369.1790, found 369.1782; ***m*/*z*** ($ES^+$) 369 ($[M+Na]^+$, 100%).

### 7.4.9 -

### Methyl (+)-(*N*,*N*-bisallyl-(*S*)-seryl)-(*S*)-alaninate 224b

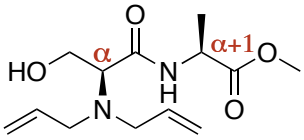


**Following GP2**: Starting with methyl (–)-*N*-[*O*-(*tert*-butyldimethyl)silyl-*N*′,*N*′-diallyl-(*S*)-seryl]-(*S*)-alaninate **232b** (195 mg, 0.507 mmol), acetic acid (150 $\mu$L, 2.62 mmol) and TBAF (2.10 mL, 1 M in THF), the reaction yielded *methyl (+)-(N,N-bisallyl-(S)-seryl)-(S)-alaninate* **224b** (121 mg, 0.448 mmol, 88%) as a colourless oil: $R_f$ 0.1 (hexane:ethyl acetate, 80:20); $[\alpha]_D^{20}$ +12.0 (*c* 0.7, $CHCl_3$);

**IR** $\nu_{max}$ (neat, $cm^{-1}$) 3356 (OH/NH), 3076, 2981, 1743 (C=O), 1653 (C=O), 1521 (NH), 1219, 1155; **$^1$H NMR** (400 MHz, $CDCl_3$) $\delta_H$ 7.83 (1H, d, *J* 7.0 Hz, CON*H*), 5.79 (2H, dddd, *J* 17.3, 10.1, 7.3, 4.7 Hz, 2 × =C*H*), 5.27-5.17 (4H, m, 2 × C$H_2$=), 4.57 (1H, dq, *J* 7.2, 7.0 Hz, $C_{\alpha+1}H$), 3.95 (1H, dd, *J* 11.2, 7.7 Hz, OC$H_a$H$_b$), 3.84-3.81 (1H, dd, *J* 11.2, 4.1 Hz, OCH$_a$$H_b$), 3.76 (3H, s, OC$H_3$), 3.48 (1H, dd, *J* 7.7, 4.1 Hz, C$_\alpha$*H*), 3.41 (1H, br s, O*H*), 3.33-3.28 (2H, m, 2 × NC$H_a$H$_b$-allyl), 3.11-3.06 (2H, m, 2 × NCH$_a$$H_b$-allyl), 1.42 (3H, d, *J* 7.2 Hz, C$H_3$); **$^{13}$C NMR** (101 MHz, $CDCl_3$) $\delta_C$ 174.1 (*C*ONH), 173.2 (*C*O$_2$CH$_3$), 135.4 (2 × =*C*H), 118.2 (2 × *C*H$_2$=), 62.8 (*C*$_\alpha$H), 58.4 (O*C*H$_2$), 53.7 (2 × N*C*H$_2$-allyl), 52.7 (O*C*H$_3$), 47.8 (*C*$_{\alpha+1}$H), 18.6 (CH*C*H$_3$); **HRMS** *m/z* (ES$^+$) calcd. for $C_{13}H_{22}N_2O_4Na$ $[M+Na]^+$ requires 293.1477, found 293.1471; ***m/z*** (ES$^+$) 293 ($[M+Na]^+$, 100%).

### 7.4.10 -

**Methyl (+)-(*N*,*N*-bisallyl-(*S*)-seryl)-(*S*)-valinate 224c**

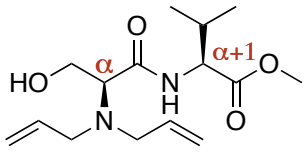


**Following GP2**: Starting with methyl (–)-*N*-[*O*-(*tert*-butyldimethyl)silyl-*N*′,*N*′-diallyl-(*S*)-seryl]-(*S*)-valinate **232c** (201 mg, 0.487 mmol), acetic acid (140 μL, 2.45 mmol) and TBAF (1.90 mL, 1 M in THF), the reaction yielded *methyl (+)-(N,N-bisallyl-(S)-seryl)-(S)-valinate* **224c** (108 mg, 0.363 mmol, 75%) as a colourless oil: $R_f$ 0.13 (hexane:ethyl acetate, 80:20); $[\alpha]_D^{20}$ +6.9 (*c* 0.5, $CHCl_3$); **IR** $\nu_{max}$ (neat, $cm^{-1}$) 3361 (OH), 2960, 2821, 1741 (C=O), 1660 (C=O), 1500 (NH), 1149; **$^1$H NMR** (300 MHz, $CDCl_3$) $\delta_H$ 7.87 (1H, d, *J* 9.0 Hz, CON*H*), 5.80 (2H, dddd,

*J* 17.3, 10.1, 7.3, 4.4 Hz, 2 × =C*H*), 5.30-5.18 (4H, m, 2 × C$H_2$=), 4.53 (1H, dd, *J* 9.0, 4.7 Hz, C$_{\alpha+1}$*H*), 3.99-3.83 (2H, m, C$H_2$OH), 3.75 (3H, s, OC$H_3$), 3.51 (1H, dd, *J* 7.5, 4.1 Hz, C$_\alpha$*H*), 3.43 (1H, br s, O*H*), 3.39-3.32 (2H, m, 2 × NC$H_a$H$_b$-allyl), 3.13-3.06 (2H, m, 2 × NCH$_a$*H*$_b$-allyl), 2.21 (1H, qqd, *J* 6.9, 6.9, 4.7 Hz, C*H*(CH$_3$)$_2$), 0.94 (3H, d, *J* 6.9 Hz, C$H_3$), 0.90 (3H, d, *J* 6.9 Hz, C$H_3$); **$^{13}$C NMR** (75.0 MHz, CDCl$_3$) $\delta_C$ 174.4 (*C*ONH), 172.2 (*C*O$_2$CH$_3$), 135.4 (2 × =*C*H), 118.1 (2 × *C*H$_2$=), 63.1 (*C*$_\alpha$H), 58.5 (*C*$_{\alpha+1}$H), 56.9 (O*C*H$_3$), 53.6 (2 × NC*H*$_2$-allyl), 52.3 (O*C*H$_2$), 31.3 (*C*H(CH$_3$)$_2$), 19.3 (CH*C*H$_3$), 17.9 (CH*C*H$_3$); **HRMS** *m/z* (ES$^+$) C$_{15}$H$_{26}$N$_2$O$_4$Na [M+Na]$^+$ requires 321.1790, found 321.1787; ***m/z*** (ES$^+$) 321 ([M+Na]$^+$, 100%).

### 7.4.11 -

**Methyl (+)-*N*-[(2*R*)-3-(diallylamino)-2-fluoropropanoyl]-(*S*)-phenylalanate 227a** & **Methyl (+)-*N*-[(2*R*)-2-(diallylamino)-3-fluoropropanoyl]-(*S*)-phenylalanate 228a**

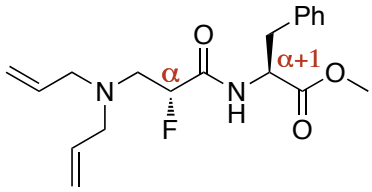


**227a**

**Following GP3**: Starting with methyl (+)-(*N,N*-bisallyl-(*S*)-seryl)-(*S*)-phenylalaninate **224a** (181 mg, 0.522 mmol) and diethylaminosulfur trifluoride **32** (90.0 $\mu$L, 0.682 mmol), to yield *methyl (+)-N-[(2R)-3-(diallylamino)-2-fluoropropanoyl]-(S)-phenylalanate* **227a** (78.1 mg, 0.224 mmol, 43%) as a colourless oil: ***R$_f$*** 0.24 (hexane:ethyl acetate, 7:3); **[α]$_D^{20}$** +69.8 (*c* 2.3, CHCl$_3$); **IR** $\nu_{max}$ (neat, cm$^{-1}$) 3429 (NH), 3070, 2924, 1747 (C=O), 1676 (C=O), 1525 (NH), 1278, 1217;

**$^1$H NMR** (500 MHz, $CDCl_3$) $\delta_H$ 7.22-7.03 (5H, m, 5 × Ar-*H*), 6.94 (1H, br d, *J* 4.7 Hz, CON*H*), 5.71 (2H, dddd, *J* 17.0, 10.3, 6.5, 6.5 Hz, 2 × =C*H*), 5.11-5.05 (4H, m, 2 × C$H_2$=), 4.90 (1H, ddd, *J* 49.9, 7.1, 2.8 Hz, C*H*F), 4.83-4.79 (1H, m, $C_{\alpha+1}$H), 3.67 (3H, s, OC$H_3$), 3.14-3.03 (6H, m, 2 × NC$H_2$-allyl and C$H_2$Ph), 2.94 (1H, ddd, *J* 30.1, 14.9, 2.8 Hz, C$H_a$H$_b$CHF), 2.84 (1H, ddd, *J* 23.9, 14.9, 7.1 Hz, CH$_a$$H_b$CHF); **$^{13}$C NMR** (125 MHz, $CDCl_3$) $\delta_C$ 171.5 (*C*$O_2$$CH_3$), 168.6 (d, *J* 20.0 Hz, *C*ONH), 135.6 (Ar-*C*), 135.1 (2 × =*C*H), 129.3 (2 × Ar-*C*H), 128.7 (2 × Ar-*C*H), 127.3 (Ar-*C*H), 118.1 (2 × *C*$H_2$=), 91.2 (d, *J* 187.8 Hz, *C*HF), 57.4 ($C_{\alpha+1}$H), 54.5 (d, *J* 19.3 Hz, *C*$H_2$CHF), 52.9 (2 × N*C*$H_2$-allyl), 52.5 (O*C*$H_3$), 38.0 (*C*$H_2$Ph); **$^{19}$F NMR** (470 MHz, $CDCl_3$) $\delta_F$ -190.7 (dddd, *J* 49.9, 30.1, 23.9, 4.0 Hz, CH*F*); **HRMS** *m*/*z* ($ES^+$) calcd. for $C_{19}H_{25}FN_2O_3Na$ $[M+Na]^+$ requires 371.1747, found 371.1741; ***m*/*z*** ($ES^+$) 371 ($[M+Na]^+$, 100%).

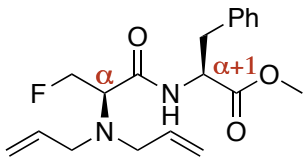


**228a**

Further elution of the reaction mixture from the above preparation furnished *methyl (+)-N-[(2R)-2-(diallylamino)-3-fluoropropanoyl]-(S)-phenylalanate* **228a** (68.8 mg, 0.197 mmol, 38%) as a colourless oil: ***R*$_f$** 0.15 (hexane:ethyl acetate, 70:30); $[\alpha]_D^{20}$ +21.9 (*c* 2.8, $CHCl_3$); **IR** $\nu_{max}$ (neat, $cm^{-1}$) 3360 (NH) , 2951, 1743 (C=O), 1674 (C=O), 1496 (NH), 1201, 1006; **$^1$H NMR** (500 MHz, $CDCl_3$) $\delta_H$ 7.75 (1H, d, *J* 7.7 Hz, CON*H*), 7.21-7.02 (5H, m, 5 × Ar-*H*), 5.53 (2H, dddd, *J* 17.4, 10.0, 7.5, 4.6 Hz, 2 × =C*H*), 5.10-5.03 (4H, m, 2 × C$H_2$=), 4.89-4.70 (3H, m, C$H_2$F and $C_{\alpha+1}$*H*), 3.68 (3H, s, OC$H_3$), 3.62 (1H, ddd, *J* 23.9, 6.7, 3.5 Hz, $CH_2FC_\alpha$*H*), 3.17-2.99 (6H, m,

2 × NC$H_2$-allyl and C$H_2$Ph); **$^{13}$C NMR** (125 MHz, $CDCl_3$) $\delta_C$ 172.0 ($CO_2CH_3$), 170.1 (d, *J* 10.3 Hz, *C*ONH), 135.9 (Ar-*C*), 135.4 (2 × =*C*H), 129.2 (2 × Ar-*C*H), 128.7 (2 × Ar-*C*H), 127.2 (Ar-*C*H), 118.1 (2 × $CH_2$=), 81.1 (d, *J* 171.1 Hz, *C*$H_2$F), 62.6 (d, *J* 18.9 Hz, $C_\alpha$H), 53.9 (2 × NC$H_2$-allyl), 53.0 ($C_{\alpha+1}$H), 52.5 (O*C*$H_3$), 37.9 (*C*$H_2$Ph); **$^{19}$F NMR** (470 MHz, $CDCl_3$) $\delta_F$ -227.1 (dt, *J* 47.2, 23.9 Hz, $CH_2F$); **HRMS** *m*/*z* ($ES^+$) calcd. for $C_{19}H_{25}FN_2O_3Na$ $[M+Na]^+$ requires 371.1747, found 371.1746; ***m*/*z*** ($ES^+$) 371 ($[M+Na]^+$, 100%).

### 7.4.12 -

**Methyl (+)-[(2*R*)-3-(diallylamino)-2-fluoropropanoyl]-(*S*)-alaninate 227b** &

**Methyl (–)-*N*-[(2*R*)-2-(diallylamino)-3-fluoropropanoyl]-(*S*)-alaninate 228b**

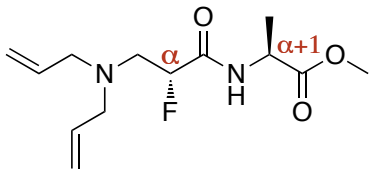


**227b**

**Following GP3:** Starting with methyl (+)-(*N*,*N*-diallyl-(*S*)-seryl)-(*S*)-alaninate **224b** (98.5 mg, 0.366 mmol) and diethylaminosulfur trifluoride **32** (65.9 mg, 54 $\mu$L, 0.409 mmol), the reaction yielded *methyl (+)-[(2R)-3-(diallylamino)-2-fluoropropanoyl]-(S)-alaninate* **227b** (18.9 mg, 69.4 $\mu$mol, 18%) as a colourless oil: $R_f$ 0.34 (hexane:ethyl acetate, 80:20); $[\alpha]_D^{20}$ +15.2 (*c* 1.8, $CHCl_3$); **$^1$H NMR** (400 MHz, $CDCl_3$) $\delta_H$ 7.03-7.02 (1H, br m, CON*H*), 5.83 (2H, dddd, *J* 17.0, 10.3, 6.6, 6.6 Hz, 2 × =C*H*), 5.21-5.14 (4H, m, 2 × $CH_2$=), 5.00 (1H, ddd, *J* 50.1, 7.2, 2.8 Hz, C*H*F), 4.63-4.59 (1H, dq, *J* 7.2, 6.7 Hz, $C_{\alpha+1}H$), 3.76 (3H, s, O$CH_3$), 3.26-3.14 (4H, m, 2 × NC$H_2$-allyl), 3.05 (1H, ddd, *J* 30.7, 14.9, 2.8 Hz, C$H_aH_b$CHF), 2.94 (1H, ddd, *J* 24.0, 14.9, 7.2 Hz, C$H_aH_b$CHF), 1.45 (3H, d, *J* 7.2 Hz, C$H_3$); **$^{13}$C NMR** (101 MHz,

$CDCl_3$) $\delta_C$ 173.0 ($CO_2CH_3$), 168.6 (d, *J* 19.1 Hz, *C*ONH), 135.2 (2 × =*C*H), 118.2 (2 × $CH_2$=), 91.4 (d, *J* 187.9 Hz, *C*HF), 57.6 (2 × N$CH_2$-allyl), 54.7 (d, *J* 19.1 Hz, $CH_2$), 52.7 ($C_{\alpha+1}$H), 47.8 (O$CH_3$), 18.5 ($CH_3$); **$^{19}$F NMR** (376 MHz, $CDCl_3$) δ -191.0 (dddd, *J* 50.1, 30.7, 24.0, 3.7 Hz, CH*F*); **HRMS** *m/z* ($ES^+$) calcd. for $C_{13}H_{22}FN_2O_3$ $[M+H]^+$ requires 273.1614, found 273.1621; ***m/z*** ($ES^+$) 273 ($[M+H]^+$, 100%).

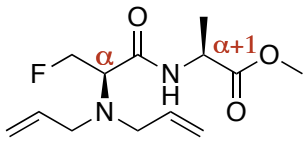


**228b**

Further elution of the reaction mixture from the above preparation furnished *methyl (–)-N-[(2R)-2-(diallylamino)-3-fluoropropanoyl]-(S)-alaninate* **228b** (36.3 mg, 0.133 mmol, 36%) as a colourless oil: ***R*$_f$** 0.20 (hexane:ethyl acetate, 80:20); $[\alpha]_D^{20}$ -1.7 (*c* 3.6, $CHCl_3$); **IR** $\nu_{max}$ (neat, $cm^{-1}$) 3365 (NH), 2983, 1745 (C=O), 1674 (C=O), 1500 (NH), 1450, 1157; **$^1$H NMR** (400 MHz, $CDCl_3$) $\delta_H$ 7.88 (1H, d, *J* 7.2 Hz, CONH), 5.82 (2H, dddd, *J* 17.3, 10.1, 7.3, 4.9 Hz, 2 × =C*H*), 5.28-5.18 (4H, m, 2 × C$H_2$=), 4.96 (1H, ddd, *J* 46.7, 10.3, 3.5 Hz, C$H_a$$H_b$F), 4.90 (1H, ddd, *J* 47.8, 10.3, 6.6 Hz, CH$_a$$H_b$F), 4.56 (1H, dq, *J* 7.2, 7.2 Hz, $C_{\alpha+1}H$), 3.75 (3H, s, OC$H_3$), 3.74 (1H, ddd, *J* 23.8, 6.6, 3.5 Hz, $CH_2FC_\alpha H$), 3.41-3.19 (4H, m, 2 × N$CH_2$-allyl) 1.39 (3H, d, *J* 7.2 Hz, C$H_3$); **$^{13}$C NMR** (101 MHz, $CDCl_3$) $\delta_C$ 173.3 ($CO_2CH_3$), 169.9 (d, *J* 16.1 Hz, *C*ONH), 135.3 (2 × =*C*H), 118.2 (2 × $CH_2$=), 81.1 (d, *J* 170.8 Hz, $CH_2$F), 62.5 (d, *J* 19.1 Hz, $C_\alpha$H), 54.0 (2 × N$CH_2$-allyl), 52.6 ($C_{\alpha+1}$H), 47.8 (O$CH_3$), 18.6 ($CH_3$); **$^{19}$F NMR** (376 MHz, $CDCl_3$) $\delta_F$ -228.9 (ddd, *J* 47.8, 46.7, 23.8 Hz, $CH_2F$); **HRMS** *m/z* ($ES^+$) calcd. for $C_{13}H_{22}FN_2O_3$ $[M+H]^+$ requires 273.1614, found 273.1612; ***m/z*** ($ES^+$) 273 ($[M+H]^+$, 100%).

### 7.4.13 -

**Methyl (+)-*N*-[(2*R*)-3-(diallylamino)-2-fluoropropanoyl]-(*S*)-valinate 227c & Methyl (+)-*N*-[(2*R*)-2-(diallylamino)-3-fluoropropanoyl]-(*S*)-valinate 228c**

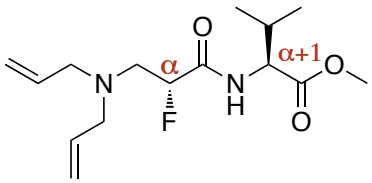


**227c**

**Following GP3**: Starting with methyl (+)-(*N,N*-bisallyl-(*S*)-seryl)-(*S*)-valinate **224c** (136 mg, 0.455 mmol) and diethylaminosulfur trifluoride (65.0 $\mu$L, 0.492 mmol), to yield *methyl (+)-N-[(2R)-3-(diallylamino)-2-fluoropropanoyl]-(S)-valinate* **227c** (12.7 mg, 42.3 $\mu$mol, 12%) as a colourless oil: $\boldsymbol{R_f}$ 0.50 (hexane:ethyl acetate, 80:20); $[\boldsymbol{\alpha}]_{\mathbf{D}}^{\mathbf{20}}$ +24.1 (*c* 1.3, $CHCl_3$); **$^1$H NMR** (400 MHz, $CDCl_3$) $\delta_H$ 6.97 (1H, br d, *J* 5.3 Hz, CON*H*), 5.83 (2H, dddd, *J* 17.0, 10.3, 6.6, 6.6 Hz, 2 × =C*H*), 5.21-5.14 (4H, m, 2 × C$H_2$=), 5.04 (1H, ddd, *J* 50.1, 7.0, 2.8 Hz, C*H*F), 4.56 (1H, dd, *J* 8.9, 5.3 Hz, $C_{\alpha+1}H$), 3.75 (3H, s, OC$H_3$), 3.26-3.14 (4H, m, 2 × NC$H_2$-allyl), 3.05 (1H, ddd, *J* 29.4, 14.9, 2.8 Hz, C$H_a$H$_b$CHF), 2.95 (1H, ddd, *J* 24.9, 14.9, 7.0 Hz, CH$_a$$H_b$CHF), 2.24-2.16 (1H, m, C*H*(CH$_3$)$_2$), 0.95 (3H, d, *J* 6.9 Hz, C$H_3$), 0.93 (3H, d, *J* 6.9 Hz, C$H_3$); **$^{13}$C NMR** (101 MHz, $CDCl_3$) $\delta_C$ 172.0 (*C*O$_2$CH$_3$), 169.0 (d, *J* 19.1 Hz, *C*ONH), 135.2 (2 × =*C*H), 118.2 (2 × *C*H$_2$=), 91.5 (d, *J* 187.9 Hz, *C*HF), 57.6 (2 × NCH$_2$-allyl), 56.9 ($C_{\alpha+1}$H), 54.6 (d, *J* 19.1 Hz, *C*H$_2$CHF), 52.4 (OCH$_3$), 31.5 (*C*H(CH$_3$)$_2$), 19.1 (*C*H$_3$), 17.9 (*C*H$_3$); **$^{19}$F NMR** (376 MHz, $CDCl_3$) $\delta_F$ -190.8 (dddd, *J* 50.1, 29.4, 24.9, 4.3 Hz, CH*F*); **HRMS** *m/z* (ES$^+$) calcd. for $C_{15}H_{26}FN_2O_3$ $[M+H]^+$ requires 301.1927, found 301.1925; ***m/z*** (ES$^+$) 301 ($[M+H]^+$, 100%).

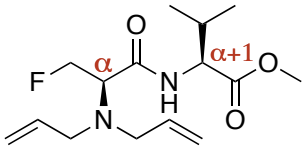


**228c**

Further elution provided *methyl (+)-N-[(2R)-2-(diallylamino)-3-fluoropropanoyl]-(S)-valinate* **228c** (50.8 mg, 0.169 mmol, 35%) as a colourless oil: $R_f$ 0.4 (hexane:ethyl acetate, 80:20); $[\alpha]_D^{20}$ +2.1 (*c* 5.0, $CHCl_3$); **IR** $\nu_{max}$ (neat, $cm^{-1}$) 3367 (NH), 2962, 1741 (C=O), 1680 (C=O), 1500 (NH), 1149,; **$^1$H NMR** (400 MHz, $CDCl_3$) $\delta_H$ 7.91 (1H, br d, *J* 9.2 Hz, CONH), 5.83 (2H, dddd, *J* 17.3, 10.2, 7.3, 4.6 Hz, 2 × =C*H*), 5.30-5.19 (4H, m, 2 × C$H_2$=), 4.96 (1H, ddd, *J* 46.8, 10.3, 3.5 Hz, C$H_a$H$_b$F), 4.92 (1H, ddd, *J* 47.8, 10.3, 6.3 Hz, CH$_a$$H_b$F), 4.53 (1H, dd, *J* 9.2, 4.6 Hz, C$_{α+1}$*H*), 3.74 (1H, ddd, *J* 24.8, 6.3, 3.5 Hz, CH$_2$FC$_α$*H*), 3.74 (3H, s, OC$H_3$), 3.45-3.39 (2H, m, 2 × NC$H_a$H$_b$-allyl), 3.25-3.20 (2H, m, 2 × NCH$_a$$H_b$-allyl), 2.25-2.15 (1H, m, C*H*(CH$_3$)$_2$), 0.92 (3H, d, *J* 6.9 Hz, CHC$H_3$), 0.87 (3H, d, *J* 6.9 Hz, CHC$H_3$); **$^{13}$C NMR** (101 MHz, $CDCl_3$) $\delta_C$ 172.3 (*C*O$_2$CH$_3$), 170.2 (d, *J* 10.1 Hz, *C*ONH), 135.3 (2 × =*C*H), 118.2 (2 × *C*H$_2$=), 81.1 (d, *J* 171.5 Hz, *C*H$_2$F), 62.8 (d, *J* 11.1 Hz, CH$_2$F*C*$_α$H), 56.9 (*C*$_{α+1}$H), 53.9 (2 × NCH$_2$-allyl), 52.3 (OCH$_3$), 31.3 (*C*H(CH$_3$)$_2$), 19.2 (*C*H$_3$), 17.7 (*C*H$_3$); **$^{19}$F NMR** (376 MHz, $CDCl_3$) $\delta_F$ -227.6 (ddd, *J* 47.8, 46.8, 24.8 Hz, CH$_2$*F*); **HRMS** *m*/*z* (ES$^+$) calcd. for $C_{15}H_{26}FN_2O_3$ $[M+H]^+$ requires 301.1927, found 301.1921; ***m*/*z*** (ES$^+$) 301 ($[M+H]^+$, 100%).

### 7.4.14 -

**(–)-(2*S*)-3-[(*tert*-Butyldimethylsilyl)oxy]-2-(diallylamino)-*N*-methyl-*N*-[(*S*)-1-phenylethyl]propanamide 240a**

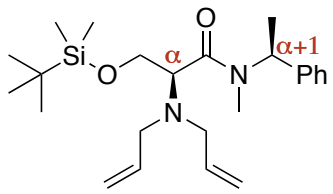


**Following GP1**: Starting with (2*S*)-3-[(*tert*-butyldimethylsilyl)oxy]-2-diallylamino-propanoic acid (*S*)-**230** (205 mg, 0.685 mmol), (*S*)-(–)-*N*,α-dimethylbenzylamine (188 mg, 200 μL, 1.39 mmol), diisopropylethylamine (450 μL, 2.58 mmol) and T3P (470 μL, 50% *w*/*w* ethyl acetate), the reaction yielded *(–)-(2S)-3-[(tert-butyldimethylsilyl)oxy]-2-(diallylamino)-N-methyl-N-[(S)-1-phenylethyl]propanamide* **240a** (231 mg, 0.561 mmol, 82%) as a colourless oil: $R_f$ 0.25 (hexane:ethyl acetate, 90:10); $[\alpha]_D^{20}$ -87.0 (*c* 1.3, $CHCl_3$); **IR** $\nu_{max}$ (neat, $cm^{-1}$) 2927, 2854, 1635 (C=O), 1404, 1095, 920 (Si–C); **$^1$H NMR** (400 MHz, $CDCl_3$) $\delta_H$ (major rotamer) 7.34-7.21 (5H, m, 5 × Ar-*H*), 6.07 (1H, q, *J* 7.1 Hz, $C_{\alpha+1}H$), 5.84-5.73 (2H, m, 2 × =C*H*), 5.18-5.03 (4H, m, 2 × $CH_2$=), 4.07 (1H, dd, *J* 9.5, 7.6 Hz, $OCH_aH_b$), 3.91 (1H, dd, *J* 9.5, 5.4 Hz, $OCH_aH_b$), 3.84 (1H, dd, *J* 7.6, 5.4 Hz, $C_\alpha H$), 3.32-3.28 (4H, m, 2 × $NCH_2$-allyl), 2.70 (3H, s, $NCH_3$), 1.44 (3H, d, *J* 7.1 Hz, $CHCH_3$), 0.85 (9H, s, $C(CH_3)_3$), 0.05 (3H, s, $SiCH_3$), 0.03 (3H, s, $SiCH_3$); **$^{13}$C NMR** (101 MHz, $CDCl_3$) $\delta_C$ 172.0 (*C*ONH), 140.8 (Ar-*C*), 137.2 (2 × =*C*H), 128.4 (2 × Ar-*C*H), 127.5 (2 × Ar-*C*H), 117.5 (Ar-*C*H), 116.9 (2 × $CH_2$=), 62.1 ($CH_2$), 60.9 ($C_\alpha$H), 54.0 (2 × $NCH_2$-allyl), 50.3 ($C_{\alpha+1}$H), 29.6 ($NCH_3$), 26.0 ($C(CH_3)_3$), 18.4 (Si*C*), 15.7 ($CHCH_3$), -5.3 ($SiCH_3$), -5.4 ($SiCH_3$);

**HRMS** *m*/*z* ($ES^+$) calcd. for $C_{24}H_{41}N_2O_2Si$ $[M+H]^+$ requires 417.2937, found 417.2941; ***m***/***z*** ($ES^+$) 417 ($[M+H]^+$, 100%).

### 7.4.15 -

### (–)-(2*S*)-3-[(*tert*-Butyldimethylsilyl)oxy]-2-(diallylamino)-*N*-[(*S*)-1-phenylethyl]propanamide 240b

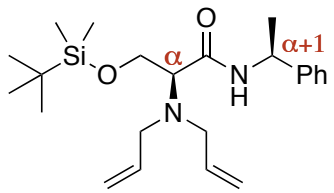


**Following GP1**: Starting with (2*S*)-3-[(*tert*-butyldimethylsilyl)oxy]-2-bisallylamino-propanoic acid (*S*)-**230** (104 mg, 0.347 mmol), (*S*)-(-)-α-methylbenzylamine (85.0 μL, 0.668 mmol), diisopropylethylamine (230 μL, 1.34 mmol) and T3P (390 μL, 50% w/w in ethyl acetate), the reaction yielded *(–)-N'-α-(S)-methylbenzyl-((2S)-N,N-bisallylamino-3-(tert-butyldimethylsilyloxy)) propanamide* **240b** (109 mg, 0.270 mmol, 78%) as a colourless oil: $R_f$ 0.5 (hexane:ethyl acetate, 80:20); $[\alpha]_D^{20}$ -50.3 (*c* 1.0, $CHCl_3$); **IR** $\nu_{max}$ (neat, $cm^{-1}$) 3365 (NH), 2953, 1747 (C=O), 1674 (C=O), 1498 (NH), 1259, 920 (Si–C); **$^1$H NMR** (400 MHz, $CDCl_3$) $\delta_H$ 7.73 (1H, d, *J* 8.0 Hz, CON*H*), 7.33-7.20 (5H, m, 5 × Ar-*H*), 5.81-5.71 (2H, m, 2 × =C*H*), 5.18-5.08 (4H, m, 2 × C$H_2$=), 5.02 (1H, dq, *J* 8.0, 6.9 Hz, $C_{\alpha+1}H$), 4.20 (1H, dd, *J* 11.1, 4.2 Hz, OC$H_aH_b$), 3.98 (1H, dd, *J* 11.1, 7.8 Hz, OC$H_aH_b$), 3.51 (1H, dd, *J* 7.8, 4.2 Hz, $C_\alpha H$), 3.36-3.27 (4H, m, 2 × NC$H_2$-allyl), 1.42 (3H, d, *J* 6.9 Hz, CHC$H_3$), 0.88 (9H, s, C(C$H_3$)$_3$), 0.05 (3H, s, SiC$H_3$), 0.04 (3H, s, SiC$H_3$); **$^{13}$C NMR** (101 MHz, $CDCl_3$) $\delta_C$ 171.2 (*C*ONH), 143.6 (Ar-*C*), 136.2 (2 × =*C*H), 128.7 (2 × Ar-*C*H),

127.3 (Ar-*C*H), 126.1 (2 × Ar-*C*H), 117.5 (2 × $CH_2$=), 64.1 ($C_{\alpha}$H), 61.5 (O$CH_2$), 54.0 (2 × N$CH_2$-allyl), 48.4 ($C_{\alpha+1}$H), 26.0 (C($CH_3$)$_3$), 22.5 ($CH_3$), 18.2 (Si*C*), -5.4 (Si$CH_3$), -5.5 (Si$CH_3$); **HRMS** *m/z* ($ES^+$) $C_{23}H_{39}N_2O_2Si$ $[M+H]^+$ 403.2781, found 403.2787; ***m/z*** ($ES^+$) 425 ($[M+Na]^+$, 30%), 403 ($[M+H]^+$, 100%).

### 7.4.16 - (–)-(2*S*)-2-(Diallylamino)-3-hydroxy-*N*-methyl-*N*-[(*S*)-1-phenylethyl]propanamide 241a

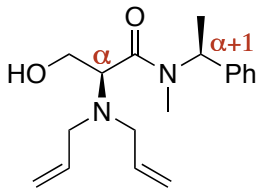


**Following GP2**: Starting with (–)-(2*S*)-3-[(*tert*-butyldimethylsilyl)oxy]-2-(diallylamino)-*N*-methyl-*N*-[(*S*)-1-phenylethyl]propanamide **240a** (102 mg, 0.245 mmol), acetic acid (60.0 $\mu$L, 1.00 mmol) and TBAF (1.00 mL, 1 M in THF), the reaction yielded *(–)-(2S)-2-(diallylamino)-3-hydroxy-N-methyl-N-[(S)-1-phenylethyl]propanamide* **241a** (58 mg, 0.192 mmol, 78%) as a colourless oil: $\boldsymbol{R_f}$ 0.15 (hexane:ethyl acetate, 80:20); $[\boldsymbol{\alpha}]_{\mathbf{D}}^{\mathbf{20}}$ -54.2 (*c* 0.8, $CHCl_3$); **IR** $\nu_{max}$ (neat, $cm^{-1}$) 3419 (OH), 2926, 1630 (C=O), 1404, 1282, 1122, 995; **$^1$H NMR** (500 MHz, $CDCl_3$) $\delta_H$ (major rotamer) 7.31-7.17 (5H, m, 5 × Ar-*H*), 5.98 (1H, q, *J* 7.1 Hz, $C_{\alpha+1}H$), 5.74-5.61 (2H, m, 2 × =C*H*), 5.15-5.11 (4H, m, 2 × $CH_2$=), 3.94 (1H, dd, *J* 10.9, 6.9 Hz, $C_{\alpha}H$), 3.76-3.70 (2H, m, $CH_2$OH), 3.41 (1H, br s, $CH_2OH$), 3.32 (2H, m, 2 × N$CH_aH_b$-allyl), 3.17 (2H, m, 2 × N$CH_aH_b$-allyl), 2.70 (3H, s, O$CH_3$), 1.41 (3H, d, *J* 7.1 Hz, $CH_3$); **$^{13}$C NMR** (126 MHz, $CDCl_3$) $\delta_C$ 172.5 (*C*ONH), 140.2 (Ar-*C*),

136.1 (2 × =*C*H), 128.8 (2 × Ar-*C*H), 127.5 (2 × Ar-*C*H), 118.4 (Ar-*C*H), 117.8 (2 × *C*$H_2$=), 60.8 ($C_\alpha$H), 58.0 (O*C*$H_2$), 53.8 (2 × N*C*$H_2$-allyl), 50.7 ($C_{\alpha+1}$H), 29.7 (N*C*$H_3$), 15.7 (*C*$H_3$); **HRMS** *m*/*z* ($ES^+$) calcd. for $C_{18}H_{26}N_2O_2Na$ $[M+Na]^+$ requires 325.1892, found 325.1885; ***m*/*z*** ($ES^+$) 325 ($[M+Na]^+$, 100%).

### 7.4.17 -

### (–)-(2*S*)-2-(Diallylamino)-3-hydroxy-*N*-[(*S*)-1-phenylethyl]propanamide 241b

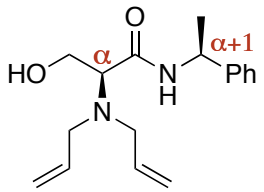


**Following GP2**: Starting with (–)-(2*S*)-3-[(*tert*-butyldimethylsilyl)oxy]-2-(diallylamino)-*N*-[(*S*)-1-phenylethyl]propanamide **240b** (93 mg, 0.231 mmol), acetic acid (66 $\mu$L, 1.16 mmol) and TBAF (900 $\mu$L, 1 M in THF), the reaction yielded *(–)-(2S)-2-(diallylamino)-3-hydroxy-N-[(S)-1-phenylethyl]propanamide* **241b** (51.0 mg, 0.180 mmol, 77%) as a colourless oil: $R_f$ 0.11 (hexane:ethyl acetate, 80:20); $[\alpha]_D^{20}$ -25.2 (*c* 0.7, $CHCl_3$); **IR** $\nu_{max}$ (neat, $cm^{-1}$) 3325 (OH/NH), 3064, 2926, 1647 (C=O), 1521 (NH), 1494, 1280, 1128, 993; **$^1$H NMR** (300 MHz, $CDCl_3$) $\delta_H$ (major rotamer) 7.63 (1H, d, *J* 7.8 Hz, CON*H*), 7.35-7.22 (5H, m, 5 × Ar-*H*), 5.74 (2H, dddd, *J* 17.3, 10.1, 7.3, 4.6 Hz, 2 × =C*H*), 5.23-5.12 (4H, m, 2 × C$H_2$=), 5.06 (1H, dq, *J* 7.8, 6.9 Hz, $C_{\alpha+1}H$), 3.94 (1H, dd, *J* 11.1, 7.9 Hz, OC$H_aH_b$), 3.79 (1H, dd, *J* 11.1, 3.9 Hz, OC$H_aH_b$), 3.58 (1H, br s, O*H*), 3.42 (1H, dd, *J* 7.9, 3.9 Hz, $C_\alpha H$), 3.34-3.26 (2H, m, 2 × NC$H_aH_b$-allyl), 3.08-3.01 (2H, m, 2 × NC$H_aH_b$-allyl), 1.45 (3H, d, *J* 6.9 Hz, C$H_3$); **$^{13}$C NMR** (75 MHz, $CDCl_3$) $\delta_C$ 173.6 (*C*ONH), 143.1 (Ar-*C*),

135.4 (2 × =*C*H), 128.9 (2 × Ar-*C*H), 127.5 (Ar-*C*H), 126.0 (2 × Ar-*C*H), 118.1 (2 × $C$H$_2$=), 62.7 ($C_{\alpha}$H), 58.2 (O$C$H$_3$), 53.7 (2 × $C$H$_2$-allyl), 48.5 ($C_{\alpha+1}$H), 22.4 ($C$H$_3$); **HRMS** *m/z* (ES$^+$) calcd. for $C_{17}H_{24}N_2O_2Na$ [M+Na]$^+$ requires 311.1735, found 311.1739; ***m/z*** (ES$^+$) 311 ([M+Na]$^+$, 100%), 289 ([M+H]$^+$, 20%).

### 7.4.18 - (–)-(2*R*)-3-(Diallylamino)-2-fluoro-*N*-methyl-*N*-[(1*S*)-1-phenylethyl]propanamide 242a

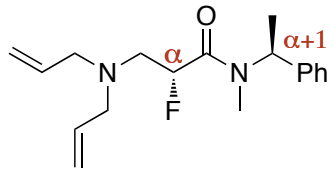


**Following GP3**: Starting with (–)-(2*S*)-2-(diallylamino)-3-hydroxy-*N*-methyl-*N*-[(*S*)-1-phenylethyl]propanamide **241a** (50.0 mg, 0.165 mmol) and diethylaminosulfur trifluoride **32** (25 $\mu$L, 0.189 mmol), to yield *(–)-(2R)-3-(diallylamino)-2-fluoro-N-methyl-N-[(1S)-1-phenylethyl]propanamide* **242a** (41.0 mg, 0.135 mmol, 81%) as a colourless oil: $R_f$ 0.09 (hexane:ethyl acetate, 90:10); $[\alpha]_D^{20}$ -125 (*c* 1.8, $CHCl_3$); **$^1$H NMR** (400 MHz, $CDCl_3$) $\delta_H$ (major rotamer) 7.32-7.18 (5H, m, 5 × Ar-*H*), 5.96 (1H, qq, *J* 7.1, 1.6 Hz, $C_{\alpha+1}H$), 5.83-5.70 (2H, m, 2 × =C*H*), 5.48-5.23 (1H, m, C*H*F), 5.16-5.03 (4H, m, 2 × C$H_2$=), 3.20-3.10 (4H, m, 2 × NC$H_2$-allyl), 3.04-2.90 (2H, m, C$H_2$CHF), 2.63 (3H, d, *J* 1.6 Hz, NC$H_3$), 1.43 (3H, d, *J* 7.1 Hz, C$H_3$); **$^{13}$C NMR** (101 MHz, $CDCl_3$) $\delta_C$ 168.2 (d, *J* 20.0 Hz, *C*ONH), 139.9 (Ar-*C*), 135.3 (2 × =*C*H), 128.6 (2 × Ar-*C*H), 127.5 (2 × Ar-*C*H), 126.8 (Ar-*C*H), 118.2 (2 × $C$H$_2$=), 89.0 (d, *J* 181.3 Hz, $C_{\alpha}$HF), 57.9 (2 × NCH$_2$-allyl), 54.4 (d,

*J* 21.9 Hz, *C*$H_2$CHF), 51.0 ($C_{\alpha+1}$H), 28.5 (N*C*$H_3$), 15.5 (*C*$H_3$); **$^{19}$F NMR** (376 MHz, $CDCl_3$) $\delta_F$ -184.5 (ddd, *J* 50.3, 28.9, 21.0 Hz, CH*F*-minor), -186.8 (ddd, *J* 49.3, 28.3, 20.6 Hz, CH*F*-major); **HRMS** *m*/*z* ($ES^+$) calcd. for $C_{18}H_{25}FN_2O_3Na$ $[M+Na]^+$ requires 327.1849, found 327.1844; ***m*/*z*** ($ES^+$) 327 ($[M+Na]^+$, 100%), 305 ($[M+Na]^+$, 30%).

### 7.4.19 -

**Methyl (+)-(2*S*)-*N*-allyl-phenylalanine**[232] **247**

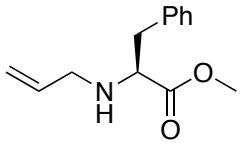


Allyl bromide (1.0 mL, 12 mmol, 2.5 eq) was added to a solution of L-phenylalanine methyl ester hydrochloride **231a** (1.00 mg, 4.6 mmol, 1.0 eq) and diisopropylethylamine (2.80 mL, 16 mmol, 3.5 eq) in DMF (15 mL) at 0 ºC. The solution was slowly warmed to rt and stirred for 48 h and quenched by the addition of water (10 mL) and the organics extracted with ether (3 × 20 mL). The organics were combined, washed with brine (20 mL), dried over $Na_2SO_4$, filtered and the solvent remove *in vacuo*. The product was purified by silica gel chromatography eluting with ethyl acetate, hexane and triethylamine (8:2 with 5% triethylamine), to yield methyl (2*S*)-*N*-allyl-phenylalaninate **247** (385 mg, 1.76 mmol, 38%) as a colourless oil: $[\boldsymbol{\alpha}]_{\mathbf{D}}^{\mathbf{20}}$ +23.2 (*c* 1.0, $CH_3OH$) [Lit.[233] $[\boldsymbol{\alpha}]_{\mathbf{D}}^{\mathbf{20}}$ +23 (*c* 1.0, $CH_3OH$)]; **$^1$H NMR** (300 MHz, $CDCl_3$) $\delta_H$ 7.32-7.09 (5H, m, 5 × Ar-*H*), 5.80 (1H, dddd, *J* 17.2, 10.2, 6.0, 6.0 Hz, =C*H*), 5.15-5.04 (2H, m, C$H_2$=), 3.64 (3H, s, OC$H_3$), 3.56 (1H, t, *J* 6.9 Hz, $CH_2$C*H*N), 3.26 (1H, dddd, *J* 13.9, 6.0, 1.5, 1.5 Hz, NC$H_a$$H_b$-allyl), 3.11 (1H, dddd, *J* 13.9, 6.0, 1.4,

1.4 Hz, $NCH_aH_b$-allyl), 2.96 (2H, d, *J* 6.9 Hz, $CH_2Ph$), 1.74 (1H, br s, N*H*); ***m/z*** ($ES^+$) 242 ($[M+Na]^+$, 60%), 220 ($[M+H]^+$, 100%).

### 7.4.20 -

**Methyl (–)-*N*-[*O*-(*tert*-butyldimethylsilyl)-*N′*,*N′*-diallyl-(*S*)-seryl]-*N*-allyl-(*S*)-phenylalaninate 248**

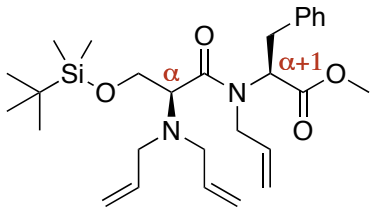


$^t$Bu P4 phosphazene **255** (1 M in hexanes, 1.00 mL, 1.00 mmol, 0.93 eq) was gradually added dropwise to a solution of methyl (+)-*N*-[*O*-(*tert*-butyldimethyl)silyl-*N′*,*N′*-diallyl-(*S*)-seryl]-(*S*)-phenylalaninate **232a** (500 mg, 1.09 mmol, 1.0 eq) and allyl bromide (500 $\mu$L, 5.79 mmol, 5.3 eq) in THF (15 mL) at -100 ºC. The resulting mixture was gradually warmed to -78 ºC and stirred at this temperature for 20 h before being diluted with ethyl acetate (10 mL) and washed with HCl (1 M, 2 × 10 mL). The organic fractions were dried over $Na_2SO_4$, filtered and the solvent removed *in vacuo*. The reaction mixture was purified by silica gel column chromatography, eluting with hexane and ethyl acetate (90:10), to yield *methyl (–)-N-[O-(tert-butyldimethylsilyl)-N′,N′-diallyl-(S)-seryl]-N-allyl-(S)-phenylalaninate* **248** (286 mg, 0.57 mmol, 53%) as a colourless oil: $R_f$ 0.10 (hexane:ethyl acetate, 90:10); $[\alpha]_D^{20}$ -102.3 (*c* 2.3, $CHCl_3$); **IR** $\nu_{max}$ (neat, $cm^{-1}$) 2951, 2856, 1747 (C=O), 1670 (C=O), 1259, 1093, 920 (Si–C); **$^1$H NMR** (300 MHz, $CDCl_3$) $\delta_H$ (major rotamer) 7.30-7.17 (5H, m, 5 × Ar-*H*), 5.79-5.67 (2H, m, 2 × =C*H*), 5.66-5.58 (1H, m, =C*H*), 5.17-5.06 (4H, m, 2 × $CH_2$=),

5.09-4.96 (2H, m, C$H_2$=), 4.19 (1H, dd, *J* 9.6, 5.4 Hz, $C_{\alpha+1}H$), 4.06-3.88 (4H, m, OC$H_2$ and N′C$H_2$-allyl), 3.71-3.67 (1H, m, $C_\alpha H$), 3.64 (3H, s, OC$H_3$), 3.40-3.08 (6H, m, 2 × NC$H_2$-allyl and C$H_2$Ph), 0.91 (9H, s, C(C$H_3$)$_3$), 0.10 (3H, s, SiC$H_3$), 0.08 (3H, s, SiC$H_3$); **$^{13}$C NMR** (101 MHz, $CDCl_3$) $\delta_C$ 171.4 (*C*ONH), 171.3 (*C*$O_2$CH$_3$), 138.5 (Ar-*C*), 136.7 (2 × =C*H*), 134.5 (=C*H*), 129.6 (2 × Ar-*C*H), 128.6 (2 × Ar-*C*H), 126.6 (Ar-*C*H), 118.0 (*C*$H_2$=), 117.5 (2 × C$H_2$=), 61.3 (*C*$_\alpha$H), 60.4 (*C*$_{\alpha+1}$H), 59.9 (O*C*H$_2$), 53.6 (2 × N*C*H$_2$-allyl), 52.0 (O*C*H$_3$), 51.3 (N′*C*H$_2$-allyl), 34.9 (*C*H$_2$Ph), 26.1 (C(*C*H$_3$)$_3$), 18.5 (Si*C*), -5.2 (Si*C*H$_3$), -5.3 (Si*C*H$_3$); **HRMS** *m/z* (ES$^+$) calcd. for $C_{28}H_{44}N_2O_4SiNa$ $[M+Na]^+$ requires 523.2968, found 523.2969; ***m/z*** (ES$^+$) 523 ($[M+Na]^+$, 100%), 501 ($[M+H]^+$, 80%).

### 7.4.21 -

**Methyl (–)-*N*-[*O*-(*tert*-butyldimethyl)silyl-*N′*,*N′*-diallyl-(*S*)-seryl]-(*R*,*S*)-a-allyl-phenylalaninate 254**

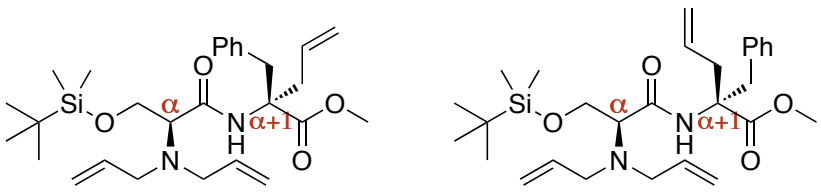


Potassium hexamethyldisilazide (1 M soln. in THF, 0.1 mL, 0.10 mmol, 0.90 eq) was added dropwise to a solution of methyl (+)-*N*-[*O*-(*tert*-butyldimethyl)silyl-*N′*,*N′*-diallyl-(*S*)-seryl]-(*S*)-phenylalaninate **232a** (50 mg, 0.11 mmol, 1.0 eq) and allyl bromide (50 μL, 0.58 mmol, 5.3 eq) in dry THF (2.5 mL) at -78 ºC. The resulting mixture was stirred at -78 ºC for 20 h before being diluted with ethyl acetate (5 mL) and washed with HCl (1 M, 2 × 5 mL). The organic fractions were dried over $Na_2SO_4$, filtered and the solvent removed *in vacuo*. The reaction mixture was purified by silica

gel column chromatography, eluting with hexane and ethyl acetate (90:10), to yield *methyl (–)-N-[O-(tert-butyldimethyl)silyl-N',N'-diallyl-(S)-seryl]-(R,S)-a-allyl-phenylalaninate* **254** (27.1 mg, 0.31 mmol, 53%) as a colourless oil: $[\alpha]_D^{20}$ -21.4 (1:1 mix of diastereoisomers, *c* 2.7, $CHCl_3$); **$^1$H NMR** (400 MHz, $CDCl_3$) $\delta_H$ (diastereoisomer A) 8.45 (1H, s, CON*H*), 7.25-6.98 (5H, m, 5 × Ar-*H*), 5.63-5.51 (3H, m, 3 × =C*H*), 5.10-4.99 (6H, m, 3 × C$H_2$=), 4.28 (1H, dd, *J* 11.0, 4.1 Hz, OC$H_a$H$_b$), 3.99 (1H, dd, *J* 11.0, 9.1 Hz, OCH$_a$$H_b$), 3.76 (3H, s, $OCH_3$), 3.73 (1H, d, *J* 13.4 Hz, C$H_a$H$_b$Ph), 3.57 (1H, dd, *J* 9.1, 4.1 Hz, C$_\alpha$*H*), 3.44-3.06 (6H, m, CH$_a$$H_b$Ph, 2 × NC$H_2$-allyl and NC$H_a$H$_b$-allyl), 2.66-2.61 (1H, m, NCH$_a$$H_b$-allyl), 0.92 (9H, s, C(C$H_3$)$_3$), 0.10 (6H, s, 2 × SiC$H_3$); $\delta_H$ (diastereomer B) 8.39 (1H, s, N*H*), 7.25-6.98 (5H, m, 5 × Ar-*H*), 5.63-5.51 (3H, m, 3 × =C*H*), 5.10-4.99 (6H, m, 3 × C$H_2$=), 4.28 (1H, dd, *J* 11.0, 4.1 Hz, OC$H_a$H$_b$), 3.93 (1H, dd, *J* 11.0, 9.1 Hz, OCH$_a$$H_b$), 3.79 (3H, s, $OCH_3$), 3.67 (1H, d, *J* 13.4 Hz, C$H_a$H$_b$Ph), 3.56 (1H, dd, *J* 9.1, 4.1 Hz, C$_\alpha$*H*), 3.44-3.06 (6H, m, CH$_a$$H_b$Ph, 2 × NC$H_2$-allyl and NC$H_a$H$_b$-allyl), 2.61-2.56 (1H, m, NCH$_a$$H_b$-allyl), 0.92 (9H, s, C(C$H_3$)$_3$), 0.10 (6H, s, 2 × SiC$H_3$); **$^{13}$C NMR** (75 MHz, $CDCl_3$) $\delta_C$ (diastereoisomer A) 173.3 (CON*H*), 171.5 (*C*O$_2$CH$_3$), 136.8 (2 × =*C*H), 136.6 (Ar-*C*), 132.6 (=*C*H), 129.8 (2 × Ar-*C*H), 128.3 (2 × Ar-*C*H), 127.0 (Ar-*C*H), 119.1 (*C*H$_2$=), 117.5 (2 × *C*H$_2$=), 65.9 (*C*$_{\alpha+1}$), 63.6 (*C*$_\alpha$H), 61.4 (O*C*H$_2$), 54.1 (2 × N*C*H$_2$-allyl), 52.6 (O*C*H$_3$), 40.6 (*C*H$_2$Ph), 39.6 (N*C*H$_2$-allyl), 26.1 (C(*C*H$_3$)$_3$), 18.3 (Si*C*), -5.4(8) (Si*C*H$_3$), -5.4(3) (Si*C*H$_3$); $\delta_C$ (diastereoisomer B) 173.1 (CON*H*), 171.4 (*C*O$_2$CH$_3$), 136.7 (2 × =*C*H), 136.5 (Ar-*C*), 132.4 (=*C*H), 129.7 (2 × Ar-*C*H), 128.3 (2 × Ar-*C*H), 126.9 (Ar-*C*H), 118.9 (*C*H$_2$=), 117.3 (2 × *C*H$_2$=), 65.5 (*C*$_{\alpha+1}$), 63.6 (*C*$_\alpha$H), 61.1 (O*C*H$_2$), 53.9 (2 × N*C*H$_2$-allyl), 52.5 (O*C*H$_3$), 40.5 (*C*H$_2$Ph), 39.5 (N*C*H$_2$-allyl), 26.1 (C(*C*H$_3$)$_3$), 18.3 (Si*C*), -5.4(8) (Si*C*H$_3$), -5.4(3) (Si*C*H$_3$);

**HRMS** *m*/*z* ($ES^+$) calcd. for $C_{28}H_{45}N_2O_4Si$ $[M+H]^+$ requires 501.3149, found 501.3153; ***m*/*z*** ($ES^+$) 523 ($[M+Na]^+$, 100%), 501 ($[M+H]^+$, 70%).

### 7.4.22 -

**Methyl (–)-*N*-[*O*-(*tert*-butyldimethyl)silyl-*N′*,*N′*-diallyl-(*S*)-seryl]-dibenzylglycinate 256, Methyl (–)-*N*-[*O*-(*tert*-butyldimethylsilyl)-*N′*,*N′*-diallyl-(*S*)-seryl]-*N*-benzyl-(*S*)-phenylalaninate 257 & Benzyl (–)-*N*-[*O*-(*tert*-butyldimethylsilyl)-*N′*,*N′*-diallyl-(*S*)-seryl]-(*S*)-phenylalaninate 258**

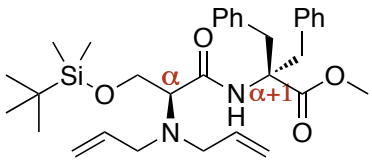


**256**

P4 phosphazene **255** (1 M soln. in hexanes, 0.10 mL, 1.00 mmol, 0.90 eq) was added dropwise to a solution of methyl (+)-*N*-[*O*-(*tert*-butyldimethyl)silyl-*N′*,*N′*-diallyl-(*S*)-seryl]-(*S*)-phenylalaninate **232a** (50.0 mg, 0.11 mmol, 1.0 eq) and benzyl bromide (50 $\mu$L, 0.58 mmol, 5.3 eq) in THF (2 mL) at -78 ºC. The resulting mixture was stirred at -78 ºC for 20 h before being diluted with ethyl acetate (5 mL) and washed with HCl (1 M, 2 × 5 mL). The organic fractions were dried over $Na_2SO_4$, filtered and the solvent removed *in vacuo*. The reaction mixture was purified by silica gel column chromatography, eluting with hexane and ethyl acetate (90:10), to yield *methyl (–)-N-[O-(tert-butyldimethyl)silyl-N',N'-diallyl-(S)-seryl]-dibenzylglycinate* **256** (12.0 mg, 0.22 $\mu$mol, 20%) as a colourless oil: $[\alpha]_D^{20}$ -19.8 (*c* 0.8, $CHCl_3$); **$^1$H NMR** (500 MHz, $CDCl_3$) $\delta_H$ 8.43 (1H, s, N*H*), 7.39-7.00 (10H, m, 10 × Ar-*H*), 5.31-5.23 (2H, m, 2 × =C*H*), 4.93-4.89 (4H, m, 2 × C$H_2$=), 4.35 (1H, dd, *J* 11.0, 4.0 Hz, OC$H_a$$H_b$),

3.96-3.93 (1H, dd, *J* 11.0, 9.5 Hz, OCH$_a$*H*$_b$), 3.94 (2H, AB, *J* 13.5 Hz, C*H*$_2$Ph), 3.79 (3H, s, OC*H*$_3$), 3.55 (1 H, dd, *J* 9.5, 4.0 Hz, C$_\alpha$*H*), 3.30 (1H, AB, *J* 13.5 Hz, C*H*$_a$H$_b$Ph), 3.19 (1H, AB, *J* 13.3, CH$_a$*H*$_b$Ph), 3.05-2.92 (4H, m, 2 × NC*H*$_2$-allyl), 0.9 (9H, s, C(C*H*$_3$)$_3$), 0.13 (3H, s, SiC*H*$_3$), 0.12 (3H, s, SiC*H*$_3$); **$^{13}$C NMR** (126 MHz, CDCl$_3$) δ$_C$ 172.9 (*C*ONH), 171.7 (*C*O$_2$CH$_3$), 136.7 (Ar-*C*), 136.7 (Ar-*C*), 136.5 (2 × =*C*H), 129.7 (2 × Ar-*C*H), 129.7 (2 × Ar-*C*H), 128.3 (2 × Ar-*C*H), 128.3 (2 × Ar-*C*H), 127.1 (Ar-*C*H), 126.9 (Ar-*C*H), 117.3 (2 × *C*H$_2$=), 67.4 (*C*$_{α+1}$), 63.4 (*C*$_α$H), 61.2 (*C*H$_2$), 53.8 (2 × NC*H*$_2$-allyl), 52.5 (OC*H*$_3$), 41.2 (*C*H$_2$Ph), 40.9 (*C*H$_2$Ph), 26.1 (C(*C*H$_3$)$_3$), 18.3 (Si*C*), -5.3 (Si*C*H$_3$), -5.4 (Si*C*H$_3$); **HRMS** *m/z* (ES$^+$) calcd. for C$_{32}$H$_{46}$N$_2$O$_4$SiNa [M+Na]$^+$ requires 573.3125, found 573.3117; ***m/z*** (ES$^+$) 573 ([M+Na]$^+$, 100%).

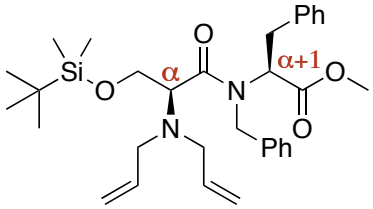


**257**

Further separation of the material enabled the isolation of *methyl (–)-N-[O-(tert-butyldimethylsilyl)-N',N'-diallyl-(S)-seryl]-N-benzyl-(S)-phenylalaninate* **257** (11.0 mg, 20 μmol, 18%) as a colourless oil: $[\alpha]_D^{20}$ -80.1 (*c* 0.7, CHCl$_3$); **$^1$H NMR** (500 MHz, CDCl$_3$) δ$_H$ 7.30-7.00 (10H, m, 10 × Ar-*H*), 5.71 (2H, dddd, *J* 17.2, 10.0, 7.4, 5.5 Hz, 2 × =C*H*), 5.20-5.03 (4H, m, 2 × C*H*$_2$=), 4.60 (1H, AB, *J* 15.6 Hz, N′C*H*$_a$H$_b$Ph), 4.13 (1H, dd, *J* 9.5, 7.5 Hz, OC*H*$_a$H$_b$), 4.06 (1H, dd, *J* 7.7, 6.5 Hz, C$_{α+1}$*H*), 4.01 (1H, AB, *J* 15.6 Hz, N′CH$_a$*H*$_b$Ph), 3.93 (1H, dd, *J* 9.5, 5.3 Hz, OC*H*$_a$H$_b$), 3.81 (1H, dd, *J* 7.5, 5.3 Hz, C$_α$*H*), 3.50 (3H, s, OC*H*$_3$), 3.41-3.07 (6H, m, C*H*$_2$Ph and 2 × NC*H*$_2$-allyl),

0.93 (9H, s, C(C*H*$_3$)$_3$), 0.12 (3H, s, SiC*H*$_3$), 0.10 (3H, s, SiC*H*$_3$); **$^{13}$C NMR** (126 MHz, $CDCl_3$) $\delta_C$ 171.4 (*C*ONH), 170.9 (*C*O$_2$CH$_3$), 138.5 (Ar-*C*), 136.4 (2 × =*C*H), 136.2 (Ar-*C*), 129.5 (2 × Ar-*C*H), 128.5 (2 × Ar-*C*H), 128.4 (2 × Ar-*C*H), 128.4 (2 × Ar-*C*H), 127.6 (Ar-*C*H), 126.5 (Ar-*C*H), 117.5 (2 × *C*H$_2$=), 61.3 (*C*$_\alpha$H), 60.2 (*C*$_{\alpha+1}$H), 59.4 (O*C*H$_2$), 53.6 (2 × N*C*H$_2$-allyl), 51.8 (O*C*H$_3$), 51.6 (N′*C*H$_2$Ph), 35.2 (*C*H$_2$Ph), 26.0 (C(*C*H$_3$)$_3$), 18.4 (Si*C*), -5.2 (2 × Si*C*H$_3$); **HRMS** *m*/*z* (ES$^+$) calcd. for $C_{32}H_{46}N_2O_4Si$ $[M+H]^+$ requires 551.3305, found 551.3320; ***m*/*z*** (ES$^+$) 573 ([M+Na]$^+$, 100%), 551 ([M+H]$^+$, 5%).

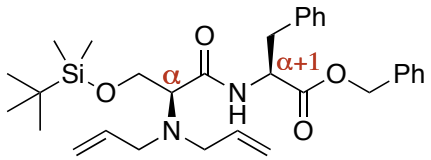


**258**

Yet further separation furnished *benzyl (–)-N-[O-(tert-butyldimethylsilyl)-N′,N′-diallyl-(S)-seryl]-(S)-phenylalaninate* **258** (9.0 mg, 16 *μ*mol, 15%) as a colourless oil: $[\alpha]_D^{20}$ -9.7 (*c* 0.6, $CHCl_3$); **$^1$H NMR** (500 MHz, $CDCl_3$) $\delta_H$ 7.94 (1H, d, *J* 7.9 Hz, CONH), 7.37-7.27 (5H, m, 5 × Ar-*H*), 7.21-7.03 (5H, m, 5 × Ar-*H*), 5.61-5.53 (2H, m, 2 × =C*H*), 5.14 (2H, ABq, *J* 12.2 Hz, OC*H*$_2$Ph), 5.12-5.02 (4H, m, 2 × C*H*$_2$=), 4.86 (1H, ddd, *J* 7.9, 6.4, 5.9 Hz, C$_{\alpha+1}$*H*), 4.16 (1H, dd, *J* 11.1, 4.1 Hz, OC*H*$_a$H$_b$), 3.90 (1H, dd, *J* 11.1, 8.4 Hz, OCH$_a$*H*$_b$), 3.53 (1H, dd, *J* 8.4, 4.1 Hz, C$_\alpha$*H*), 3.21-3.18 (4H, m, 2 × NC*H*$_2$-allyl), 3.15 (1H, dd, *J* 14.0, 5.9 Hz, C*H*$_a$H$_b$Ph), 3.08 (1H, dd, *J* 14.0, 6.4 Hz, CH$_a$*H*$_b$Ph), 0.89 (9H, s, C(C*H*$_3$)$_3$), 0.06 (6H, s, 2 × SiC*H*$_3$); **$^{13}$C NMR** (126 MHz, $CDCl_3$) $\delta_C$ 171.9 (*C*ONH), 171.4 (CO$_2$Bn), 136.4 (2 × =*C*H), 136.1 (Ar-*C*), 135.3 (Ar-*C*), 129.4 (2 × Ar-*C*H), 128.7 (2 × Ar-*C*H), 128.7 (2 × Ar-*C*H), 128.6 (2 × Ar-*C*H), 128.6 (Ar-*C*H), 127.1 (Ar-*C*H), 117.4 (2 × *C*H$_2$=), 67.3 (O*C*H$_2$Ph),

63.8 ($C_{\alpha}$H), 61.3 (O$CH_2$), 54.0 (2 × N$CH_2$-allyl), 53.1 ($C_{\alpha+1}$H), 38.1 ($CH_2$Ph), 26.0 (C($CH_3$)$_3$), 18.2 (Si*C*), -5.4 (2 × Si$CH_3$); **HRMS** *m*/*z* ($ES^+$) calcd. for $C_{31}H_{45}N_2O_4Si$ $[M+H]^+$ 537.3149, found 537.3161; ***m*/*z*** ($ES^+$) 559 ($[M+Na]^+$, 100%), 537 ($[M+H]^+$, 10%).

### 7.4.23 -

**Methyl (–)-*N*-[*N′*,*N′*-diallyl-(*S*)-seryl]-*N*-allyl-(*S*)-phenylalaninate 244**

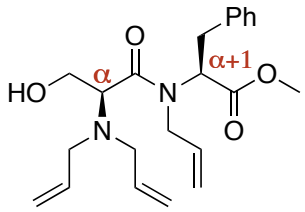


**Following GP2**: Starting with methyl (–)-*N*-[*O*-(*tert*-butyldimethylsilyl)-*N′*,*N′*-diallyl-(*S*)-seryl]-*N*-allyl-(*S*)-phenylalaninate **248** (206 mg, 0.411 mmol), acetic acid (120.0 $\mu$L, 2.06 mmol) and TBAF (1.6 mL, 1 M in THF), the reaction yielded *methyl (–)-N-[N′,N′-diallyl-(S)-seryl]-N-allyl-(S)-phenylalaninate* **244** (133 mg, 0.345 mmol, 84%) as a colourless oil: $R_f$ 0.12 (hexane:ethyl acetate, 70:30); $[\alpha]_D^{20}$ -124 (*c* 1.2, $CHCl_3$); **IR** $\nu_{max}$ (neat, $cm^{-1}$) 3446 (OH), 3078, 2949, 1743 (C=O), 1635 (C=O), 1436, 1274, 1195, 993; **$^1$H NMR** (400 MHz, $CDCl_3$) $\delta_H$ (major rotamer) 7.25-7.06 (5H, m, 5 × Ar-*H*), 5.63 (2H, dddd, *J* 17.3, 10.0, 7.4, 5.4 Hz, 2 × =C*H*), 5.59-5.50 (1H, m, =C*H*), 5.11-5.03 (4H, m, 2 × C$H_2$=), 5.03-4.92 (2H, m, C$H_2$=), 4.12 (1H, dd, *J* 10.2, 5.2 Hz, $C_{\alpha+1}H$), 4.00-3.94 (1H, m, N′C$H_a$$H_b$-allyl), 3.88 (1H, dd, *J* 11.3, 7.3 Hz, OC$H_a$$H_b$), 3.69 (1H, dd, *J* 11.3, 5.0 Hz, OC$H_a$$H_b$), 3.62 (3H, s, OC$H_3$), 3.60 (1H, dd, *J* 7.3, 5.0 Hz, $C_{\alpha}H$), 3.32 (1H, dd, *J* 14.0, 5.2, C$H_a$$H_b$Ph), 3.22-3.04 (6H, m, C$H_a$$H_b$Ph, 2 × NC$H_2$-allyl and N′C$H_a$$H_b$-allyl), 2.27 (1H, br s, O*H*); **$^{13}$C NMR** (101 MHz,

$CDCl_3$) $\delta_C$ 172.5 (*C*ON), 170.9 (*C*$O_2CH_3$), 138.0 (Ar-*C*), 136.1 (2 × =*C*H), 133.8 (=*C*H), 129.4 (2 × Ar-*C*H), 128.8 (2 × Ar-*C*H), 126.9 (Ar-*C*H), 118.8 (*C*$H_2$=), 118.1 (2 × *C*$H_2$=), 60.8 ($C_\alpha$H), 60.4 ($C_{\alpha+1}$H), 57.8 (O*C*$H_2$), 53.5 (2 × N*C*$H_2$-allyl), 52.2 (O*C*$H_3$), 51.6 (N′*C*$H_2$-allyl), 34.7 (*C*$H_2$Ph); **HRMS** *m/z* ($ES^+$) calcd. for $C_{22}H_{30}N_2O_4Na$ $[M+Na]^+$ requires 409.2103, found 409.2090; ***m/z*** ($ES^+$) 409 ($[M+Na]^+$, 100%).

### 7.4.24 -

**Methyl (–)-*N*-[(2*R*)-3-(diallylamino)-2-fluoropropanoyl]-*N*-allyl-(*S*)-phenylalanate 245**

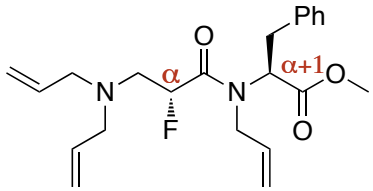


**Following GP3**: Starting with methyl (–)-*N*-[*N*′,*N*′-diallyl-(*S*)-seryl]-*N*-allyl-(*S*)-phenylalaninate **244** (76.3 mg, 0.197 mmol) and diethylaminosulfur trifluoride **32** (30.0 μL, 0.265 mmol), to yield *methyl (–)-N-[(2R)-3-(diallylamino)-2-fluoropropanoyl]-N-allyl-(S)-phenylalanate* **245** (56 mg, 0.144 mmol, 73%) as a colourless oil: $R_f$ 0.1 (hexane:ethyl acetate, 90:10); $[\alpha]_D^{20}$ -39.2 (*c* 1.3, $CHCl_3$); **IR** $\nu_{max}$ (neat, $cm^{-1}$) 3076, 2949, 1743 (C=O), 1653 (C=O), 1436, 1222, 1166, 993; **$^1$H NMR** (500 MHz, $CDCl_3$) $\delta_H$ (major rotamer) 7.25-7.09 (5H, m, 5 × Ar-*H*), 5.74 (2H, dddd, *J* 17.0, 10.3, 6.6, 6.6 Hz, 2 × =C*H*), 5.52-5.44 (1H, m, =C*H*), 5.12-5.04 (6H, m, 3 × C$H_2$=), 5.06 (1H, ddd, *J* 49.7, 8.0, 3.2 Hz, C*H*F), 4.31 (1H, dd, *J* 10.3, 5.3 Hz, $C_{\alpha+1}H$), 3.86-3.82 (2H, m, N′C$H_2$-allyl), 3.64 (3H, s, OC$H_3$), 3.30 (1H,

dd, *J* 14.1, 5.3 Hz, C*H*$_a$H$_b$Ph), 3.17 (1H, dd, *J* 14.1, 10.3 Hz, CH$_a$*H*$_b$Ph), 3.13-3.03 (4H, m, 2 × NC*H*$_2$-allyl), 2.82 (1H, ddd, *J* 18.1, 15.0, 8.0 Hz, C*H*$_a$H$_b$CHF), 2.68 (1H, ddd, *J* 31.8, 15.0, 3.2 Hz, CH$_a$*H*$_b$CHF); **$^{13}$C NMR** (125 MHz, $CDCl_3$) $\delta_C$ 170.5 (*C*O$_2$CH$_3$), 168.5 (d, *J* 20.4 Hz, *C*ON), 137.6 (Ar-*C*), 135.3 (2 × =*C*H), 133.1 (=*C*H), 129.4 (2 × Ar-*C*H), 128.7 (2 × Ar-*C*H), 126.9 (Ar-*C*H), 118.4 (*C*H$_2$=), 118.1 (2 × *C*H$_2$=), 88.4 (d, *J* 180.7 Hz, *C*HF), 60.8 (*C*$_{\alpha+1}$H), 57.7 (2 × NCH$_2$-allyl), 54.3 (d, *J* 21.6 Hz, *C*H$_2$CHF), 52.4 (O*C*H$_3$), 50.8 (d, *J* 4.1 Hz, N′*C*H$_2$-allyl), 34.8 (*C*H$_2$Ph); **$^{19}$F NMR** (470 MHz, $CDCl_3$) $\delta_F$ -185.4 (ddd, *J* 49.6, 33.5, 19.0 Hz, CH*F*-minor rotamer), -187.2 (ddd, *J* 49.7, 31.8, 18.1 Hz, CH*F*-major rotamer); **HRMS** *m/z* (ES$^+$) calcd. for $C_{22}H_{29}FN_2O_3Na$ $[M+Na]^+$ requires 411.2060, found 411.2058; ***m/z*** (ES$^+$) 411 ($[M+Na]^+$, 100%).

### 7.4.25 -

**Methyl (–)-*N*-[(2*R*)-3-amino-2-fluoropropanoyl]-*N*-allyl-(*S*)-phenylalanate hydrochloride 260**

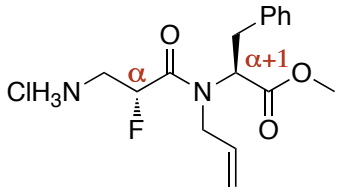


1,4-Di(phenylphosphino)butane (16.5 mg, 37.3 μmol, 30.0 mol%) was added to a solution of tris(dibenzylideneacetone)dipalladium (22.2 mg, 24.2 μmol, 25.0 mol%) in THF (5 mL) and stirred for 15 min until the solution turned yellow. This solution was added *via* canula to a solution of *methyl (–)-N-[(2R)-3-(diallylamino)-2-fluoropropanoyl]-N-allyl-(S)-phenylalanate* **254** (51.6 mg, 0.133 mmol, 1.0 eq) and

2-mercaptosalicylic acid (60.0 mg, 0.389 mmol, 2.9 eq) in THF (7.0 mL) and the solution was brought to reflux for 3 h. The reaction was cooled to rt and water (10 mL) and HCl (1 M, 0.2 mL) were added. The precipitate was isolated by filtration and washed repeatedly with water with the filtrate collected and the solvent removed *in vacuo* to furnish a yellow solid. This solid was reconstituted in water and re-filtered and the sample lyophilised to yield *methyl (–)-N-[(2R)-3-amino-2-fluoropropanoyl]-N-allyl-(S)-phenylalanate hydrochloride* **260** (41 mg, 0.20 mmol, 93%) as a colourless solid which was used without further purification: $[\alpha]_D^{20}$ -41.7 (*c* 1.0, $D_2O$); **$^1$H NMR** (500 MHz, $D_2O$) $\delta_H$ (major rotamer) 7.36-7.22 (5H, m, 5 × Ar-*H*), 5.62 (1H, ddd, *J* 48.0, 7.4, 3.4 Hz, $C_\alpha$*H*F), 5.58-5.51 (1H, m, =C*H*), 5.18-5.14 (2H, m, C$H_2$=), 4.65 (1H, dd, *J* 10.7, 5.1 Hz, $C_{\alpha+1}$*H*), 3.94 (1H, m, N′C$H_a$$H_b$-allyl), 3.71 (3H, s, OC$H_3$), 3.41-3.32 (2H, m, C$H_2$CHF), 3.29-3.16 (3H, m, C$H_2$Ph and N′C$H_a$$H_b$-allyl); **$^{13}$C NMR** (101 MHz, $D_2O$) $\delta_C$ 172.2 (*C*$O_2$$CH_3$), 167.5 (d, *J* 19.8 Hz, *C*ONH), 136.9 (Ar-*C*), 131.6 (=*C*H), 129.4 (2 × Ar-*C*H), 128.8 (2 × Ar-*C*H), 127.1 (Ar-*C*H), 119.3 (*C*$H_2$=), 84.3 (d, *J* 179 Hz, *C*HF), 61.3 ($C_{\alpha+1}$H), 53.0 (O*C*$H_3$), 51.5 (N′*C*$H_2$-allyl), 40.0 (d, *J* 21.3 Hz, *C*$H_2$CHF), 33.5 (*C*$H_2$Ph); **$^{19}$F NMR** (376 MHz, $D_2O$) $\delta_F$ -193.9 (ddd, *J* 48.0, 27.9, 20.2 Hz, CH*F*-minor rotamer), -194.7 (ddd, *J* 48.0, 26.8, 21.5 Hz, CH*F*-major rotamer); **HRMS** *m*/*z* ($ES^+$) calcd. for $C_{16}H_{22}FN_2O_3$ $[M+H]^+$ requires 309.1614, found 309.1621; ***m*/*z*** ($ES^+$) 331 ($[M+Na]^+$, 50%), 309 ($[M+H]^+$, 100%).

### 7.4.26 -

**Methyl (–)-*N*-{(2*R*)-3-[(*tert*-butoxycarbonyl)amino]-2-fluoropropanoyl}-*N*-allyl-(*S*)-phenylalanate 265**

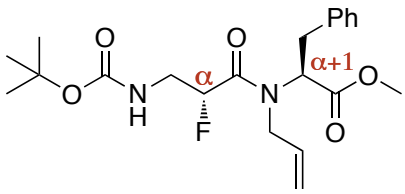


Diisopropylethylamine (40.0 $\mu$L, 0.230 mmol, 3.0 eq) and di-*tert*-butyl dicarbonate (22.0 mg, 0.101 mmol, 1.3 eq) were added to a solution of methyl (–)-*N*-((2*R*)-3-amino-2-fluoropropanoyl)-*N*-allyl-(*S*)-phenylalanate hydrochloride **260** (24.0 mg, 69.6 $\mu$mol, 1.0 eq) in aqueous dioxane (2 mL, 25% v/v) and the mixture was stirred at rt for 24 h. The reaction was quenched by the addition of saturated aqueous $Na_2CO_3$ (2 mL) and the aqueous phase extracted with ethyl acetate (2 × 2 mL). The organic extracts were combined, dried over $Na_2SO_4$, filtered and the solvent removed *in vacuo* to yield an oil. The product was purified by silica gel column chromatography, eluting with hexane and ethyl acetate (90:10), to yield *methyl (–)-N-{(2R)-3-[(tert-butoxycarbonyl)amino]-2-fluoropropanoyl}-N-allyl-(S)-phenylalanate* **265** (20.1 mg, 49.2 $\mu$mol, 71%) as a colourless oil: $[\alpha]_D^{20}$ -52.1 (*c* 2.0, $CHCl_3$); **$^1$H NMR** (400 MHz, $CDCl_3$) $\delta_H$ (major rotamer) 7.31-7.16 (5H, m, 5 × Ar-*H*), 5.55-5.46 (1H, m, =C*H*), 5.17-5.10 (2H, m, C$H_2$=), 5.15-5.02 (1H, m, C$_\alpha$*H*F), 4.93 (1H, t, *J* 6.3 Hz, N*H*Boc), 4.40 (1H, dd, *J* 10.4, 5.1 Hz, C$_{\alpha+1}$*H*), 3.96-3.87 (1H, m, N′C*H*$_a$H$_b$-allyl), 3.73 (3H, s, OC$H_3$), 3.58-3.29 (3H, m, C$H_2$CHF and N′CH$_a$*H*$_b$-allyl), 3.38 (1H, dd, *J* 14.2, 5.1 Hz, C*H*$_a$H$_b$Ph), 3.24 (1H, dd, *J* 14.2, 10.4 Hz, CH$_a$*H*$_b$Ph), 1.44 (9H, s, C(C$H_3$)$_3$); **$^{13}$C NMR** (75 MHz, $CDCl_3$) $\delta_C$ 170.5 (*C*O$_2$CH$_3$), 167.8 (d, *J* 20.3 Hz, *C*ONH),

156.0 (O*C*O$^t$Bu), 137.5 (Ar-*C*), 132.8 (=*C*H), 129.5 (2 × Ar-*C*H), 128.7 (2 × Ar-*C*H), 127.0 (Ar-*C*H), 119.0 (*C*$H_2$=), 86.4 (d, *J* 181 Hz, *C*HF), 60.9 ($C_{\alpha+1}$H), 52.5 (O*C*$H_3$), 51.1 (N′*C*$H_2$-allyl), 41.7 (d, *J* 23.8 Hz, *C*$H_2$CHF), 34.8 (*C*$H_2$Ph), 30.0 (*C*$(CH_3)_3$), 28.5 (C$(CH_3)_3$); **$^{19}$F NMR** (376 MHz, $CDCl_3$) $\delta_F$ -191.5 (ddd, *J* 47.3, 25.4, 19.6 Hz, CH*F*-minor rotamer), -192.5 (ddd, *J* 48.0, 22.9, 17.4 Hz, CH*F*-major rotamer); **HRMS** *m/z* ($ES^+$) calcd. for $C_{21}H_{29}FN_2O_5Na$ $[M+Na]^+$ requires 431.1958, found 431.1948; ***m/z*** ($ES^+$) 431 ($[M+Na]^+$, 100%).

### 7.4.27 -

**Methyl (–)-*N*-{(2*R*)-3-[(*tert*-butoxycarbonyl)amino]-2-fluoropropanoyl}-*N*-formyl-(*S*)-phenylalanate 267**

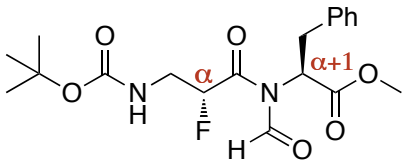


$Ru(CO)HCl(PPh_3)_3$ (4.7 mg, 4.9 μmol, 10 mol%) was added to a solution of methyl (–)-*N*-{(2*R*)-3-[(*tert*-butoxycarbonyl)amino]-2-fluoropropanoyl}-*N*-allyl-(*S*)-phenylalanate **265** (20 mg, 48.9 μmol, 1.0 eq) in toluene (2 mL) and the mixture was brough to reflux for 3 h. The solution was cooled to rt and the solvent removed *in vacuo*. $RuCl_3$ (1.0 mg, 1.7 μmol, 3.5 mol%) and $NaIO_4$ (20.8 mg, 97.8 mmol, 2 eq) in aqueous 1,2-dichloroethane (50% *v*/*v*, 1 mL) were added to the isomerised product and the mixture was stirred at rt for 24 hr. The reaction was quenched by the addition of saturated aqueous $Na_2CO_3$ (1 mL) and the organics extracted with ethyl acetate (2 × 2 mL). The organic phases were combined washed with brine (1 mL) and dried over $Na_2SO_4$, filtered and the solvent removed *in vacuo* to yield an oil. The

product was purified by silica gel chromatography to yield *methyl (–)-N-{(2R)-3-[(tert-butoxycarbonyl)amino]-2-fluoropropanoyl}-N-formyl-(S)-phenylalanate* **267** (11.5 mg, 29 $\mu$mol, 59%) as a colourless oil: $[\alpha]_D^{20}$ -30.2 (*c* 1.1, $CHCl_3$); **$^1$H NMR** (500 MHz, $CDCl_3$) $\delta_H$ 8.97 (1H, s, C*H*O), 7.29-7.10 (5H, m, 5 × Ar-*H*), 5.49 (1H, dd, *J* 10.2, 5.2 Hz, N*H*Boc), 5.35-5.26 (1H, br m, C*H*F), 4.74 (1H, m, $C_{\alpha+1}H$), 3.76 (3H, s, $OCH_3$), 3.52 (1H, dd, *J* 14.2, 5.4 Hz, $CH_aH_bPh$), 3.54-3.34 (1H, m, $CH_aH_bCHF$), 3.28 (1H, dd, *J* 14.2, 11.1 Hz, $CH_aH_bPh$), 3.32-3.23 (1H, m, $CH_aH_bCHF$), 1.44 (9H, s, $C(CH_3)_3$); **$^{13}$C NMR** (126 MHz, $CDCl_3$) $\delta_C$ 169.1 ($CO_2CH_3$), 168.8 (*C*HO), 161.3 (d, *J* 9.6 Hz, *C*ONH), 155.7 (O*C*O$^t$Bu), 136.3 (Ar-*C*), 129.2 (2 × Ar-*C*H), 128.6 (2 × Ar-*C*H), 127.1 (Ar-*C*H), 87.0 (d, *J* 186 Hz, *C*HF), 60.4 (1H, s, $C_{\alpha+1}H$), 52.8 ($OCH_3$), 41.8 (d, *J* 23.1 Hz, $CH_2CHF$), 34.3 ($CH_2Ph$), 29.7 ($C(CH_3)_3$), 28.3 ($C(CH_3)_3$); **$^{19}$F NMR** (470 MHz, $CDCl_3$) $\delta_F$ -190.5 (br m, CH*F*-minor rotamer), -191.5 (br m, CH*F*-major rotamer); **HRMS** *m/z* ($ES^+$) calcd. for $C_{19}H_{25}FN_2O_6Na$ $[M+Na]^+$ 419.1594, found 419.1588; ***m/z*** ($ES^+$) 419 ($[M+Na]^+$, 100%).

### 7.4.28 -

**Methyl (–)-*N*-{(2*R*)-3-[(*tert*-butoxycarbonyl)amino]-2-fluoropropanoyl}-(*S*)-phenylalanate 268**

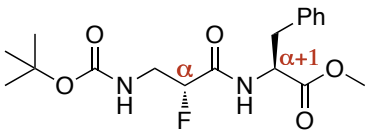


Saturated aqueous sodium carbonate (0.5 mL) was added to a solution of $NaHCO_3$ (1.0 mg, 9.4 $\mu$mol, 0.33 eq) and methyl (–)-*N*-{(2*R*)-3-[(*tert*-butoxycarbonyl)amino]-2-fluoropropanoyl}-*N*-formyl-(*S*)-phenylalanate **267** (11.0 mg,

28 $\mu$mol, 1.0 eq) in aqueous acetone (25% *v*/*v*, 1 mL) and the mixture was stirred vigorously for 12 h at rt. The mixture was diluted with water (1 mL) and ethyl acetate (2 mL), the organic phase was separated and the aqueous layer further extracted with ethyl acetate (2 mL). The organic phases were combined, washed with brine (1 mL), dried with $Na_2SO_4$, filtered and the solvent removed *in vacuo*. The oil was purified by silica gel column chromatography, to yield *methyl (–)-N-{(2R)-3-[(tert-butoxycarbonyl)amino]-2-fluoropropanoyl}-(S)-phenylalanate* **268** (4.7 mg, 12 $\mu$mol, 46%) as a colourless solid: $[\alpha]_D^{20}$ -26.1 (*c* 0.1, $CHCl_3$); **$^1$H NMR** (500 MHz, $CDCl_3$) $\delta_H$ 7.34-7.11 (5H, m, 5 × Ar-*H*), 6.70 (1H, br d, *J* 4.9 Hz, CONH), 4.95-4.84 (3H, m, C*H*F, $C_{\alpha+1}H$ and N*H*Boc), 3.82-3.72 (1H, m, C$H_aH_b$CHF), 3.75 (3H, s, OC$H_3$), 3.54-3.44 (1H, m, C$H_aH_b$CHF), 3.19 (1H, dd, *J* 14.0, 5.7 Hz, C$H_aH_b$Ph), 3.12 (1H, dd, *J* 14.0, 6.5 Hz, C$H_aH_b$Ph), 1.43 (9H, s, C(C$H_3$)$_3$); **$^{13}$C NMR** (126 MHz, $CDCl_3$) $\delta_C$ 171.2 (*C*$O_2CH_3$), 167.9 (d, *J* 20.7 Hz, *C*ONH), 155.7 (O*C*O$^t$Bu), 135.3 (Ar-*C*), 129.1 (2 × Ar-*C*H), 128.8 (2 × Ar-*C*H), 127.4 (Ar-*C*), 90.0 (d, *J* 194.5 Hz, *C*HF), 52.8 ($C_{\alpha+1}$H), 52.6 (O*C*$H_3$), 42.1 (d, *J* 21.1 Hz, *C*$H_2$CHF), 37.7 (*C*$H_2$Ph), 29.7 (*C*(C$H_3$)$_3$), 28.3 (C(*C*$H_3$)$_3$); **$^{19}$F NMR** (470 MHz, $CDCl_3$) $\delta_F$ -195.3 (ddd, *J* 48.1, 23.7, 23.7 Hz, CH*F*); **HRMS** *m*/*z* ($ES^+$) calcd. for $C_{18}H_{25}FN_2O_5Na$ $[M+Na]^+$ requires 391.1645, found 391.1645; ***m*/*z*** ($ES^+$) 391 ($[M+Na]^+$, 100%).

# References


1. A. Tressaud, *Angew. Chem., Int. Ed.*, 2006, **45**, 6792-6796.

2. N. N. Greenwood and A. Earnshaw, *Chemistry of the Elements*, Elsevier, Oxford, 2nd edn., 2005, vol. Elsevier.

3. J. R. Breen, G. Sandford, D. S. Yufit, J. A. K. Howard, J. Fray, and B. Patel, *Beilstein J. Org. Chem.*, 2011, **7**, 1048-1054.

4. T. Furuya, C. A. Kuttruff, and T. Ritter, *Curr. Opin. Drug Discovery Dev.*, 2008, **11**, 803-819.

5. C. Hollingworth and V. Gouverneur, *Chem. Commun.*, 2012, **48**, 2929-2942.

6. D. H. R. Barton, L. S. Godinho, R. H. Hesse, and M. M. Pechet, *Chem. Commun.*, 1968, 804-806.

7. T. Umemoto, S. Fukami, G. Tomizawa, K. Harasawa, K. Kawada, and K. Tomita, *J. Am. Chem. Soc.*, 1990, **112**, 8563-8575.

8. S. Sing, D. D. DesMarteau, S. S. Zuberi, M. Witz, and H.-N. Haung, *J. Am. Chem. Soc.*, 1987, **109**, 7194-7196.

9. E. Differding and R. W. Lang, *Tetrahedron Lett.*, 1988, **29**, 6087-6090.

10. T. D. Beeson and D. W. C. MacMillan, *J. Am. Chem. Soc.*, 2005, **127**, 8826-8828.

11. M. Marigo, D. Fielenbach, A. Braunton, A. Kjærsgaard, and K. A. Jørgensen, *Angew. Chem., Int. Ed.,* 2005, **44**, 3703-3706.

12. D. D. Steiner, N. Mase, and C. F. Barbas, *Angew. Chem., Int. Ed.,* 2005, **44**, 3706-3710.

13. R. E. Banks, *J. Fluorine Chem.*, 1998, **87**, 1-17.

14. P. T. Nyffeler, S. G. Durón, M. D. Burkart, S. P. Vincent, and C.-H. Wong, *Angew. Chem., Int. Ed.,* 2005, **44**, 192-212.

15. V. Rauniyar, A. D. Lackner, G. L. Hamilton, and F. D. Toste, *Science*, 2011, **334**, 1681-1684.

16. T. Furuya, A. E. Strom, and T. Ritter, *J. Am. Chem. Soc.*, 2009, **131**, 1662-1663.

17. H. Teare, E. G. Robins, A. Kirjavainen, S. Forsback, G. Sandford, O. Solin, S. K. Luthra, and V. Gouverneur, *Angew. Chem., Int. Ed.,* 2010, **49**, 6821-6824.

18. J. H. Clark, *Chem. Rev.*, 1980, **80**, 429-452.

19. D. O'Hagan, *Chem. Soc. Rev.*, 2008, **37**, 308-319.

20. C. W. Tullock and D. D. Coffman, *J. Org. Chem.*, 1960, **25**, 2016-2019.

21. I. Shahak and E. D. Bergmann, *J. Chem. Soc. C*, 1967, 319-320.

22. M. H. Litt, A.-M. Weidler-Kubanek, and F. P. Avonda, *J. Org. Chem.*, 1968, **33**, 1837-1839.

23. W. J. Middleton, *J. Org. Chem.*, 1975, **40**, 574-578.

24. M. J. Tozer and T. F. Herpin, *Tetrahedron*, 1996, **52**, 8619-8683.

25. H. Hayashi, H. Sonoda, and T. Nagata, *Chem. Commun.*, 2002, 1618-1619.

26. F. Beaulieu, L.-P. Beauregard, G. Courchesne, M. Couturier, F. LaFlamme, and A. L'Heureux, *Org. Lett.*, 2009, **11**, 5050-5053.

27. A. L'Heureux, F. Beaulieu, C. Bennett, D. R. Bill, S. Clayton, F. LaFlamme, M. Mirmehrabi, S. Tadayon, D. Tovell, and M. Couturier, *J. Org. Chem.*, 2010, **75**, 3401-3411.

28. E. J. Cho, T. D. Senecal, T. Kinzel, Y. Zhang, D. A. Watson, and S. L. Buchwald, *Science*, 2010, **328**, 1679-1681.

29. Y. Ji, T. Brueckl, R. D. Baxter, Y. Fujiwara, I. B. Seiple, S. Su, D. G. Blackmond, and P. S. Baran, *Proc. Natl. Acad. Sci. USA*, 2011, **108**, 14411-14415.

30. D. A. Nagib and D. W. C. MacMillan, *Nature*, 2011, **480**, 224-248.

31. B. R. Langlois, E. Laurent, and N. Roidot, *Tetrahedron Lett.*, 1991, **32**, 7525-7528.

32. A. T. Parsons and S. L. Buchwald, *Nature*, 2011, **480**, 184-185.

33. T. Besset, C. Schneider, and D. Cahard, *Angew. Chem., Int. Ed.*, 2012, **51**, 5048-5050.

34. M. Pagliaro and R. Ciriminna, *J. Mater. Chem.*, 2005, **15**, 4981-4991.

35. H.-J. Böhm, D. Banner, S. Bendels, M. Kansy, B. Kuhn, K. Müller, U. Obst-Sander, and M. Stahl, *ChemBioChem*, 2004, **5**, 637-643.

36. S. Purser, P. R. Moore, S. Swallow, and V. Gouverneur, *Chem. Soc. Rev.*, 2008, **37**, 320-330.

37. K. Müller, C. Faeh, and F. Diederich, *Science*, 2007, **317**, 1881-1886.

38. P. Jeschke, *ChemBioChem*, 2004, **5**, 571-589.

39. W. K. Hagmann, *J. Med. Chem.*, 2008, **51**, 4359-4369.

40. A. Bondi, *J. Phys. Chem.*, 1964, **68**, 441-451.

41. B. E. Smart, *J. Fluorine Chem.*, 2001, **109**, 3-11.

42. D. M. Lemal, *J. Org. Chem.*, 2004, **69**, 1-11.

43. M. H. Abraham, P. L. Grellier, D. V. Prior, P. P. Duce, J. J. Morris, and P. J. Taylor, *J. Chem. Soc., Perkin Trans. 2*, 1989, 699-711.

44. M. H. Abraham, P. L. Grellier, D. V. Prior, J. J. Morris, and P. J. Taylor, *J. Chem. Soc., Perkin Trans. 2*, 1990, 521-529.

45. S. B. Rosenblum, T. Huynh, A. Afonso, H. R. Davis, N. Yumibe, J. W. Clader, and D. A. Burnett, *J. Med. Chem.*, 1998, **41**, 973-980.

46. C. Heidelberger, N. K. Chaudhuri, P. Danneberg, D. Mooren, L. Griesbach, R. Duschinsky, R. J. Schnitzer, E. Pleven, and J. Scheiner, *Nature*, 1957, **179**, 663-666.

47. J. E. Barrett, D. A. Maltby, D. V. Santi, and P. G. Schultz, *J. Am. Chem. Soc.*, 1998, **120**, 449-450.

48. J. G. Bundy, E. M. Lenz, D. Osborn, J. M. Weeks, J. C. Lindon, and J. K. Nicholson, *Xenobiotica*, 2002, **32**, 479-490.

49. C. J. Duckett, I. D. Wilson, D. S. Douce, H. J. Walker, F. R. Abou-Shakra, J. C. Lindon, and J. K. Nicholson, *Xenobiotica*, 2007, **37**, 1378-1393.

50. C. Schaffrath, S. L. Cobb, and D. O'Hagan, *Angew. Chem., Int. Ed.,* 2002, **41**, 3913-3915.

51. M. Onega, R. P. McGlinchey, H. Deng, J. T. G. Hamilton, and D. O'Hagan, *Chem. Commun.*, 2007, **35**, 375-385.

52. S. Klimasauskas, T. Szyperski, S. Serva, and K. Wüthrich, *EMBO J.*, 1998, **17**, 317-324.

53. M. A. Danielson and J. J. Falke, *Annu. Rev. Biophys. Biomol. Struct.*, 1996, **25**, 163-195.

54. S. L. Cobb and C. Murphy, *J. Fluorine Chem.*, 2009, **130**, 132-143.

55. R. Moumne, M. Pasco, E. Prost, T. Lecourt, L. Micouin, and C. Tisne, *J. Am. Chem. Soc.*, 2010, **132**, 13111-13113.

56. F. Chung, C. Tisné, T. Lecourt, B. Seijo, F. Dardel, and L. Micouin, *Chem. Eur. J.*, 2009, **15**, 7109-7116.

57. F. Chung, C. Tisné, T. Lecourt, F. Dardel, and L. Micouin, *Angew. Chem., Int. Ed.*, 2007, **46**, 4489-4491.

58. S. Bresciani, T. Lebl, A. M. Z. Slawin, and D. O'Hagan, *Chem. Commun.*, 2010, **46**, 5434-5436.

59. J. Battiste and R. Newmark, *Prog. Nucl. Magn. Reson. Spectrosc.*, 2006, **48**, 1-23.

60. T. M. O'Connell, S. A. Gabel, and R. E. London, *Biochem.*, 1994, **33**, 10985-10992.

61. F. R. Souza, M. P. Freitas, and R. Rittner, *J. Mol. Struct.: THEOCHEM*, 2008, **863**, 137-140.

62. L. Goodman, H. Gu, and V. Pophristic, *J. Phys. Chem. A*, 2005, **109**, 1223-1229.

63. I. V. Alabugin, K. M. Gilmore, and P. W. Peterson, *Wiley Interdiscip. Rev.: Comput. Mol. Sci.*, 2011, **1**, 109-141.

64. D. Y. Buissonneaud, T. van Mourik, and D. O'Hagan, *Tetrahedron*, 2010, **66**, 2196-2202.

65. D. O'Hagan, *J. Org. Chem.*, 2012, **77**, 3689-3699.

66. D. Wu, A. Tian, and H. Sun, *J. Phys. Chem. A*, 1998, **102**, 9901-9905.

67. D. Farran, A. M. Z. Slawin, P. Kirsch, and D. O'Hagan, *J. Org. Chem.*, 2009, **74**, 7168-7171.

68. L. Hunter, A. M. Z. Slawin, P. Kirsch, and D. O'Hagan, *Angew. Chem., Int. Ed.,* 2007, **46**, 7887-7890.

69. L. Hunter, P. Kirsch, A. M. Z. Slawin, and D. O'Hagan, *Angew. Chem., Int. Ed.,* 2009, **48**, 5457-5460.

70. A. G. Myers, J. K. Barbay, and B. Zhong, *J. Am. Chem. Soc.*, 2001, **123**, 7207-7219.

71. K. B. Wiberg and P. R. Rablen, *J. Am. Chem. Soc.*, 1993, **115**, 614-625.

72. J. W. Banks, A. S. Batsanov, J. A. K. Howard, D. O'Hagan, H. S. Rzepa, and S. Martin-Santamaria, *J. Chem. Soc., Perkin Trans. 2*, 1999, 2409-2411.

73. C. R. S. Briggs, D. O'Hagan, J. A. K. Howard, and D. S. Yu, *J. Fluorine Chem.*, 2003, **119**, 9-13.

74. C. F. Tormena, N. S. Amadeu, R. Rittner, and R. J. Abraham, *J. Chem. Soc., Perkin Trans. 2*, 2002, 773-778.

75. P. R. Olivato, S. A. Guerrero, M. H. Yreijo, R. Rittner, and C. F. Tormena, *J. Mol. Struct.*, 2002, **607**, 87-99.

76. R. I. Mathad, B. Jaun, O. Flögel, J. Gardiner, M. Löweneck, J. D. C. Codée, P. H. Seeberger, and D. Seebach, *Helv. Chim. Acta*, 2007, **90**, 2251-2273.

77. B. Jaun, D. Seebach, and R. I. Mathad, *Helv. Chim. Acta*, 2011, **94**, 355-361.

78. C. R. S. Briggs, M. J. Allen, D. O'Hagan, D. J. Tozer, A. M. Z. Slawin, A. E. Goeta, and J. A. K. Howard, *Org. Biomol. Chem.*, 2004, **2**, 732-740.

79. N. E. J. Gooseman, D. O'Hagan, M. J. G. Peach, A. M. Z. Slawin, D. J. Tozer, and R. J. Young, *Angew. Chem., Int. Ed.*, 2007, **46**, 5904-5908.

80. A. Sun, D. C. Lankin, K. Hardcastle, and J. P. Snyder, *Chem.-Eur. J.*, 2005, **11**, 1579-1591.

81. N. E. J. Gooseman, D. O'Hagan, A. M. Z. Slawin, A. M. Teale, D. J. Tozer, and R. J. Young, *Chem. Commun.*, 2006, 3190-3192.

82. N. E. J. Gooseman, Ph.D. Thesis, University of St Andrews, Scotland, 2008.

83. L. E. Zimmer, C. Sparr, and R. Gilmour, *Angew. Chem., Int. Ed.*, 2011, **50**, 11860-11871.

84. C. Sparr, W. B. Schweizer, H. M. Senn, and R. Gilmour, *Angew. Chem., Int. Ed.*, 2009, **48**, 3065-3068.

85. A. Lattanzi, *Org. Lett.*, 2005, **7**, 2579-2582.

86. M. D. Clift, H. Ji, G. P. Deniau, D. O'Hagan, and R. B. Silverman, *Biochemistry*, 2007, **46**, 13819-13828.

87. G. Deniau, A. M. Z. Slawin, T. Lebl, F. Chorki, J. P. Issberner, T. van Mourik, J. M. Heygate, J. J. Lambert, L.-A. Etherington, K. T. Sillar, and D. O'Hagan, *ChemBioChem*, 2007, **8**, 2265-2274.

88. I. Yamamoto, G. P. Deniau, N. Gavande, M. Chebib, G. A. R. Johnston, and D. O'Hagan, *Chem. Commun.*, 2011, **47**, 7956-7958.

89. L. Hunter, *Beilstein J. Org. Chem.*, 2010, **6**, 14pp.

90. L. Hunter, K. A. Jolliffe, M. J. T. Jordan, P. Jensen, and R. B. Macquart, *Chem. Eur. J.*, 2011, 2340-2343.

91. I. Yamamoto, M. J. T. Jordan, N. Gavande, M. R. Doddareddy, M. Chebib, and L. Hunter, *Chem. Commun.*, 2012, **48**, 829-831.

92. T. Ohba, E. Ikeda, and H. Takei, *Bioorg. Med. Chem. Lett.*, 1996, **6**, 1875-1880.

93. L. Somekh and A. Shanzer, *J. Am. Chem. Soc.*, 1982, **104**, 5836-5837.

94. D. F. Hook, F. Gessier, C. Noti, P. Kast, and D. Seebach, *ChemBioChem*, 2004, **5**, 691-706.

95. T.-X. Métro, B. Duthion, D. G. Pardo, and J. Cossy, *Chem. Soc. Rev.*, 2010, **39**, 89-102.

96. M. K. Edmonds, F. H. M. Graichen, J. Gardiner, and A. D. Abell, *Org. Lett.*, 2008, **10**, 885-887.

97. S. G. Davies, N. M. Garrido, D. Kruchinin, O. Ichihara, L. J. Kotchie, P. D. Price, A. J. P. Mortimer, A. J. Russell, and A. D. Smith, *Tetrahedron: Asymmetry*, 2006, **17**, 1793-1811.

98. P. J. Duggan, M. Johnston, and T. L. March, *J. Org. Chem.*, 2010, **75**, 7365-7372.

99. X.-L. Qiu and F.-L. Qing, *Eur. J. Org. Chem.*, 2011, 3261-3278.

100. Nobel Prize, *The 2009 Nobel Prize in Physiology or Medicine Nobelprize.org. Feb 2012 www.nobelprize.org/nobel_prizes/medicine/laureates/2009/press.html*, 2009.

101. J. W. Szoztak and E. H. Blackburn, *Cell*, 1982, **29**, 245-255.

102. C. W. Greider and E. H. Blackburn, *Cell*, 1985, **43**, 405-413.

103. C. W. Greider and E. H. Blackburn, *Nature*, 1989, **337**, 331-337.

104. J. A. Londono-Vallejo, *Biochimie*, 2008, **90**, 73-82.

105. R. K. Moyzis, J. M. Buckingham, L. S. Cram, M. Dani, L. L. Deaven, M. D. Jones, J. Meyne, R. L. Ratliff, and J. R. Wu, *Proc. Natl. Acad. Sci. USA*, 1988, **85**, 6622-6626.

106. S. Neidle and G. Parkinson, *Nat. Rev. Drug Discovery*, 2002, **1**, 383-393.

107. J. W. Shay and W. E. Wright, *Nat. Rev. Mol. Cell. Biol.*, 2000, **1**, 72-76.

108. J. W. Shay and W. E. Wright, *FEBS Letters*, 2010, **584**, 3819-3825.

109. T. M. Bryan and T. R. Cech, *Curr. Opin. Cell Biol.*, 1999, **11**, 318-324.

110. J. Feng, W. D. Funk, S. S. Wang, S. L. Weinrich, A. A. Avilion, C. P. Chiu, R. R. Adams, E. Chang, R. C. Allsopp, and J. Yu, *Science*, 1995, **269**, 1236-1241.

111. J.-L. Chen, M. A. Blasco, and C. W. Greider, *Cell*, 2000, 100, 503-514.

112. K. Yashima, A. Maitra, B. B. Rogers, C. F. Timmons, A. Rathi, H. Pinar, W. E. Wright, J. W. Shay, and A. F. Gazdar, *Cell Growth Differ.*, 1998, **9**, 805-813.

113. W. E. Wright, M. A. Piatyszek, W. E. Rainey, W. Byrd, and J. W. Shay, *Dev. Genet.*, 1996, **18**, 173-179.

114. N. R. Forsyth, W. E. Wright, and J. W. Shay, *Differentiation*, 2002, **69**, 188-197.

115. N. W. Kim, M. A. Piatyszek, K. R. Prowse, C. B. Harley, M. D. West, P. L. Ho, G. M. Coviello, W. E. Wright, S. L. Weinrich, and J. W. Shay, *Science*, 1994, **266**, 2011-2015.

116. J. W. Shay and W. E. Wright, *Nat. Rev. Drug Discovery*, 2006, **5**, 577-584.

117. T. de Lange, *Genes Dev.*, 2005, **19**, 2100-2110.

118. W. E. Wright, V. M. Tesmer, K. E. Huffman, S. D. Levene, and J. W. Shay, *Genes Dev.*, 1997, **11**, 2801-2809.

119. R. McElligott and R. J. Wellinger, *EMBO J.*, 1997, **16**, 3705-3714.

120. K. E. Huffman, S. D. Levene, V. M. Tesmer, J. W. Shay, and W. E. Wright, *J. Biol. Chem.*, 2000, **275**, 19719-19722.

121. H. Takai, A. Smogorzewska, and T. D. Lange, *Curr. Biol.*, 2003, **13**, 1549-1556.

122. F. d'Adda di Fagagna, P. M. Reaper, L. Clay-Farrace, H. Fiegler, P. Carr, T. von Zglinicki, G. Saretzki, N. P. Carter, and S. P. Jackson, *Nature*, 2003, **426**, 194-198.

123. Z. Lou and J. Chen, *Exp. Cell Res.*, 2006, **312**, 2641-2646.

124. E. H. Blackburn, *Nature*, 2000, **408**, 53-56.

125. D. Hockemeyer, J.-P. Daniels, H. Takai, and T. de Lange, *Cell*, 2006, **126**, 63-77.

126. S. J. Froelich-Ammon, B. A. Dickinson, J. M. Bevilacqua, S. C. Schultz, and T. R. Cech, *Genes & Development*, 1998, **12**, 1504-1514.

127. M. Gellert, M. N. Lipsett, and D. R. Davies, *Proc. Natl. Acad. Sci. USA*, 1962, **48**, 2013-2018.

128. S. M. Haider, G. N. Parkinson, and S. Neidle, *J. Mol. Biol.*, 2003, **326**, 117-125.

129. DeLanoScientific, *The PyMOL Molecular Graphics System*, 2002, Version 0.99.

130. J. T. Davis, *Angew. Chem., Int. Ed.,* 2004, **43**, 668 - 698.

131. T. J. Pinnavaia, C. L. Marshall, C. M. Mettler, C. L. Fisk, T. Miles, and E. D. Becker, *J. Am. Chem. Soc.*, 1978, **100**, 3625-3627.

132. P. Tougard, J.-F. Chantot, and W. Guschlbauer, *Biochim. Biophys. Acta, Nucleic Acids Protein Synth.*, 1973, **308**, 9-16.

133. S. B. Zimmerman, G. H. Cohen, and D. R. Davies, *J. Mol. Biol.*, 1975, **92**, 181-192.

134. Z. B. Steven, *J. Mol. Biol.*, 1976, **106**, 663-672.

135. T.-M. Ou, Y.-J. Lu, J.-H. Tan, Z.-S. Huang, and K.-Y. Wong, *ChemMedChem*, 2008, **3**, 690-713.

136. E. Henderson, C. C. Hardin, S. K. Walk, I. Tinoco Jr., and E. H. Blackburn, *Cell*, 1987, **51**, 899-908.

137. J. R. Williamson, M. K. Raghuraman, and T. R. Cech, *Cell*, 1989, **59**, 871-880.

138. S. Burge, G. N. Parkinson, P. Hazel, A. K. Todd, and S. Neidle, *Nucleic Acids Res.*, 2006, **34**, 5402-5415.

139. G. N. Parkinson, in *Quadruplex Nucleic Acids*, eds. S. Neidle and S. Balasubramanian, RSC Publishing, 1st edn., 2006, pp. 17-19.

140. S. Neidle and G. N. Parkinson, *Biochemie*, 2008, **90**, 1184-1196.

141. S. Haider, G. N. Parkinson, and S. Neidle, *J. Mol. Biol.*, 2002, **320**, 189-200.

142. F. W. Smith and J. Feigon, *Nature*, 1992, **356**, 164-168.

143. P. Schultze, N. V. Hud, F. W. Smith, and J. Feigon, *Nucleic Acids Res.*, 1999, **27**, 3018-3028.

144. M. Crnugelj, P. Sket, and J. Plavec, *J. Am. Chem. Soc.*, 2003, **125**, 7866-7871.

145. P. Hazel, G. N. Parkinson, and S. Neidle, *J. Am. Chem. Soc.*, 2006, **128**, 5480-5487.

146. R. Rodriguez, K. M. Miller, J. V. Forment, C. R. Bradshaw, M. Nikan, S. Britton, T. Oelschlaegel, B. Xhemalce, S. Balasubramanian, and S. P. Jackson, *Nat. Chem. Biol.*, 2012, **8**, 301-310.

147. D. Sen and W. Gilbert, *Nature*, 1990, **334**, 410-414.

148. Y. Wang and D. J. Patel, *Structure*, 1993, **1**, 263-282.

149. G. N. Parkinson, M. P. H. Lee, and S. Neidle, *Nature*, 2002, **417**, 876-880.

150. A. M. Zahler, J. R. Williamson, T. R. Cech, and D. M. Prescott, *Nature*, 1991, **350**, 718-720.

151. S. Neidle, *FEBS Journal*, 2010, **277**, 1118-1125.

152. P. Murat, Y. Singh, and E. Defrancq, *Chem. Soc. Rev.*, 2011, **40**, 5293-5307.

153. A. Ambrus, D. Chen, J. Dai, T. Bialis, R. A. Jones, and D. Yang, *Nucleic Acids Res.*, 2006, **34**, 2723-2735.

154. C. C. Hardin, T. Watson, M. Corregan, and C. Bailey, *Biochemistry*, 1992, **31**, 833-841.

155. P. K. Patel and R. V. Hosur, *Nucleic Acids Res.*, 1999, **27**, 2457-2464.

156. P. K. Patel, A. S. R. Koti, and R. V. Hosur, *Nucleic Acids Res.*, 1999, **27**, 3836-3843.

157. N. H. Campbell and G. N. Parkinson, *Methods*, 2007, **43**, 252-263.

158. J.-L. Mergny, L. Lacroix, C. Hounsou, L. Guittat, M. Hoarau, P. B. Arimondo, J.-P. Vigneron, J.-M. Lehn, J.-F. Roui, T. Garestier, and C. Helene, *Proc. Natl. Acad. Sci. USA*, 2001, **98**, 3062-3067.

159. A. D. Cian, L. Guittat, M. Kaiser, B. Saccà, S. Amrane, A. Bourdoncle, P. Alberti, M.-P. Teulade-Fichou, L. Lacroix, and J.-L. Mergny, *Methods*, 2007, **42**, 183-195.

160. B.-S. Herbert, A. E. Hochreiter, W. E. Wright, and J. W. Shay, *Nat. Protoc.*, 2006, **1**, 1583-1590.

161. D. Monchaud and M.-P. Teulade-Fichou, *Org. Biomol. Chem.*, 2008, **6**, 627-636.

162. K. Shin-Ya, K. Wierzba, K.-I. Matsuo, T. Ohtani, Y. Yamada, K. Furihata, Y. Hayakawa, and H. Seto, *J. Am. Chem. Soc.*, 2001, **123**, 1262-1263.

163. M.-Y. Kim, H. Vankayalapati, K. Shin-Ya, K. Wierzba, and L. H. Hurley, *J. Am. Chem. Soc.*, 2002, **124**, 2098-2099.

164. T. Doi, M. Yoshida, K. Shin-ya, and T. Takahashi, *Org. Lett.*, 2006, **8**, 4165-4167.

165. C. M. Barbieri, A. R. Srinivasan, S. G. Rzuczek, J. E. Rice, E. J. Lavoie, and D. S. Pilch, *Nucleic Acids Res.*, 2007, **35**, 3272-3286.

166. M. Tera, Y. Sohtome, H. Ishizuka, T. Doi, M. Takagi, K. Shin-ya, and K. Nagasawa, *Heterocycles*, 2006, **69**, 505-514.

167. R. T. Wheelhouse, D. Sun, H. Han, F. X. Han, and L. H. Hurley, *J. Am. Chem. Soc.*, 1998, **120**, 3261-3262.

168. N. V. Anantha, M. Azam, and R. D. Sheardy, *Biochemistry*, 1998, **37**, 2709-2714.

169. F. X. Han, R. T. Wheelhouse, and L. H. Hurley, *J. Am. Chem. Soc.*, 1999, **121**, 3561-3570.

170. G. N. Parkinson, R. Ghosh, and S. Neidle, *Biochemistry*, 2007, **46**, 2390-2397.

171. J. Ren and J. B. Chaires, *Biochemistry*, 1999, **38**, 16067-16075.

172. M.-P. Teulade-Fichou, C. Carrasco, L. Guittat, C. Bailly, P. Alberti, J.-L. Mergny, A. David, J.-M. Lehn, and W. D. Wilson, *J. Am. Chem. Soc.*, 2003, **125**, 4732-4740.

173. S. Neidle and M. A. Read, *Biopolymers*, 2001, **56**, 195-208.

174. R. J. Harrison, A. P. Reszka, S. M. Haider, B. Romagnoli, J. Morrell, M. A. Read, S. M. Gowan, C. M. Incles, L. R. Kelland, and S. Neidle, *Bioorg. Med. Chem. Lett.*, 2004, **14**, 5845-5849.

175. M. A. Read, A. A. Wood, J. R. Harrison, S. M. Gowan, L. R. Kelland, H. S. Dosanjh, and S. Neidle, *J. Med. Chem.*, 1999, **42**, 4538-4546.

176. R. J. Harrison, S. M. Gowan, L. R. Kelland, and S. Neidle, *Bioorg. Med Chem. Lett.*, 1999, **9**, 2463-2468.

177. M. Read, R. J. Harrison, B. Romagnoli, F. A. Tanious, S. M. Gowan, A. P. Reszka, W. D. Wilson, L. R. Kelland, and S. Neidle, *Proc. Natl. Acad. Sci. USA*, 2001, **98**, 4844-4849.

178. R. J. Harrison, J. Cuesta, G. Chessari, M. A. Read, S. K. Basra, A. P. Reszka, J. Morrell, S. M. Gowan, C. M. Incles, F. A. Tanious, W. D. Wilson, L. R. Kelland, and S. Neidle, *J. Med. Chem.*, 2003, **46**, 4463-4476.

179. C. M. Incles, C. M. Schultes, H. Kempski, H. Koehler, L. R. Kelland, and S. Neidle, *Mol. Cancer Ther.*, 2004, **3**, 1201-1206.

180. A. M. Burger, F. Dai, C. M. Schultes, A. P. Reszka, M. J. Moore, J. A. Double, and S. Neidle, *Cancer Res.*, 2005, **65**, 1489-1496.

181. S. M. Gowan, J. R. Harrison, L. Patterson, M. Valenti, M. A. Read, S. Neidle, and L. R. Kelland, *Mol. Pharmacol.*, 2002, **61**, 1154-1162.

182. N. H. Campbell, M. Patel, A. B. Tofa, R. Ghosh, G. N. Parkinson, and S. Neidle, *Biochemistry*, 2009, **48**, 1675-1680.

183. N. H. Campbell, G. N. Parkinson, A. P. Reszka, and S. Neidle, *J. Am. Chem. Soc.*, 2008, **130**, 6722-6724.

184. M. J. B. Moore, C. M. Schultes, J. Cuesta, F. Cuenca, M. Gunaratnam, F. A. Tanious, W. D. Wilson, and S. Neidle, *J. Med. Chem.*, 2006, **49**, 582-599.

185. C. L. Perrin and J. B. Nielson, *Annu. Rev. Phys. Chem.*, 1997, **48**, 511-544.

186. C. Thibaudeau, J. Plavec, and J. Chattopadhyaya, *J. Org. Chem.*, 1998, **63**, 4967-4984.

187. P. Emsley and K. Cowtan, *Acta Crystallogr., Sect. D: Biol. Crystallogr.*, 2004, **60**, 2126-2132.

188. C. Ye and J. M. Shreeve, *J. Fluorine Chem.*, 2004, **125**, 1869-1872.

189. A. Cheguillaume, S. Lacroix, and J. Marchand-Brynaert, *Tetrahedron Lett.*, 2003, **44**, 2375-2377.

190. P. E. Floreancig, S. E. Swalley, J. W. Trauger, and P. B. Dervan, *J. Am. Chem. Soc.*, 2000, **122**, 6342-6350.

191. S. Neidle, R. J. Harrison, L. Kelland, S. M. Gowan, M. A. Read, and A. Reszka, 2003, US 2003/0207909 A1.

192. K. Matsumura, *J. Am. Chem. Soc.*, 1929, **51**, 816-820.

193. S. A. Gamage, N. Tepsiri, P. Wilairat, S. J. Wojcik, D. P. Figgitt, R. K. Ralph, and W. A. Denny, *J. Med. Chem.*, 1994, **37**, 1486-1494.

194. C. A. Faler and M. M. Joullie, *Tetrahedron*, 2006, **47**, 7229-7231.

195. K.-W. Yang, J. G. Cannon, and J. G. Rose, *Tetrahedron Lett.*, 1970, **21**, 1791-1794.

196. B. Duthion, D. G. Pardo, and J. Cossy, *Org. Lett.*, 2010, **12**, 4620-4623.

197. P. G. M. Wuts and T. W. Greene, in *Greene's Protective Groups in Organic Synthesis*, John Wiley & Sons, Inc., 2006, p. 4th Edition.

198. Q. Yang, X.-Y. Li, H. Wu, and W.-J. Xiao, *Tetrahedron*, 2006, **47**, 3893-3896.

199. Q. Yang, W.-J. Xiao, and Z. Yu, *Org. Lett.*, 2005, **7**, 871-874.

200. O. Songis, A. M. Z. Slawin, and C. S. J. Cazin, *Chem. Commun.*, 2012, **48**, 1266-1268.

201. C. Enkisch and C. Schneider, *Eur. J. Org. Chem.*, 2009, **32**, 5549-5564.

202. A. F. Abdel-Magid, K. G. Carson, B. D. Harris, C. A. Maryanoff, and R. D. Shah, *J. Org. Chem.*, 1996, **61**, 3849-3862.

203. A. J. Phillips, Y. Uto, P. Wipf, M. J. Reno, and D. R. Williams, *Org. Lett.*, 2000, **2**, 1165-1168.

204. J. R. Dunetz, Y. Xiang, A. Baldwin, and J. Ringling, *Org. Lett.*, 2011, **13**, 5048-5051.

205. B. Kuhn, P. Mohr, and M. Stahl, *J. Med. Chem.*, 2010, **53**, 2601-2611.

206. S. T. Cheung and N. L. Benoiton, *Can. J. Chem.*, 1977, **55**, 906 -910.

207. L. Aurelio, R. T. C. Brownlee, and A. B. Hughes, *Chem. Rev.*, 2004, **104**, 5823-5846.

208. J. Coste, E. Frérot, P. Jouin, and B. Castro, *Tetrahedron Lett.*, 1991, **32**, 1967-1970.

209. V. T. Pietzonka and D. Seebach, *Angew. Chem., Int. Ed.,* 1992, **31**, 1481-1482.

210. R. Schwesinger, H. Schlemper, C. Hasenfratz, J. Willaredt, T. Dambacher, T. Breuer, C. Ottaway, M. Fletschinger, J. Boele, H. Fritz, D. Putzas, H. W. Rotter, F. G. Bordwell, A. V. Satish, G.-Z. Ji, E.-M. Peters, K. Peters, H. G. V. Schnering, and L. Walz, *Liebigs. Ann.*, 1996, 1055-1081.

211. S. Escoubet, S. Gastaldi, and M. Bertrand, *Eur. J. Org. Chem.*, 27, **2005**, 3855-3873.

212. M. Schelhaas and H. Waldmann, *Angew. Chem., Int. Ed.*, 1996, **35**, 2056-2083.

213. F. Guibé, *Tetrahedron*, 1998, **54**, 2967-3042.

214. N. Ohmura, A. Nakamura, A. Hamasaki, and M. Tokunaga, *Eur. J. Org. Chem.*, 2008, **30**, 5042-5045.

215. B. Alcaide, P. Almendros, and J. M. Alonso, *Chem. Eur. J.*, 2006, **12**, 2874-2879.

216. K. Kajihara, M. Arisawa, and S. Shuto, *J. Org. Chem.*, 2008, **73**, 9494-9496.

217. M. J. Zacuto and F. Xu, *J. Org. Chem.*, 2007, **72**, 6298-6300.

218. D. P. Spalding, G. W. Moersch, H. S. Mosher, and F. C. Whitmore, *J. Am. Chem. Soc.*, 1964, **68**, 1596-1598.

219. A. Klapars, X. Huang, and S. L. Buchwald, *J. Am. Chem. Soc.*, 2002, **124**, 7421-7428.

220. D. P. Phillips, X.-F. Zhu, T. L. Lau, X. He, K. Yang, and H. Liu, *Tetrahedron Lett.*, 2009, **50**, 7293-7296.

221. D. H. Paull, M. T. Scerba, E. Alden-Danforth, L. R. Widger, and T. Lectka, *J Am. Chem. Soc.*, 2008, **130**, 17260-17261.

222. D. P. Galonic, N. D. Ide, W. A. V. D. Donk, and D. Y. Gin, *J. Am. Chem. Soc.*, 2005, **127**, 7359-7369.

223. W. L. F. Armarego and C. L. L. Chai, *Purification of Laboratory Chemicals*, Butterworth-Heinemann, Oxford, 6th edn., 2009.

224. W. C. Still, M. Kahn, and A. Mitra, *J. Org. Chem.*, 1978, **43**, 2923-2925.

225. B. M. Trost and M. T. Rudd, *Org. Lett.*, 2003, **5**, 4599-4602.

226. A. N. Hulme, C. H. Montgomery, and D. K. Henderson, *J. Chem. Soc., Perkin Trans. 1*, 2000, 1837-1841.

227. D. Gani, P. B. Hitchcock, and D. W. Young, *J. Chem. Soc., Perkin Trans. 1*, 1985, 1363-1372.

228. G. P. Deniau, Ph.D., University of St Andrews, Scotland, 2007.

229. N. S. Chandrakumar, P. K. Yonan, A. Stapelfeld, M. Savage, E. Rorbacher, P. C. Contreras, and D. Hammond, *J. Med. Chem.*, 1992, **35**, 223-233.

230. K. Matsumura, *J. Am. Chem. Soc.*, 1929, **51**, 816-820.

231. A. W. McConnaughie and T. C. Jenkins, *J. Med. Chem.*, 1995, **38**, 3488-3501.

232. Y. Tong, Y. M. Fobian, M. Wu, N. D. Boyd, and K. D. Moeller, *J. Org. Chem.*, 2000, **65**, 2484-2493.

233. J. H. Cho and B. M. Kim, *Tetrahedron Lett.*, 2002, **43**, 1273-1276.

**Appendix 1.1**- *Crystallographic information for (R,R)-**144** with O.nova telomeric DNA*

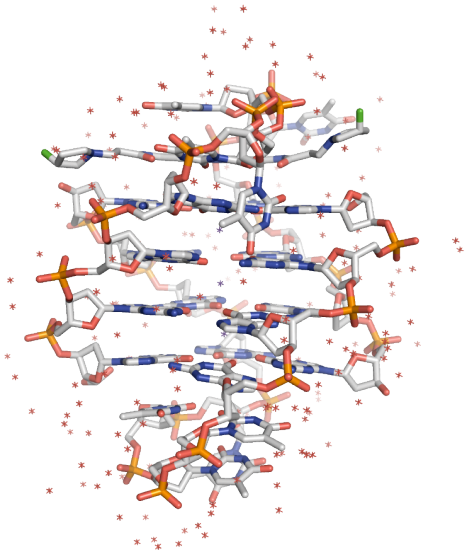

**PDB ID -** 3NYP*

| | | |
|---|---|---|
| **Data collection** | | |
| | Total number of reflections collected | 85447 |
| | Number of unique reflections | 23982 |
| | Space Group | P21212 |
| | Cell dimensions: *a*,*b* and *c* (Å) | 57.80, 44.46, 28.14 |
| | Angle (°) $\alpha$, $\beta$, $\gamma$ | 90.00, 90.00, 90.00 |
| | Maximum resolution (Å) | 1.18 |
| | $R_{merge}$ | 0.051 |
| | $I/\sigma I$ | 15.5 |
| | I/σ (highest resolution shell) | 5.7 |
| | Completeness (%) | 97.7 |
| | Redundancy | 3.6 |
| **Refinement** | | |
| | Resolution range used in refinement (Å) | 21.99-1.18 |
| | Number of unique reflections used in refinement | 23275 |
| | Completeness (%) | 94.6 |
| | $R_{factor}$(%) | 16.6 |
| | $R_{free}$(%) | 18.8 |
| | Number of G-quadruplexes/asymmetric unit | 1 |
| | Number of ligands/asymmetric unit | 1 |
| | Number of asymmetric units per unit cell | 4 |
| **Number of atoms** | | |
| | DNA | 506 |
| | Ligand | 36 |
| | Potassium ions | 4 |
| | Water | 177 |

**Appendix 1.2** - *Crystallographic information for (S,S)-**144** with O. nova telomeric DNA*

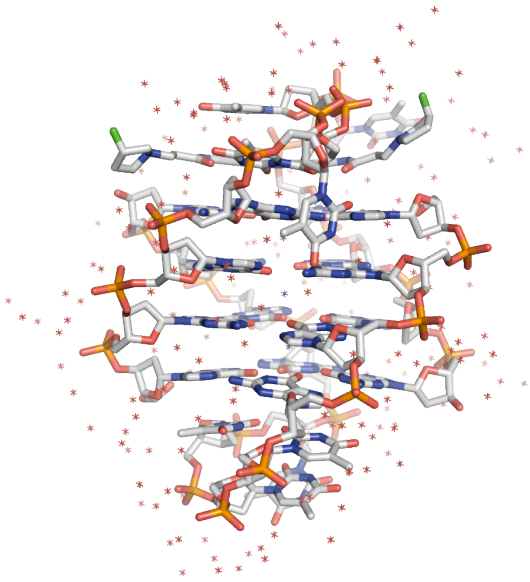

**PDB ID -** 3NZ7 **

| | | |
|---|---|---|
| **Data collection** | | |
| | Total number of reflections collected | 248167 |
| | Number of unique reflections | 25994 |
| | Space Group | P21212 |
| | Cell dimensions: *a*, *b* and *c* (Å) | 55.57, 42.70, 27.00 |
| | Angle (°) $\alpha$, $\beta$, $\gamma$ | 90.00, 90.00, 90.00 |
| | Maximum resolution (Å) | 1.1 |
| | $R_{merge}$ | 0.073 |
| | *I*/σ*I* | 25.4 |
| | *I*/σ (highest resolution shell) | 6.8 |
| | Completeness (%) | 97.1 |
| | Redundancy | 5 |
| **Refinement** | | |
| | Resolution range used in refinement (Å) | 7.80 - 1.10 |
| | Number of unique reflections used in refinement | 25901 |
| | Completeness (%) | 97 |
| | $R_{factor}$(%) | 13.8 |
| | $R_{free}$(%) | 15.9 |
| | Number of G-quadruplexes/asymmetric unit | 1 |
| | Number of ligands/asymmetric unit | 1 |
| | Number of asymmetric units/unit cell | 4 |
| **Number of atoms** | | |
| | DNA | 506 |
| | Ligand | 36 |
| | Potassium ions | 4 |
| | Water | 188 |

## **Appendix 1.3** - *Crystallographic information for **234***

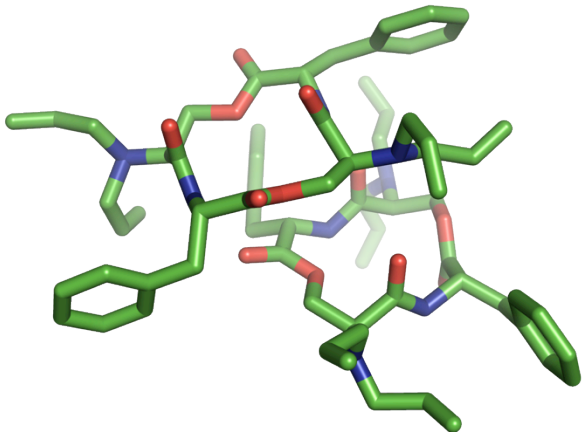

### A. Crystal Data

dsdh4

| | |
|---|---|
| Empirical Formula | $C_{36}H_{44}N_4O_6$ |
| Formula Weight | 628.77 |
| Crystal Color, Habit | colorless, prism |
| Crystal Dimensions | 0.200 × 0.020 × 0.020 mm |
| Crystal System | orthorhombic |
| Lattice Type | Primitive |
| No. of Reflections Used for Unit Cell Determination (2θ range) | 6233 (81.8 - 139.0 °) |
| Lattice Parameters | a = 16.681(5) Å<br>b = 17.399(6) Å<br>c = 24.279(8) Å<br>V = 7047(4) Å$^3$ |
| Space Group | $P2_12_12_1$(#19) |
| Z value | 8 |
| $D_{calc}$ | 1.185 g/cm$^3$ |
| $F_{000}$ | 2688.00 |
| μ(CuK*α*) | 6.576 cm$^{-1}$ |

### B. Intensity Measurements

| | |
|---|---|
| Diffractometer Radiation | CuK*α* (λ = 1.54187 Å)<br>multi-layer mirror monochromated |
| Take-off Angle | 2.8 ° |
| Detector Aperture | 2.0 - 2.5 mm horizontal, 2.0 mm vertical |
| Crystal to Detector Distance | 21 mm |
| Voltage, Current | 40kV, 20mA |
| Temperature | -100.0 °C |
| Scan Type | ω-2θ |
| $2\theta_{max}$ | 137.0 ° |
| No. of Reflections Measured | Total: 73332, Unique: 12756 ($R_{int}$ = 0.1119)<br>Friedel pairs: 5732 |
| Corrections | Lorentz-polarization<br>Absorption (trans. factors: 0.472 - 0.987) |

### C. Structure Solution and Refinement

| | |
|---|---|
| Structure Solution | Direct Methods |
| Refinement | Full-matrix least-squares on F2 |
| Function Minimized | $\Sigma$ w (Fo2 - $Fc^2)^2$ |
| Least Squares Weights | w = 1/ [ $\sigma 2(Fo^2)$ + $(0.1213 \cdot P)^2$ + 0.1830 · P ] where P = (Max($Fo^2$,0) + $2Fc^2$)/3 |
| $2\theta_{max}$ cutoff | 137.0° |
| Anomalous Dispersion | All non-hydrogen atoms |
| No. Observations (All reflections) | 12756 |
| No. Variables | 845 |
| Reflection/Parameter Ratio | 15.10 |
| Residuals: R1 (I>2.00σ(I)) | 0.0707 |
| Residuals: R (All reflections) | 0.0761 |
| Residuals: wR2 (All reflections) | 0.1914 |
| Goodness of Fit Indicator | 1.059 |
| Flack Parameter (Friedel pairs = 5732) | 0.14(17) |
| Max Shift/Error in Final Cycle | 0.001 |
| Maximum peak in Final Diff. Map | 0.69 $e^-/Å^3$ |
| Minimum peak in Final Diff. Map | -0.38 $e^-/Å^3$ |

## **Appendix 1.4** - *Selected NMR*

### *1.4.1 - $^{1}$H NMR of (S,S)-**196**.HCl*

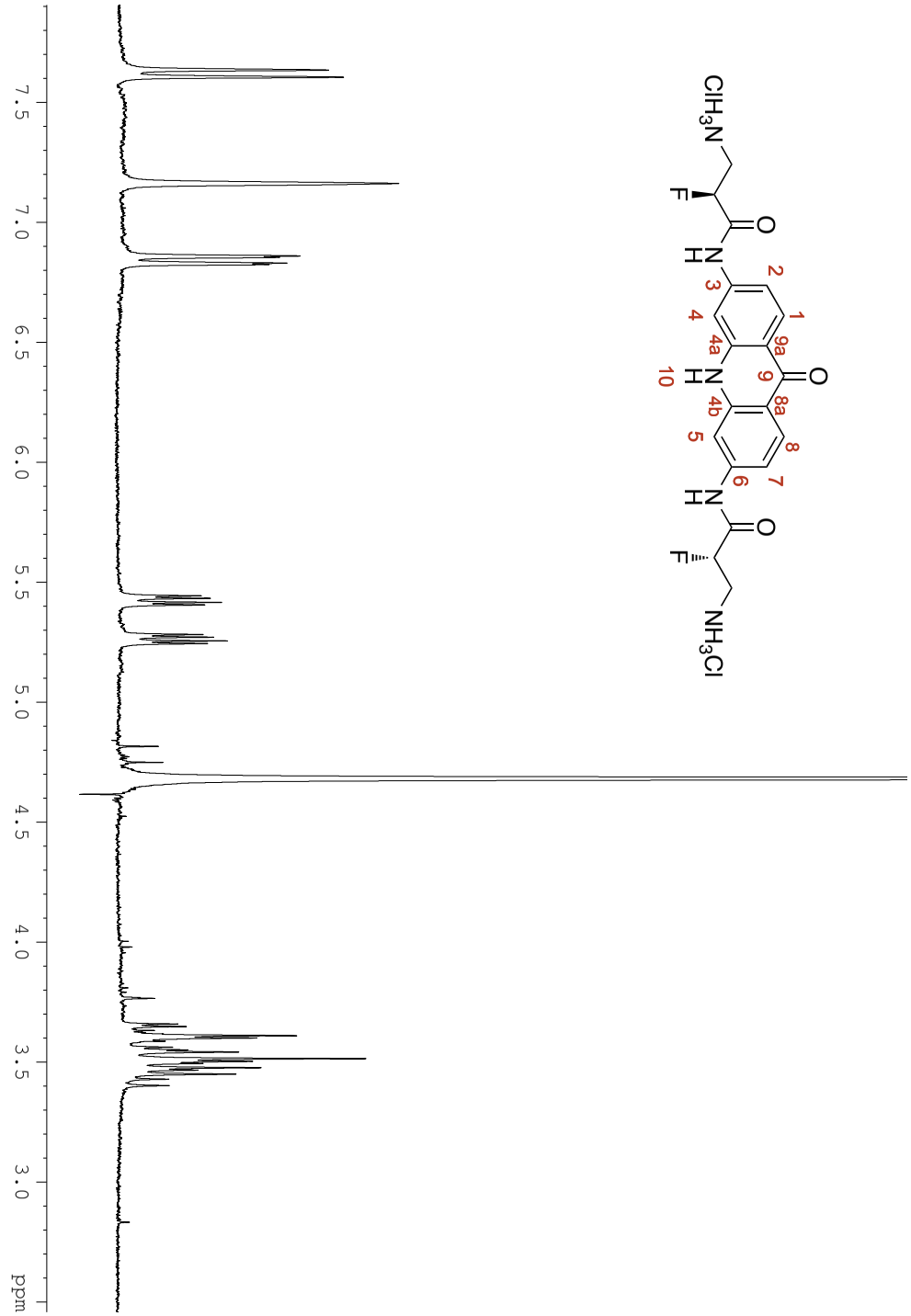

### 1.4.2 - $^{19}F$ NMR of (S,S)-**196**.HCl

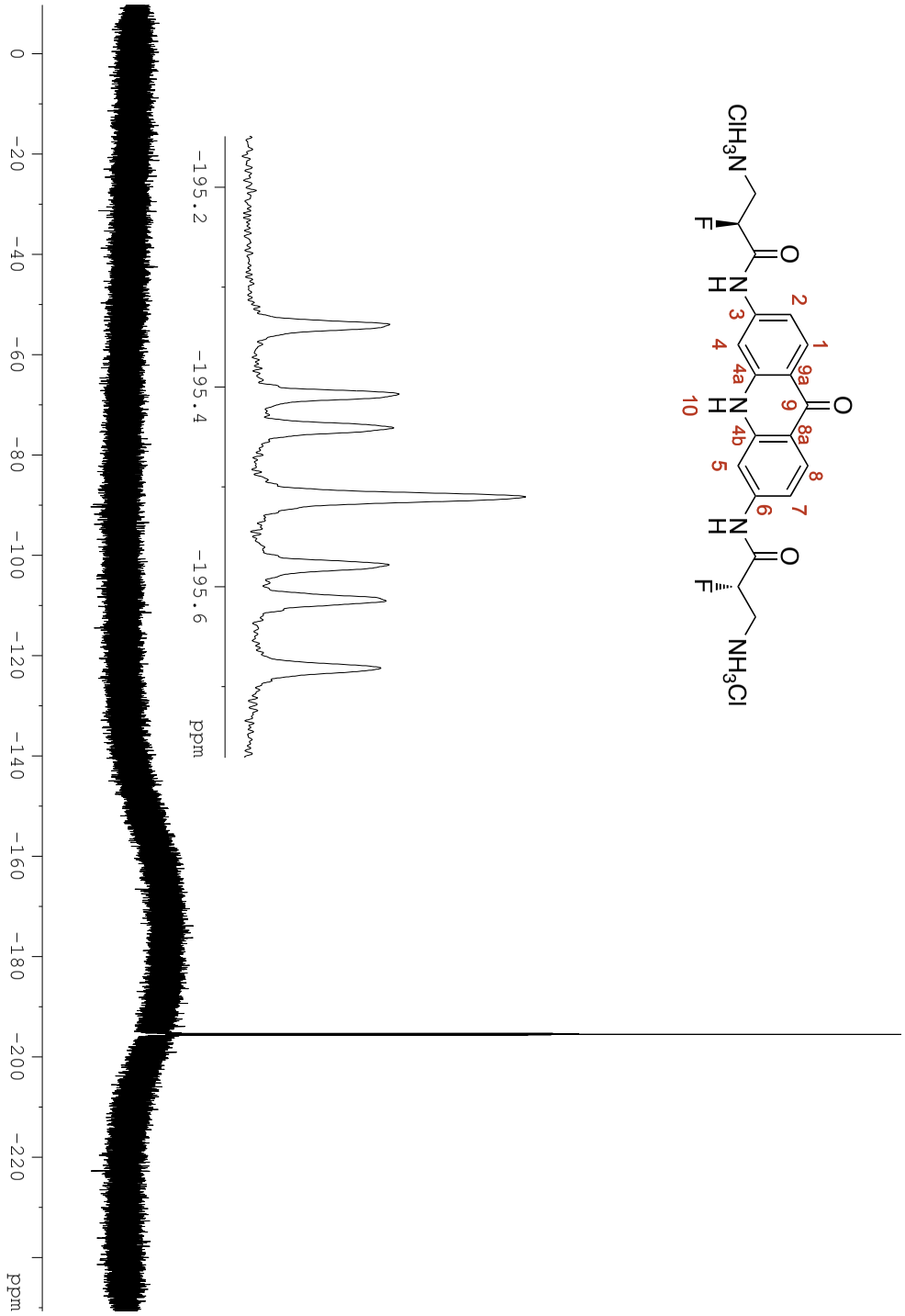

### 1.4.3 - $^{1}H$ NMR of (S,S)-**206**

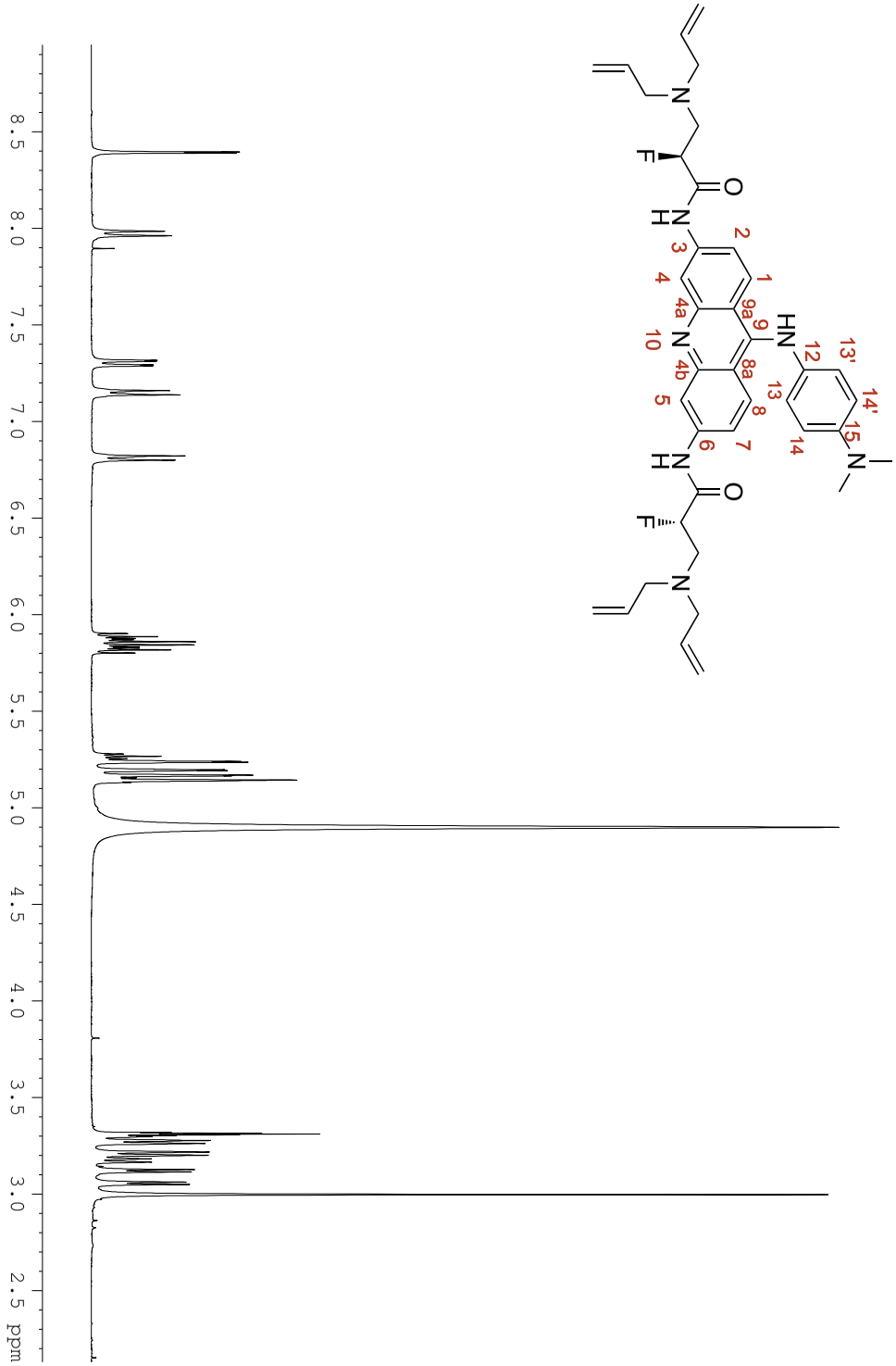

### 1.4.4 - $^{19}F$ NMR of (S,S)-**206**

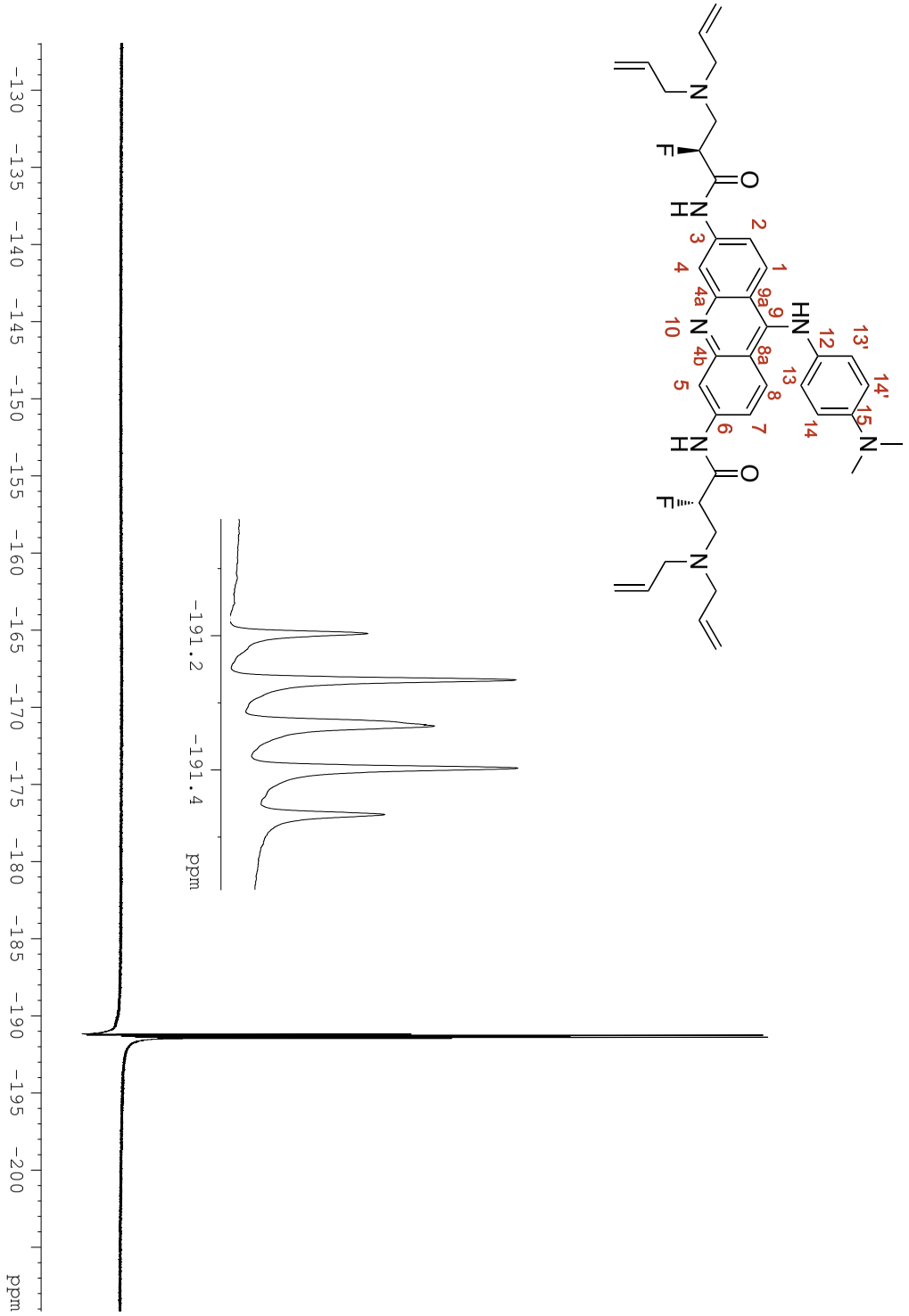

*1.4.5 - $^{13}C$ NMR of (S,S)-**206***

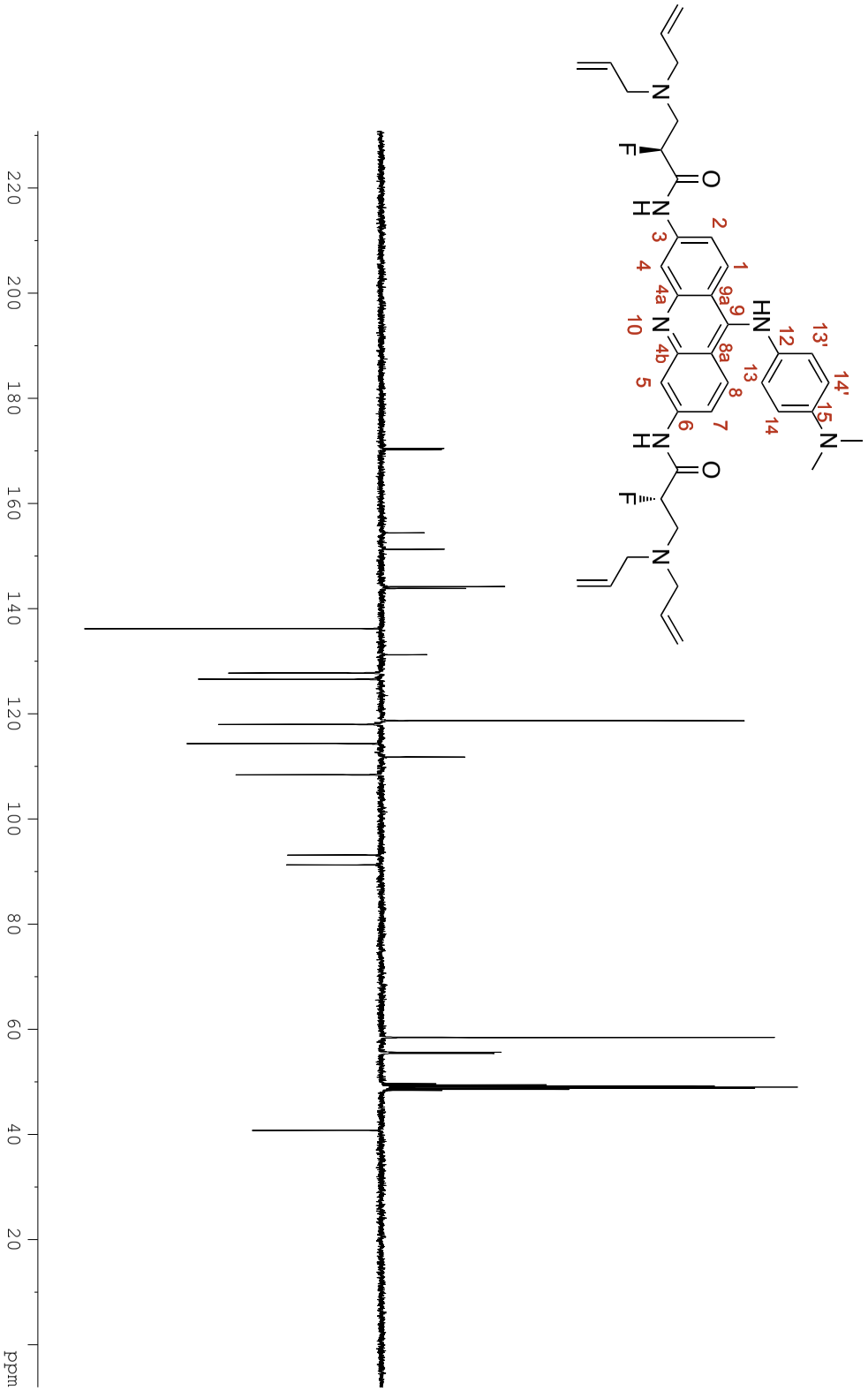

### *1.4.6 - $^{1}$H NMR (S,S)-**208**.HCl*

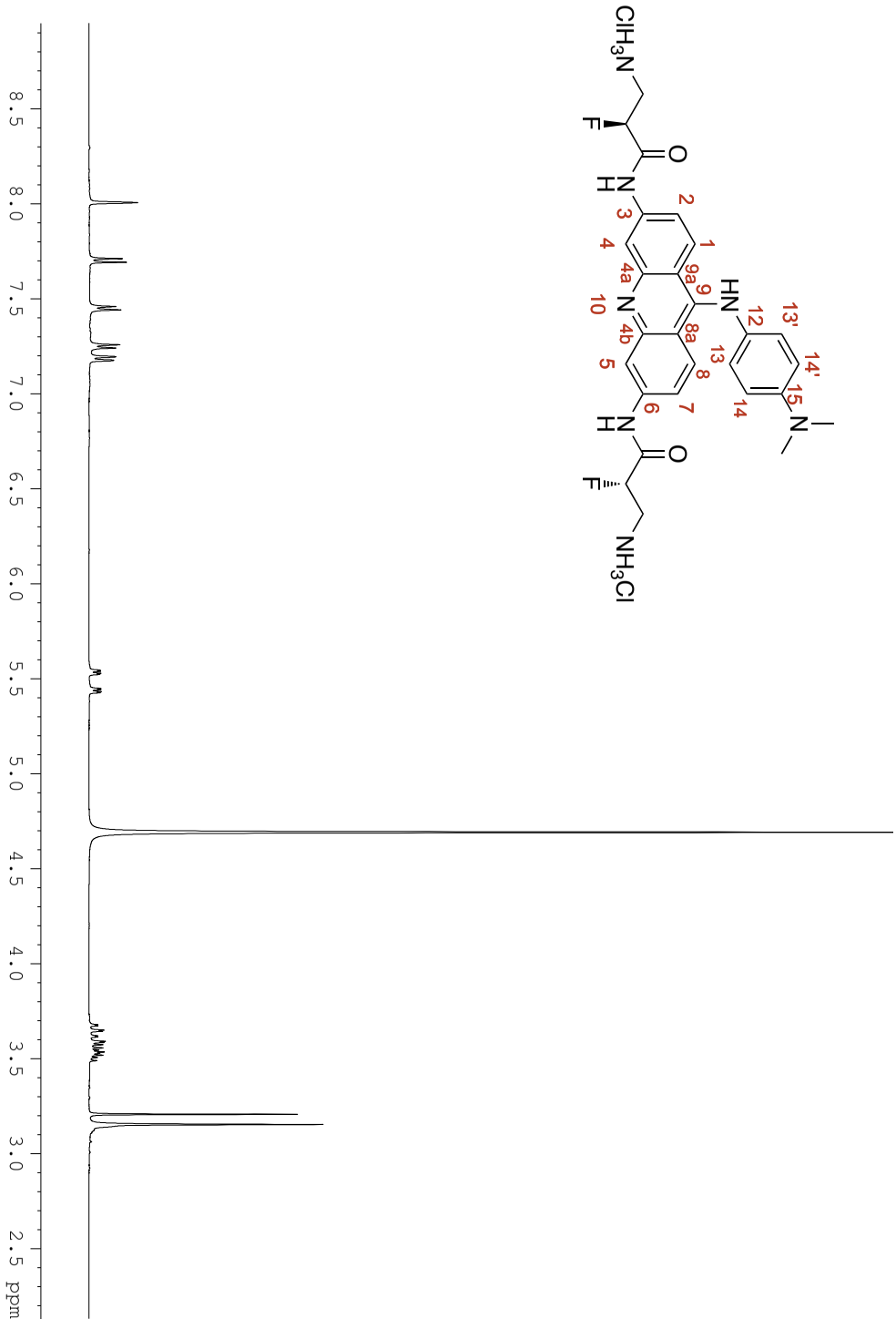

### 1.4.7 - $^{1}H$ NMR (S,S)-**208**.HCl

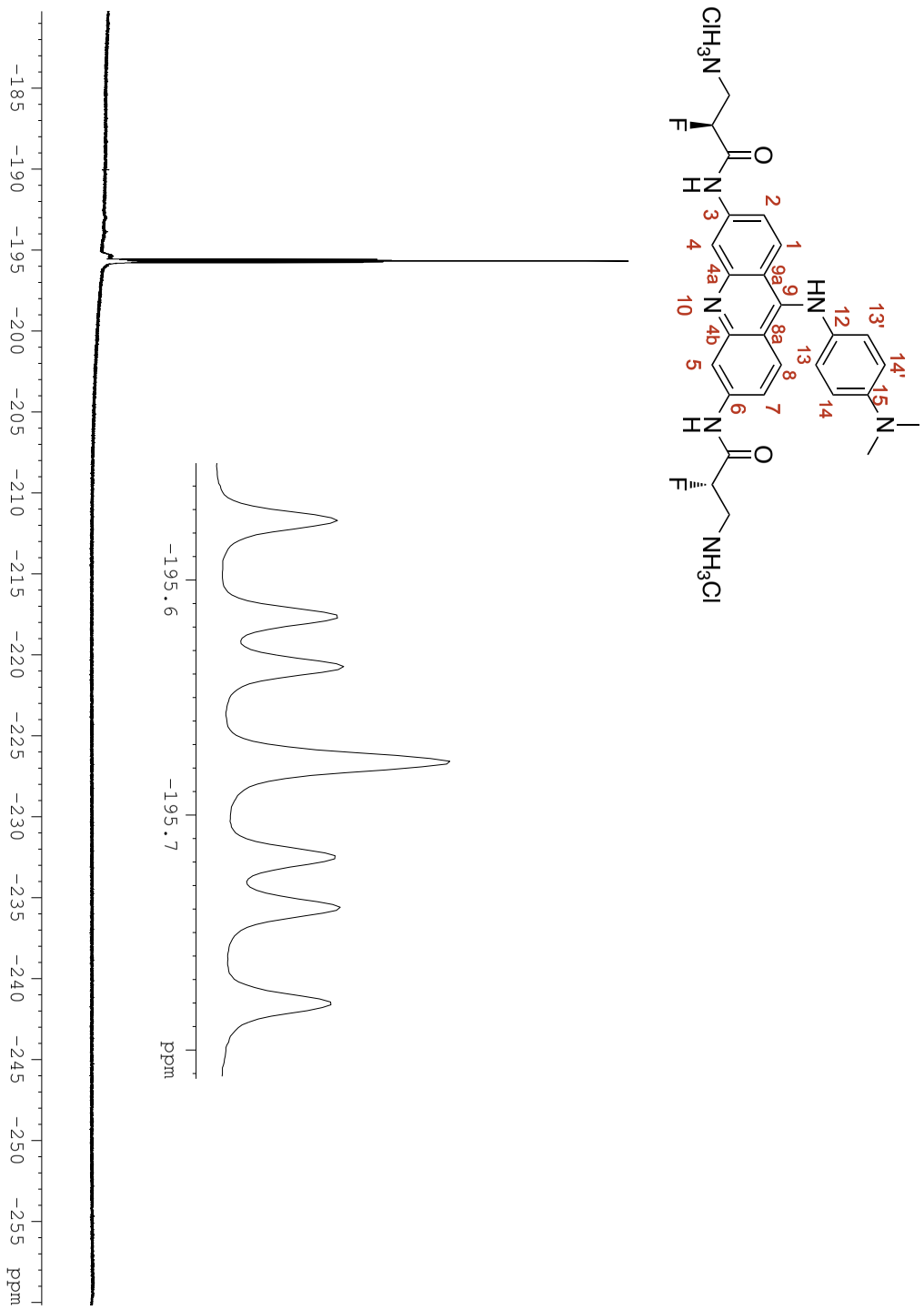

### *1.4.8 - $^{1}$H NMR of (S,S)-**210***

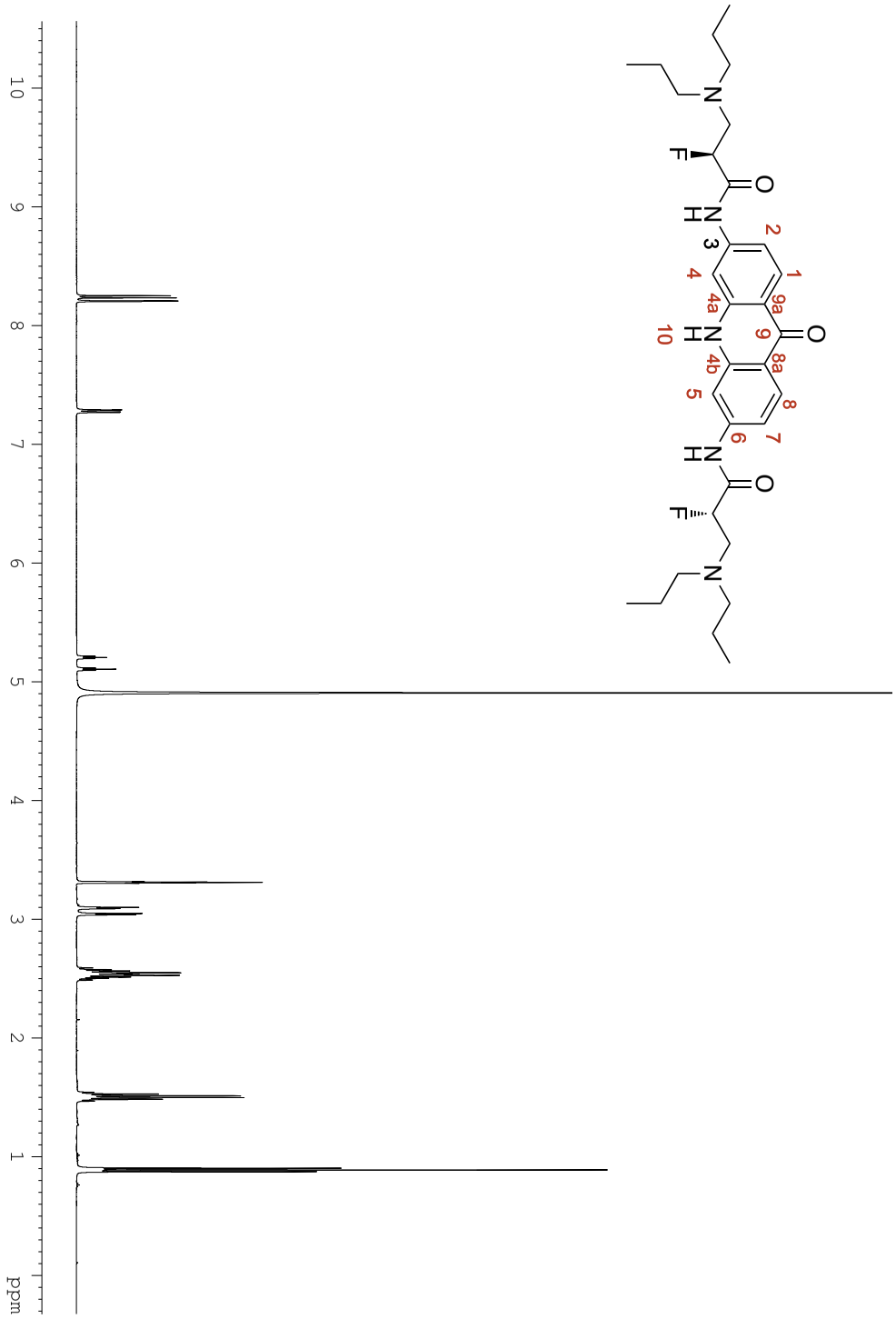

### 1.4.9 - $^{19}F$ NMR of (S,S)-**210**

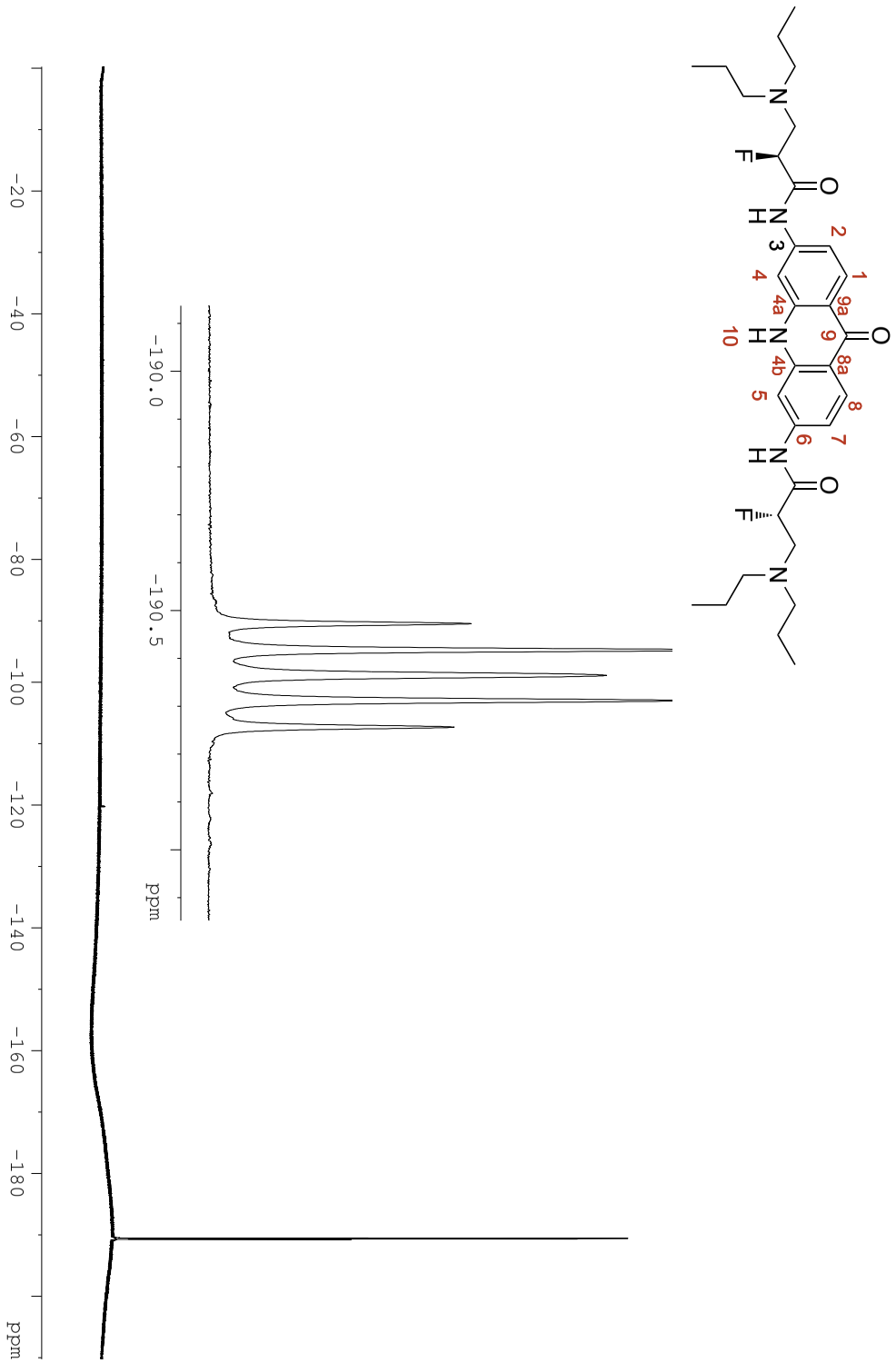

### 1.4.10 - $^{13}$C NMR of (S,S)-***210***

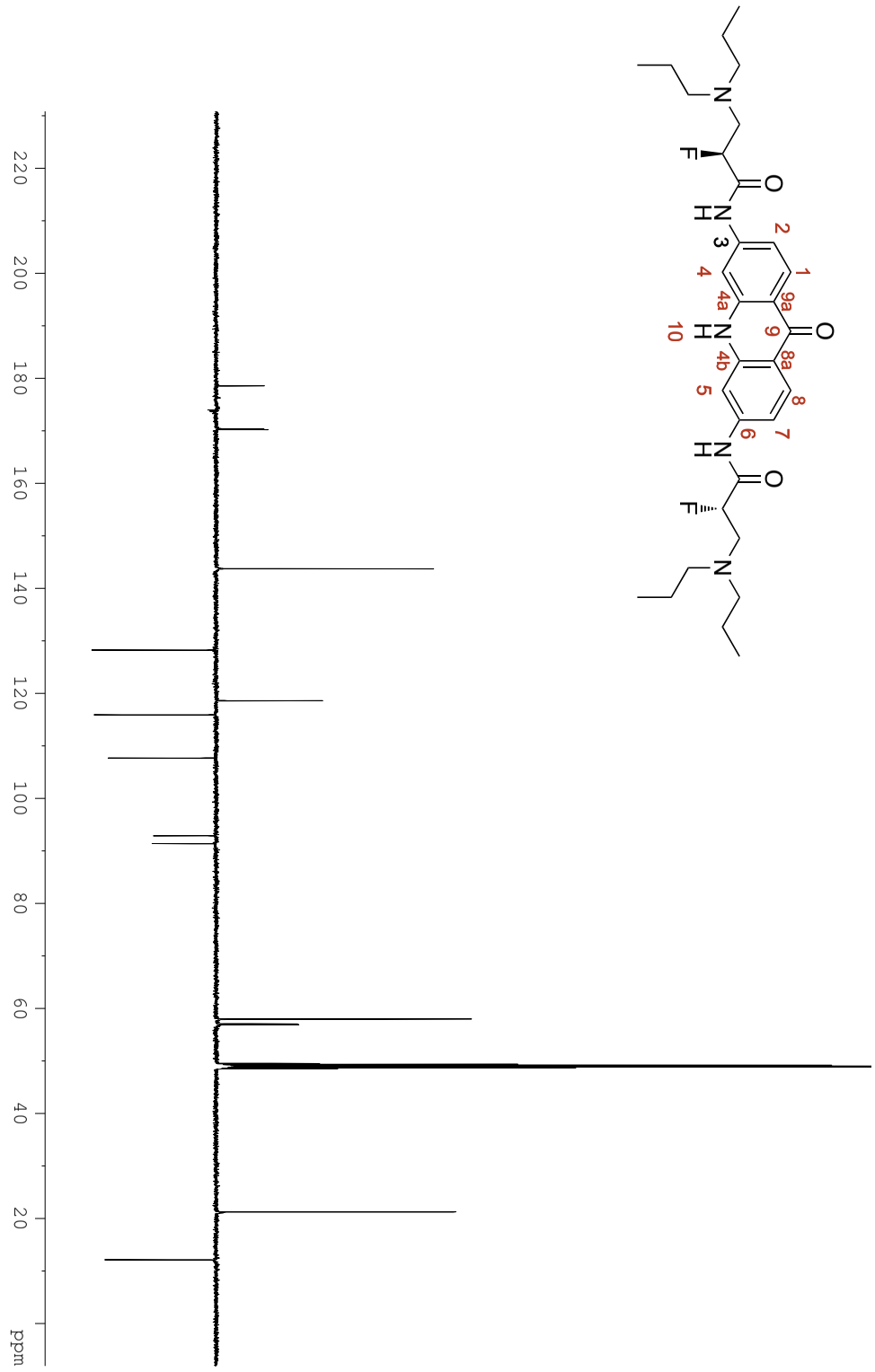

### 1.4.11 - $^{1}H$ NMR of (S,S)-***212***

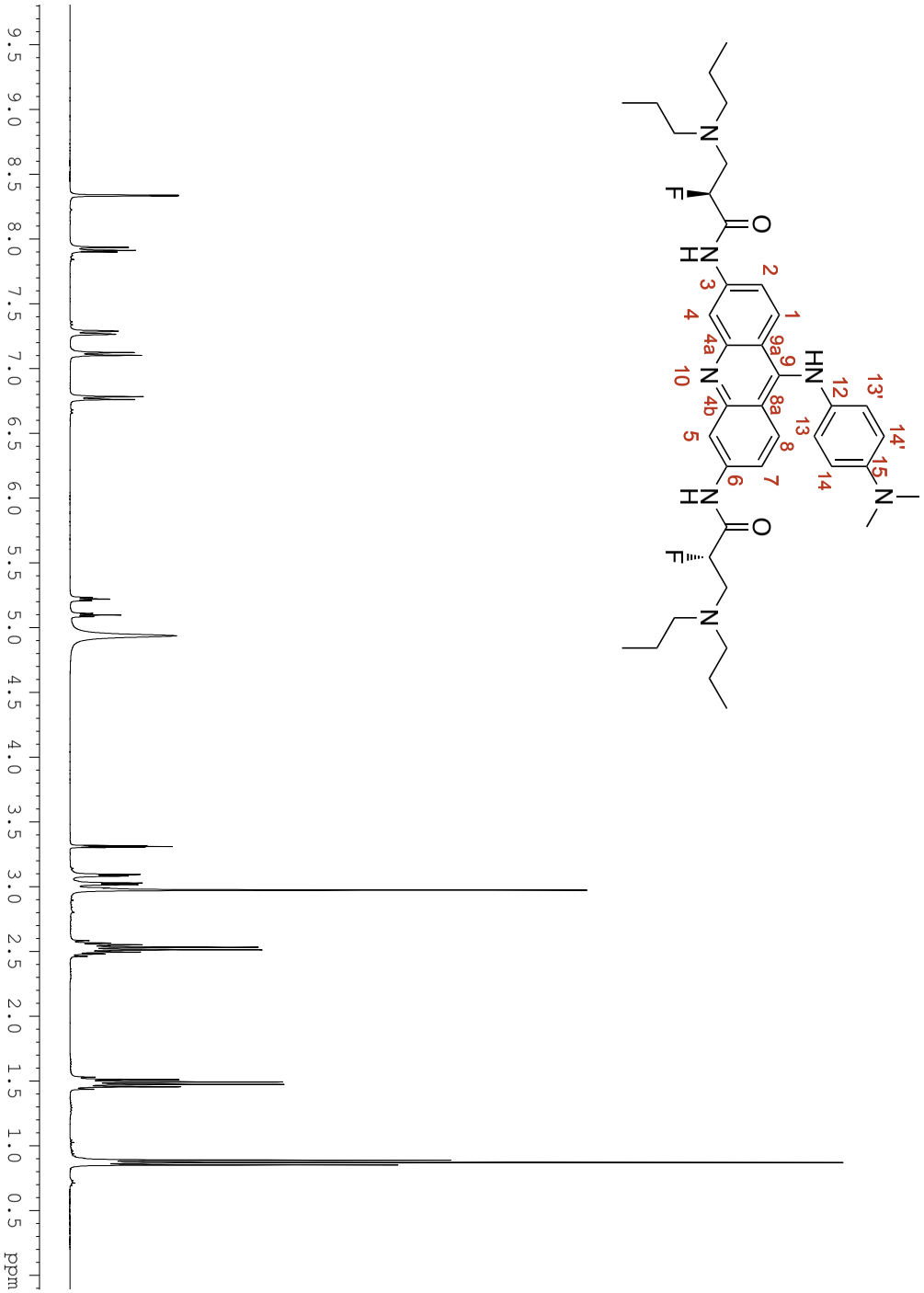

### 1.4.12 - $^{19}F$ NMR of (S,S)-**212**

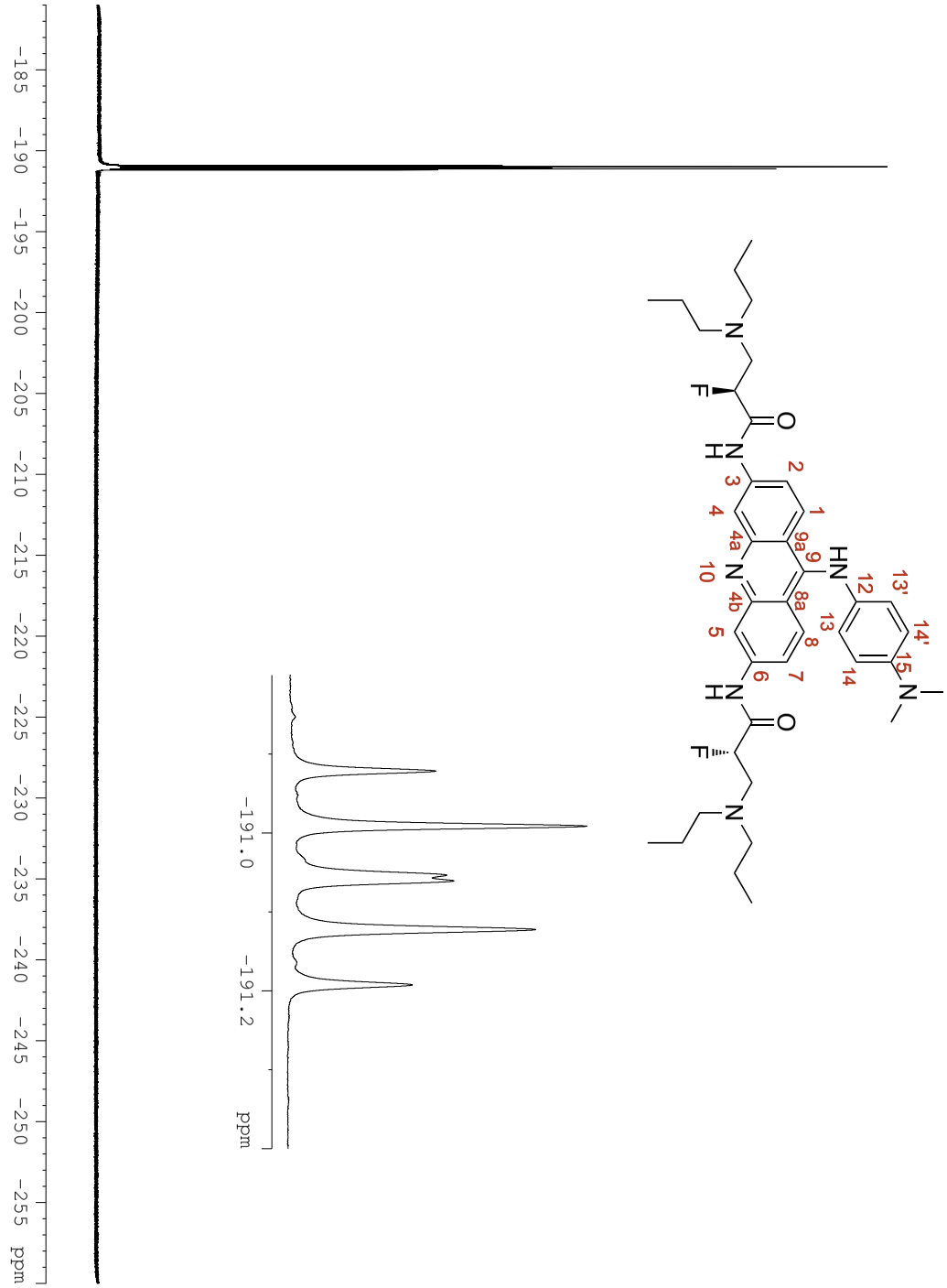

### 1.4.13 - $^{13}C$ NMR of (S,S)-**212**

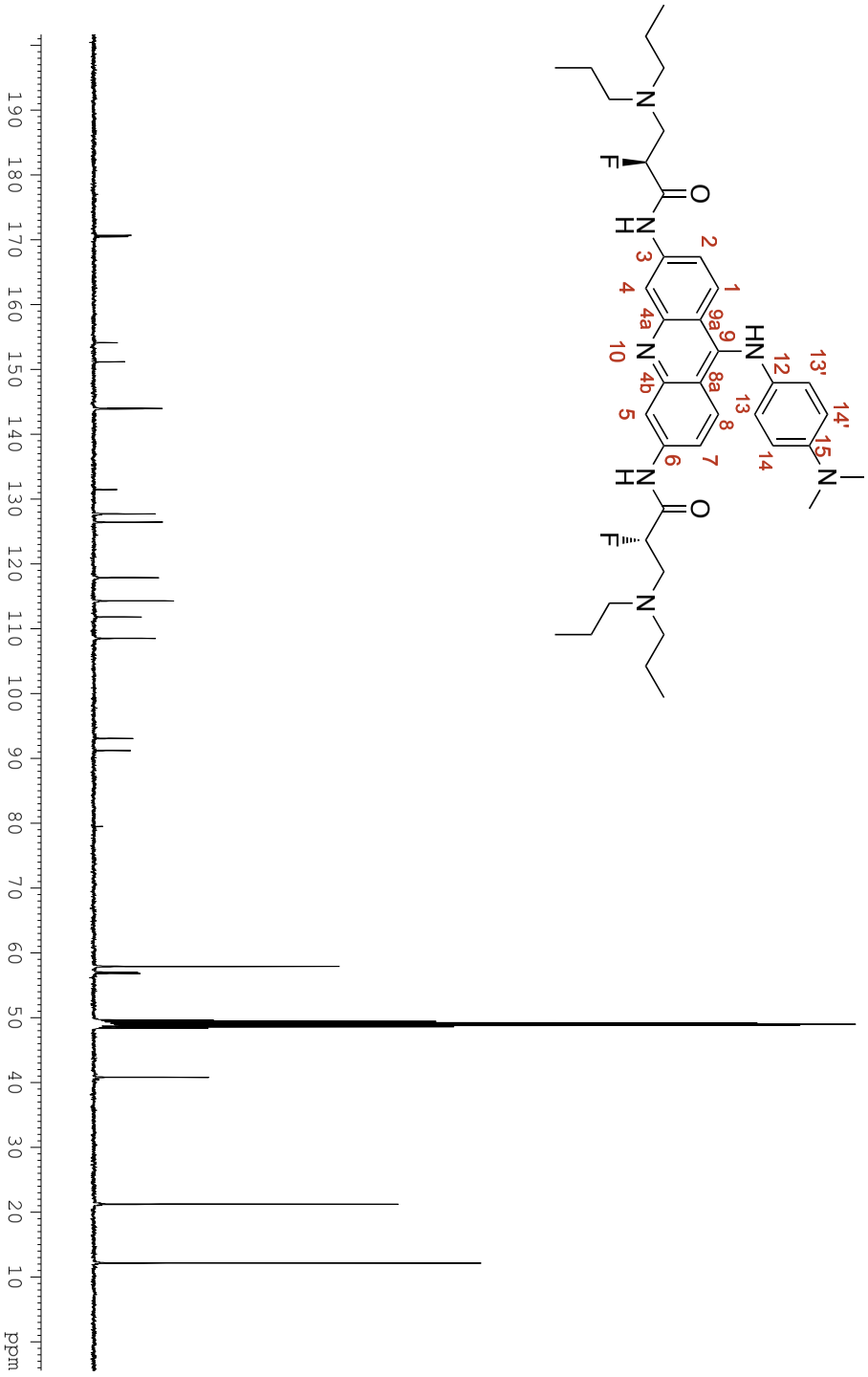

### *1.4.14 - $^{1}H$ NMR of (S)-**229***

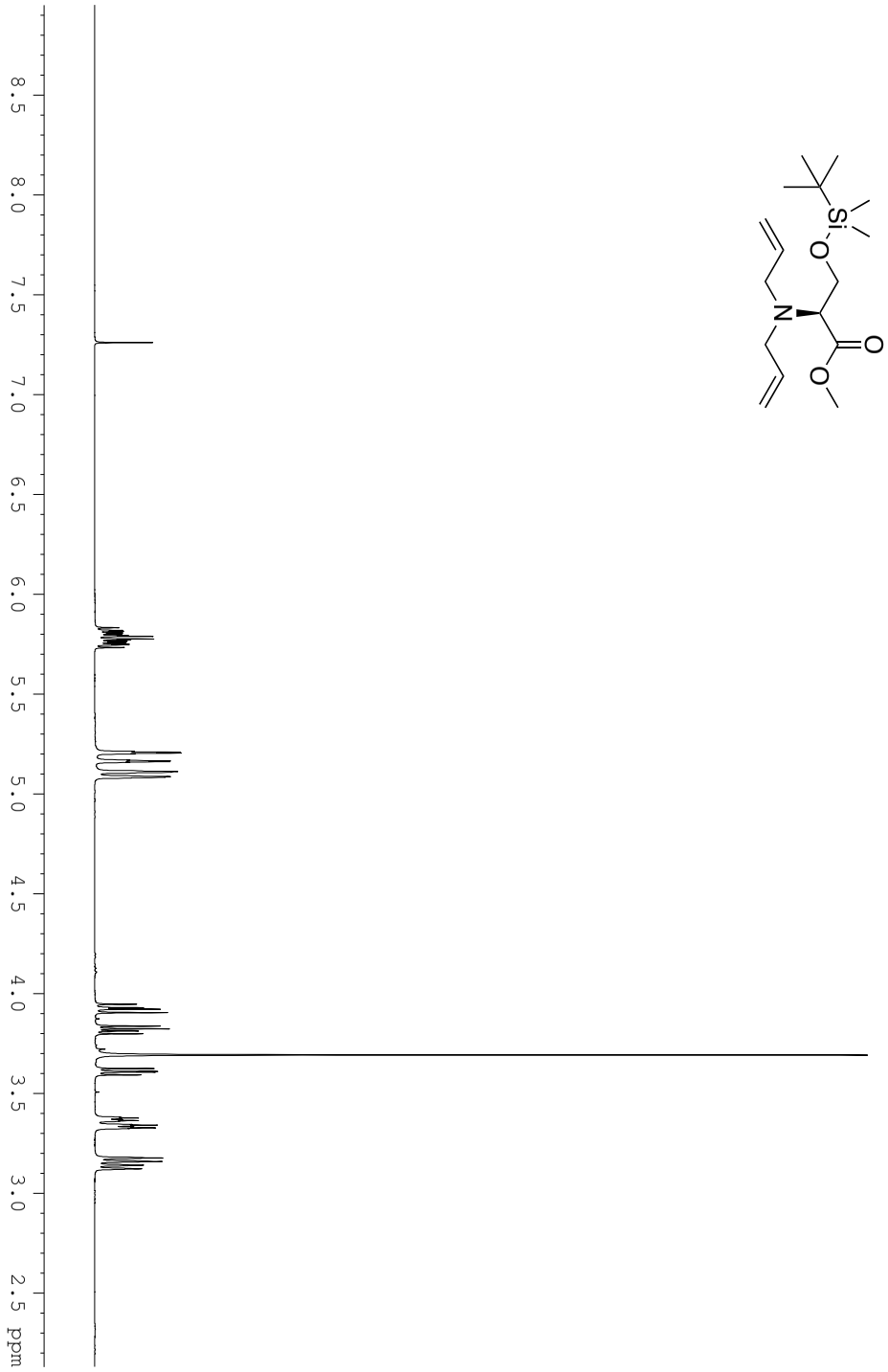

### 1.4.15 - $^{13}C$ NMR of (S)-**229**

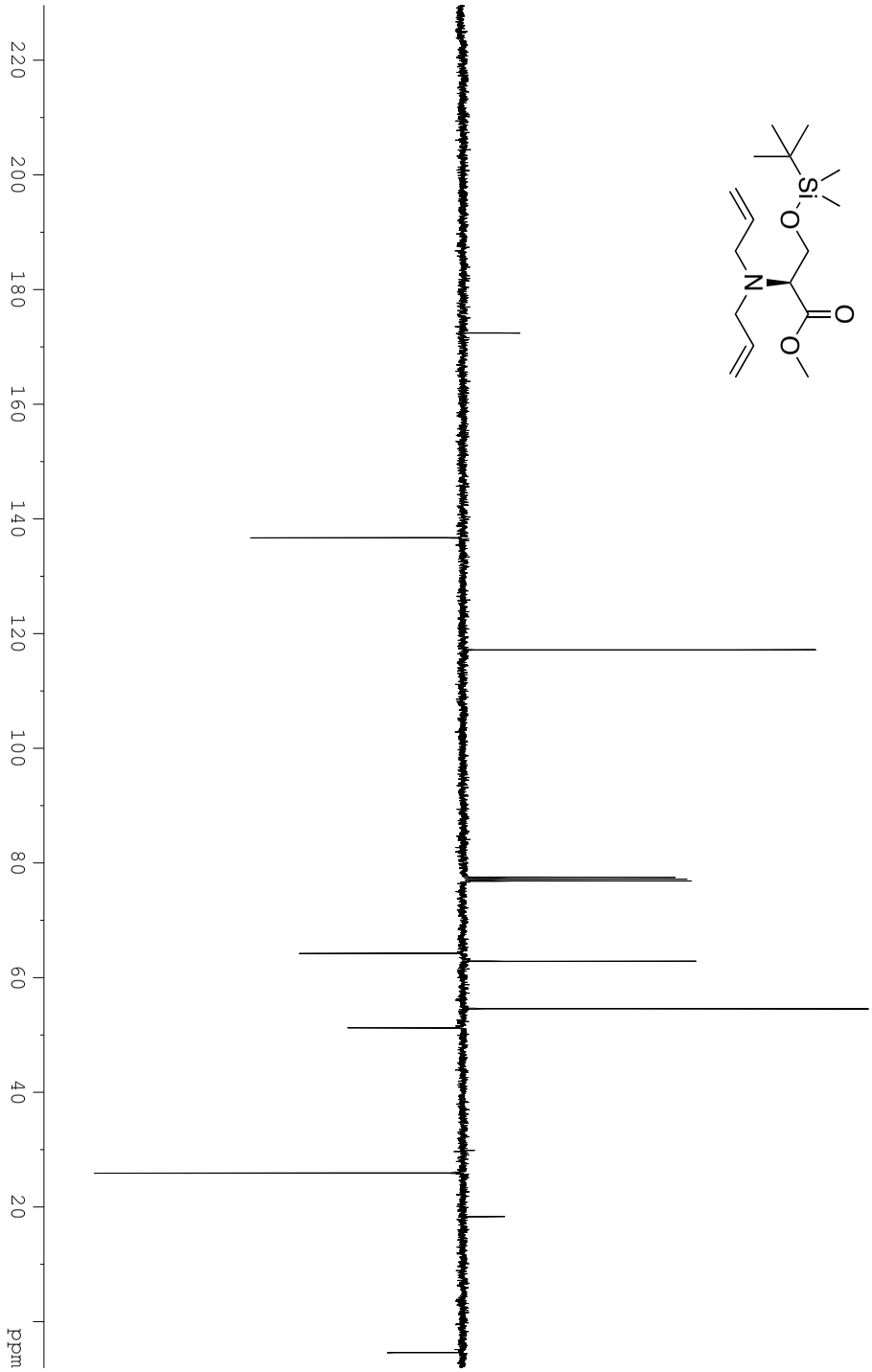

### *1.4.16 - $^{1}H$ NMR **224c***

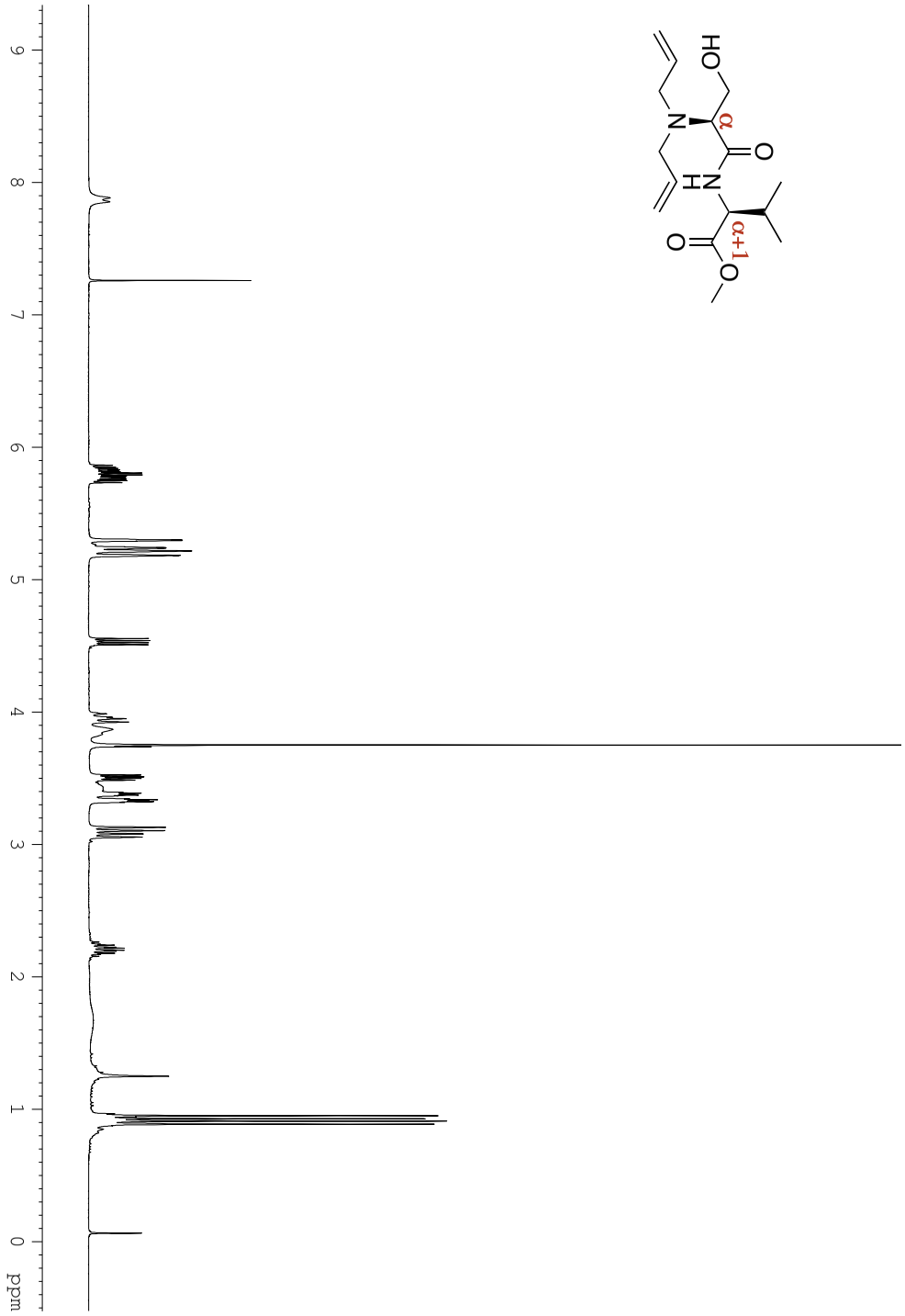

### 1.4.17 - $^{13}C$ NMR of ***224c***

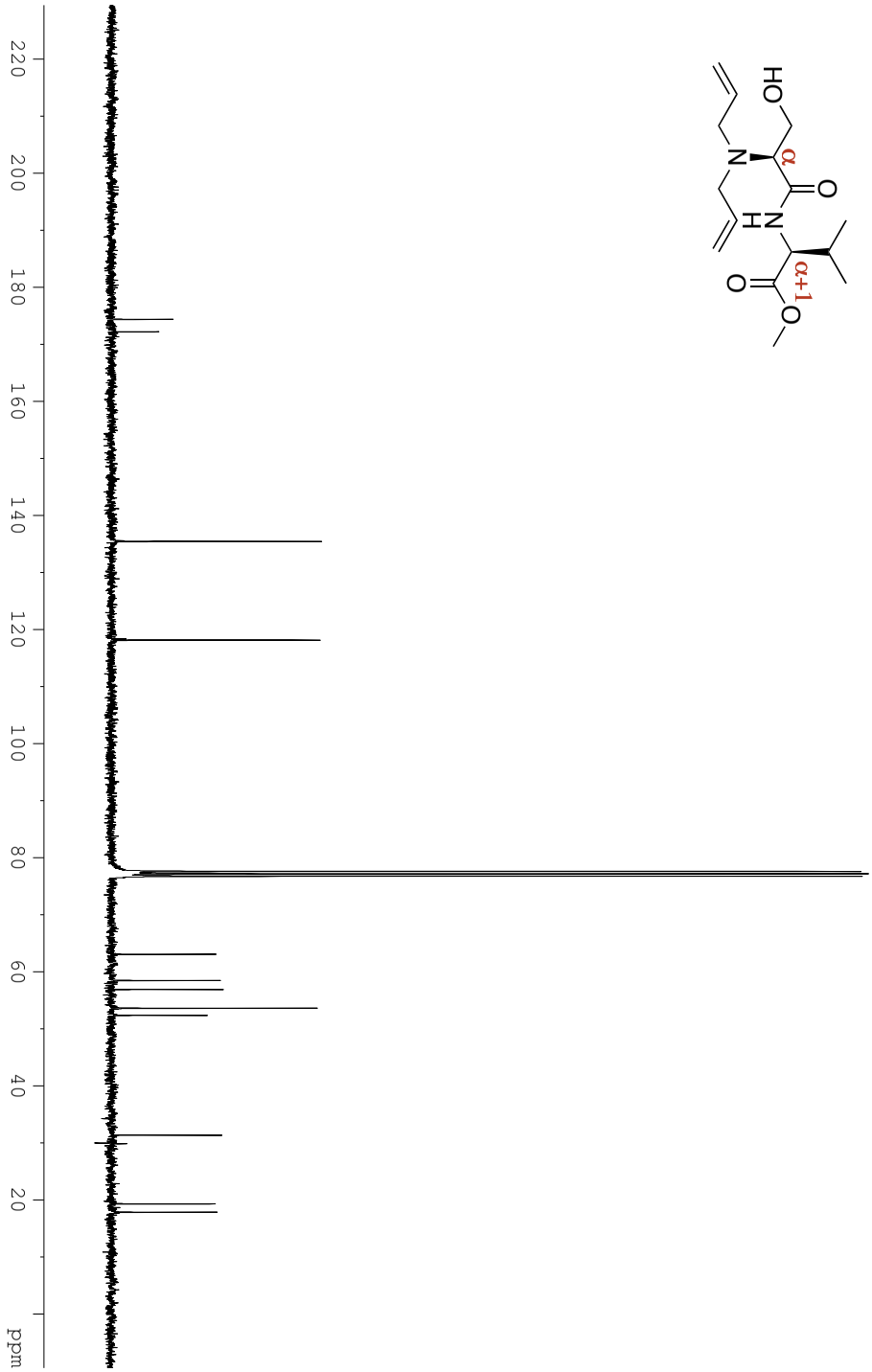

### *1.4.18 - $^{1}H$ NMR of **227c***

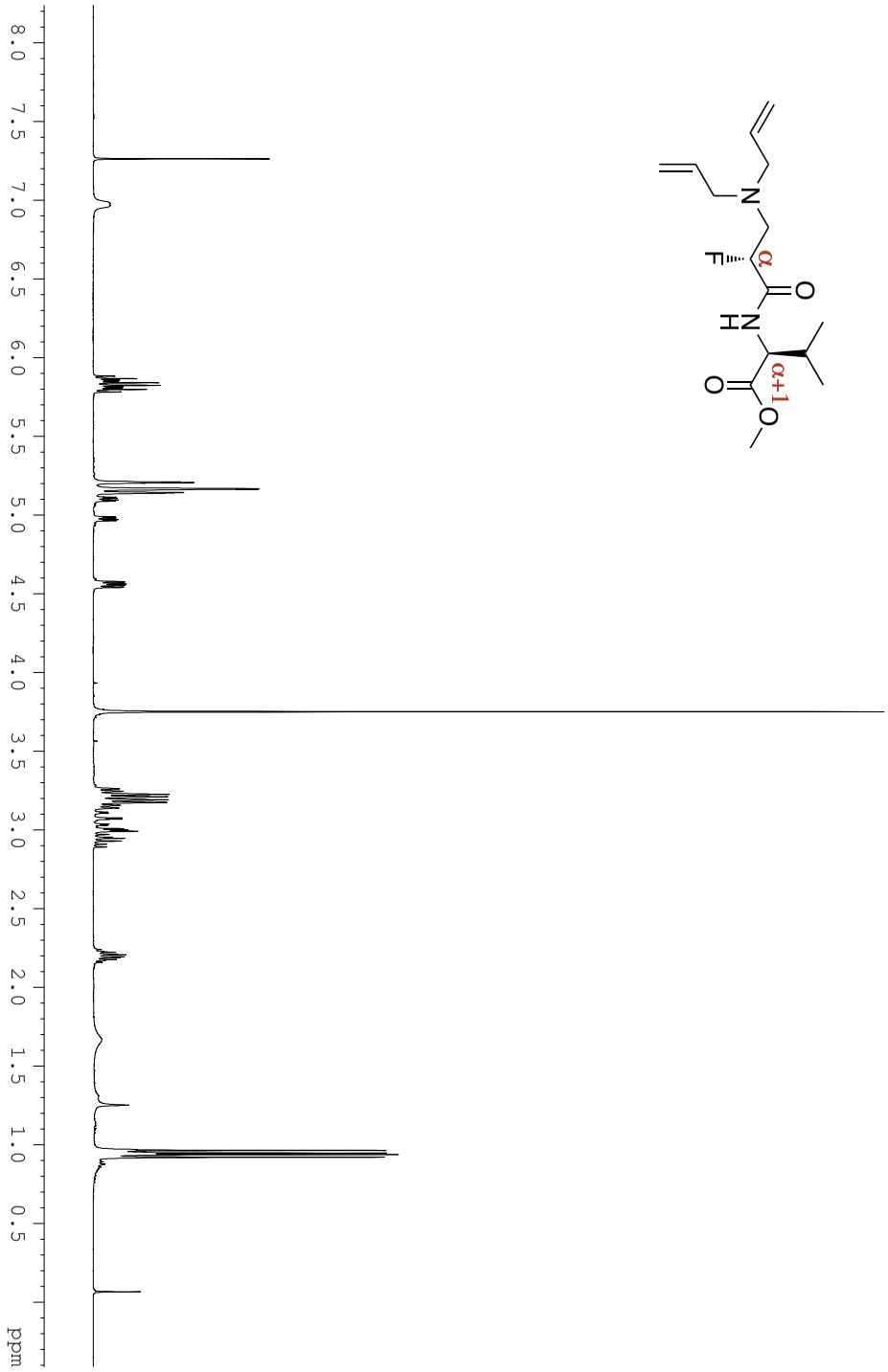

### *1.4.19 - $^{19}F$ NMR of **227c***

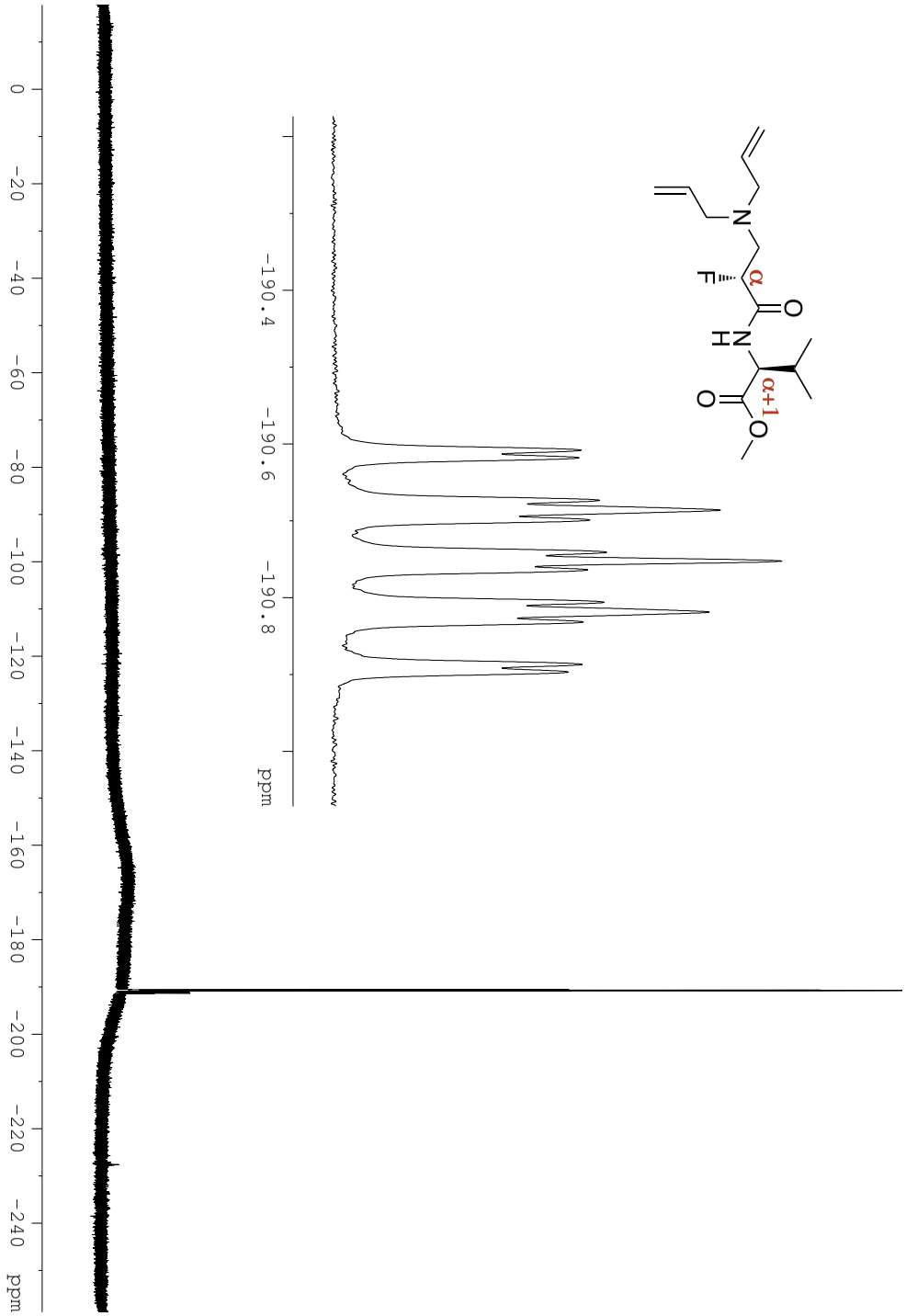

### 1.4.20 - $^{13}C$ NMR of ***227c***

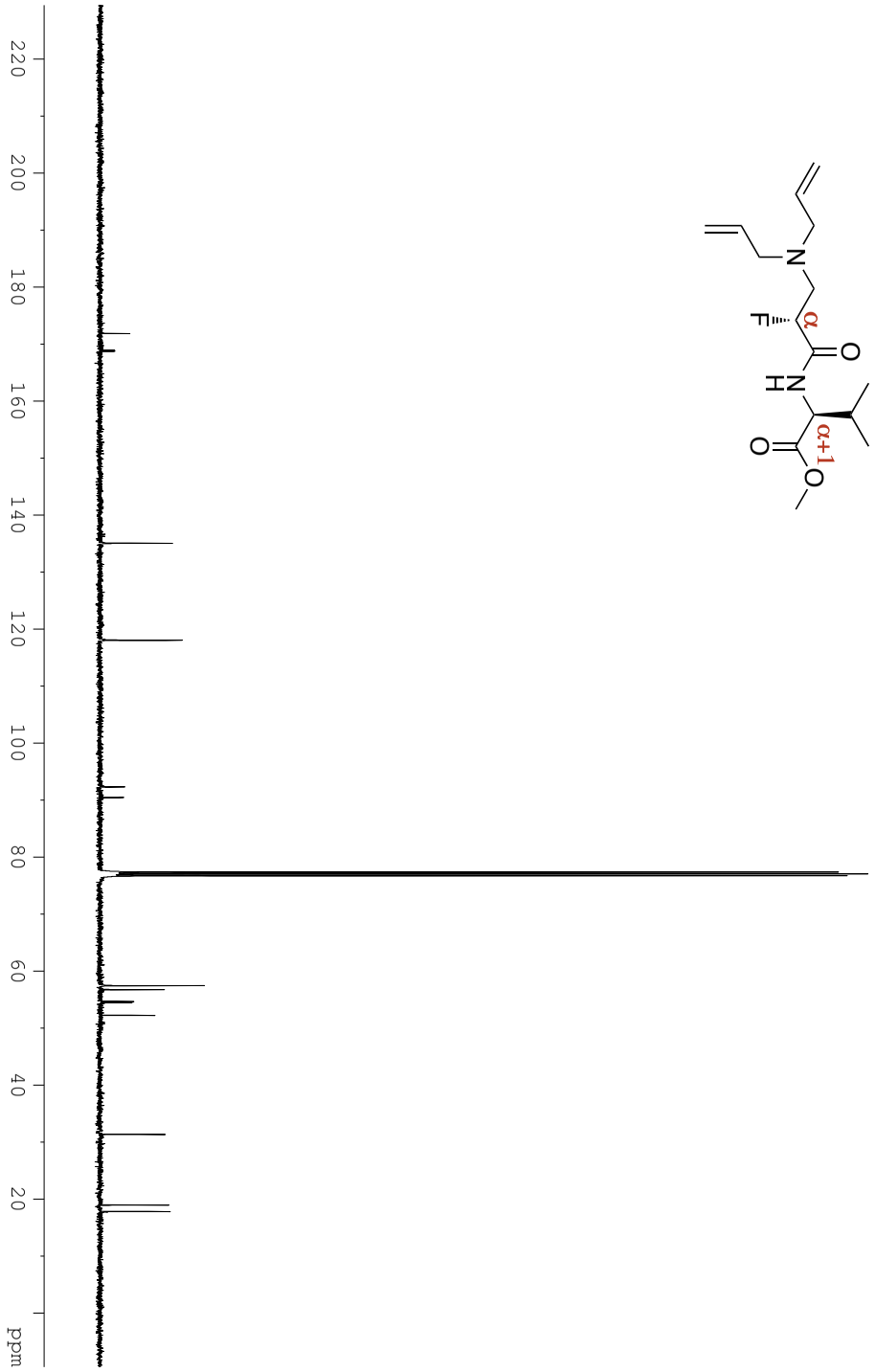

### *1.4.21 - $^{1}H$ NMR of **228c***

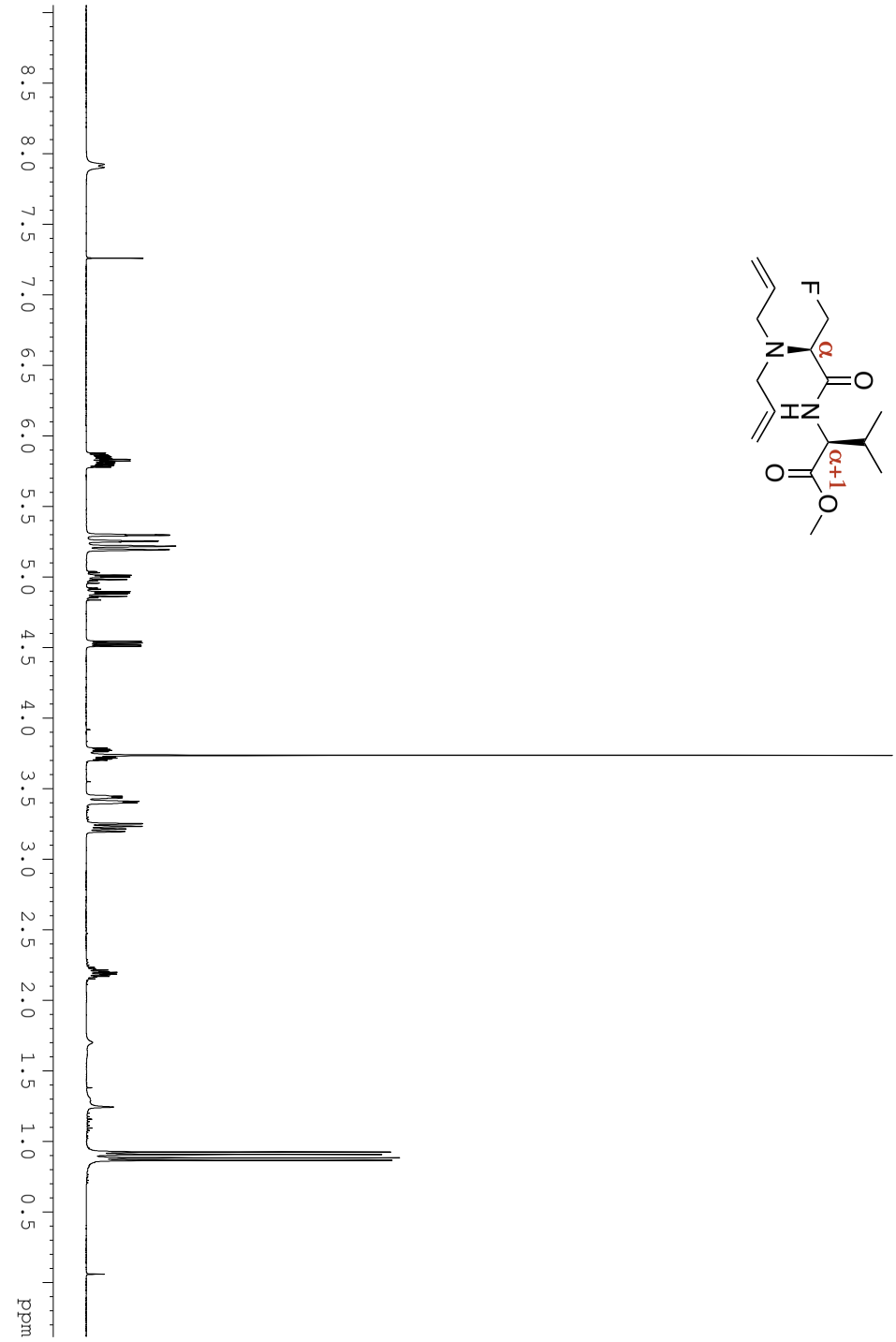

### 1.4.22 - $^{19}F$ NMR of **228c**

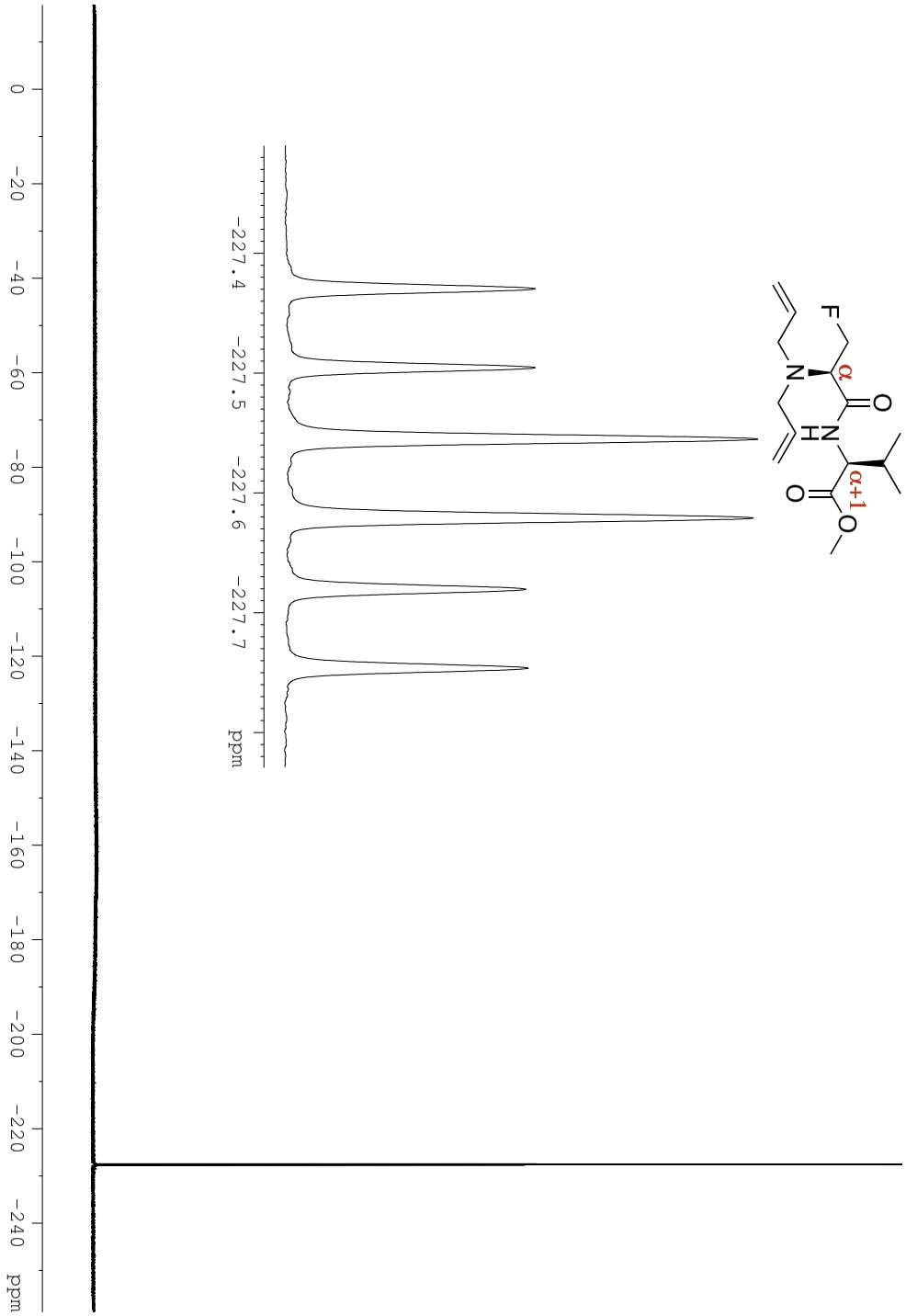

### *1.4.23 - $^{13}C$ NMR of **228c***

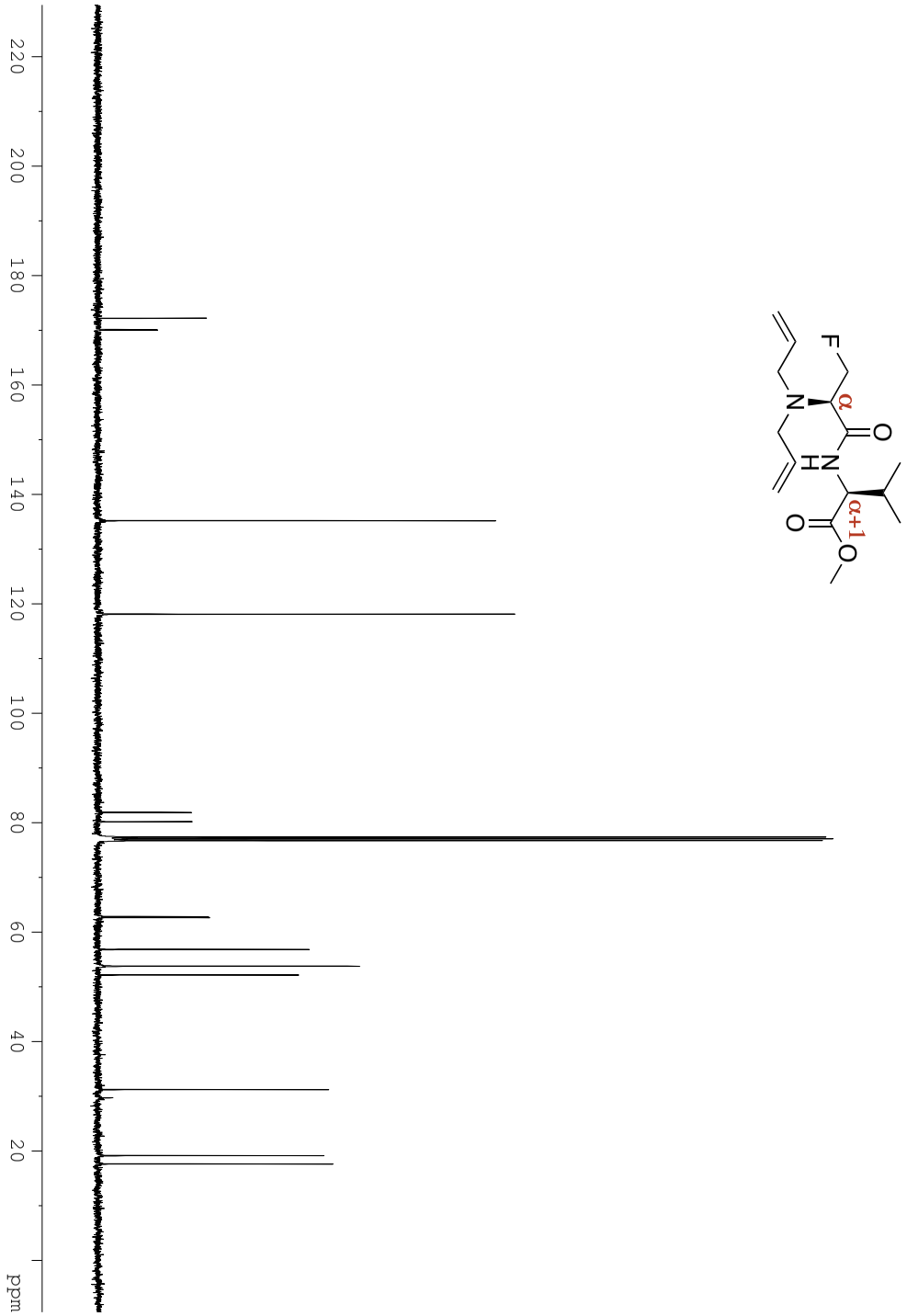

### *1.4.24 - $^{1}H$ NMR of **248***

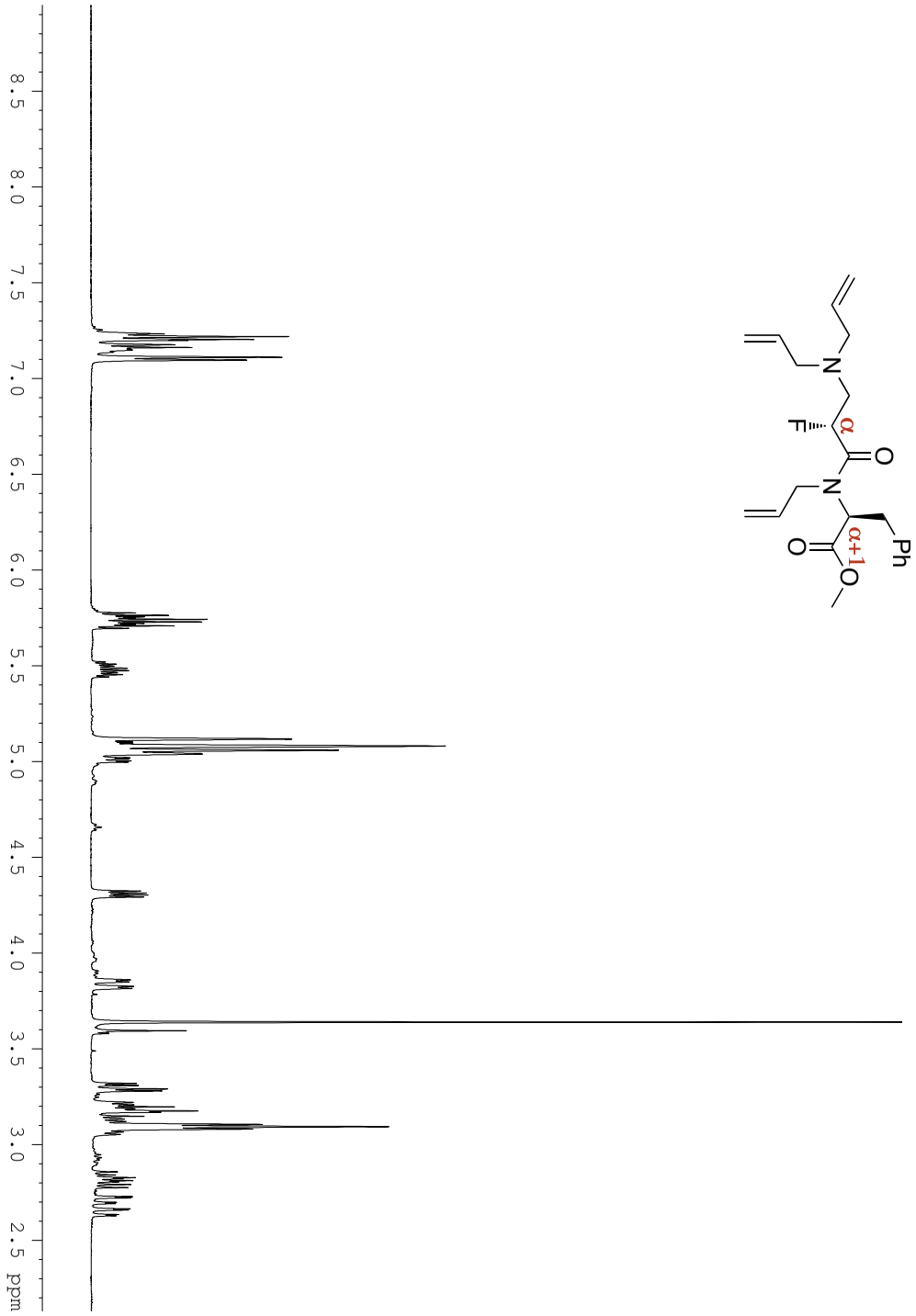

### *1.4.25 - $^{19}$F NMR of **248***

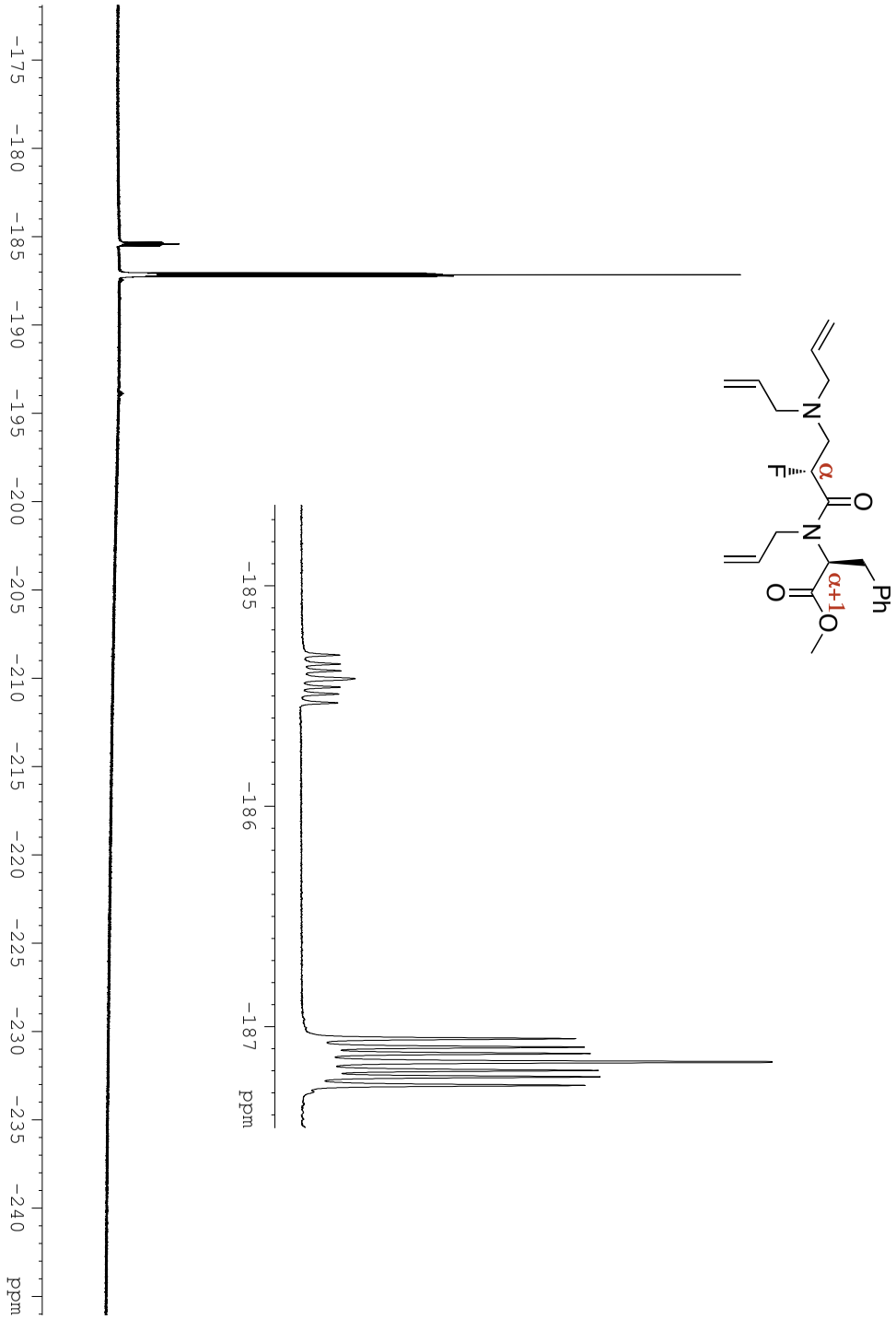

### 1.4.26 - $^{13}C$ NMR of **248**